

# BLACK HOLES AND HOLOGRAPHY

A thesis  
submitted to the



Tata Institute of Fundamental Research,  
Mumbai, India - 400005

for the degree of

Doctor of Philosophy  
in Physics

by

**Pushkal Shrivastava**



International Centre for Theoretical Sciences  
Tata Institute of Fundamental Research  
Bengaluru, India - 560089

August, 2020

Final version submitted in June, 2021



## DECLARATION

This thesis is a presentation of my original research work. Wherever contributions of others are involved, every effort is made to indicate this clearly, with due reference to the literature, and acknowledgement of collaborative research and discussions.

The work was done under the guidance of Prof. Suvrat Raju, at the International Centre for Theoretical Sciences, Bengaluru.



Pushkal Shrivastava

In my capacity as supervisor of the candidate's thesis, I certify that the above statements are true to the best of my knowledge.



Prof. Suvrat Raju

Date: June 12, 2021



*To Bhaiya, Mummy and Papa,  
for years of support and affection*

*§*

*To Prachi,  
for endless motivation.*



## Publications

1. S. Raju and P. Shrivastava, *Critique of the fuzzball program*, *Phys. Rev. D* **99** (2019) 066009, [[1804.10616](#)].
2. S. Banerjee, K. Papadodimas, S. Raju, P. Samantray and P. Shrivastava, *A Bound on Thermal Relativistic Correlators at Large Spacelike Momenta*, *SciPost Phys.* **8** (2020) 064, [[1902.07203](#)].
3. K. Papadodimas, S. Raju and P. Shrivastava, *A simple quantum test for smooth horizons*, [1910.02992](#).
4. A. Laddha, S. G. Prabhu, S. Raju and P. Shrivastava, *The Holographic Nature of Null Infinity*, [2002.02448](#).



## Acknowledgments

First and foremost, I would like to thank Prof. Suvrat Raju for the opportunity to work on some of the most fascinating ideas in physics today. I am grateful for his remarkable patience and support. I have learned a lot from him and will continue to learn more in the future.

My interactions with members of the strings group at ICTS have been extremely helpful. I would like to thank Prof. Loganayagam for the string theory reading course and other helpful discussions. I joined the group with Chandan Jana and we learned a lot together, through numerous discussions. I would also like to thank Siddharth Prabhu, Chandramouli Chowdhury, Sudip Ghosh, Soumyadeep Chaudhuri, Junggi Yoon, and all other present and past members of the group.

I would like to thank all my collaborators, especially, Kyriakos Papadodimas, Alok Laddha, and Siddharth Prabhu, for illuminating discussions.

The ICTS administration is extremely efficient and helpful, and I thank them all. Jeeva and Madhulika have provided instant clarifications to a myriad of inquiries throughout my stay at ICTS. Irshad has always gone above and beyond to sort all sorts of IT problems. I would like to thank the cleaning, security, transport, sports complex, and canteen staff at ICTS for their service, which made each day easier.

I would like to thank my friends Rahul, Mukesh, Sumith, Chandan, and Ganga for making the stay at ICTS memorable.

My interest in physics stems from countless childhood discussions with my father. Apart from the fascination with physics, I hope to have assimilated a fraction of his values as well. My family has always been very loving, caring and supportive. My mother has always been overly proud and happy with little milestones, and my brother has been silently watchful. I dedicate my thesis to them.

I also dedicate my thesis to Prachi for her infinite affection and understanding. You have always been a source of motivation, encouragement as well as honest criticism. You challenge me to push myself and not be complacent. Somehow, even from thousands of miles away, you manage to provide perspective.



# Contents

<b>Publications</b>	<b>v</b>
<b>Acknowledgments</b>	<b>vii</b>
<b>1 Introduction</b>	<b>1</b>
1.1 Motivation and summary of results . . . . .	1
1.2 The black hole information paradox . . . . .	4
1.3 Structure of the thesis . . . . .	9
<b>2 Holographic encoding of information in quantum gravity</b>	<b>11</b>
2.1 Introduction . . . . .	11
2.2 Review of 4-dimensional asymptotically flat spacetimes . . . . .	13
2.2.1 Phase space and conserved charges . . . . .	15
2.2.2 The Hilbert space of massless excitations . . . . .	17
2.2.3 Algebra in the neighbourhood of a cut . . . . .	19
2.3 Holographic storage of information . . . . .	20
2.3.1 Information at the past of future null infinity . . . . .	21
2.3.2 The nested structure of information on cuts of null infinity . . . . .	26
2.3.3 Some comments . . . . .	29
2.4 Implications of holography for black hole information paradox . . . . .	32
2.4.1 A constant Page curve . . . . .	32
2.4.2 Strong subadditivity and cloning paradox . . . . .	36
2.5 Discussion . . . . .	36
<b>3 Critique of the fuzzball program</b>	<b>39</b>
3.1 Introduction . . . . .	39
3.2 A statistical-mechanics evaluation of the fuzzball program . . . . .	41
3.2.1 Some results from statistical mechanics . . . . .	41
3.2.2 Implications for the fuzzball program . . . . .	48

3.2.3	Indirect arguments for horizon structure . . . . .	57
3.3	Quantum aspects of the two-charge solutions . . . . .	59
3.3.1	One-point functions . . . . .	62
3.3.2	Fluctuations . . . . .	68
3.3.3	Analysis of the results . . . . .	75
3.4	Probing multi-charge solutions . . . . .	79
3.4.1	Review of the solution . . . . .	80
3.4.2	Physical quantities of interest . . . . .	81
3.4.3	Propagation of a massless scalar . . . . .	83
3.4.4	Energy gap . . . . .	86
3.4.5	Large $\gamma$ Wightman function and commutator . . . . .	88
3.4.6	Numerical verification . . . . .	91
3.4.7	Analysis of the result . . . . .	93
3.5	Discussion . . . . .	98
<b>4</b>	<b>Bound on thermal Wightman correlators</b>	<b>99</b>
4.1	Introduction . . . . .	99
4.2	Proof of the bound . . . . .	102
4.2.1	First part: on the analyticity domain of position-space thermal correlators . . . . .	103
4.2.2	Second part: decay of spacelike correlators . . . . .	106
4.2.3	Third part: an extremization problem . . . . .	107
4.3	Weakly coupled theories . . . . .	110
4.3.1	Two-point functions . . . . .	115
4.3.2	Three-point functions . . . . .	118
4.3.3	Higher-point functions . . . . .	122
4.4	Holographic theories . . . . .	125
4.4.1	Two-point functions . . . . .	126
4.4.2	Interactions and higher-point functions . . . . .	133
4.5	Discussion . . . . .	143
<b>5</b>	<b>A quantum test for strong cosmic censorship</b>	<b>145</b>
5.1	Introduction . . . . .	145
5.2	Entangled modes across a null surface . . . . .	149

5.3	The Reissner-Nordström black hole in AdS . . . . .	161
5.3.1	The classical geometry . . . . .	162
5.3.2	Quantum fields on the RN background . . . . .	164
5.3.3	Relationship between near-horizon modes and global modes . . . . .	166
5.3.4	Constraints on two-point functions . . . . .	168
5.3.5	Numerical results for the Reissner-Nordström black hole . . . . .	170
5.4	The BTZ black hole . . . . .	173
5.4.1	Classical geometry and propagation of fields . . . . .	174
5.4.2	Near-horizon modes and constraints from entanglement . . . . .	177
5.4.3	Checking the constraints on approaching the inner horizon . . . . .	180
5.4.4	Extending the field behind the inner horizon . . . . .	182
5.5	Discussion . . . . .	187
<b>6</b>	<b>Conclusions</b>	<b>191</b>
<b>A</b>	<b>Asymptotic charges as observables</b>	<b>193</b>
<b>B</b>	<b>Thermal perturbation theory</b>	<b>199</b>
<b>C</b>	<b>Scattering in the Reissner-Nordström geometry at large angular momenta</b>	<b>215</b>
	<b>References</b>	<b>221</b>



# Chapter 1

## Introduction

### 1.1 Motivation and summary of results

In the absence of a complete quantum mechanical understanding, careful analysis of the semiclassical theory offer surprisingly deep lessons and insights into the working of gravity. Intuitions from quantum field theories in *fixed* background can often break down once we allow the geometry to *fluctuate*. A lack of understanding of these subtleties can lead to apparent inconsistencies and paradoxes, such as the black hole information paradox.

One of the key results of this thesis is the *holographic* storage of information in a theory of quantum gravity in asymptotically flat spacetimes. The *holographic principle* refers to the proposition that in gravity the true quantum degrees of freedom in a region are encoded in its boundary. This expectation stems from the fact that the entropy of a black hole is proportional to the area [1], and not the volume, of the *event horizon*. The most explicit and well understood realization of the holographic principle comes from string theory. The anti-de-Sitter space/conformal field theory conjecture [2, 3, 4], or AdS/CFT for short, suggests that quantum gravity in asymptotically AdS spacetimes is dual to a non-gravitational field theory in one lower dimension. Although this explicit realization is built from string theory, we would argue that we do not need detailed high energy structure of gravity to indicate holography. A semiclassical analysis is enough to show that any reasonable theory of quantum gravity must be holographic.

To be precise, we show that in a theory of quantum gravity in 4-dimensional asymptotically flat spacetimes, all operators on the future null infinity ( $\mathcal{I}^+$ ) can be approximated by an operator in the neighbourhood of the past boundary of future null infinity ( $\mathcal{I}_-^+$ ), with arbitrary precision [5]. This suggests that the quantum

degrees of freedom in gravity are holographic. This leads to a complete breakdown of *locality*. As  $\mathcal{I}^+$  is a Cauchy slice, operators which do not have overlapping support would commute, in a local theory. Even in gauge theories, we can define gauge invariant operators localized in an interval of  $\mathcal{I}^+$ , that commute with all operators which have no support on the interval. However, in gravity, no operator defined over any interval of  $\mathcal{I}^+$  commutes with all operators near  $\mathcal{I}_-^+$ .

The holographic encoding of degrees of freedom implies that all information about the quantum state is always available at the boundary. So, any excitation in some bounded region can be detected from the boundary, instantaneously. This is not surprising, if we take seriously the notion of holography. As the boundary degrees of freedom already encode all degrees of freedom, including those in the bounded region, quantum state in some region cannot be changed independently of the quantum state near the boundary. This has immediate implications for the black hole information paradox (see section 1.2 for an introduction to the information paradox). In particular, the notion of information escaping from the black hole is unfounded, as all information about the quantum state is always available at the boundary. As we discuss in detail later, this resolves many of the paradoxes associated with black holes which are based on the incorrect premise of locality.

Our results only rely on simple assumptions about the low energy sector of the theory, motivated from the semiclassical analysis. One of the physical feature responsible for such an identification of degrees of freedom is the access to all charges and the Hamiltonian, at  $\mathcal{I}_-^+$ . This ensures that a vacuum state can be identified through measurements in the neighbourhood of  $\mathcal{I}_-^+$ . Such a result can never hold in usual quantum field theories, where Hamiltonian is an integral over the full Cauchy slice. Related results for asymptotically AdS spacetimes can be found in [6, 7]. The analysis in flat space is more intricate due to the presence of infinitely many conserved charges [8] that render the vacuum degenerate.

Over the years, various resolutions have been proposed for the black hole information paradox. One such proposal is the *fuzzball* proposal [9]. Fuzzballs are smooth solutions in higher dimensional supergravity theories that have same charges as black holes, but no horizons. The size of compact directions, in these geometries, shrink to zero at a distance larger than the radius of corresponding black hole horizon. The fuzzball proposal posits that classical fuzzball geometries parameterize the phase

space of black hole microstates. If true, the fuzzball proposal would have two immediate implications. First, it would account for the entropy of black holes. Second, it would suggest that typical microstates of black holes do not have a horizon, hence, bypassing the information paradox. However, this proposal has not been realized for any macroscopic black hole yet.

In [10] we undertook a statistical analysis of the fuzzball program. We argued that a typical fuzzball geometry can only differ from the conventional black hole geometry at a Planck scale distance from the horizon. This can happen only if such geometries explicitly contain Planck scale structures by introducing a length scale which is at most of the order of Planck scale. However these length scales receive quantum corrections of the same order. These quantum fluctuations render the classical geometry unreliable. Hence, it is fallacious to conclude that typical black hole microstates do not have a horizon. As an explicit check, we studied fuzzball solutions obtained in [11, 12] and quantized in [13]. These solutions are dual to a microscopic black hole of zero horizon radius. We computed the fluctuations in the geometry of typical fuzzball solutions and showed that fluctuations were indeed large close to the horizon. We also studied fuzzball solutions in the context of AdS/CFT correspondence to provide further evidence to our assertion that fuzzballs do not appear to be relevant for the black hole information paradox.

In [14], we proved a *universal* bound on  $n$ -point thermal Wightman functions in any relativistic quantum field theory. In the limit when the momenta are large and spacelike, that is frequencies are much smaller than spatial momenta, thermal Wightman functions decay exponentially. The exponent is bounded by a universal geometric quantity that depends only on the temperature and spatial momenta of the operators in the correlation functions. We explored this bound in perturbative quantum field theories and strongly coupled holographic theories. A special case of such a bound was used in [10] to demonstrate the difference between fuzzball geometries and black holes.

Application of semiclassical techniques can be useful in providing answers to other fundamental questions about gravity. It is a long-lasting problem to understand whether or not gravity is deterministic. This problem is especially acute for black holes with multiple horizons, such as Kerr-black holes or Reissner Nordström black holes. Such black holes have an inner horizon, which is also the boundary of space-

time beyond which the Cauchy problem is not well defined. That is why inner horizons are often known as *Cauchy horizons*. Initial conditions cannot fix the evolution of fields beyond the Cauchy horizon uniquely. Hence, a smooth Cauchy horizon could lead to a breakdown of determinism. To prevent such loss of determinism, it was conjectured that for generic initial data, maximal Cauchy development should be complete. This is a formulation of the *strong cosmic censorship* conjecture [15]. For black holes, the conjecture implies that generic perturbations should render inner horizons unstable. The validity of this conjecture has been a matter of much interest in recent years. However, most of the works on this issue have focused solely on classical perturbations. In [16], we developed a necessary quantum test for violation of the strong cosmic censorship conjecture. We used this test to demonstrate that Reissner Nordström black holes in anti-de-Sitter space do not violate the conjecture. We also studied BTZ black holes and found that our test did not rule out violations. We explored the constraints on extension of spacetime behind the inner horizon.

Before proceeding to the structure of the thesis, we provide a brief pedagogical introduction to the relevant aspects of the black hole information paradox.

## 1.2 The black hole information paradox

The study of quantum fields in the presence of a black hole reveals that they emit thermal radiation [17]. Such thermal radiation is an inevitable consequence of the assumption of a smooth horizon. Locally, the horizon is no different from any other region of spacetime. For large black holes, the strength of the gravitational field and tidal forces are small near the horizon. Hence, an astronaut crossing a horizon does not experience anything out of the ordinary. This is simply a consequence of Einstein's equivalence principle. As local gravitational effects are not arbitrarily large near the horizon, it is reasonable to expect that the experience of the astronaut would remain qualitatively the same, even after inclusion of quantum effects. This justifies the assumption of smoothness of the horizon. It is a general property of quantum field theories that smoothness entails entanglement. In particular, if a quantum state is smooth across a null surface, then degrees of freedom across the surface must be entangled [16]. Hence, if our measurements are restricted to one

side of the surface, the quantum state would appear to be mixed. This entanglement is the reason behind the Hawking radiation. It is important to realize that Hawking radiation alone does not accord special status to black hole horizons. Even in Minkowski space, if we restrict to observables on one side of any null surface, then we would perceive a similar thermal radiation. Such a restriction can be achieved by *choosing* to study only accelerated observers. Locally, the source of this radiation is identical to the source of the Hawking radiation, i.e., entanglement across a null surface. Hawking radiation can be viewed as a consequence of a quantum version of the equivalence principle. The global properties of a black hole spacetimes make Hawking radiation more *physical* as no observer outside the black hole can access all the degrees of freedom inside the black hole, if the theory is *local*. The temperature of the Hawking radiation is universal and depends only on the surface gravity at the horizon.

As the black hole radiates and shrinks, degrees of freedom inside the black hole gets more and more entangled with the degrees of freedom outside. However, a finite-size black hole only has a finite entropy. Eventually, the black hole would not have enough internal degrees of freedom to accommodate the large entanglement with the exterior. Hence, any more radiation out of the black hole must be entangled with early radiation. Entanglement between late and early radiation is necessary to get the Page curve of entanglement entropy between radiation and black holes [18, 19], which is required for a unitary evaporation process. However, this seems to be at odds with the assumption of smoothness of horizon, which requires the Hawking quanta to be entangled with degrees of freedom inside the black hole. This apparent inconsistency can be formalized into the strong subadditivity paradox [20].

We will briefly describe the Page curve and strong subadditivity paradox in this section.

### The page curve

Consider a collapsing shell in pure state that forms a black hole. We define the *radiation* to be the collection of all degrees of freedom restricted to the region outside the black hole. If the theory is local, then the full Hilbert space is a direct product of black hole subspace and radiation subspace. In what follows, we will assume that

such a factorization is possible<sup>1</sup>.

Initially, when the black hole is formed, there is no entanglement between the radiation and black hole. However, Hawking showed that black holes radiate. As discussed, this radiation is a consequence of entanglement across the horizon. Hence, as more and more Hawking quanta radiate, the black hole gets more and more entangled with the radiation. Hawking's calculations suggests that this should continue until the black hole evaporates completely and we are left with a gas of radiation with non-zero von-Neumann entropy. However, since the black hole has radiated away, the radiation is now the full quantum system. It seems that we started with a pure initial state and ended with a mixed final state. This is not possible in a unitary theory.

Violation of unitarity is subject to the purity of the final state of radiation. It is extremely complicated to determine whether or not a state picked from an ensemble is pure. A pure state can mimic a mixed state with corrections that are suppressed exponentially in entropy of the ensemble. Hence the question of purity of the final state of Hawking radiation cannot be answered in a usual perturbative analysis. Since Hawking's calculations are only perturbative, we cannot conclude that quantum gravity is not unitary.

However, if the black hole evaporation process is unitary, then the final state must be pure. Hence the entanglement entropy of radiation must go to zero when the black hole completely evaporates. This suggests that the entanglement entropy of radiation should follow the Page curve [18, 19], Figure 1.1. The time at which the Page curve reaches the maxima is called the Page time.

### The strong subadditivity paradox

The Page curve immediately leads to a paradox that cannot be resolved by invoking small corrections. Consider the Penrose diagram of an evaporating black hole in Figure 1.2. The Cauchy slice  $\Sigma$  represents a late time slice, i.e., after Page time. We have divided the Cauchy slice into three sub-regions. The region  $A$  corresponds to the black hole.  $B$  is some region very close to the horizon, which contains all the radiation escaping from the black hole at this instant. Finally region  $C$  contains

---

<sup>1</sup>One of the main result of this thesis is that such a factorization is not possible. However, this assumption is implicit in the formulation of the black hole information paradox.

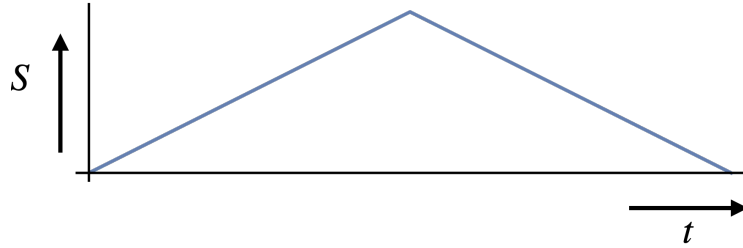


Figure 1.1: *The Page curve of black hole radiation.* Entanglement entropy of radiation as a function of time. If unitarity is respected, then the entanglement entropy of radiation must go to zero once the black hole completely evaporates.

the earlier radiation. Unitarity requires the degrees of freedom in region  $B$  to be entangled with  $C$ . That is,

$$S_{BC} < S_C. \quad (1.1)$$

However, if the horizon is smooth, then  $A$  must be entangled with  $B$ ,

$$S_{BA} < S_A. \quad (1.2)$$

So,  $B$  is entangled with both  $A$  and  $C$ . This violates the monogamy of entanglement. More precisely, the equations above are in contradiction with the following property of entanglement entropy, known as the strong subadditivity.

$$S_{BA} + S_{BC} \geq S_A + S_C. \quad (1.3)$$

This is known as the strong subadditivity paradox and this cannot be resolved via small corrections [20].

A related paradox is the cloning paradox. Unitarity can be preserved only if all information about the quantum state can be retrieved from Hawking radiation. However, consider a Cauchy slice that intersects with an observer that has fallen into the black hole and also collects most of the Hawking radiation, Figure 1.3. Then the information about the observer can be determined from the interior of the black hole, as well as Hawking radiation. It seems that quantum information has been

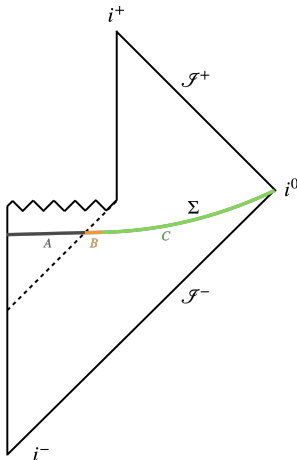


Figure 1.2: *Strong subadditivity paradox*: The Penrose diagram of an evaporating black hole in flat space.  $\Sigma$  depicts a slice at a time later than the Page time. Smooth horizon requires  $B$  to be entangled with  $A$ . Unitarity requires  $B$  to be entangled with  $C$ . This violates the monogamy of entanglement.

cloned, which is not possible in a quantum theory.

This suggests that *not all* of the following statements can be correct in a theory of quantum gravity.

1. Black holes have an interior.
2. Black holes have a smooth horizon.
3. Black holes evaporate completely.
4. Black hole evaporation is unitary.
5. Quantum gravity is local.

Various proposed resolutions have focused on various of these assumptions. For instance, the fuzzball proposal [21] suggests that black holes have no horizon and interior. The firewall proposal [22] suggests that the horizon is not smooth. Instead, an infalling observer experiences an infinite flux of radiation. Planck scale remnants of the evaporation process have been proposed. Even loss of unitarity has been considered.

However, the most overlooked assumption is that of locality. In [5] we demonstrated that the last item in the above list is an *incorrect* assumption. Careful

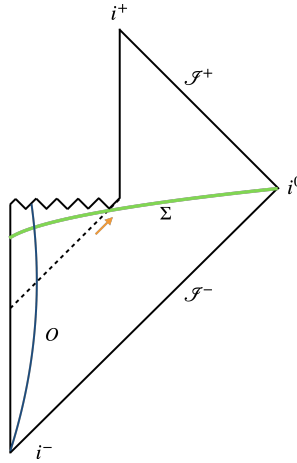


Figure 1.3: *Cloning paradox*: The Cauchy slice  $\Sigma$  intersects the observer  $O$  inside the black hole. It also collects a large fraction of the Hawking radiation. If the evaporation process is unitary, then the information about  $O$  can also be retrieved from the radiation. This is in violation of quantum mechanics, which prohibits cloning of information.

analysis of semiclassical gravity forces us to conclude that quantum gravity is holographic. Holography is a feature of quantum gravity, and not a choice. This feature immediately resolves the strong subadditivity paradox and the cloning paradox, as we will explore in chapter 2.

### 1.3 Structure of the thesis

In chapter 2, based on [5], we argue for holographic storage of information in quantum gravity in asymptotically flat spacetimes. We detail the implications of holography, especially for the black hole information paradox.

In chapter 3, based on [10], we explore the fuzzball resolution to the information paradox. We argue that fuzzballs may not be relevant for the black hole information paradox. We study study explicit fuzzball solutions to support our contention.

In chapter 4, based on [14], we describe and prove a universal bound on thermal Wightman correlators in the limit when momenta are large and spacelike. We study this bound in perturbative quantum field theories and holographic theories.

In chapter 5, based on [16], we show that a quantum state across a null surface can be smooth only if degrees of freedom across the surface are entangled and use

this to develop a test for strong cosmic censorship conjecture. We implement the test for Reissner Nordström black holes in anti-de-Sitter spacetime and BTZ black holes. We also mention some constraints on extension of spacetime beyond the inner horizon.

In chapter 6, we summarize the thesis and end with some open problems and future directions.

## Chapter 2

# Holographic encoding of information in quantum gravity

### 2.1 Introduction

As discussed in chapter 1, it is often expected that quantum gravity is holographic, i.e., it can be described by a lower dimensional theory in absence of gravity. Can we better understand holography without invoking detailed structure of the *ultraviolet completion* of quantum gravity? Holography implies that it should be possible to embed all degrees of freedom in a codimension-1 surface, in quantum gravity. Hence, a necessary first step towards answering this question is to show that any theory of gravity must encode quantum information holographically.

Over the past two decades, holography in asymptotically AdS spacetimes has been explored extensively. The AdS/CFT conjecture [2, 3, 4], motivated by string theory, suggests that quantum gravity in asymptotically AdS spacetimes can be described by a lower dimensional conformal field theory. The operators in the dual conformal field theory are related to asymptotic operators in AdS through the extrapolate dictionary [23]. This suggests that the gravity degrees of freedom indeed resides in the boundary of the AdS. The holographic nature of gravity can be inferred even without invoking the AdS/CFT conjecture. In [6, 7] it was demonstrated that any two quantum states distinguishable by a localized operator anywhere on some Cauchy slice, can also be distinguished by an operator localized near the boundary of the same slice, without relying on the details of the high energy structure of the theory. This suggests that all information in a quantum theory of gravity in asymptotically AdS spacetimes is contained in the boundary.

The aim of this chapter is to explore holographic storage of information in asymptotically flat spacetimes. A lot of work has been devoted to understanding holo-

raphy in flat space [24], however, unlike in AdS, our understanding of holography in flat spacetimes remain primitive. There is no counter part of AdS/CFT correspondence for flat space, yet. Hence, the question of understanding holography without reference to string theory, or any other completion of gravity, is of immense importance.

In this chapter, based on [5], we argue that the following statements hold in a theory of quantum gravity in 4-dimensional asymptotically flat spacetimes.

1. All operators on the future null infinity,  $\mathcal{I}^+$ , can be approximated by an operator in a neighbourhood of the past boundary of future null infinity,  $\mathcal{I}_-^+$ , with arbitrary precision.
2. On future null infinity, all operators to the future of a cut can be approximated by an operator in a neighbourhood of the cut, with arbitrary precision.

Precisely analogous statements hold for past null infinity,  $\mathcal{I}^-$ . All operators on past null infinity,  $\mathcal{I}^-$ , can be approximated by operators in a neighbourhood of the future boundary of past null infinity,  $\mathcal{I}_+^-$ . Also, all operators to the past of a cut can be approximated by an operator in a neighbourhood of the cut. These statements elucidate the holographic encoding of degrees of freedom in quantum gravity. Result (1) suggests that all information about massless particles can be obtained from measurements near the past boundary of future null infinity. Result (2) suggests a nested structure of storage of information on  $\mathcal{I}^+$ . A cut of null infinity contains all information to the future of the cut. These results are in contrast with the intuition from local quantum field theories, where operators with non-overlapping support on  $\mathcal{I}^+$  commute.

To get result (1), we assume that in the full UV complete theory, there are operators in a neighbourhood of  $\mathcal{I}_-^+$  can identify the vacua and map any vacua to any other. We also assume that the Hamiltonian in the full theory is bounded from below. In the semiclassical gravity, all asymptotic charges and the Hamiltonian are boundary observables. Hence, the assumptions about the vacua are valid in semiclassical gravity. Moreover, as these assumptions pertain to the low energy structure of the theory, we expect any reasonable UV completion to preserve this feature. It should be noted that Hamiltonian is a boundary observable only in a theory of gravity. Hence, result (1) does not hold in usual quantum field theories, including gauge

theories.

The stronger result (2) assumes that certain commutation relation in semiclassical gravity are corrected only by local terms in the full theory. This assumption is valid to all orders in perturbation theory.

The holographic encoding of information has important implications for the information paradox. It immediately resolves the strong subadditivity paradox reviewed in section 1.2. Moreover, as we explain in detail below, our results imply that the often discussed Page curve of entanglement entropy is not the correct expectation. Since all information of the quantum state, including that of the degrees of freedom inside the black hole, is always available at the boundary, the correct Page curve should be a constant. The notion of information escaping the black hole through the Hawking radiation is based on the incorrect assumption of locality, and leads to apparent paradoxes.

In section 2.2, we review some results from the quantization of 4-dimensional asymptotically flat spacetimes. In section 2.3 we prove the holographic storage of information. In section 2.4 we list some implications of holography, especially for the black hole information paradox. Finally, in section 2.5 we end the chapter with some concluding remarks.

## 2.2 Review of 4-dimensional asymptotically flat spacetimes

The objective of this section is to review aspects of quantum gravity in asymptotically flat spacetimes relevant for us. This has been subject to extensive study and we refer the readers to review articles [25, 26] for details and further references. In [27] it was noted that the symplectic structure of the *full nonlinear theory* takes a remarkably simple form when the phase space is parameterized by data on null infinity. Upon quantization, this structure leads to a Hilbert space that is the direct sum of an infinite number of “soft” sectors, and this has received renewed attention in light of the conservation laws associated to BMS symmetry [8, 28, 29].

In order to study quantum gravity in asymptotically flat spacetimes, we need to first define the phase space. The space of all asymptotically flat space-times can be parameterized in terms of the retarded *Bondi* [30] co-ordinates ( $u = t - r$ ,  $r$ ,  $\Omega =$

$(\theta, \phi)$  as

$$\begin{aligned}
 ds^2 = & - du^2 - 2dudr + r^2\gamma_{AB}d\Omega^A d\Omega^B \\
 & + rC_{AB}d\Omega^A d\Omega^B + \frac{2m_B}{r}du^2 + \gamma^{DA}D_D C_{AB}dud\Omega^B + \dots,
 \end{aligned} \tag{2.1}$$

where  $\gamma_{AB}$  is the unit metric on  $S^2$ , with the corresponding derivative operator  $D_A$ .  $C_{AB}(u, \Omega)$  is known as the shear field and contains complete information about the radiative degrees of freedom. In the Bondi frame,  $C_{AB}$  is trace free,  $\gamma^{AB}C_{AB} = 0$ . This radiative data, in fact, ‘‘lives at’’ future null infinity  $\mathcal{I}^+ := S^2 \times \mathbf{R}$  with coordinates  $(\Omega, u)$ . Viewed in this way,  $S^2$  is a sphere at null infinity with the intrinsic metric  $\gamma_{AB}$ , and is known as the celestial sphere. We will denote the  $S^2$  that lives at  $u \rightarrow -\infty$  by  $\mathcal{I}^-$ .  $m_B(u, \Omega^A)$  is called the Bondi mass aspect. In our analysis, we allow inclusion of massless matter fields, for example scalar field  $\phi(r, u, \Omega)$ . We define  $O(u, \Omega) = \lim_{r \rightarrow \infty} r\phi(r, u, \Omega)$ .

The components of the metric and the matter fields at null infinity are not all independent. The rate of change of the Bondi mass aspect  $m_B(u, \Omega)$  is determined in terms of the radiative data via the following constraint

$$\partial_u m_B = \frac{1}{4}\partial_u D^A D^B C_{AB} - \frac{1}{8}N_{AB}N^{AB} - 4\pi G T_{uu}^{M(0)}, \tag{2.2}$$

where  $N_{AB} = \partial_u C_{AB}$  is known as the Bondi news tensor.  $T_{uu}^{M(0)}$  is the leading  $\frac{1}{r^2}$  coefficient of the matter stress tensor  $T_{uu}^{M(0)} = \lim_{r \rightarrow \infty} r^2 T_{uu}^M$ . It is a function of the radiative data for the matter fields. In the case of the scalar field,  $T_{uu}^{M(0)} = \frac{1}{2}\partial_u \mathcal{O} \partial_u \mathcal{O}$ . From eqn.(2.2), we see that  $m_B(u, \Omega)$  is determined in terms of radiative data and the integration constant  $m_B(u = -\infty, \Omega)$ .

The symmetries associated with gravity in asymptotically flat spacetimes are an infinite dimensional group of supertranslations<sup>1</sup> [30, 31], generated by vector fields,

$$\zeta = f(\Omega)\partial_u - \frac{1}{r}D^A f(\Omega)\partial_A + \frac{1}{2}D^A D_A f(\Omega)\partial_r + \dots, \tag{2.3}$$

where  $f$  is some function on the sphere. Action of supertranslation on fields can be obtained by Lie-derivatives along the generator,  $\zeta$ . For instance, the shear trans-

---

<sup>1</sup>We will label the vacua only by their supertranslation charges. Superrotations may further refine the vacuum structure, however, our analysis will remain unaffected.

forms as,

$$\mathcal{L}_\zeta C_{AB}(u, \Omega) = f(\Omega) \partial_u C_{AB}(u, \Omega) - 2(D_A D_B f(\Omega))^{\text{TF}}, \quad (2.4)$$

where TF denotes the trace free component of a tensor,  $T_{AB}^{\text{TF}} = T_{AB} - \gamma_{AB} T_C^C$ .

The integration constant,  $m_B(u = -\infty, \Omega)$ , can be used to define infinitely many conserved charges by smearing with functions on the sphere,

$$\mathcal{Q}_{\ell, m} = \frac{1}{4\pi G} \int \sqrt{\gamma} d^2\Omega m_B(u = -\infty, \Omega) Y_{\ell, m}(\Omega). \quad (2.5)$$

These are called the *supertranslation charges* as they will turn out to be the generators of supertranslations (2.4). To see how, we need to analyze the symplectic structure. The charge with  $\ell = m = 0$  is the Bondi mass at  $u \rightarrow -\infty$ , and it was shown in [32] that this coincides with the standard ADM Hamiltonian [33].

### 2.2.1 Phase space and conserved charges

It was shown by [34] that the space of free data  $C_{AB}(u, \Omega)$  is the radiative phase space of gravity in which the fall-off conditions on the shear field are given by

$$C_{AB}(u, \Omega)|_{u \rightarrow \pm\infty} = C_{AB}^{(0)\pm}(\Omega) + O\left(\frac{1}{|u|^\delta}\right), \quad (2.6)$$

with  $\delta > 0$ . It was also shown in [34] that the Poisson bracket structure of the radiative data at  $\mathcal{I}^+$  is given by,

$$\begin{aligned} \{N_{AB}(u, \Omega), C_{MN}(u', \Omega')\} &= -16\pi G \delta(u - u') \frac{1}{\sqrt{\gamma}} \delta^2(\Omega - \Omega') \\ &\times \left[ \gamma_{A(M} \gamma_{N)B} - \frac{1}{2} \gamma_{AB} \gamma_{MN} \right]. \end{aligned} \quad (2.7)$$

The phase space of the full non-linear theory trivializes on  $\mathcal{I}^+$  and is generated by free fields. However, as noted earlier, the fields are related by the constraint (2.2). Using these results, we can now demonstrate that  $\mathcal{Q}_{\ell, m}$  in (2.5) are indeed the supertranslation charges. To see this, we first integrate the constraint (2.2) to get,

$$m_B(u = -\infty, \Omega) = -\frac{1}{4} \int_{-\infty}^{\infty} du \left[ -D^A D^B N_{AB} + \frac{1}{2} N_{AB} N^{AB} + 16\pi G T_{uu}^{\text{M}(0)} \right]. \quad (2.8)$$

The boundary term at the future of future null infinity,  $\mathcal{I}_+^+$ , can be set to zero in the absence of massive excitations<sup>2</sup>, which reach time-like infinity. The supertranslation charges can then be written as a sum of two terms,

$$\mathcal{Q}_{\ell,m} = \mathcal{Q}_{\ell,m}^{\text{soft}} + \mathcal{Q}_{\ell,m}^{\text{hard}}, \quad (2.9)$$

where,

$$\begin{aligned} \mathcal{Q}_{\ell,m}^{\text{soft}} &= \frac{1}{16\pi G} \int_{-\infty}^{\infty} du d^2\Omega \sqrt{\gamma} Y_{\ell,m}(\Omega) [ D^A D^B N_{AB} ], \\ \mathcal{Q}_{\ell,m}^{\text{hard}} &= -\frac{1}{16\pi G} \int_{-\infty}^{\infty} du d^2\Omega \sqrt{\gamma} Y_{\ell,m}(\Omega) \left[ \frac{1}{2} N_{AB} N^{AB} + 16\pi G T_{uu}^{\text{M}(0)} \right]. \end{aligned} \quad (2.10)$$

The soft charge is generated by “zero mode” of the news tensor given by,

$$\lim_{\omega \rightarrow 0} \int_{-\infty}^{\infty} du e^{-i\omega u} N_{AB}(u, \Omega) =: \lim_{\omega \rightarrow 0} \tilde{N}_{AB}(\omega, \Omega), \quad (2.11)$$

and the hard charge depends on the total (gravitational and matter) stress tensor at  $\mathcal{I}^+$ . The action of supertranslation charges on various fields can be determined from the symplectic structure. For instance, the action on shear is,

$$\{C_{MN}(u, \Omega), \mathcal{Q}_{\ell,m}\} = Y_{\ell,m}(\Omega) \partial_u C_{MN}(u, \Omega) - 2(D_M D_N Y_{\ell,m}(\Omega))^{\text{TF}}. \quad (2.12)$$

This precisely matches with the transformation of shear under supertranslations (2.4), hence justifying the name.

## Quantization

The theory can be quantized by promoting the Poisson brackets to commutators. The elementary operators in the theory are the News tensor  $N_{AB}$ . This approach to quantization of gravity in 4-dimensional asymptotically flat spacetimes is known

---

<sup>2</sup>In this chapter, we only consider massless excitations. However, we believe that these arguments can be generalized to include massive excitations as well.

as the asymptotic quantization program [27, 35, 36].

$$\begin{aligned}
 [ N_{AB}(u, \Omega), N_{CD}(u', \Omega') ] &= i16\pi G \partial_u \delta(u - u') \frac{1}{\sqrt{\gamma}} \delta^2(\Omega - \Omega') \\
 & \quad [ \gamma_{A(C} \gamma_{D)B} - \frac{1}{2} \gamma_{AB} \gamma_{CD} ].
 \end{aligned} \tag{2.13}$$

One can also define the algebra generated by the shear operators and the zero mode of the news  $N_{AB}^{(0)}(\Omega') = \int du N_{AB}(u, \Omega')$  as [36, 25, 28]

$$\begin{aligned}
 [ C_{AB}(u, \Omega), C_{CD}(u', \Omega') ] &= -i8\pi G \Theta(u - u') \frac{1}{\sqrt{\gamma}} \delta^2(\Omega - \Omega') \\
 & \quad [ \gamma_{A(C} \gamma_{D)B} - \frac{1}{2} \gamma_{AB} \gamma_{CD} ],
 \end{aligned} \tag{2.14}$$

where  $\Theta(x) = \text{sign}(x)$ .

### 2.2.2 The Hilbert space of massless excitations

News tensor and matter fields can be decomposed into positive and negative frequencies to define “creation” and “annihilation” operators,

$$\begin{aligned}
 \tilde{N}_{AB}^{\pm}(\omega, \Omega) &= \int du e^{\pm i\omega u} N_{AB}(u, \Omega); \\
 \tilde{O}^{\pm}(\omega, \Omega) &= \int du e^{\pm i\omega u} O(u, \Omega),
 \end{aligned} \tag{2.15}$$

The positive frequency part of matter fields and News tensor would annihilate the vacuum. However, this is not sufficient to fix the vacuum completely. Action of the soft modes of News tensor must be specified. This can be done by specifying the eigenvalue under all supertranslations.

$$\mathcal{Q}_{\ell, m} |\{s\}\rangle = s_{\ell, m} |\{s\}\rangle. \tag{2.16}$$

This eigenvalue is also the eigenvalue of the “soft” part of the supertranslation charge, since the “hard” part annihilates all the vacua. So, the set of all possible vacua are given by specifying a (countably) infinite set of real numbers  $s_{\ell, m}$ . The vacua,  $|\{s\}\rangle$ ,

are normalized such that,

$$\langle \{s\} | \{s'\} \rangle = \prod_{\ell, m} \delta(s_{\ell, m} - s'_{\ell, m}). \quad (2.17)$$

On top of *each* such vacuum, one can construct a Fock space comprising the states

$$\mathcal{H}_{\{s\}} = \text{span of } \{N(f_1)N(f_2) \dots N(f_n)O(h_1) \dots O(h_m)\} | \{s\}, \quad (2.18)$$

where  $f_1^{AB}(u, \Omega) \dots f_n^{AB}(u, \Omega)$  and  $h_1(u, \Omega) \dots h_m(u, \Omega)$  are test functions on  $\mathbf{R} \times S^2$  and

$$\begin{aligned} N(f_i) &\equiv \int \sqrt{\gamma} N_{AB}(u, \Omega) f_i^{AB}(u, \Omega) du d^2\Omega, \\ O(h_i) &\equiv \int \sqrt{\gamma} O(u, \Omega) h_i(u, \Omega) du d^2\Omega. \end{aligned} \quad (2.19)$$

Each such space gives an irreducible representation of the algebra of news operators and of the massless matter fields. But the full Hilbert space is obtained by taking the *direct sum* of all of these Hilbert spaces

$$\mathcal{H} = \bigoplus_{\{s\}} \mathcal{H}_{\{s\}}, \quad (2.20)$$

where the sum is over all possible values of all soft charges.

We now show that the full Hilbert space is closed under the action of all operators in the theory. From the definition of the Hilbert space, it is evident that the action of news tensor and matter fields do not generate any new state. As shear can be obtained from the news tensor, up to a  $u$ -independent function, we only need to consider the action of constant shear mode,  $C_{AB}^{(0)}(\Omega)$  on a soft vacua,

$$e^{-\frac{i}{2} \int \sqrt{\gamma} F^{AB}(\Omega) C_{AB}^{(0)}(\Omega) d^2\Omega} | \{s\} \rangle = | \{s'\} \rangle, \quad (2.21)$$

where

$$s'_{\ell, m} = s_{\ell, m} + \int \sqrt{\gamma} F^{AB}(\Omega) \left( D_A D_B - \frac{1}{2} \ell(\ell + 1) \gamma_{AB} \right) Y_{\ell, m}(\Omega) d^2\Omega. \quad (2.22)$$

Clearly, constant shear mode does not generate any new state. We also note that the action of constant shear mode is *irreducible* on the Hilbert space,  $\mathcal{H}$ . This operator can map any soft sector to any other. This point would be crucial to our analysis later.

The only other operator in the theory is the Bondi mass aspect,  $m_B$ . However, the action of  $m_B$  is completely fixed by the action of other operators using the constraint Eq. (2.2). Hence, Bondi mass aspect maps states in  $\mathcal{H}$  to another state in the same Hilbert space. This shows that the Hilbert space  $\mathcal{H}$  is closed under action of all operators.

In our analysis, we only restrict attention to massless excitations. However, inclusion of massive particles would not invalidate our results as the Hilbert space of massive modes is independent of the Hilbert space  $\mathcal{H}$ .

Also, we have labeled the vacua only by their supertranslation soft charges, recent studies in asymptotic symmetries indicate that the so-called superrotation soft charges commute with the supertranslation soft charges [37], and this may further refine the vacuum structure of the theory. As we explain below, our analysis will not be affected by such refinements, and so, for the sake of simplicity in presentation, we restrict our vacuum-labels to supertranslations.

To avoid any confusion we make the following definition.

**Definition 1.** *The Hilbert space of massless particles,  $\mathcal{H}$ , refers to the space obtained by starting with all possible vacua, exciting each vacuum with operators on  $\mathcal{I}^+$  and then taking the span of all states so obtained.*

In the semiclassical theory, this leads to the space described by Eqn. (2.20) but the definition above holds generally.

### 2.2.3 Algebra in the neighbourhood of a cut

We denote by  $A(\mathcal{I}^+)$ , the set of all operators on future null infinity. We are especially interested in the algebra of operators on a cut of null infinity, which we define now.

**Definition 2.** *The algebra associated with an  $\epsilon$ -neighbourhood of a cut  $u_0$  is denoted by  $\mathcal{A}_{u_0, \epsilon}$  and consists of all possible functions of asymptotic operators with a  $u$ -coordinate lying in  $(u_0, u_0 + \epsilon)$ .*

The algebra  $\mathcal{A}_{u_0, \epsilon}$  comprises of all functions of operators  $m_B(u, \Omega)$ ,  $C_{AB}(u, \Omega)$ , and the massless matter fields collectively denoted as  $O(u, \Omega)$ , such that  $u \in (u_0, u_0 + \epsilon)$  and  $\Omega$  ranges over the entire celestial sphere<sup>3</sup>. For instance some of the lowest order polynomials that are elements of  $\mathcal{A}_{u_0, \epsilon}$  are

$$\begin{aligned} \mathcal{A}_{u_0, \epsilon} = \{ & m_B(u_1, \Omega), C_{AB}(u_1, \Omega_1), O(u_1, \Omega_1), m_B(u_1, \Omega_1)C_{AB}(u_2, \Omega_2), \\ & m_B(u_1, \Omega_1)O(u_2, \Omega_2), C_{AB}(u_1, \Omega_1)O(u_2, \Omega_2), O(u_1, \Omega_1)O(u_2, \Omega_2) \dots \}, \end{aligned} \quad (2.23)$$

where  $u_i \in (u_0, u_0 + \epsilon)$ .

As is standard in the analysis of algebras in quantum field theory, our algebra includes polynomials and other functions constructed out of the elementary operators as well as their spectral projections<sup>4</sup>. Indeed, the spectral projections can themselves be obtained just as limits of functions of the operators.

Finally an important special case of the definition above is the algebra obtained near the boundary of null infinity.

**Definition 3.** *The algebra near the past boundary of future null infinity,  $\mathcal{A}_{-\infty, \epsilon}$  is the set of all functions of operators on  $\mathcal{I}^+$  with  $u$ -coordinate in  $(-\infty, -\frac{1}{\epsilon})$ .*

## 2.3 Holographic storage of information

Having established the framework, we now turn to the main results of this chapter. The results, stated and proved in this section, are based on reasonable assumptions about the UV complete theory that are motivated from the low energy structure of the theory, discussed in section 2.2. We will detail and justify the assumptions below. Result (2.1) is a special case of result (2.2), and is based on more conservative assumptions.

---

<sup>3</sup>It was argued in [38] that the Bondi mass may not be observable because, taking a naive limit of the bulk metric as  $r \rightarrow \infty$  seems to lead to an operator with large quantum fluctuations. However, as we explain in appendix A, if the limit is taken carefully, these quantum fluctuations do not appear.

<sup>4</sup>Spectral projection corresponding to eigenvalue  $\lambda$  of an operator  $A$  is the orthogonal projection on the kernel of  $A - \lambda I$ .

### 2.3.1 Information at the past of future null infinity

In line with our motivation of understanding holography from semiclassical analysis, the first result shows how all degrees of freedom in quantum gravity in 4-dimensional asymptotically flat spacetimes are encoded in the boundary.

**Result 2.1.** *Consider any operator on future null infinity,  $A \in A(\mathcal{I}^+)$ . There exists an operator near the past boundary of future null infinity,  $\tilde{A} \in \mathcal{A}_{-\infty, \epsilon}$ , such that*

$$A \doteq \tilde{A},$$

where  $\doteq$  denotes equality of at the level of matrix elements. That is,

$$\langle \Psi_1 | A | \Psi_2 \rangle = \langle \Psi_1 | \tilde{A} | \Psi_2 \rangle, \quad \forall \psi_i \in \mathcal{H}.$$

Loosely, result (2.1) implies that the algebra near the past boundary contains all operators in the theory; or more precisely,

$$\mathcal{A}_{-\infty, \epsilon} \doteq A(\mathcal{I}^+). \tag{2.24}$$

The following corollary is immediately implied by result (2.1).

**Corollary 2.1.1.** *Any two distinct states in the Hilbert space of massless particles can be distinguished just by observables in an infinitesimal neighbourhood of  $\mathcal{I}_-^+$ .*

Suppose two states,  $|\Psi_1\rangle$  and  $|\Psi_2\rangle$  can be distinguished by an operator on future null infinity,  $A$ , i.e.,  $\langle \Psi_1 | A | \Psi_1 \rangle \neq \langle \Psi_2 | A | \Psi_2 \rangle$ . Then, as a consequence of result (2.1), these states can also be distinguished by an operator near the past of future null infinity,  $\tilde{A} \in \mathcal{A}_{-\infty, \epsilon}$ . Hence, all information is encoded holographically.

Now, we will state and justify the assumptions involved. The first two assumptions pertain to the low energy structure of the theory.

**Assumption 2.1.1.** *The vacua in the full theory of quantum gravity can be completely identified by the values of operators near  $\mathcal{I}_-^+$*

**Assumption 2.1.2.** *All operators that map the space of vacua back to itself are contained in  $\mathcal{A}_{-\infty, \epsilon}$ .*

We now explain the validity of these assumptions in the framework elaborated in section 2.2. As noted earlier, the vacua are labeled by eigen values of supertranslation charges. These charges are defined at the past boundary of future null infinity (2.5). However, note that, these charges alone cannot identify the vacua. We also need the ADM Hamiltonian, which once again is an element of  $\mathcal{A}_{-\infty,\epsilon}$ . Note that, if the vacua are labeled by additional charges, then our analysis would go through as long as those charges can be defined at  $\mathcal{I}_-^+$ <sup>5</sup>.

Recall that the algebra,  $\mathcal{A}_{-\infty,\epsilon}$ , also contain all projectors of operators. Hence, the projector onto the space of vacua is also an element of the algebra. The projector,  $P_0$ , can be expanded as,

$$P_0 = \int \left( \prod_{\ell,m} ds_{\ell,m} \right) |\{s\}\rangle\langle\{s\}| \in \mathcal{A}_{-\infty,\epsilon}. \quad (2.25)$$

Now we can perform a spectral decomposition for each supertranslation charge<sup>6</sup>

$$\mathcal{Q}_{\ell,m} = \int ds s \mathcal{P}_{\ell,m}[s]. \quad (2.26)$$

Now, this supertranslation charge includes both hard and soft parts but by multiplying the projector onto the space of vacua with an infinite product of  $\mathcal{P}_{\ell,m}[s]$  we can select a *specific soft vacuum*.

$$P_0 \prod_{\ell,m} \mathcal{P}_{\ell,m}[s_{\ell,m}] = |\{s\}\rangle\langle\{s\}| \in \mathcal{A}_{-\infty,\epsilon}. \quad (2.27)$$

Clearly, assumption (2.1.1) is justified in the framework of asymptotic quantization. To see validity of assumption (2.1.2), recall that the constant shear mode acts irreducibly on the Hilbert space  $\mathcal{H}$ . The action of shear, coupled with the projector

---

<sup>5</sup>This is true for additional superrotation charges discussed earlier.

<sup>6</sup>The vacuum projector can be constructed explicitly as a limit of a bounded functions on  $\mathcal{A}_{-\infty,\epsilon}$  through  $P_0 = \lim_{\alpha \rightarrow \infty} e^{-\alpha M(-\infty)}$ . The operator,  $\mathcal{P}_{\ell,m}[s]$ , which we use for ease of notation, selects a delta-function normalized state so it is not bounded. But the spectral projector onto any range of values of  $\mathcal{Q}_{\ell,m}$  can also be constructed as a limit of bounded functions on  $\mathcal{A}_{-\infty,\epsilon}$ :  $\int_s^{s'} \mathcal{P}_{\ell,m}[x] dx = \lim_{T \rightarrow \infty} \frac{1}{2\pi} \int_{-T}^T e^{i\theta \mathcal{Q}_{\ell,m}} \frac{e^{-i\theta s} - e^{-i\theta s'}}{i\theta} d\theta$ .

onto the space of vacua can map one vacua to any other vacua.

$$P_0 e^{-\frac{i}{2} \int_{-\infty}^{-\frac{1}{\epsilon}} \sqrt{\gamma} C_{AB}(u, \Omega) G^{AB}(u, \Omega) d^2 \Omega} |\{s\}\rangle = |\{s'\}\rangle, \quad (2.28)$$

where we see from (2.22) that

$$s'_{\ell, m} = s_{\ell, m} + \int_{-\infty}^{-\frac{1}{\epsilon}} du d^2 \Omega \sqrt{\gamma} G^{AB}(u, \Omega) \left( D_A D_B - \frac{1}{2} \ell(\ell + 1) \gamma_{AB} \right) Y_{\ell, m}(\Omega). \quad (2.29)$$

Since we can choose  $G$  to be arbitrary, we can attain any value of  $s'_{\ell, m}$  starting with a given value of  $s_{\ell, m}$ . Therefore, using operator from the algebra, one can not only select a particular vacuum but also cause transitions to any other vacuum.

$$T_{\{s\}, \{s'\}} = |\{s'\}\rangle \langle \{s\}| \in \mathcal{A}_{-\infty, \epsilon}. \quad (2.30)$$

So, in the canonical theory, any operator that maps the space of vacua back to itself can be written as a linear combination of the transition operators above.

Having justified the assumptions semi-classically, we note once again that these assumptions only pertain to the low energy structure of the theory. It is reasonable to expect that the full theory of quantum gravity would not modify the vacuum structure. Hence, we will extrapolate these assumptions to the full UV complete quantum gravity.

The final assumption that we require is stated below. Finally, we need a third physical assumption.

**Assumption 2.1.3.** *The spectrum of the Hamiltonian of the full theory of quantum gravity is bounded below.*

This seems, to us, to be a very natural assumption, and so we do not justify it any further. We merely note that the assumption above is weaker than any of the commonly used energy conditions since it says nothing about the local positivity of energy but merely about its global positivity. For convenience, we choose this lower bound to be 0 and simply assume, below, that the energy eigenvalues are positive.

The assumption (2.1.3) immediately leads to the following Lemma.

**Lemma 1.** *The Hilbert space  $\mathcal{H}$  can also be generated by starting with all possible*

*vacua and acting with operators from an infinitesimal neighbourhood of the the past of future null infinity.*

First consider the sector built on top of a particular vacuum as displayed in Eqn. (2.18) by smeared news and matter operators. What we need to prove is that all these states can be generated just by acting with operators near the past of future null infinity

$$\mathcal{H}_{\{s\}} = \text{span of } \{N(\tilde{f}_1)N(\tilde{f}_2)\dots N(\tilde{f}_n)O(\tilde{h}_1)\dots O(\tilde{h}_m)\}|\{s\}\rangle, \quad (2.31)$$

where the notation is the same as (2.19) except that  $\tilde{f}_i$  and  $\tilde{h}_i$  have support *only* for  $u \in (-\infty, -\frac{1}{\epsilon})$ . Note that this support is very different from the support of the functions  $f_i$  and  $h_i$  in equation (2.18) that could be the entire real line.

We will prove the statement via contradiction. Imagine that there exists a state,  $|\Psi_\perp\rangle$ , that belongs to the Hilbert space but is orthogonal to all states of the form above. This implies that whenever  $u_i \in (-\infty, -\frac{1}{\epsilon})$ , the following correlator vanishes.

$$\begin{aligned} \kappa(u_i) = \langle \Psi_\perp | N_{A_1 B_1}(u_1, \Omega_1) \dots N_{A_n B_n}(u_n, \Omega_n) \\ O(u_{n+1}, \Omega_{n+1}) \dots O(u_{n+m}, \Omega_{n+m}) | \{s\} \rangle = 0. \end{aligned} \quad (2.32)$$

We may now insert a complete set of eigenstates of the full Hamiltonian to evaluate the correlator above.

$$\kappa(u_i) = \sum_{E_i} \langle \Psi_\perp | N_{A_1 B_1}(0, \Omega_1) | E_1 \rangle \dots \langle E_{n+m-1} | O(0, \Omega_{n+m}) | \{s\} \rangle e^{i \sum_{i=1}^{n+m-1} E_i (u_{i+1} - u_i)}.$$

Now consider the variables

$$z_1 = u_2 - u_1; \dots z_{n+m} = u_{n+m} - u_{n+m-1}. \quad (2.33)$$

As a function of these variables, and as a result of our assumption about the *positivity* of the  $E_i$  above, we find that  $\kappa$  is analytic when we extend the  $z_i$  to the *upper half plane*.

Now, by the *edge of the wedge* theorem [39], if  $\kappa$  vanishes for all  $u_i \in (-\infty, -\frac{1}{\epsilon})$ , it must vanish for all real  $u_i$ . But this is impossible since, by assumption,  $|\Psi_\perp\rangle$  is itself generated by acting with news operators on the vacuum. Therefore, we have

reached a contradiction with our initial assumption. So  $|\Psi_\perp\rangle$  cannot exist. This proves the lemma.  $\square$

We would like to make two short remarks. Although we have focused on a neighbourhood near  $\mathcal{I}_-^+$ , the same argument above shows that any sector of the Hilbert space can be generated by acting with operators from *any* infinitesimal neighbourhood of future null infinity. Second the argument above shows that Assumption 2.1.2 can also be phrased as an assumption about  $\mathcal{A}(\mathcal{I}^+)$  rather than an assumption about  $\mathcal{A}_{-\infty,\epsilon}$ .

**Proof of result 2.1:** We now move to the proof of result (2.1). Any operator on future null infinity can be expanded as,

$$A = \sum_{s,s',n,m} c(n, m, s, s') |n_{\{s\}}\rangle \langle m_{\{s'\}}|, \quad (2.34)$$

where the state  $|n_{\{s\}}\rangle$  belongs to the sector of the Hilbert space built on top of the soft vacuum  $|\{s\}\rangle$  i.e.  $|n_{\{s\}}\rangle \in \mathcal{H}_{\{s\}}$ , the state  $|m_{\{s'\}}\rangle$  belongs to the sector of the Hilbert space built on top of the soft vacuum  $|\{s'\}\rangle$  i.e.  $|m_{\{s'\}}\rangle \in \mathcal{H}_{\{s'\}}$ , and the coefficients  $c(n, m, s, s')$  are  $c$ -numbers.

But, by the result above, we can write

$$|n\rangle \doteq X_n |\{s\}\rangle; \quad |m\rangle \doteq X_m |\{s'\}\rangle, \quad (2.35)$$

where the operators  $X_n, X_m$  both belong to the algebra that lives near the past boundary of future null infinity:  $X_n, X_m \in \mathcal{A}_{-\infty,\epsilon}$ . Combining this with the assumption about operators in the space of vacua above, we find that we can write the entire operator as

$$A \doteq \sum c(n, m, s, s') X_{n_i} T_{\{s\},\{s'\}} X_{m_j}^\dagger = \tilde{A} \in \mathcal{A}_{-\infty,\epsilon}. \quad (2.36)$$

Since we started with an arbitrary operator in  $A(\mathcal{I}^+)$ , we get the following result,

$$\forall A \in A(\mathcal{I}^+), \exists \tilde{A} \in \mathcal{A}_{-\infty,\epsilon}, \text{ such that } A \doteq \tilde{A}. \quad (2.37)$$

This completes the proof of result (2.1).  $\blacksquare$

An analogous result holds for past null infinity, where all operators are encoded in the neighbourhood of future boundary of past null infinity.

### 2.3.2 The nested structure of information on cuts of null infinity

The second result of this chapter shows that the future null infinity stores information in an intricate, nested structure.

**Result 2.2.** *Consider any operator,  $B$ , localized on future null infinity to the future of a cut at  $u = u_0$ . There exists an operator in the neighbourhood of the cut  $u = u_0$ ,  $\tilde{B} \in \mathcal{A}_{u_0, \epsilon}$ , such that*

$$B \doteq \tilde{B}.$$

This suggests that all degrees of freedom in a semi-infinite interval to the future of a cut are encoded holographically on the cut, which is the past boundary of the semi-infinite interval.

An immediate corollary is the following.

**Corollary 2.2.1.** *Any two states that are distinguishable by operators in  $\mathcal{A}_{u_1, \epsilon}$  can be distinguished by operators in  $\mathcal{A}_{u_0, \epsilon}$  for any  $u_0 < u_1$ .*

If we visualize the future null infinity as a Cauchy slice, then this suggests that all information in a bounded region is contained in the boundary of the region.

We note that the result (2.2) is stronger than the result (2.1). The first result is a limit of the second result,  $u_0 \rightarrow \infty$ . The second result is built on stronger assumptions.

To motivate this result, we first integrate the constraint equation for the Bondi mass aspect, given in (2.2), over the sphere. We find that the Bondi mass,  $M(u)$  defined as

$$M(u) = \int \sqrt{\gamma} m_B(u, \Omega) d^2\Omega, \quad (2.38)$$

satisfies the constraints

$$\partial_u M(u) = - \int \sqrt{\gamma} d^2\Omega \left[ \frac{1}{8} N_{AB} N^{AB} + 4\pi G T_{uu}^{M(0)} \right]. \quad (2.39)$$

Using the news-news commutators and the constraint equation given in (2.2), we

see immediately that

$$[\partial_u M(u), C_{AB}(u', \Omega)] = 4\pi G i \partial_{u'} C_{AB}(u', \Omega) \delta(u - u'). \quad (2.40)$$

The stress-tensor of the matter fields that appears in (2.2) has simple commutators with the matter field

$$[T_{uu}^{M(0)}(u, \Omega), O(u', \Omega')] = \frac{-i}{\sqrt{\gamma}} \partial_{u'} O(u', \Omega) \delta(u - u') \delta^2(\Omega - \Omega'). \quad (2.41)$$

Therefore we see that the commutator of the derivative of the Bondi mass with any matter field also has the same form as its commutator with components of the metric

$$[\partial_u M(u), O(u', \Omega)] = 4\pi G i \partial_{u'} O(u', \Omega) \delta(u - u'). \quad (2.42)$$

Note that no factor of  $\gamma$  appears in this expression.

We now need to set initial conditions to derive the commutator of the Bondi mass with dynamical fields. We assume that, even in the full quantum theory, as  $u \rightarrow -\infty$ , the integrated Bondi mass tends to the canonical Hamiltonian

$$\lim_{u \rightarrow -\infty} \frac{1}{4\pi G} M(u) = H. \quad (2.43)$$

We expect that the commutator of the Hamiltonian with the metric and matter fields at null infinity simply generates translations along null infinity

$$\begin{aligned} [H, C_{AB}(u, \Omega)] &= -i \partial_u C_{AB}(u, \Omega), \\ [H, O(u, \Omega)] &= -i \partial_u O(u, \Omega). \end{aligned} \quad (2.44)$$

Then using the constraint equation on  $M(u)$  above and the commutators of  $M(u)$  with the news, this leads to the following commutators of  $M$ .

$$\begin{aligned} [M(u), C_{AB}(u', \Omega)] &= -4\pi G i \partial_{u'} C_{AB}(u', \Omega) \theta(u' - u), \\ [M(u), O(u', \Omega)] &= -4\pi G i \partial_{u'} O(u', \Omega) \theta(u' - u). \end{aligned} \quad (2.45)$$

The commutators above can be simply generalized to *any polynomial* in the metric and matter fields, and have a very simple form. Taking a commutator of any

observable at  $u'$  with the Bondi mass at  $u$  is just like taking a  $u'$ -derivative of the observable if  $u' > u$ ; otherwise the commutator vanishes.

The commutators (2.45) are exact in the full nonlinear Einstein theory. To prove our second result above, we will need to make the following assumption.

**Assumption 2.2.1.** *In the full theory of quantum gravity, the commutators of the Bondi mass,  $M(u)$ , with other asymptotic fields (given in (2.45)) and the evolution equation for the Bondi mass (given in (2.2)) are exact up to possible corrections by local operators in the algebra at  $u$ .*

This seemingly strong assumption can be proved to all orders in perturbation theory. The commutators only depend on the *weak-field* structure of the theory. This implies that even if we add infinite number of terms that only modify the non-linear interaction terms in the Lagrangian, the commutators at null infinity would remain unchanged. Even if this assumption fails nonperturbatively, our results would hold to all orders in perturbation theory.

**Proof of result 2.2:** Subject to the assumption above, result (2.2) now follows in a single step from our analysis. The commutators (2.45) lead to a differential equation for the dynamical fields in the theory. Consider two points  $u, u' \in (u_0, u_0 + \epsilon)$  with  $u' > u$ . Since the algebra in the vicinity of the cut at  $u$  includes both  $M(u)$  and the matter and metric fields at  $u'$ , we can use these to set the initial conditions for the differential equation. This differential equation has a *unique* solution as we evolve towards the future of null infinity. Explicitly, we have

$$\begin{aligned} C_{AB}(u' + U, \Omega) &= e^{\frac{iM(u)}{4\pi G}U} C_{AB}(u', \Omega) e^{-\frac{iM(u)}{4\pi G}U}; \\ O(u' + U, \Omega) &= e^{\frac{iM(u)}{4\pi G}U} O(u', \Omega) e^{-\frac{iM(u)}{4\pi G}U}; \end{aligned} \tag{2.46}$$

for any  $U > 0$ .<sup>7</sup> Once we have the operator values for all the matter fields, we may obtain the value of  $M(u + U)$  by solving the constraint equation (2.2). This way, we get all operators to the future of the cut  $u = u_0$ . ■

Note that this process is *not* reversible and the equation (2.46) does not hold for  $U < 0$  because the differential equation ceases to be valid in that domain due to

---

<sup>7</sup>We start evolving the fields from  $u' > u$  rather than  $u$  to avoid any subtleties with the the value of the theta function when its argument is exactly 0.

the  $\theta$ -function in (2.45). So, the structure of future null infinity is asymmetric in its information content. As we move towards the future, we lose information.

Of course, an analogous result holds at past null infinity. There, the information in any cut of past null infinity is also contained in any cut to the future.

### 2.3.3 Some comments

#### Locality and causality

The results proved above are strikingly different from our expectations based on local field theories. In a usual field theory, measurements over all of null infinity  $\mathcal{I}^+$  is required to determine the state. However, as we have demonstrated above, in gravity measurements close to the past boundary of future null infinity is sufficient to determine the state. At first, this sounds extremely counter intuitive. For instance, this suggests that one can, in principle, detect a null signal supposed to reach  $\mathcal{I}^+$  at  $u = 0$  from measurements much earlier, at  $u \rightarrow \infty$ .

One may naively think that our results imply a complete breakdown of the causal structure. However, this conclusion is not correct. Instead our results imply a breakdown of *locality*. The reason why all information can be obtained even “before” the signal has reached is due to non-local identification of degrees of freedom. Holography implies that a quantum state in some bounded region,  $R$ , cannot be changed without simultaneously changing the state near the boundary. This is because the degrees of freedom in  $R$  are already encoded in the degrees of freedom in the boundary. Hence, it is not that we have measured the signal “before” it reaches  $\mathcal{I}^+$ , rather the signal is already present at  $\mathcal{I}_-^+$ .

#### Importance of gravity

As stated earlier, gravity was crucial to establish holography. We reiterate this point here.

Result (2.1) crucially depended on the fact that the vacuum can be uniquely identified through asymptotic measurements, i.e., assumption (2.1.1). Identification of a vacuum state requires access to the asymptotic charges, as well as projector onto the vacuum subspace. As we have already seen, this projector can be constructed from the semiclassical Hamiltonian, which is a boundary observable only in a theory

of gravity. Hence result (2.1) does not hold in usual quantum field theories, including gauge theories.

The argument that leads to result (2.2) also cannot be generalized to a non-gravitational setting since there is no analogue of the Bondi mass at a cut in a nongravitational theory that can be used to evolve operators into the future.

Indeed in nongravitational theories it is easy to construct a counterexample to (2.1) and (2.2). Consider any states  $|\Psi\rangle$  and another state  $U|\Psi\rangle$  obtained by exciting the original state with a *gauge-invariant* unitary operator from the algebra near the cut at  $u = 0$ . For instance, in QED we may take

$$U = e^{i \lim_{r \rightarrow \infty} r^2 \int \sqrt{\gamma} F_{\mu\nu}(r, u, \Omega) F^{\mu\nu}(r, u, \Omega) f(u, \Omega) d^2\Omega du}, \quad (2.47)$$

where  $f$  smears the operator in a small region near  $u = 0$ . In the absence of gravity, such an operator commutes with all operators in the algebra near any cut except for the algebra near the cut at  $u = 0$ . So it is impossible to distinguish  $|\Psi\rangle$  and  $U|\Psi\rangle$  either at  $\mathcal{I}_-^+$  or at any cut at negative  $u$ .

### Perturbative verification

Our results leads to implications that can be verified even in perturbation theory. The analysis here is based on [40].

Consider a vacuum,  $|\Omega\rangle$  formed by taking an arbitrary superposition of the soft vacua detailed above and normalized so that  $\langle\Omega|\Omega\rangle = 1$ . Now, we excite this vacuum by acting on it with a unitary operator that comprises the news insertion smeared with a function of *compact support* near  $u = 0$ .

$$|f\rangle = e^{i\lambda \int dud^2\Omega \sqrt{\gamma} N_{AB}(u, \Omega) f^{AB}(u, \Omega)} |\Omega\rangle. \quad (2.48)$$

The challenge is to back-calculate the function  $f^{AB}$  using observations only in the vicinity of  $u = -\infty$ . The construction above is just like (2.47) but in gravity, unlike QED, the challenge can be met.

A simple calculation shows that this can be done by considering the *two-point* func-

tion of the Bondi mass at  $\mathcal{I}_-^+$  and news operator insertions in the interval  $(-\infty, -\frac{1}{\epsilon})$ .

$$\langle f|M(-\infty)N_{CD}(u, \Omega')|f\rangle = \lambda \int dx 16G \frac{f^{AB}(x, \Omega')}{(x-u-i\epsilon)^3} [\gamma_{A(M}\gamma_{N)B} - \frac{1}{2}\gamma_{AB}\gamma_{MN}] + O(\lambda^2). \quad (2.49)$$

Since the function on the right hand side is analytic when  $u$  is extended in the upper half plane given its value for  $u \in (-\infty, -\frac{1}{\epsilon})$  we can reconstruct  $f^{AB}$ . A similar calculation allows one to extract  $f^{AB}$  from the neighbourhood of any cut for negative  $u$ .

This calculation also explains why we need an *infinitesimal interval* rather than a cut. Using the value of the two point correlator, (2.49), for only for a fixed value of  $u$  it is not possible to reconstruct  $f^{AB}$ . It may still be possible to reconstruct  $f^{AB}$  by using correlators of arbitrarily complicated operators at a single value of  $u$ . But using a small interval obviates the need for such complicated correlators and allows a perturbative examination of how holographic information is stored. As explained above, this computation crucially relies on gravity and on the nonvanishing commutators of the Bondi mass with other operators.

### Importance of quantum mechanics

Our results have no classical analogs. Classically, we can only measure product of one-point functions, such as the average value of Bondi mass,  $\langle M(u) \rangle$ . To obtain information about the quantum state, we need quantum correlators.

### Nongravitational limit

In the limit where we take  $M_{\text{pl}} \rightarrow \infty$  and ignore the information in gravitational correlators, we recover the usual picture of local quantum field theory where information is stored locally rather than holographically. When such a decoupling limit is possible, results (2.1) and (2.2) remain true but may not be relevant from a practical perspective.

All quantum-information experiments that are feasible with current technology fall into the category above. For instance, if one is given a sealed box of qubits, in the real world, it is not practical to read off the qubits just by making measurements of the quantum fluctuations of the metric around the box, and the only practical

possibility is to open the box and directly examine the qubits.

This is an obvious point but nevertheless we urge the reader to keep it in mind. Our everyday intuition about the localization of quantum information is built by our experiences in a regime where  $M_{\text{pl}}$  is very large compared to other energy scales. Results (2.1) and (2.2) are in conflict with this intuition because they are relevant in a regime where effects suppressed by  $M_{\text{pl}}$  are important.

## 2.4 Implications of holography for black hole information paradox

Holography has striking implications for the black hole information paradox. A pedagogical introduction to the relevant aspects of black hole information paradox was given in chapter 1. In this section we explain how holography modifies the expectation for Page curve and resolves the strong subadditivity and cloning paradoxes. The crucial point is that the paradox is built on the incorrect assumption of locality.

Before proceeding we point out that the effects of holography are *always* relevant for the black hole information paradox. The reason is that the entropy of a black hole scales with the Planck scale,

$$S = \frac{A}{4\ell_{\text{pl}}^2}, \tag{2.50}$$

where  $A$  is the area of the horizon and  $\ell_{\text{pl}}$  is the Planck length.

To determine whether state of the black hole radiation is pure or not, we would at least need  $S$ -point correlators with exponential,  $e^{-S}$ , accuracy. Since the entropy of a black hole always scales with the  $M_{\text{pl}}$ , there is no way to consistently decouple quantum gravity corrections when answering *fine-grained* questions about the purity of a state.

### 2.4.1 A constant Page curve

In this chapter we have explored how all information about a quantum state is always present at the boundary,  $\mathcal{I}_-^+$ , including the information encoded in the interior of a black hole. There is no sense in which information comes out of the black holes.

This can be formalized in the following two results, which follow immediately from our previous results.<sup>8</sup>

**Result 2.3.** *The fine-grained von Neumann entropy of the segment  $(-\infty, u_0)$  of  $\mathcal{I}^+$  is independent of  $u_0$  for any pure or mixed state on  $\mathcal{H}$ .*

This result requires only result (2.1) as we show below. If we also assume result (2.2), we find a stronger result

**Result 2.4.** *The fine-grained von Neumann entropy of the segment  $(u_1, u_2)$  of  $\mathcal{I}^+$  with  $u_2 > u_1$  is independent of  $u_2$  for any state.*

We first establish these results and then discuss their interpretation.

**Proof of result 2.3:** First, we review how the von Neumann entropy of the state at future null infinity up to a cut at  $u_0$  is defined.

The first step is to consider the algebra,  $\mathcal{B}_{-\infty, u_0}$ , formed by considering all possible functions of operators on  $\mathcal{I}^+$  that lie in  $(-\infty, u_0)$ . The definition is precisely analogous to the definition of the algebras in the vicinity of a cut that we have considered previously, except that we allow the operators to be localized within a larger interval.

$$\begin{aligned} \mathcal{B}_{-\infty, u_0} = \{ & m(u_1, \Omega_1), C_{AB}(u_1, \Omega_1), O(u_1, \Omega_1), m(u_1, \Omega_1)C_{AB}(u_2, \Omega_2), \\ & m(u_1, \Omega_1)O(u_2, \Omega_2), C_{AB}(u_1, \Omega_1)O(u_2, \Omega_2) \dots \} \end{aligned} \quad (2.51)$$

where  $u_i \in (-\infty, u_0)$ .

Now consider any density matrix from the Hilbert space  $\mathcal{H}$ , which we denote by  $\sigma$ . Recall that by the definition of  $\mathcal{H}$  above that the algebra  $\mathcal{B}_{-\infty, u_0}$  maps  $\mathcal{H}$  back to itself. Now the *reduced* density matrix associated with a segment is defined to be the element of the algebra of the segment  $\mathcal{B}_{-\infty, u_0}$  that, when traced with any other observable in the algebra, reproduces the expectation value of the observable given

---

<sup>8</sup>We frame these results in terms of density matrices, traces and von Neumann entropy since we anticipate that these concepts are more familiar to most readers even if they need to be carefully defined and regulated. For the more rigorously-minded reader, we note that similar results hold for the relative-entropy of two states: it is independent of the upper-bound of the segment of  $\mathcal{I}^+$  on which it is evaluated.

by the density matrix  $\sigma$ . More precisely, we choose the reduced density matrix of the segment,  $\rho_{-\infty, u_0}$ , to satisfy

$$\mathrm{Tr}(\rho_{-\infty, u_0} b) = \mathrm{Tr}(\sigma b), \quad \forall b \in \mathcal{B}_{-\infty, u_0}, \quad (2.52)$$

subject to the condition that  $\rho_{-\infty, u_0} \in \mathcal{B}_{-\infty, u_0}$ . The von Neumann entropy of the segment is now defined as

$$S_{-\infty, u_0} = -\mathrm{Tr}(\rho_{-\infty, u_0} \log(\rho_{-\infty, u_0})). \quad (2.53)$$

However, in result (2.3) we proved that *any operator* that mapped  $\mathcal{H} \rightarrow \mathcal{H}$  could be approximated arbitrarily well by an operator in  $\mathcal{A}_{-\infty, \epsilon}$ . So  $\sigma \in \mathcal{A}_{-\infty, \epsilon}$ . Therefore, we can always choose

$$\rho_{-\infty, u_0} = \sigma \in \mathcal{A}_{-\infty, \epsilon}, \quad (2.54)$$

But this choice is independent of  $u_0$ . Therefore

$$S_{-\infty, u_0} = -\mathrm{Tr}(\sigma \log(\sigma)), \quad (2.55)$$

which is manifestly independent of  $u_0$ ! ■

**Proof of result 2.4:** The proof of result (2.4) is precisely analogous to the proof above and so we only sketch it.

To define the reduced density matrix associated with a segment, we first define the algebra  $\mathcal{B}_{u_1, u_2}$  in precisely the same fashion as above. Now consider a density matrix,  $\mu$ , in the full quantum theory and for the purposes of this result, such a state may have both *both massless and massive* excitations. Then the reduced density matrix we are looking for is defined by the condition

$$\mathrm{Tr}(\rho_{u_1, u_2} b) = \mathrm{Tr}(\mu b), \quad \forall b \in \mathcal{B}_{u_1, u_2}, \quad (2.56)$$

subject to the constraint  $\rho_{u_1, u_2} \in \mathcal{B}_{u_1, u_2}$ . But since, by result (2.2) *any* in  $\mathcal{B}_{u_1, u_2}$  can be written as an operator in  $\mathcal{A}_{u_1, \epsilon}$  we can always choose

$$\rho_{u_1, u_2} \in \mathcal{A}_{u_1, \epsilon}. \quad (2.57)$$

This choice is manifestly independent of  $u_2$  and so the von Neumann entropy of this density matrix is also independent of  $u_2$ . ■.

### Failure of Page argument

The naive expectation of the Page curve [18], Figure 2.1, is based on the incorrect assumption of *factorization* of the Hilbert space as a tensor product of Hilbert space of sub-regions. From result (2.4), it is clear that the true Page curve should be a constant, Figure 2.2. Note that the constant need not be zero, as we have not included massive particles in our analysis.

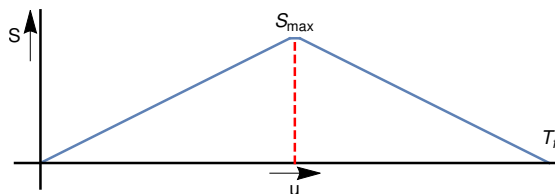


Figure 2.1: *The naive Page curve. If one incorrectly assumes that the Hilbert space factorizes into degrees of freedom outside and inside the black hole, the von Neumann entropy of the radiation that has emerged till retarded time  $u$  on  $\mathcal{I}^+$  is expected to obey the curve above indicating that “information is gradually returned to the exterior.”*

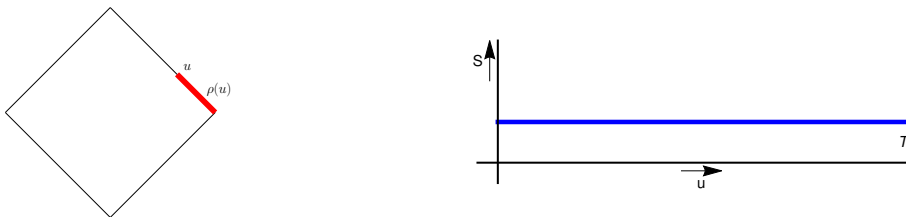


Figure 2.2: *The fine-grained von Neumann entropy (right) of any state of massless excitations reduced on a segment that extends till the cut at  $u$  marked on the left figure. The result directly follows from the arguments above. The information is always outside, and so the entropy never goes up or comes down!*

Recently, it has been suggested that the naive page curve, Figure 2.1, can be derived from a semiclassical analysis [41]. These works are not in contradiction with our results as the setup is very different. The naive Page curve has been achieved by

forcing a factorization of the Hilbert space by coupling the spacetime with a non-gravitational *reservoir*, and *identifying* the radiation and the reservoir. We make two comments.

1. In these setup gravity *switches-off* at large distances. However, this is not true for black holes in our world, where gravity is always present. Hence, the relevance of these works remain unclear.
2. Identifying the radiation and the reservoir is misleading as the reservoir necessarily excludes some of the radiation which continues to be described by the gravitational theory.

**Note:** We are *not* claiming that there exist no sub-algebra of operators which results in the traditional Page curve. For instance, if we restrict our attention to the news operators alone, then we would be able to define sub-algebra of operators on different cuts of  $\mathcal{I}^+$  that commute. Hence, we may tweak the question such that the answer is the Page curve. However, an observer at infinity can access other operators as well, including the Bondi mass. Hence, a more *physical* algebra would contain all asymptotic operators. In such a scenario, we will get the constant Page curve. We reiterate the key point: *all information is always available at the boundary*.

### 2.4.2 Strong subadditivity and cloning paradox

The strong subadditivity and cloning paradox are based on the incorrect assumption of the factorization of the Hilbert space into a Hilbert space of the black hole and a Hilbert space of the radiation. However, we have shown that such a factorization is not possible. Hence, the premise of these paradoxes breaks down.

## 2.5 Discussion

### Summary

In this chapter we have demonstrated that the degrees of freedom in a theory of quantum gravity in 4-dimensional asymptotically flat spacetimes are encoded holographically. Result (2.1) states that all operators on the future null infinity can be approximated with arbitrary precision by an operator in the past boundary of future

null infinity. To prove this result, we assumed that the vacua can be identified by operators near the past boundary of future null infinity. Moreover, operators that transition between any two soft vacua is also accessible at  $\mathcal{I}_-^+$ . We also assumed that the Hamiltonian of the full theory is bounded from below.

We realized these assumptions explicitly in the framework of asymptotic quantization. We noted that this result is not valid in a non-gravitational theory as we can never project onto the space of vacua by using operators that are localized near the past boundary of the future null infinity, hereby violating our assumptions.

The result (2.1) implies that all information is always present at  $\mathcal{I}_-^+$ . This suggests that the Page curve of black hole evaporation should be a constant, result (2.3).

We proved a stronger result (2.2) based on stronger assumptions. We showed that future null infinity encodes the degrees of freedom in a nested structure. All operators to the future of a cut can be approximated with arbitrary precision by operators in the neighbourhood of the cut. This result assumes that certain commutation relations hold even in the full UV complete theory. We argued that this assumption is true to all orders in perturbation theory. Hence, our results at least holds to all order in perturbation theory. This result implies that all information to the future of a cut of  $\mathcal{I}^+$  is also encoded in the cut, see result (2.4).

Since the Hilbert space fails to factorize into the subspace of interior and exterior, our results resolved the cloning and strong subadditivity paradox.

## Outlook

In our analysis, we did not include massive excitations. Extension of our results for massive particles is an immediate future direction.

We restricted to study of 4-dimensional asymptotically flat spacetimes. Generalizing these results to other dimensions is another avenue that remains to be explored. There is some debate in the literature on the vacuum structure of gravity in other spacetime dimensions. However, regardless of the answer to this question, it appears likely that the vacua should be identifiable by charges supported near spatial infinity. If so, the program outlined in this chapter should carry through to other spacetime dimensions.

Another question to explore is whether we can make more refined statements, such as the counter part of entanglement wedge reconstruction conjecture in AdS/CFT.



## Chapter 3

# Critique of the fuzzball program

### 3.1 Introduction

Fuzzballs are smooth solutions in higher dimensional supergravity theories that have same charges as black holes, but no horizons. The size of compact directions, in these geometries, shrink to zero at a distance larger than the radius of corresponding black hole horizon. The fuzzball proposal [21, 42] posits that classical fuzzball geometries parameterize the phase space of black hole microstates. If true, the fuzzball proposal would have two immediate implications. First, it would account for the entropy of black holes. Second, it would suggest that typical microstates of black holes do not have a horizon, hence, bypassing the information paradox.

The fuzzball proposal has garnered a lot of attention in the literature. Considerable efforts have been devoted to finding these *microstate geometries*. However, this proposal has not been carried through in any setting corresponding to macroscopic black hole, i.e., black holes with finite horizon radius. In this chapter, based on [10], we undertake a careful statistical-mechanical analysis of the fuzzball proposal.

We first begin by noting some facts from quantum statistical mechanics concerning *typical* states in subspace of Hilbert spaces with large dimensions. Consider a subspace  $H_E$  with energy  $E \pm \Delta$  and dimension  $e^S$ . Our goal is to understand the properties of *typical* states of this subspace. It can be shown that a state picked at random from the subspace, would mimic the maximally mixed state in  $H_E$  with exponential accuracy. More precisely, the expectation of any operator in the typical state is the same as expectation in maximally mixed state, with  $e^{-\frac{S}{2}}$  corrections. It can also be shown that the subspace cannot be spanned by an atypical basis. Almost all elements of the basis of  $H_E$  must be typical.

These results greatly constrain the geometry of typical black hole microstates. We

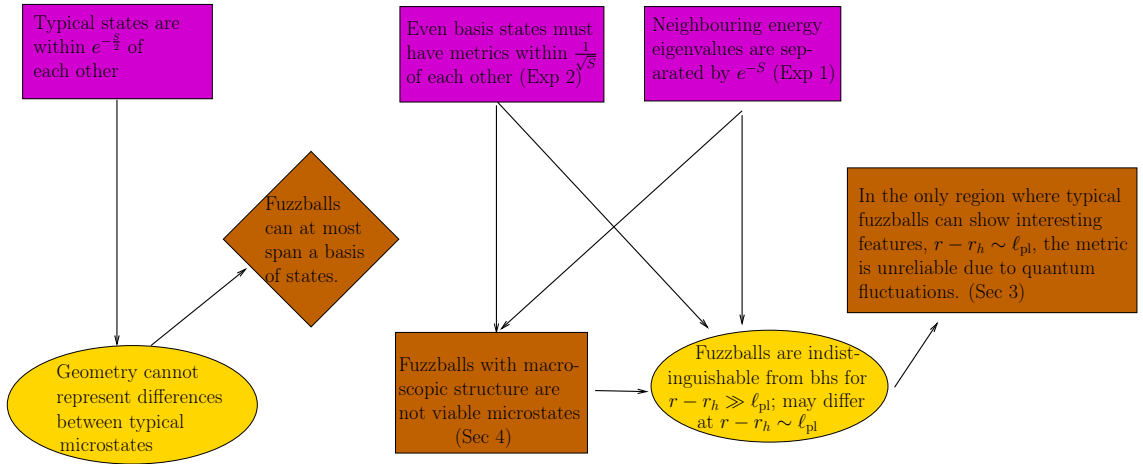


Figure 3.1: Logical flowchart. Statistical mechanics results are in magenta rectangles. The physical expectation that they rely on is referred to in brackets. Implications for the fuzzball are in orange ovals. Major conclusions are in brown boxes. Sections where a conclusion is verified are given in brackets.

argue that if distinct fuzzball geometries parameterize the phase space of black hole microstates, then these geometries must remain exponentially close to the conventional black hole geometry, outside Planck scale distance from the horizon. Hence, fuzzball geometries that are relevant for black holes can only differ from the conventional geometry within Planck scale of the horizon. This can only be realized by introducing explicit structures at a length scale, which is of the order of Planck scale. Since any scale in quantum gravity undergoes fluctuations of the order of Planck scale, the fluctuations in this scale is at least of the order of the scale itself. Hence, the classical structures controlled by these scales cannot be trusted. This makes distinct classical fuzzball geometries unreliable. Instead, all typical black holes should have a classical geometry that is identical to the conventional black hole geometry. These arguments are explained in detail in section 3.2.

As explicit checks, in section 3.3, we explore two-charge Lunin-Mathur geometries corresponding to ground states in the D1-D5 system [12, 43]. These solutions were quantized in [13]. In this case, we can explicitly verify the claims made in section 3.2.

In section 3.4 we analyze a class of asymptotically AdS solutions that correspond to 1/4-BPS states in the D1-D5 system [44]. Such 1/4-BPS states are described by

a black hole with finite horizon area [45] but the geometries of [44] differ macroscopically from the black-hole geometry. We show that these differences can be easily detected through simple asymptotic boundary observables. Since all fuzzball solutions for this case are not known, we can only study a specific class of fuzzball geometries. However, we believe that our conclusions can be realized more generally.

Figure 3.1 outlines the flow of logic in this chapter and explains how our calculations in sections 3 and 4 fit into this flow.

## 3.2 A statistical-mechanics evaluation of the fuzzball program

In this section, we review some simple results from quantum statistical mechanics, and explain their implications for the fuzzball program. These results will motivate our calculations in section 3.3 and 3.4. We have organized this section into three subsections: in subsection 3.2.1 we review some results from statistical mechanics; in subsection 3.2.2 we explain the relevance of these results for the fuzzball program; in subsection 3.2.3 we discuss the “Hawking theorem” described in [20] which is sometimes used to indirectly infer properties of fuzzballs.

Some readers may be concerned that our arguments in this section are too abstract. We urge these readers to read this section in conjunction with section 3.3 and section 3.4 where we have performed a number of calculations that support our deductions in specific examples.

### 3.2.1 Some results from statistical mechanics

We now discuss some results that characterize (a) typical states in high-dimensional quantum statistical systems (b) the extent to which elements of a complete basis can differ from one another and (c) the gap between neighbouring energy eigenstates.

**Result 3.1.** *Consider any subspace  $H_E$  of a Hilbert space. Let  $\dim(H_E) = e^S$  and let  $\mu_\psi$  be the Haar measure on  $H_E$  in the neighbourhood of a state  $|\psi\rangle$ . Then typical pure states in  $H_E$  are exponentially close to the maximally mixed state on  $H_E$  in the*

sense that for any Hermitian operator  $A$ , we have

$$\langle A \rangle \equiv \int \langle \Psi | A | \Psi \rangle d\mu_\psi = \text{Tr}(\rho A), \quad (3.1)$$

where the density matrix,  $\rho = e^{-S} P$ , and  $P$  is the projector onto  $H_E$ . Moreover, deviations from this mean value are exponentially suppressed

$$\int (\langle \Psi | A | \Psi \rangle - \langle A \rangle)^2 d\mu_\psi \leq \frac{\sigma_{ens}^2}{e^S + 1}, \quad (3.2)$$

where  $\sigma_{ens}^2 \equiv \text{Tr}(\rho A^2) - [\text{Tr}(\rho A)]^2$ .

To our knowledge this result was first described in [46]. To prove this result we choose some basis for the subspace, and we label its elements by  $|f_1\rangle, |f_2\rangle \dots |f_{e^S}\rangle$ . Then an arbitrary state in this subspace can be written as  $|\Psi\rangle = \sum_i a_i |f_i\rangle$ . The Haar measure is given by

$$d\mu_\Psi = \frac{1}{V} \delta\left(\sum_{i=1}^{e^S} |a_i|^2 - 1\right) \prod_{j=1}^{e^S} da_j, \quad (3.3)$$

where  $V$  is a normalization-constant which can be set by demanding that  $\int d\mu_\Psi = 1$ , which leads to  $V^{-1} = \frac{\pi^{e^S}}{\Gamma(e^S)}$ . We emphasize that the measure (3.3) is *independent* of the choice of basis.

Now consider an arbitrary Hermitian operator,  $A$  and denote its matrix elements in the basis above by  $A_{ij} = \langle f_j | A | f_i \rangle$ . Then

$$\int \langle \Psi | A | \Psi \rangle d\mu_\psi = \int d\mu_\psi \left[ \sum_{i=1}^{e^S} |a_i|^2 A_{ii} + \sum_{i \neq j} a_i a_j^* A_{ij} \right] = \frac{1}{e^S} \sum A_{ii} = \text{Tr}(\rho A), \quad (3.4)$$

where we have used the fact that  $\int d\mu_\psi a_i a_j^* = \frac{1}{e^S} \delta_{ij}$ .

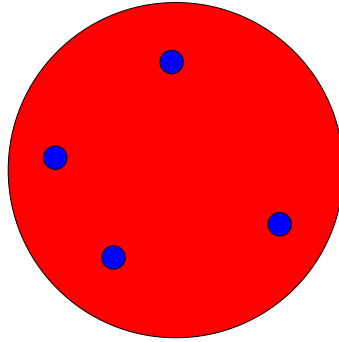


Figure 3.2: The subspace,  $H_E$ , is a compact manifold. Most pure states in the space are very close to the maximally mixed state. An exponentially small volume of states (displayed in blue) can be atypical.

A simple computation yields the variance in the second part of the result.

$$\begin{aligned}
 & \int \left[ \langle \Psi | A | \Psi \rangle - \text{Tr}(\rho A) \right]^2 d\mu_\psi = \int \left[ \sum_{i,j} A_{ij} a_i a_j^* - \sum_i A_{ii} |a_i|^2 \right]^2 \\
 & = \int \left[ \sum_{i \neq j, l \neq m} A_{ij} A_{lm} a_i a_j^* a_l a_m^* \right] d\mu_\psi = \int \left[ \sum_{i \neq j} |A_{ij}|^2 |a_i|^2 |a_j|^2 \right] d\mu_\psi \quad (3.5) \\
 & = \frac{1}{e^S (e^S + 1)} \sum_{i \neq j} |A_{ij}|^2 \leq \frac{1}{e^S + 1} \sigma_{\text{ens}}^2.
 \end{aligned}$$

Here, in the second line we used the fact that unless  $i = m$  and  $j = l$ , the summand vanishes upon integration. In the third line, we used the fact that  $\int d\mu_\psi |a_i|^2 |a_j|^2 = \frac{1}{e^S (e^S + 1)}$  for  $i \neq j$ . A small subtlety in the final step is that

$$\frac{1}{e^S} \sum_{i \neq j} |A_{ij}|^2 = \text{Tr}(\rho (PAP)^2) - \text{Tr}(\rho A)^2 \leq \sigma_{\text{ens}}^2. \quad (3.6)$$

This difference arises because  $A$  might have matrix elements that link states in  $H_E$  to states outside  $H_E$ .

This result should be interpreted as follows: “On almost all of the volume of the subspace, the expectation value of the operator differs from the typical expectation value by an exponentially small amount. The expectation value may differ significantly from the typical expectation value only an exponentially small region of the

subspace.” The reader may consult Figure 3.2 for intuition.

This result tells us that *typical* microstates of  $H_E$  are described by a universal set of correlators. By itself, this does not disallow the possibility of an atypical basis of states for  $H_E$ . This is because the basis vectors themselves occupy only zero volume in the Hilbert space. We now bound the atypicality of a basis in some cases of interest.

**Result 3.2.** (*Limit on atypicality of a basis*) Assume that the ratio  $\frac{\sigma_{\text{ens}}}{\langle A \rangle}$  vanishes as  $\frac{1}{S^\alpha}$  for large  $S$  and some positive number  $\alpha$ . Given any basis,  $|f_1\rangle \dots |f_{e^S}\rangle$ , for  $H_E$ , let  $|f_{\alpha_1}\rangle \dots |f_{\alpha_M}\rangle$  be those of its elements where  $\left| \frac{\langle f_{\alpha_j} | A | f_{\alpha_j} \rangle - \langle A \rangle}{\langle A \rangle} \right| \geq O\left(\frac{1}{S^\beta}\right)$  in the thermodynamic limit, with  $\beta < \alpha$ . Then  $\frac{M}{e^S}$  vanishes at least as fast as  $O\left(\frac{1}{S^{2(\alpha-\beta)}}\right)$ .

This result follows from simple inequalities.

$$\begin{aligned} \sigma_{\text{ens}}^2 &= \frac{1}{e^S} \sum_i \langle f_i | A^2 | f_i \rangle - \langle A \rangle^2 \\ &= \frac{1}{e^S} \sum_i (\langle f_i | A^2 | f_i \rangle - \langle f_i | A | f_i \rangle^2) + \frac{1}{e^S} \sum_i (\langle f_i | A | f_i \rangle - \langle A \rangle)^2 \\ &\geq \frac{1}{e^S} \sum_{j=1}^M (\langle f_{\alpha_j} | A | f_{\alpha_j} \rangle - \langle A \rangle)^2 \geq \frac{M \kappa^2 \langle A \rangle^2}{e^S}, \end{aligned} \quad (3.7)$$

where  $\kappa = \inf_j \left| \frac{\langle f_{\alpha_j} | A | f_{\alpha_j} \rangle - \langle A \rangle}{\langle A \rangle} \right|$ . By assumption  $\kappa = O\left(\frac{1}{S^\beta}\right)$  in the thermodynamic limit, and since  $\frac{\sigma_{\text{ens}}^2}{\langle A \rangle^2}$  vanishes like  $\frac{1}{S^{2\alpha}}$ , therefore  $\frac{M}{e^S}$  must vanish like  $\frac{1}{S^{2(\alpha-\beta)}}$ .

The result above is very simple, but it is relevant for those observables that take on a finite *classical expectation value*. These are the observables where  $\frac{\sigma_{\text{ens}}}{\langle A \rangle}$  vanishes as  $S \rightarrow \infty$ . For such observables, the result states that one cannot construct a basis whose elements are all individually very different, and only average out to give some mean.

So far our results have been kinematical. We now state a dynamical *expectation* about the spectrum, which should be true in almost all interacting systems. Let  $S$  be the entropy at energy  $E$ . (We deliberately use the same notation as above since  $e^S = \dim(H_E)$  if  $H_E$  is taken to the subspace corresponding to the microcanonical ensemble.)

**Expectation 1.** (*Almost continuous spectrum*) The gap between the energy eigen-

values of typical neighbouring high-energy eigenstates is  $O(e^{-S})$  in an interacting theory in the thermodynamic limit.

The motivation for this expectation is as follows. Between the energy  $[E - \Delta, E + \Delta]$  We expect to have  $e^S$  states in a finite band of energies,  $2\Delta$ . Except for an *exactly* free theory, interactions generically break all degeneracies. Therefore, the energy gap between neighbouring states scales like  $e^{-S}$  in the thermodynamic limit.

Expectation (1) also holds in theories with supersymmetry. Supersymmetry might ensure that some states, which saturate the BPS bound, are degenerate. However, as soon as we move slightly away from the BPS bound, the gap between eigenvalues becomes exponentially small.

Some systems may have a forbidden-zone of energies in which states cannot exist. For example, superconformal field theories may have BPS representations that are separated from other representations with the same charges by a finite mass gap. (See, for example, the “**b**” representations in [47].) However, outside the forbidden zone, we again expect exponentially small gaps between neighbouring eigenvalues.

Expectation (1) also holds in *integrable* systems. The statistical mechanics literature contains considerable discussion of the *statistics* of the distribution of energy eigenstates. The statistics of eigenvalues differ in integrable and chaotic systems (See, for example, [48].) But the fact that the energy gap is  $O(e^{-S})$  holds almost universally.

In the context of the fuzzball proposal, there has been some discussion that the correct gap between energy-eigenstates, even at the supergravity point of the D1-D5 system, should be an inverse power of  $N_1 N_5$  (the product of the number of D1 and D5 branes) rather than an inverse exponential of this product [49, 50]. This is based on the fact that, at the orbifold point, the D1-D5 CFT does have a gap that scales with  $\frac{1}{N_1 N_5}$ . However, the orbifold CFT is a *free* theory. The moment we turn on the moduli that are necessary to reach the supergravity point, we expect that the degeneracies in the orbifold CFT will be destroyed. The entropy at energy  $E$  scales as  $S \propto \sqrt{N_1 N_5 E}$ , and we expect that the gap between neighbouring energy eigenstates is of order  $e^{-S}$  at a generic point in moduli space.

The exponentially small gap can be easily detected by a two-point function. For example, let  $A(t)$  be a simple operator localized in time. Then, given any typical

high energy basis state,  $|f\rangle$  of energy  $E$  (which may *not* be an eigenstate), consider

$$G_{\mathfrak{F}}(\omega_0) = \int dt \langle f|A(t)A(0)|f\rangle \mathfrak{F}_{\omega_0}(t) dt, \quad (3.8)$$

where  $\mathfrak{F}_{\omega_0}(t)$  is a function whose Fourier transform is centered around  $\omega_0$  with a width  $\delta \gg Ee^{-S}$ . But we can take  $\delta$  to be very narrow. For example, in the D1-D5 theory, we may take  $\delta = \frac{1}{(N_1 N_5)^4}$  since this is still larger than  $e^{-S}$ .

Then, by inserting a complete set of energy eigenstates,  $|E_i\rangle$ ,

$$G_{\mathfrak{F}}(\omega_0) = \sum_{i,j} \langle f|E_i\rangle \langle E_i|A(0)|E_j\rangle \langle E_j|A(0)|f\rangle \left[ \int \mathfrak{F}_{\omega_0}(t) e^{i(E_i - E_j)t} dt \right]. \quad (3.9)$$

Since the difference  $E_i - E_j$  takes on almost a continuous range of values we see that  $G_{\mathfrak{F}}(\omega_0)$  has support for a *continuous range* of  $\omega_0$ . Even if the state  $|f\rangle$  is a supersymmetric state, we can choose an appropriate operator  $A$  that moves us off the BPS bound and whose two-point function displays a continuous spectrum.

States, where the two-point function does not have a continuous spectrum for *any* simple operator typically correspond to microstates of a phase of zero-entropy. For such states, the three point function  $\langle E_j|A(0)|f\rangle$  that appears above vanishes for almost all except an exponentially small set of eigenstates,  $|E_j\rangle$ . For example, the boundary two-point function of light primary operators in the state dual to thermal AdS is expected to have a discrete spectrum.

In the paper [51], it was argued that fuzzballs might represent typical states and still not show the continuous spectrum described above. The paper [51] suggested that the matrix elements  $\langle E_j|A(0)|f\rangle$  could be subject to a *selection rule*: the matrix element vanishes unless  $E_j - E = nE_{\text{gap}}$  where  $E_{\text{gap}} \gg e^{-S}$  is some large gap and  $n$  is an *integer*. Thus probing a particular fuzzball microstate with simple operators only excites a tower of integrally spaced excitations on top of that microstate. A probe of another microstate excites a parallel tower and it is impossible to move between towers by probing the system with simple operators. (See Figure 3.3.) The number of towers must be exponentially large to account for the total number of states.

This picture would suggest that the matrix elements between different states not only violate the eigenstate thermalization hypothesis (see below) but most matrix

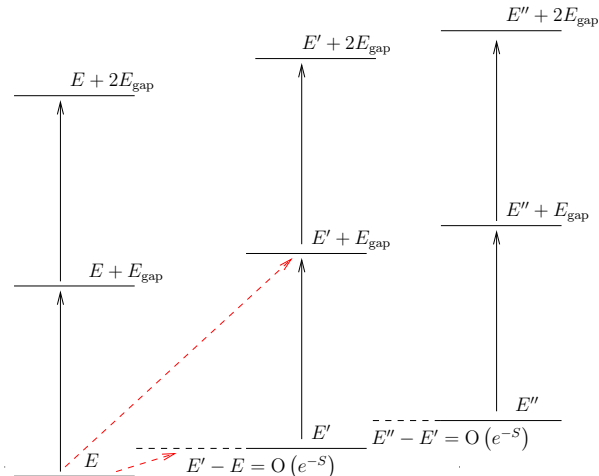


Figure 3.3: An unusual possibility for the dynamics of fuzzball microstates. Probes of one microstate only excite other microstates in a single tower (solid black lines) and transitions between towers (dashed red lines) are disallowed.

elements actually vanish. Moreover, since it is impossible to transition between towers using simple operators, the system effectively breaks up into an exponentially large number of disconnected phases. If the D1-D5 system, or any gravitational system shows such *unusual* statistical behaviour, there should be a dynamical explanation for this. The selection rule above cannot just be *postulated* to save the fuzzball program from potential contradictions. In the absence of such a dynamical explanation, the simplest possibility is just that fuzzballs and other states where the two-point function does not show a continuous spectrum represent isolated states whose degeneracy is exponentially small compared to the set of all microstates.

**Relation to eigenstate thermalization.** Before, we conclude our discussion on general statistical expectations, we should clarify the relation to the commonly discussed *eigenstate thermalization hypothesis* (ETH) [52].

The ETH is usually stated for energy eigenstates. However, it really only relies on the assumption that, in a large statistical system, the eigenstates of most observables are likely to be highly scrambled versions of eigenstates of the Hamiltonian. So, given some basis of states for the microcanonical ensemble,  $|f_i\rangle$ , the ETH can be stated

as

$$\langle f_j | A | f_i \rangle = A(E_i) \delta_{ij} + B\left(\frac{E_i + E_j}{2}\right) e^{-\frac{s}{2}} R_{ij}, \quad (3.10)$$

where  $R$  is a matrix of random phases and  $E_i, E_j$  are the expectation values of the Hamiltonian in  $|f_i\rangle, |f_j\rangle$  and  $A, B$  are smooth functions of their arguments. Note that  $A(E)$  is the microcanonical average of the observable at energy  $E$ .

If the ETH holds for some basis of states, this implies that most elements of such a basis are typical even for operators where the standard deviation is not parametrically small in the thermodynamic limit.

The ETH is a significantly stronger assumption than the vanishing of the microcanonical standard deviation for classical observables that is an input to result 3.2. The ETH implies the typicality of most elements of the basis even for observables that have large  $\sigma_{\text{ens}}$ . The ETH arises from an assumption of quantum chaos, and in such a system expectation 1 also holds.

Therefore, the ETH is *stronger* than the assumptions of result 3.2 and expectation 1. Nevertheless, we expect the ETH to hold in theories with holographic duals [53].

### 3.2.2 Implications for the fuzzball program

Now we discuss several implications of these results for the fuzzball program. In what follows, to make contact with the results above, we take the Hilbert space  $H_E$ , to be the subspace that corresponds to black holes. If we consider large black holes in the AdS/CFT correspondence, then this subspace can simply be taken to be the microcanonical ensemble. However, note that the subspace corresponding to black holes exists even in flat space, where black holes do *not* dominate the canonical or microcanonical ensemble.

**Information-free nature of the horizon/stretched horizon.** The fuzzball program is often motivated by the idea that the horizon should be replaced by the surface of a fuzzball that would contain “information” about the initial state. It is claimed that this structure would correct Hawking radiation at  $\mathcal{O}(1)$ .

We now apply result 3.1. Let  $A$  correspond to an operator that measures correlations between different Hawking quanta. For example,  $A$  may be a product of curvature invariants at distinct points. Since we are considering smooth geometries,

such invariants are bounded and their fluctuations cannot be exponentially large. Then result 3.1 tells us that such observations in a typical microstate yield only an exponentially small amount of information.

In particular, it *cannot* be the case that Hawking radiation differs by  $O(1)$  amounts between different typical microstates. It is sometimes claimed that “high energy” observables would take on a universal form but “low energy” observables at the scale of the Hawking radiation would differ between microstates [54]. However result 3.1 allows no such freedom. *In a typical microstate, both high-energy and low-energy observables take on a universal value, and all features of the microstate can only be determined by exponentially precise observations.*

The idea that the surface of a black hole should contain “information” is often presented by making an analogy with a piece of coal. (For instance, see page 3 of [9].) When coal burns, the properties of the outgoing radiation are strongly affected by the nature of its surface. However, this is a misleading analogy: everyday pieces of coal are *not* completely thermalized. They have a number of distinctive features because they are in highly *atypical* states. A better example, to visualize a thermalized system, is a gas of radiation in a box. This gas is entirely featureless. Individual photons that emerge from the box contain almost no information about the state of the radiation inside the box; it is only by making exponentially precise measurements on the radiation that we can discern the state of the radiation.

**The universal fuzzball geometry.** Above, we argued that correlation functions of Hawking radiation measured in a typical microstate must take on a universal value. We now argue that these correlators should correspond to correlators computed in effective field theory about an *approximately classical average bulk geometry* in the limit where the Planck length is smaller than all other scales.

The signature of an approximately classical bulk geometry is that correlators of local operators factorize into products of lower-point functions [55].

In AdS/CFT the factorization of *boundary correlators* in the microcanonical/canonical ensemble can be proved at large- $N$  using the standard factorization arguments. We can then use the standard HKLL construction [56, 57, 58] to construct approximately local operators and the factorization of boundary correlators implies the factorization of bulk correlators. This implies that, in AdS/CFT, the microcanon-

ical/canonical ensemble is dual to an approximately classical bulk geometry. By result 3.1 this is also the geometry dual to a typical microstate. This geometry can also be used to compute n-point functions of simple operators to excellent accuracy.

In flat space, we cannot make such a clear argument that averages computed in  $H_E$  correspond to an approximately classical bulk. But, even here we expect that S-matrix elements will factorize if the Planck length is much smaller than other length scales in the problem. These S-matrix elements can be used to reconstruct a bulk geometry that is approximately classical.

A priori, we do not know what this universal classical geometry should be. In section 3.3, we will *compute* this average geometry for the two-charge Lunin-Mathur solutions that have been quantized. However, in more general settings that correspond to large black holes, we cannot compute this average geometry since all fuzzball solutions have neither been found nor quantized. So, in the remainder of this chapter, we will simply proceed with the following expectation.

**Expectation 2.** (Conventional geometry as average) *The conventional black-hole geometry — after incorporating classical string-theory corrections — correctly computes the average value of bulk observables such as the metric and correlation functions of the metric as long as we are more than Planck length outside the horizon.*

We believe that this is a fairly uncontroversial assumption. If the geometry obtained by averaging over all microstates differs significantly from the black-hole geometry, this has significant implications for AdS/CFT: it would imply the computations in a thermal state in the CFT should be matched to bulk computations in this special average fuzzball geometry (whatever it may be) rather than the black hole. This would be the case even for time-ordered correlators that are obtained naturally from *Euclidean computations*. Therefore any claim that expectation 2 is violated must be accompanied by an explanation for why the Euclidean saddle point is not adequate for correlators outside the horizon. We are not aware of any place in the literature where such a strong claim has been made.

Expectation 2 allows for the possibility that the average geometry to have Planck-scale deviations from the conventional geometry. We discuss these deviations in greater detail below.

**Distinct fuzzballs as a basis?** Result (3.1) implies that the geometries corresponding to *typical* states can only differ by an exponentially small amount from the average geometry. We certainly do not expect to represent such exponentially small deviations in terms of a classical metric, and therefore the idea that fuzzballs can represent typical microstates is entirely untenable. Typical microstates are represented by the *same* average geometry.

One might imagine that while it is impossible to describe the different typical microstates using geometries, perhaps one could use a set of distinguishable geometries as a *basis* for all microstates of the black hole. However, we will now show that result 3.2, together with expectation 2 constrains how much the typical element of the basis can differ from the conventional black hole. To make this precise, we pause to define some useful intermediate quantities that we will use later as well.

**The “difference” and “quantumness” parameters.** Let  $\hat{O}(r)$  be a simple *bulk* observable. For example,  $\hat{O}(r)$  may be some coordinate invariant function of the metric. Here  $r$  denotes the “radial” coordinate in a coordinate system where the horizon is at  $r = r_h$  and  $r = \infty$  is the asymptotic region. To make physical meaningful comparisons,  $r$  should be defined through the physical area of a compact submanifold in the geometry.

Let  $O^{\text{bh}}(r)$  be the expectation value of this observable in the black-hole, For a fuzzball microstate,  $|f\rangle$ , we denote

$$\langle f|\hat{O}(r)|f\rangle = O^{\text{fuzz}}(r). \quad (3.11)$$

The quantum fluctuations of this operator, in the fuzzball state, are measured by

$$\sigma^2(r) = \langle f|\hat{O}(r)^2|f\rangle - \langle f|\hat{O}(r)|f\rangle^2, \quad (3.12)$$

where the product of operators at a point may need to suitably renormalized.

We now define two parameters. The *difference parameter*,  $\mathbf{d}$  is defined as

$$\mathbf{d}_{\mathcal{O}}(r) = \left| \frac{O^{\text{bh}}(r) - O^{\text{fuzz}}(r)}{O^{\text{fuzz}}(r)} \right|. \quad (3.13)$$

The *quantumness parameter*,  $\mathfrak{q}$  is defined as

$$\mathfrak{q}_{\mathcal{O}}(r) = \left| \frac{\sigma(r)}{O^{\text{fuzz}}(r)} \right|. \quad (3.14)$$

For a classical solution to be “interesting” we require that the difference parameter be large. On the other hand, for the classical solution to be reliable, the quantumness parameter must be parametrically suppressed. This is particularly important in a non-linear theory like gravity. It makes no sense to trust classical general relativity in a regime where quantum fluctuations of the metric are of the same order as the metric itself.

We argue below that typical fuzzballs cannot meet both conditions simultaneously. In the region where they are interesting, they also become unreliable.

**Deviations of individual fuzzballs from the average geometry.** From result 3.1, the fluctuations that enter result 3.2 are the same as quantum fluctuations in a typical state. Since we argued above that typical states correspond to the conventional black-hole geometry, we can estimate the fluctuations that enter result 3.2 by estimating quantum fluctuations in the black-hole geometry.

$$\begin{aligned} \sigma_{\text{ens}}(r) &= \frac{1}{e^S} \text{Tr}_{H_E} \hat{O}(r)^2 - \left( \frac{1}{e^S} \text{Tr}_{H_E} \hat{O}(r) \right)^2 \\ &= \langle \Psi | \hat{O}(r)^2 | \Psi \rangle - \langle \Psi | \hat{O}(r) | \Psi \rangle^2 + \mathcal{O} \left( e^{-\frac{S}{2}} \right), \end{aligned} \quad (3.15)$$

where  $|\Psi\rangle$  is a typical microstate, and we have used result 3.1 in the second equality. Note that  $\sigma_{\text{ens}}(r)$  may *not* coincide with  $\sigma(r)$  defined above if  $|f\rangle$  is not a typical state.

The leading quantum fluctuations in the black-hole geometry appear with a factor of  $\frac{1}{G_N}$  and on dimensional grounds, we expect that they are proportional to  $\left(\frac{\ell}{\ell_{\text{pl}}}\right)^{d-2}$  where  $\ell$  is the typical length scale in the geometry. If we are far away from the horizon, then we expect that  $\ell \leq r_h$ . We also note that the entropy is proportional to  $\left(\frac{r_h}{\ell_{\text{pl}}}\right)^{d-2}$ . Therefore for simple gauge-invariant observables made out of the metric,

we expect that for observables with a non-zero classical expectation value<sup>1</sup>

$$\frac{\sigma_{\text{ens}}^2(r)}{(O^{\text{bh}}(r))^2} = \mathcal{O}\left(\frac{1}{S}\right), \quad r - r_h \gg \ell_{\text{pl}}. \quad (3.16)$$

(The reader may consult [59] for a concrete calculation of quantum fluctuations in the black-hole background.)

However, then result 3.2 tells us that for all but a vanishing fraction of fuzzball states, we also have

$$\mathbf{d}_{\mathcal{O}}(r) = \left| \frac{O^{\text{bh}}(r) - O^{\text{fuzz}}(r)}{O^{\text{fuzz}}(r)} \right| = \mathcal{O}\left(\frac{1}{\sqrt{S}}\right), \quad r - r_h \gg \ell_{\text{pl}}. \quad (3.17)$$

Moreover, if  $\mathbf{d}_{\mathcal{O}}$  is very small then quantum fluctuations of the metric in the fuzzball geometry are also very close to quantum fluctuations in the black-hole geometry. Therefore

$$\mathbf{q}_{\mathcal{O}}(r) = \mathcal{O}\left(\frac{1}{\sqrt{S}}\right). \quad (3.18)$$

So the deviation of the fuzzball metric from the black-hole metric can *at most* be of the same order as the quantum fluctuations of the metric.

It is important that (3.17) continues to hold when  $r = r_h + \ell_{\text{str}}$ , where  $\ell_{\text{str}}$  is the string-length. The black hole metric is corrected at the string-scale but we can compute fluctuations of the metric, using Euclidean quantum gravity, and we do *not* expect quantum fluctuations in the black-hole geometry to become significant at the string-scale.

Since, by definition, fuzzballs have no horizon they must start to deviate appreciably from the conventional black-hole geometry at some point. The argument above tells us that for typical fuzzballs, this can only happen when  $r - r_h = \mathcal{O}(\ell_{\text{pl}})$ . This is precisely where expectation 2 also allows the average geometry to deviate from the conventional geometry.<sup>2</sup>

---

<sup>1</sup>What we will need, in subsequent sections, is just that  $\frac{\sigma_{\text{ens}}(r)}{O^{\text{bh}}(r)}$  is small — not that it takes the precise value predicted by the black-hole geometry. This may hold even if expectation 2 fails: as long as the typical microstate in  $H_E$  corresponds to an approximately classical geometry, we can estimate  $\sigma_{\text{ens}}$  by quantizing metric fluctuations in this geometry, and these quantum fluctuations will be small compared provided that typical curvatures are small.

<sup>2</sup>Standard calculations in the conventional black-hole geometry suggest that when the geometry has a macroscopic horizon, we do *not* expect any unusual effects in the near-horizon region and

But this means that the geometric solution — corresponding to a typical basis state or the average geometry — must explicitly have *Planck-scale* structures, presumably through an explicit length-scale that takes on a Planck-scale value. However, we expect that any length-scale in quantum gravity will itself undergo fluctuations of the size of the Planck-scale. Therefore, in the region where we are very close to the horizon, if the fuzzball has explicit Planck scale features, then quantum fluctuations in the metric are expected to be of the same order as these Planck-scale structures. So,

$$\mathbf{d}_{\mathcal{O}}(r) = \mathcal{O}(1), \quad \text{but} \quad \mathbf{q}_{\mathcal{O}}(r) = \mathcal{O}(1), \quad \text{when} \quad r - r_h = \mathcal{O}(\ell_{\text{pl}}). \quad (3.19)$$

But if the parameter  $\mathbf{q}_{\mathcal{O}} = \mathcal{O}(1)$ , then the classical solution becomes completely unreliable. So, if we explicitly insert Planck-scale features into the fuzzball solution in order to satisfy result 3.2, then we run into the difficulty that the geometry becomes unreliable just where it appears to be interesting.

To summarize, we have argued the following. If fuzzballs are to represent typical microstates then they must have the following features:

1. When we are far away from the horizon (in Planck units), the fuzzball geometry is indistinguishable from the black-hole geometry up to terms that are suppressed by the black-hole entropy. This follows from the fact that the *average* fluctuations of the metric — which can be computed in the black-hole geometry — are small, and then result 3.2 limits the extent to which typical basis elements can differ from the average.
2. When we approach within a Planck length of the horizon, the fuzzball geometry may appear to deviate from the conventional black hole. But such a geometry must explicitly contain Planckian structures, and then we expect that quantum fluctuations will become large and so the fuzzball geometry becomes unreliable. (Note that this is contrast to the conventional black-hole geometry, which

---

$\sigma_{\text{ens}}$  continues to be small there. However, it is difficult to *prove* this even in holography, since the HKLL construction requires very long time-bands on the boundary to represent physics in the region  $r - r_h = \mathcal{O}(\ell_{\text{pl}})$ . The length of these bands scales with  $N$  and may interfere with standard large- $N$  counting. So we make a generous assumption for the fuzzball program by allowing the possibility that some unknown hitherto unknown effect invalidates the standard calculation of  $\sigma_{\text{ens}}$  within a Planck length of the horizon and somehow makes it large.

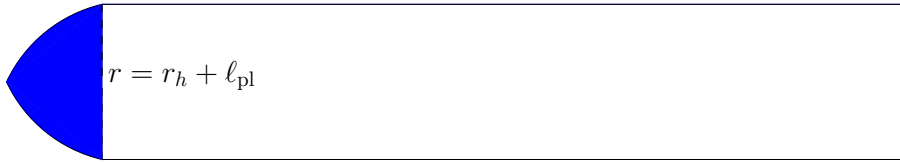


Figure 3.4: A schematic representation of what a typical fuzzball geometry must look like, if fuzzballs represent black-hole microstates. The geometry must closely resemble the black-hole geometry away from the horizon (unshaded region) and then suddenly deviate away to cause some extra-dimension to pinch off when we reach within Planck length of the horizon (blue region).

remains perfectly reliable close to the horizon.)

This picture of the fuzzball is shown schematically in Figure 3.4

Therefore, *it is wrong to think of fuzzballs as macroscopically distinct geometries, which somehow average out to give the same answer as the black hole.* Rather, typical fuzzballs must all look like Figure 3.4 to satisfy result 3.2. Fuzzballs which have structure on a scale larger than the Planck scale can only be a vanishing fraction of microstates by result 3.2.

**Requirement of large red-shifts.** The discussion above utilizes expectation 2, which is what leads to equation (3.16). However, even without invoking expectation 2, we can still use expectation 1 to justify the important aspects of the picture shown in Figure 3.4.

Consider a quantum field that propagates in the bulk whose excitations about the vacuum are gapped. In global AdS we can consider a massless field. If we are considering flat space or Poincare AdS, we can consider a massive field. Then expectation 1 implies that the *asymptotic* two-point function of this field must be supported at arbitrary frequencies even though, locally, field excitations are gapped.

The reason that black holes allow this phenomenon is because of the infinite redshift at the horizon. This red-shift allows for arbitrary low-energy excitations. This is *not* a bug; it is a *feature* of the black-hole geometry which ensures that it can be interpreted as a heavy state in a quantum-mechanical system with large entropy.

If fuzzballs are to represent black-hole microstates, they must also support a continuous spectrum. Therefore, the fuzzball geometry must also have an extremely

large-shift. In particular, *if the geometry caps off to form a fuzzball at any length-scale that is visible classically, then the inverse of this length-scale will be visible as an energy gap that would violate expectation 1*. Once again we see that the requirement of an almost continuous spectrum disallows fuzzballs that are of size  $\ell_{\text{str}}$  or any other classical length-scale.

What if the geometry caps off at  $r = r_h + \ell_{\text{pl}}$ ? Even such a geometry would not support the exponentially suppressed gap that is required around a heavy pure state since it would allow, at most, an energy gap that is power-law suppressed in the entropy. So the only possibility is for the geometry to stop making sense classically below  $r = r_h + \ell_{\text{pl}}$ . However if this happens we return to our conclusion above, displayed in Figure 3.4: fuzzballs are uninteresting in most of space (where  $r - r_h \gg \ell_{\text{pl}}$ ) and unreliable where they are interesting ( $r - r_h = \mathcal{O}(\ell_{\text{pl}})$ ).

Larger fuzzballs that are both reliable and interesting by virtue of having larger than Planck scale structure are *irrelevant* to the discussion of black-hole microstates since they do not have the right energy gap expected in a system with large entropy.

**Eigenstate thermalization.** The arguments that led to the structure expected from typical fuzzball geometries shown in Figure 3.4 assumed that the bulk metric was a good observable with small quantum fluctuations. We believe that this is a very robust assumption.

However, if we assume the ETH, then we can deduce such a structure for typical fuzzballs while restricting our discussion to only asymptotic observables. If we apply the ETH in the form (3.10) to fuzzball states, then we expect to get the microcanonical average

$$\langle f|A|f \rangle = A(E), \tag{3.20}$$

where  $E$  is the energy of the fuzzball state and  $A(E)$  is the microcanonical average of  $A$ .

Therefore, the ETH tells us that even for asymptotic observables, we should get precisely the same value in a typical fuzzball microstate as we do in the conventional black hole.

Intuitively, this rules out fuzzballs that differ at leading order from the black-hole metric. This is because if the geometry differs at leading order, then a simple scattering experiment with waves sent in from asymptotic infinity will detect this

variation and produce an answer that fails to satisfy the ETH. We will see in section 3.4 that this is precisely what happens for fuzzballs with macroscopic structures.

**A cautionary note.** We close this subsection with a note of caution. The reader will note that our arguments above have been based on simple physical expectations and general results from statistical mechanics. This makes them broadly applicable but it also means that these arguments are only suggestive of the difficulties that the fuzzball program must surmount and cannot be taken as a proof that the program is not viable.

In section 3.3 and 3.4 we will verify the correctness of these arguments in specific examples. But if the fuzzball program is to be carried through to completion in any system, this must involve a loophole in the arguments outlined above, and it would be interesting to understand the origins of such a loophole.

### 3.2.3 Indirect arguments for horizon structure

In an attempt to sidestep arguments of the kind that we have provided above, Mathur put forward indirect arguments to show that the horizon must have structure [20]. Mathur’s argument was based on the strong subadditivity and it was later used to produce the firewall paradox [22]. See section 1.2 for details.

The difficulty with this argument is that the strong-subadditivity of entropy *assumes* that the set of observables on a nice slice factorize into observables in the black hole interior, a near horizon region just outside the horizon and everything else. However, we have already seen in chapter 2 that in quantum-gravity this is simply not true. To the contrary, observables near the boundary already contain all observables. See [7, 60, 61] for related results which demonstrate breakdown of locality in quantum gravity. In fact, it was shown in [61] that if we take strong-subadditivity seriously in quantum gravity, we can construct paradoxes even in empty AdS.

Modification to classical black hole geometry is not required for recovery of information from the Hawking radiation as information can be stored in exponentially small correlations between different Hawking quanta [62].

A related set of ideas suggests that a pure-state cannot have a horizon, because a horizon has entropy whereas pure states cannot have entropy [63]. However, this

is incorrect. The thermodynamic entropy should not be conflated with the von Neumann entropy. So, pure-states can also have thermodynamic entropy which arises after we coarse-grain the system and this entropy reflects the fact that coarse-grained probes of the system leave its fine-grained features undetermined [64]. In a theory of quantum gravity, the geometry is a tool to encode expectation values of the metric and its low-point correlators — it is thus an explicitly coarse-grained probe of the full theory. So it is perfectly consistent for the geometry to be described by a metric with a horizon whose entropy reflects the fact that we have ignored the fine-grained *non-metric* degrees of freedom that are part of the full description.

We note, parenthetically, that in anti-de Sitter space, the papers [65, 66] made an entirely independent set of arguments to suggest that the black-hole interior cannot be represented in the boundary CFT. These arguments are relevant for large AdS black holes that are thermodynamically stable. Moreover, even if they are correct, they suggest that the black hole has a horizon and the interior of a black hole has a firewall rather than a fuzzball. For this reason the arguments of [65, 66] are not directly relevant here, and a detailed discussion of their merits is beyond the scope of this thesis. Nevertheless, a brief summary of their status is as follows.

Several authors [67, 68, 69, 70, 71] have pointed out that interior operators can be constructed using a suitably state-dependent construction. The authors of [72] suggested that state-dependence would lead to observable peculiarities for an infalling observer but it was explained in [73] that these effects were not observable in physically reasonable experiments.

Physically, our understanding of the origins of state-dependence has also advanced. The state-dependence of the interior can be understood as arising from a fat-tail in the inner-product of coherent states in gravity [69, 70] and this fat-tail also contributes to the fact that interior operators, when gauge-fixed in a particular manner, may fail to satisfy a non-perturbative version of the Hamiltonian constraints [74]. The origins of state-dependence can also be studied in toy-models [75]. Of course, several questions about state-dependence and the reconstruction of the black-hole interior in AdS/CFT remain to be understood.

To summarize this subsection, we have argued that indirect arguments for the relevance of fuzzballs to black-holes are invalid. This is an important point. It shows that one cannot concede the limitations of supergravity solutions — as is sometimes

done in the fuzzball program — but yet argue that black-holes do not have smooth interiors. *Neither a resolution to the information paradox nor an understanding of the black-hole entropy requires the existence of fuzzballs.* The relevance, or lack thereof, of fuzzballs to the study of black-holes must follow from a study of the known fuzzball solutions. If these solutions are irrelevant to black-holes, there is *no other valid argument for the relevance of fuzzballs* for black-holes.

### 3.3 Quantum aspects of the two-charge solutions

In this section, we examine the original two-charge fuzzball solutions that were discovered in [11, 12]. The literature on these solutions, and their relation to CFT microstates is extensive. Our analysis will be simple and independent, but we note a few salient results in the literature. In [76] and then in [77], it was pointed out that the supergravity solution was not valid for typical states and as one travels towards the fuzzball cap, it is necessary to transition out of the D1-D5 duality frame. This can indeed be done in some cases, and for specific solutions the full stringy description was analyzed in [78]. We will reach a similar conclusion, although our reasoning will be slightly different and placed within the framework developed in section 3.2.

There has also been work on identifying specific solutions with microstates in the orbifold CFT [79]. We note that even for very simple states, such an identification must be performed carefully since the supergravity point is very far from the orbifold point in the D1-D5 moduli space and, moreover, states *cannot* be uniquely identified just by specifying one-point functions of a few operators. In fact, in general, such an identification is impossible since the matching between states at different points in moduli-space is path-dependent [80]. Holographic correlators have also been calculated in these solutions [81] as we will do for multi-charge solutions in section 3.4.

For us, what is important, is that these solutions were quantized in [13], following a suggestion made in [82]. Therefore, we can study the quantum mechanics of this set of solutions and we will use this system to *verify* the arguments of section 3.2. We will compute the *average* fuzzball geometry, and we will also compute *quantum fluctuations* in this geometry. This allows us to compute the parameters  $\mathbf{d}$  (defined

in (3.13)) and  $\mathbf{q}$  (defined in (3.14)). This system differs slightly from the setup of section 3.2 because the horizon of the conventional solution is of zero size because a circle in the geometry shrinks to zero at that point. Nevertheless — using the size of this circle as a measure of the distance from this zero-size horizon — we find that

1. As the distance from the position of the conventional horizon becomes greater than the Planck length, the average fuzzball geometry tends rapidly to the classical geometry.
2. The average geometry starts deviating from the conventional geometry when we are within Planck length, and *not* string length, of the horizon. Moreover, most of the entropy of the set of solutions comes from solutions that differ from the conventional geometry at the Planck scale.
3. In the region where deviations of the average geometry from the conventional geometry are appreciable, quantum fluctuations are of the same order as the expectation values of components of the metric. Therefore the solution is entirely unreliable.

We will consider the two-charge solutions in the following form, using the conventions of [13].

$$\begin{aligned}
 ds^2 &= e^{-\frac{\phi}{2}} ds_{\text{str}}^2; & e^{-2\phi} &= \frac{f_5}{f_1}; \\
 ds_{\text{str}}^2 &= \frac{1}{\sqrt{f_1 f_5}} \left( -(dt + A)^2 + (dy + B)^2 \right) + \sqrt{f_1 f_5} d\vec{x}^2 + \sqrt{\frac{f_1}{f_5}} d\vec{z}^2; \\
 f_5 &= 1 + \frac{Q_5}{L} \int_0^L \frac{ds}{|\vec{x} - \vec{F}(s)|^2}; & f_1 &= 1 + \frac{Q_5}{L} \int_0^L \frac{|\vec{F}'(s)|^2}{|\vec{x} - \vec{F}(s)|^2}; \\
 A_i &= \frac{Q_5}{L} dx^i \int_0^L \frac{F'_i(s)}{|\vec{x} - \vec{F}(s)|^2} ds; & dB &= *_4 dA; \\
 C &= \frac{1}{f_1} (dt + A) \wedge (dy + B) + \mathcal{C}; & d\mathcal{C} &= - *_4 df_5.
 \end{aligned} \tag{3.21}$$

Here  $\vec{z}$  denotes four compact directions. The conventional solution is obtained simply by setting

$$f_1 \rightarrow 1 + \frac{Q_1}{\vec{x}^2}; \quad f_5 \rightarrow 1 + \frac{Q_5}{\vec{x}^2}. \tag{3.22}$$

and setting  $A = 0, B = 0$ .

These solutions can be systematically quantized by recognizing that the space of classical solutions can be bijectively mapped to points on the phase space; the action of the theory yields a symplectic form on this space, and the machinery of geometric quantization can then be applied to obtain a Hilbert space [83]. The result of this process is very simple. The quantization promotes the functions  $F^k(s)$  to operators as follows

$$F^k(s) = \mu \sum_{n>0} \frac{1}{\sqrt{2n}} \left( a_n^k e^{-\frac{2\pi i n s}{L}} + (a_n^k)^\dagger e^{\frac{2\pi i n s}{L}} \right), \quad (3.23)$$

where  $[a_n, a_m^\dagger] = \delta_{nm}$ . The various parameters that appear here are defined as

$$\mu = \frac{g_s}{R\sqrt{V_4}}; \quad L = \frac{2\pi Q_5}{R}. \quad (3.24)$$

Here  $R$  is the coordinate radius of the  $y$ -direction and  $V_4$  is the coordinate volume of the compact manifold. These are moduli of the solution. We are working in units where the *string length is set to unity*. The charges are related to the brane-numbers by

$$Q_5 = g_s N_5; \quad Q_1 = \frac{g_s N_1}{V_4}. \quad (3.25)$$

For the purposes of counting states, it will be useful to define the following ‘‘Hamiltonian’’

$$H = \sum_{n>0, k} n (a_n^k)^\dagger a_n^k, \quad (3.26)$$

where we have a infinite set of harmonic oscillators with creation and annihilation operators specified by  $a_n^k$  and  $k$  runs over  $1 \dots 4$ . The fuzzball states dual to the D1-D5 system with charges  $(Q_1, Q_5)$  are defined to be the states in this quantum system that have  $H = N_1 N_5$ .

We will not attempt to compute the full quantum expectation value of the metric. Instead, we will focus on the following list of quantum expectation values,

$$\langle \Psi | f_5 - 1 | \Psi \rangle, \quad \langle \Psi | f_1 - 1 | \Psi \rangle, \quad \langle \Psi | A_i | \Psi \rangle, \quad (3.27)$$

in a typical state,  $|\Psi\rangle$ . Here, ‘‘typical state’’ is used in the sense of result 3.1. These one-point expectation values were also calculated in [84], and our results

agree precisely with theirs. We will not consider  $B_i$  separately since this field is defined through the dual of  $A$ . Note that we also subtract off the uninteresting 1 in both  $f_1$  and  $f_5$ .

$A_i$  vanishes in the conventional geometry, and it will turn out that  $\langle \Psi | A_i | \Psi \rangle$  also vanishes. So the difference and quantumness parameters ((3.13) and (3.14)) are not well defined for this observable. Therefore, we will consider another one-form that does not appear in the metric but is also an interesting probe of the geometry

$$W_i = \frac{Q_5}{L} \int_0^L \frac{F_i(s)}{|\vec{x} - \vec{F}(s)|^2} ds. \quad (3.28)$$

This quantity is of interest since it vanishes in the conventional geometry but, as we will find,  $\langle \Psi | W_i | \Psi \rangle$  takes on a finite value. So one can ask if this finite value is reliable.

We will also compute the quantum fluctuations in these quantities by computing the following quantum two-point functions

$$\langle \Psi | (f_5 - 1)^2 | \Psi \rangle, \quad \langle \Psi | (f_1 - 1)^2 | \Psi \rangle, \quad \langle \Psi | W_i W_j | \Psi \rangle. \quad (3.29)$$

We will use these two-point functions to evaluate the difference and quantumness parameters for these observables. These calculations will allow us to verify all the expectations outlined in section 3.2 in a precise setting.

### 3.3.1 One-point functions

Using result 3.1, the expectation value of the observables above in a typical state can be computed by considering the microcanonical trace. Therefore, we can consider the generating function

$$\mathcal{G}(\chi, \alpha) = \frac{1}{e^{S(E)}} \text{Tr}_{\text{mic}} \left[ \int_{-\infty}^{\infty} \prod_k dg_k \int_0^{\infty} dt \int_0^L \frac{ds}{L} : e^{\mathcal{F}} : \left( \frac{t}{\pi} \right)^2 \right], \quad (3.30)$$

where

$$\mathcal{F} = - \sum_k t g_k g_k + 2it(x^k - F^k(s))g_k + \sum_j \alpha^j F^j(s) + \chi^j \frac{dF^j(s)}{ds}. \quad (3.31)$$

Here the trace is taken over all energy eigenstates of the Hamiltonian with a large total energy,

$$E = N_1 N_5, \quad (3.32)$$

and the degeneracy of states at that energy is given by  $e^{S(E)}$ . By normal ordering we mean that when we expand the exponential in terms of creation and annihilation operators, we move all annihilation operators to the right. This, of course, involves a necessary choice of how to interpret the quantum operator corresponding to the classical quantity.

From result 3.1, in a typical microstate  $|\Psi\rangle$ , we expect

$$\begin{aligned} \langle \Psi | f_5 | \Psi \rangle &= 1 + Q_5 \mathcal{G}(\chi = 0, \alpha = 0); \\ \langle \Psi | f_1 | \Psi \rangle &= 1 + Q_5 \lim_{\chi \rightarrow 0} \frac{\partial}{\partial \chi^i} \frac{\partial}{\partial \chi^i} \mathcal{G}(\chi, \alpha = 0); \\ \langle \Psi | A_i | \Psi \rangle &= Q_5 \lim_{\chi \rightarrow 0} \frac{\partial}{\partial \chi^i} \mathcal{G}(\chi, \alpha = 0); \\ \langle \Psi | W_i | \Psi \rangle &= Q_5 \lim_{\alpha \rightarrow 0} \frac{\partial}{\partial \alpha^i} \mathcal{G}(\chi = 0, \alpha). \end{aligned} \quad (3.33)$$

We can equivalently compute this object by using the equivalence of the canonical and microcanonical ensemble at large  $S(E)$

$$\mathcal{G}_\beta(\chi, \alpha) = \frac{1}{Z(\beta)} \text{Tr} \left[ e^{-\beta H} \int_{-\infty}^{\infty} \prod_k dg_k \int_0^{\infty} dt \int_0^L \frac{ds}{L} : e^{\mathcal{F}} : \left( \frac{t}{\pi} \right)^2 \right], \quad (3.34)$$

where the “temperature”,  $\beta^{-1}$ , is set by demanding that the expectation value of the Hamiltonian be  $N_1 N_5$  and  $Z(\beta) = \text{Tr}(e^{-\beta H})$ . The equivalence of ensembles implies that

$$\mathcal{G}_\beta(\chi, \alpha) = \mathcal{G}(\chi, \alpha) + \mathcal{O} \left( \frac{1}{\sqrt{S(E)}} \right), \quad (3.35)$$

and this accuracy is sufficient for our purpose. Similarly, the thermal expectation values,  $\langle f_5 \rangle_\beta, \langle f_1 \rangle_\beta, \langle W_i \rangle_\beta$  obtained from this generating function match the typical expectation values of (3.33) up to terms suppressed by the entropy.

Before evaluating the traces we need, we remind the reader of a few simple results. If we consider a *single* simple harmonic oscillator, corresponding to a given value of  $n$  and  $k$ , then in a number eigenstate of that oscillator,  $|N_n^k\rangle$ , for any values of the

c-number coefficients  $c_n^k$  and  $d_n^k$ , we have

$$\langle N_n^k | e^{c_n^k (a_n^k)^\dagger} e^{d_n^k a_n^k} | N_n^k \rangle = \sum_{r=0}^N \frac{N!}{(N-r)!(r!)^2} (c_n^k d_n^k)^r = \sum_{r=0}^{\infty} \frac{N_n^k (N_n^k - 1) \dots (N_n^k - r + 1)}{(r!)^2} (c_n^k d_n^k)^r. \quad (3.36)$$

Here in the last step, we have simply noted that the sum over  $r$  can be extended till  $\infty$ . All terms larger than  $N$  vanish because of the factor of  $(N - r + 1)$  in the numerator. If we take the thermal trace and denote  $z = e^{-\beta}$ , we find

$$\begin{aligned} \text{Tr} \left( e^{-\beta n N_n^k} e^{c_n^k (a_n^k)^\dagger} e^{d_n^k a_n^k} \right) &= \sum_{N_n^k=0}^{\infty} \sum_{r=0}^{\infty} \frac{N_n^k (N_n^k - 1) \dots (N_n^k - r + 1)}{(r!)^2} z^{n N_n^k} (c_n^k d_n^k)^r \\ &= \frac{1}{1 - z^n} \exp \left( \frac{c_n^k d_n^k z^n}{1 - z^n} \right), \end{aligned} \quad (3.37)$$

where we have used the identity

$$\sum_{N=0}^{\infty} N(N-1) \dots (N-r+1) x^N = r! \frac{x^r}{(1-x)^{r+1}}. \quad (3.38)$$

We now note that

$$\begin{aligned} \mathcal{F} &= \sum_{k,n} \frac{\mu e^{-\frac{2i\pi ns}{L}} a_n^k (-2itg_k + \alpha_k - i\frac{2\pi n}{L} \chi_k)}{\sqrt{2nL}} + \frac{\mu e^{\frac{2i\pi ns}{L}} (a_n^k)^\dagger (-2itg_k + \alpha_k + i\frac{2\pi n}{L} \chi_k)}{\sqrt{2n}} \\ &\quad - \sum_k tg_k (g_k - 2ix_k). \end{aligned} \quad (3.39)$$

The expression above is just in the form we need. We see that the thermal trace breaks up into a product of the traces over individual oscillator sectors, and moreover that for each oscillator the coefficients  $c_n^k$  and  $d_n^k$  can be identified from the expression

above. This leads to

$$\begin{aligned} \text{Tr}(e^{-\beta H} : e^{\mathcal{F}} :) = \exp & \left[ \sum_k 2itg_k x_k - tg_k^2 + \sum_n \log(1 - z^n) \right. \\ & \left. + \sum_n \frac{1}{1 - z^n} \left( \frac{-2\mu^2 t^2 g_k^2 z^n}{n} - \frac{2i\mu^2 t g_k \alpha_k z^n}{n} + \frac{2\pi^2 \mu^2 n \chi_k^2 z^n}{L^2} + \frac{\mu^2 \alpha_k^2 z^n}{2n} \right) \right]. \end{aligned} \quad (3.40)$$

Note that if we take the limit  $t, g_k, \alpha_k, \chi_k \rightarrow 0$  in (3.40), we simply get the partition function, which is

$$Z(\beta) = e^{\sum_{n,k} \log(1 - z^n)}. \quad (3.41)$$

We can expand the logarithm in a power series and the interchange the order of sums to get

$$Z(\beta) = \exp \left[ d \sum_{n,m} \frac{1}{m} z^{nm} \right] = \exp \left[ d \sum_m \frac{z^m}{m(1 - z^m)} \right]. \quad (3.42)$$

At high temperatures, we can approximate

$$\sum_m \frac{z^m}{m(1 - z^m)} = \sum_m \frac{1}{m^2 \beta} + O(1) = \frac{\pi^2}{6\beta} (1 + O(\beta)). \quad (3.43)$$

and therefore,

$$Z(\beta) = e^{\frac{2\pi^2}{6\beta}}, \quad (3.44)$$

where we have dropped the  $O(\beta)$  errors that should be understood and will not be displayed explicitly again.

From the partition function above, we find that the temperature and the energy (at large energies) are related through

$$E = \frac{2\pi^2}{3\beta^2}. \quad (3.45)$$

Moreover, the degeneracy of states at a given energy is given by

$$S(E) = \frac{4\pi^2}{3\beta} = 2\pi \sqrt{\frac{2E}{3}} = 2\pi \sqrt{\frac{2N_1 N_5}{3}}. \quad (3.46)$$

To evaluate the expression in (3.40), we need to evaluate one more infinite sum over  $n$ .

$$\sum_{n=1}^{\infty} \frac{ne^{-\beta n}}{1 - e^{-\beta n}} = \sum_{n=1, m=1}^{\infty} ne^{-\beta nm} = \sum_{m=1}^{\infty} \frac{e^{-\beta m}}{(1 - e^{-\beta m})^2} \xrightarrow{\beta \rightarrow \infty} \frac{\pi^2}{6\beta^2} + \mathcal{O}\left(\frac{1}{\beta}\right). \quad (3.47)$$

Therefore we find at “high temperatures” that

$$\begin{aligned} \mathcal{G}_\beta(\chi, \alpha) &= \int \prod_k dg_k dt \frac{ds}{L} \left(\frac{t}{\pi}\right)^2 e^{\sum_k \left[ -\left(\frac{\pi^2 \mu^2 t^2}{3\beta} + t\right) g_k^2 - g_k \left(\frac{i\pi^2 \mu^2 t \alpha_k}{3\beta} + 2itx_k\right) + \frac{\pi^2 \mu^2 \alpha_k^2}{12\beta} + \frac{\pi^4 \mu^2 \chi_k^2}{3\beta^2 L^2} \right]} \\ &= \int dt \frac{ds}{L} 9\beta^2 e^{\left(\frac{\frac{\pi^4 \mu^2 \bar{\chi}^2}{3\beta^2 L^2} + \frac{\pi^2 \bar{\alpha}^2 \mu^2 + 4t(\pi^2 \mu^2 \bar{x} \cdot \bar{\alpha} - 3\beta r^2)}{4(3\beta + \pi^2 \mu^2 t)}}\right)} \\ &= \frac{36\beta^2 e^{\frac{\pi^4 \mu^2 \bar{\chi}^2}{3\beta^2 L^2} - \frac{3\beta r^2}{\pi^2 \mu^2}} \left( e^{\frac{\pi^2 \bar{\alpha}^2 \mu^2}{12\beta} + \frac{3\beta r^2}{\pi^2 \mu^2}} - e^{\bar{x} \cdot \bar{\alpha}} \right)}{\pi^4 \bar{\alpha}^2 \mu^4 + 36\beta^2 r^2 - 12\pi^2 \beta \mu^2 \bar{x} \cdot \bar{\alpha}}, \end{aligned} \quad (3.48)$$

where  $r^2 = \sum_k x^k x^k$ .

From this generating function we can immediately read off the various “thermal” expectation values. We find that

$$\begin{aligned} \langle f_5 - 1 \rangle_\beta &= Q_5 \frac{1 - e^{-\frac{r^2}{\tau}}}{r^2}; \\ \langle f_1 - 1 \rangle_\beta &= Q_5 \frac{24\tau^2 \left(1 - e^{-\frac{r^2}{\tau}}\right)}{\mu^2 L^2 r^2} = Q_1 \frac{\left(1 - e^{-\frac{r^2}{\tau}}\right)}{r^2}; \\ \langle A_i \rangle_\beta &= 0; \\ \langle W_i \rangle_\beta &= -Q_5 \frac{\tau x_i e^{-\frac{r^2}{\tau}} \left(1 - e^{\frac{r^2}{\tau}} + \frac{r^2}{\tau}\right)}{r^4}. \end{aligned} \quad (3.49)$$

where

$$\tau = \frac{\pi^2 \mu^2}{3\beta}, \quad (3.50)$$

In the second line of (3.49) we noted that

$$\frac{24\tau^2}{\mu^2 L^2} = \frac{8\pi^4 \mu^2}{3\beta^2 L^2} = \frac{Q_1}{Q_5}. \quad (3.51)$$

As advertised,  $\langle A_i \rangle_\beta$  vanishes in the average fuzzball metric.

### Analysis of one-point functions

The expressions in (3.49) start deviating from the conventional expressions when  $r^2 = \tau$ . To understand this physically, we consider the radius of the  $y$ -circle when  $r^2 = \tau$  in the *conventional* metric. We see that this radius (in the Einstein frame) is given by

$$R_{\text{stretch}}^2 = \left(\frac{Q_5}{Q_1}\right)^{\frac{1}{4}} \left(\frac{1}{Q_1 Q_5}\right)^{\frac{1}{2}} \tau R^2. \quad (3.52)$$

Note that we have

$$\tau = \frac{\mu^2 \pi^2}{3\beta} = \frac{\mu^2 S(E)}{4} = \frac{g_s^2 S(E)}{4R^2 V_4}, \quad (3.53)$$

where we used the fact that  $\mu^2 = \frac{g_s^2}{R^2 V_4}$ . We also note that the volume of the compact manifold in the string frame is given by  $V_{\text{com}} = \left(\frac{Q_1}{Q_5}\right) V_4$ .

Putting all these factors together, and using (3.25) and (3.46), we find

$$R_{\text{stretch}}^2 = \left(\frac{Q_5}{Q_1}\right)^{\frac{1}{4}} \left(\frac{V_4}{g_s^2 N_1 N_5}\right)^{\frac{1}{2}} \frac{g_s^2 2\pi \sqrt{\frac{2N_1 N_5}{3}}}{4V_4} = \left(\frac{Q_1}{Q_5}\right)^{\frac{1}{4}} \frac{\pi}{2} \sqrt{\frac{2}{3}} \frac{g_s}{\sqrt{V_{\text{com}}}}. \quad (3.54)$$

In these units, where string scale is set to unity, the fundamental (10 dimensional) Planck scale is simply given by  $\ell_{\text{pl}}^8 = g_s^2$ . Therefore we have found that

$$R_{\text{stretch}}^2 = \frac{\pi}{2} \sqrt{\frac{2}{3}} \left(\frac{Q_1}{Q_5}\right)^{\frac{1}{4}} \frac{\ell_{\text{pl}}^4}{\sqrt{V_{\text{com}}}}. \quad (3.55)$$

Now, we should work in the duality frame, where the physical volume of the compact manifold is at least  $V_{\text{com}} \geq 1$  in string-units. If we are not in such a frame, we should use T-duality in the compact directions to reach such a frame. Moreover, we should work in the duality frame where the dilaton does not blow up at this point in space, and therefore we need  $\frac{Q_1}{Q_5} = \mathcal{O}(1)$ . Just as above, if this constraint is not

met, we can use the U-duality group to change the values of  $N_1, N_5$  while keeping  $N_1 N_5$  constant to reach such a duality frame. Putting these physical constraints into (3.55), we see that

$$R_{\text{stretch}} \ll O(\ell_{\text{pl}}). \quad (3.56)$$

Therefore, in the average fuzzball solution, the metric starts to differ from the conventional metric when the  $y$ -circle has a size that is smaller than the Planck length. The solution is *completely unreliable* since, well before this size is reached, classical string effects become important that have not been taken into account in obtaining the solution (3.21). Moreover, in this region, as one might expect — and as we compute explicitly in the next subsection — quantum fluctuations in the geometry are as large as various classical expectation values. This implies that we should *not* take (3.21) with the substitutions (3.49) seriously as a quantum-corrected geometry.

### 3.3.2 Fluctuations

We now compute the quantum fluctuations in the thermally averaged ensemble as an input to computing the quantumness parameters for these quantities. We do not compute these parameters for  $A_i$ , since it vanishes both in the conventional geometry and the black hole. We consider the generating function of the variance

$$\mathcal{V}_\beta(\chi, \alpha, \tilde{\chi}, \tilde{\alpha}) = \frac{1}{Z(\beta)} \text{Tr} \left[ e^{-\beta H} \int_{-\infty}^{\infty} \prod_k dg_k d\tilde{g}_k \int_0^{\infty} dt d\tilde{t} \int_0^L \frac{ds d\tilde{s}}{L^2} \left( \frac{t\tilde{t}}{\pi^2} \right)^2 : e^{\mathcal{F}} :: e^{\tilde{\mathcal{F}}} : \right], \quad (3.57)$$

where

$$\tilde{\mathcal{F}} = - \sum_k \tilde{t} \tilde{g}_k \tilde{g}_k + 2i\tilde{t}(x^k - F^k(\tilde{s}))\tilde{g}_k + \sum_j \tilde{\alpha}^j F^j(\tilde{s}) + \tilde{\chi}^j \frac{dF^j(\tilde{s})}{d\tilde{s}}. \quad (3.58)$$

(Note that  $\mathcal{F}$  and  $\tilde{\mathcal{F}}$  share the same value of  $x$ .) We can then obtain the required two-point functions by differentiation

$$\begin{aligned} \langle (f_5 - 1)^2 \rangle_\beta &= Q_5^2 \mathcal{V}_\beta(\chi = 0, \tilde{\chi} = 0, \alpha = 0, \tilde{\alpha} = 0); \\ \langle (f_1 - 1)^2 \rangle_\beta &= Q_5^2 \lim_{\chi^i, \tilde{\chi}^i \rightarrow 0} \sum_{i,j} \frac{\partial^4}{\partial^2 \chi^i \partial^2 \tilde{\chi}^i} \mathcal{V}_\beta(\chi, \tilde{\chi}, \alpha = 0, \tilde{\alpha} = 0); \\ \langle W_i W_j \rangle_\beta &= Q_5^2 \lim_{\alpha^i, \tilde{\alpha}^i \rightarrow 0} \frac{\partial^2}{\partial \alpha_i \partial \tilde{\alpha}_j} \mathcal{V}_\beta(\chi = 0, \alpha, \tilde{\chi} = 0, \tilde{\alpha}); \end{aligned} \quad (3.59)$$

By the equivalence of ensembles these variances coincide with microcanonical variances up to terms suppressed by the entropy. Then, by result 3.1 these variances also coincide with variances computed in a typical state:

$$\langle (f_5 - 1)^2 \rangle_\beta = \langle \Psi | (f_5 - 1)^2 | \Psi \rangle + \mathcal{O}\left(\frac{1}{\sqrt{S(E)}}\right), \quad (3.60)$$

and similarly for  $\langle (f_1 - 1)^2 \rangle_\beta$  and  $\langle W_i W_j \rangle_\beta$ .

The computation of the variance is considerably more involved than the computation of the expectation value. So, we will not compute the function  $\mathcal{V}_\beta$  for arbitrary values of its parameters, but simply compute the derivatives and limits that we are interested in.

First we note that

$$: e^{\mathcal{F}} :: e^{\tilde{\mathcal{F}}} := e^{\mathcal{F} + \tilde{\mathcal{F}}} : e^{\mathcal{N}}, \quad (3.61)$$

where the normal ordering constant  $\mathcal{N}$  arises because we need to move the creation operators inside  $\tilde{\mathcal{F}}$  past the annihilation operators of  $\mathcal{F}$ . This can be easily done through the formula

$$e^{c_n^k a_n^k} e^{d_n^k (a_n^k)^\dagger} = e^{d_n^k (a_n^k)^\dagger} e^{c_n^k a_n^k} e^{c_n^k a_n^k}. \quad (3.62)$$

In our case, we find that

$$\begin{aligned}
 \mathcal{N} &= \sum_{n,k} e^{\frac{2\pi i n(\tilde{s}-s)}{L}} \left[ \frac{1}{n} \left( -2\mu^2 t \tilde{t} g_k \tilde{g}_k - i\mu^2 t g_k \tilde{\alpha}_k - i\mu^2 \tilde{t} \tilde{g}_k \alpha_k + \frac{1}{2} \mu^2 \alpha_k \tilde{\alpha}_k \right) \right. \\
 &\quad \left. + \left( \frac{2\pi \mu^2 t g_k \tilde{\chi}_k}{L} - \frac{2\pi \mu^2 \tilde{t} \tilde{g}_k \chi_k}{L} + \frac{i\pi \mu^2 \alpha_k \tilde{\chi}_k}{L} - \frac{i\pi \mu^2 \tilde{\alpha}_k \chi_k}{L} \right) + \frac{2\pi^2 n \mu^2 \chi_k \tilde{\chi}_k}{L^2} \right] \\
 &= \left[ -\log(1 - e^{\frac{2\pi i(\tilde{s}-s)}{L}}) \left( -2\mu^2 t \tilde{t} g_k \tilde{g}_k - i\mu^2 t g_k \tilde{\alpha}_k - i\mu^2 \tilde{t} \tilde{g}_k \alpha_k + \frac{1}{2} \mu^2 \alpha_k \tilde{\alpha}_k \right) \right. \\
 &\quad \left. + \frac{1}{(1 - e^{\frac{2\pi i(\tilde{s}-s)}{L}})} \left( \frac{2\pi \mu^2 t g_k \tilde{\chi}_k}{L} - \frac{2\pi \mu^2 \tilde{t} \tilde{g}_k \chi_k}{L} + \frac{i\pi \mu^2 \alpha_k \tilde{\chi}_k}{L} - \frac{i\pi \mu^2 \tilde{\alpha}_k \chi_k}{L} \right) \right. \\
 &\quad \left. + \frac{1}{(1 - e^{\frac{2\pi i(\tilde{s}-s)}{L}})^2} \frac{2\pi^2 \mu^2 \chi_k \tilde{\chi}_k}{L^2} \right]. \tag{3.63}
 \end{aligned}$$

Also,

$$\begin{aligned}
 \mathcal{F} + \tilde{\mathcal{F}} &= \sum_{n,k} \frac{1}{2L\sqrt{n}} \\
 &\quad \times \left[ \sqrt{2} \mu a_n^k \left( e^{-\frac{2i\pi n \tilde{s}}{L}} (-2iL t g_k + L\alpha_k - 2i\pi n \chi_k) + e^{-\frac{2i\pi n s}{L}} (-2iL \tilde{t} \tilde{g}_k + L\tilde{\alpha}_k - 2i\pi n \tilde{\chi}_k) \right) \right. \\
 &\quad \left. + \sqrt{2} \mu (a_n^k)^\dagger \left( e^{\frac{2i\pi n s}{L}} (-2iL t g_k + L\alpha_k + 2i\pi n \chi_k) + e^{\frac{2i\pi n \tilde{s}}{L}} (-2iL \tilde{t} \tilde{g}_k + L\tilde{\alpha}_k + 2i\pi n \tilde{\chi}_k) \right) \right. \\
 &\quad \left. - 2L\sqrt{n} (-2ix_k(tg_k + \tilde{t}\tilde{g}_k) + tg_k^2 + \tilde{t}\tilde{g}_k^2) \right]. \tag{3.64}
 \end{aligned}$$

Therefore,

$$\langle : e^{\mathcal{F} + \tilde{\mathcal{F}}} : \rangle_\beta = e^{\sum_{n,k} \mathcal{Q}_{n,k}}, \tag{3.65}$$

with

$$\begin{aligned}
 \mathcal{Q}_{n,k} &= \frac{\mu^2 z^n}{2n(z^n - 1)} \\
 &\times \left( 2tg_k e^{\frac{2i\pi n \bar{s}}{L}} + 2\tilde{t}\tilde{g}_k e^{\frac{2i\pi n s}{L}} + i\tilde{\alpha}_k e^{\frac{2i\pi n s}{L}} + \frac{2\pi n}{L} \tilde{\chi}_k e^{\frac{2i\pi n s}{L}} + i\alpha_k e^{\frac{2i\pi n \bar{s}}{L}} + \frac{2\pi n}{L} \chi_k e^{\frac{2i\pi n \bar{s}}{L}} \right) \\
 &\times \left( 2tg_k e^{\frac{-2i\pi n s}{L}} + 2\tilde{t}\tilde{g}_k e^{\frac{-2i\pi n \bar{s}}{L}} + i\alpha_k e^{\frac{-2i\pi n s}{L}} - \frac{2\pi n}{L} \chi_k e^{\frac{-2i\pi n s}{L}} + i\tilde{\alpha}_k e^{\frac{-2i\pi n \bar{s}}{L}} - \frac{2\pi n}{L} \tilde{\chi}_k e^{\frac{-2i\pi n \bar{s}}{L}} \right) \\
 &- tg_k(g_k - 2ix_k) - \tilde{t}\tilde{g}_k(\tilde{g}_k - 2ix_k).
 \end{aligned} \tag{3.66}$$

We can compute the sums over  $n$  using the following formulas. As  $\beta \rightarrow 0$ , we have

$$\begin{aligned}
 \sum_n \frac{e^{-\beta n + 2i\pi n s}}{n(1 - e^{-n\beta})} &\rightarrow \frac{\text{Li}_2(e^{2i\pi s})}{\beta}; \\
 \sum_n \frac{e^{-\beta n + 2i\pi n s}}{1 - e^{-n\beta}} &\rightarrow -\frac{\log(1 - e^{2i\pi s})}{\beta}; \\
 \sum_n \frac{ne^{-\beta n + 2i\pi n s}}{1 - e^{-n\beta}} &\rightarrow \frac{1}{\beta(1 - e^{2i\pi s})}.
 \end{aligned} \tag{3.67}$$

We can then write

$$\mathcal{N} + \sum_{n,k} \mathcal{Q}_{n,k} = \sum_k -(g^k, \tilde{g}^k) \cdot \begin{pmatrix} \tau t^2 + t & ct\tilde{t} \\ ct\tilde{t} & \tau \tilde{t}^2 + \tilde{t} \end{pmatrix} \cdot (g^k, \tilde{g}^k) + \ell_1^k t g^k + \ell_2^k \tilde{t} \tilde{g}^k + z, \tag{3.68}$$

where

$$\tau = \frac{\pi^2 \mu^2}{3\beta}, \tag{3.69}$$

as above in section 3.3.1 and the other coefficients take on the values

$$\begin{aligned}
 c &= \frac{\mu^2}{\beta} \mathcal{L}^+ + c_{\mathcal{N}}; \\
 -i\ell_1^k &= 2x_k - \frac{\mu^2}{3\beta} \left[ \pi^2 \alpha_k + 3\tilde{\alpha}_k \mathcal{L}^+ - 6i\pi \frac{\tilde{\chi}_k}{L} \mathcal{L}^- \right] - i\ell_{1\mathcal{N}}^k; \\
 -i\ell_2^k &= 2x_k - \frac{\mu^2}{3\beta} \left[ \pi^2 (\tilde{\alpha})_k + 3\alpha_k \mathcal{L}^+ + 6i\pi \frac{\chi_k}{L} \mathcal{L}^- \right] - i\ell_{2\mathcal{N}}^k; \\
 z &= \frac{\mu^2}{12\beta^2} \left[ \pi^2 \beta \alpha_k^2 + \left( -24\pi^2 \beta \frac{\chi_k \tilde{\chi}_k}{L^2} + 4\pi^4 \frac{\chi_k^2}{L^2} + 4\pi^4 \frac{\tilde{\chi}_k^2}{L^2} \right) + \pi^2 \beta \tilde{\alpha}_k^2 \right. \\
 &\quad \left. + 12i\pi \beta \tilde{\alpha}_k \frac{\chi_k}{L} \mathcal{L}^- + \alpha_k \tilde{\alpha}_k \mathcal{L}^+ - 12i\pi \beta \frac{\tilde{\chi}_k}{L} \mathcal{L}^- \right] + z_{\mathcal{N}},
 \end{aligned} \tag{3.70}$$

where

$$\begin{aligned}
 \mathcal{L}^+ &= Li_2 \left( e^{-\frac{2i\pi(s-\bar{s})}{L}} \right) + Li_2 \left( e^{\frac{2i\pi(s-\bar{s})}{L}} \right), \\
 \mathcal{L}^- &= \log \left( 1 - e^{-\frac{2i\pi(s-\bar{s})}{L}} \right) - \log \left( 1 - e^{\frac{2i\pi(s-\bar{s})}{L}} \right).
 \end{aligned} \tag{3.71}$$

The contribution from the normal ordering constant in the coefficients above is indicated with the subscript  $\mathcal{N}$  and these numbers are given by

$$\begin{aligned}
 c_{\mathcal{N}} &= \mu^2 \mathcal{L}_{\mathcal{N}}; \\
 \ell_{1\mathcal{N}} &= -i\mu^2 \left( i\tilde{\alpha}_k \mathcal{L}_{\mathcal{N}} + \frac{2\pi \tilde{\chi}_k}{L(-1+w)} \right); \\
 \ell_{2\mathcal{N}} &= -i\mu^2 \left( i\alpha_k \mathcal{L}_{\mathcal{N}} - \frac{2\pi \chi_k}{L(-1+w)} \right); \\
 z_{\mathcal{N}} &= -\frac{\mu^2}{2(-1+w)^2} \\
 &\quad \times \left[ \alpha_k (-1+w) \left( \tilde{\alpha}_k (-1+w) \mathcal{L}_{\mathcal{N}} - 2i\pi \frac{\tilde{\chi}_k}{L} \right) - 2\pi \frac{\chi_k}{L} \left( 2\pi \frac{\tilde{\chi}_k}{L} w - i\tilde{\alpha}_k (-1+w) \right) \right],
 \end{aligned} \tag{3.72}$$

with  $w = e^{\frac{2i\pi(s-\bar{s})}{L}}$  and  $\mathcal{L}_{\mathcal{N}} = \log(1 - 1/w)$ . By comparing (3.72) to (3.70) we see that the coefficients that come from normal ordering are all negligible when  $\beta \ll 1$ .

So, for numerical purposes we will neglect these coefficients although the fact that they are non-zero will play a role below.

In this form we can immediately do the integral over  $g_k$  and  $\tilde{g}_k$ , since these are Gaussian. We find that

$$\mathcal{V}_\beta(\chi, \alpha, \tilde{\chi}, \tilde{\alpha}) = \int_0^\infty dt d\tilde{t} \int_0^L ds d\tilde{s} e^{\frac{i\tilde{t}(4\tau^2 z + \tau(\ell_1^2 + \ell_2^2) - 2c(2cz + \ell_1 \cdot \ell_2)) + (4\tau z(t + \tilde{t}) + \ell_1^2 t + \ell_2^2 \tilde{t}) + 4z}{4(i\tilde{t}(\tau^2 - c^2) + \tau(t + \tilde{t}) + 1)}}}{(i\tilde{t}(\tau^2 - c^2) + \tau(t + \tilde{t}) + 1)^2}. \quad (3.73)$$

At this stage, rather than do the  $t$ -integrals in generality, it is convenient to separate the computation of the different quantities.

$\langle(\mathbf{f}_5 - \mathbf{1})^2\rangle_\beta$ : This is the simplest  $t$ -integral to calculate since we simply set  $\chi, \tilde{\chi}, \alpha, \tilde{\alpha}$  to 0. With these substitutions,  $z \rightarrow 0$  and also  $\ell_1^k, \ell_2^k \rightarrow 2ix^k$ . We then find that

$$\begin{aligned} \mathcal{V}_\beta(\chi = 0, \alpha = 0, \tilde{\chi} = 0, \tilde{\alpha} = 0) &= \int_0^L \frac{ds}{L} \frac{d\tilde{s}}{L} \int_0^\infty dt d\tilde{t} \frac{\exp\left(-\frac{r^2(2i\tilde{t}(\tau - c) + (t + \tilde{t}))}{i\tilde{t}(\tau^2 - c^2) + \tau(t + \tilde{t}) + 1}\right)}{(i\tilde{t}(\tau^2 - c^2) + \tau(t + \tilde{t}) + 1)^2} \\ &= \int_0^L \frac{ds}{L} \frac{d\tilde{s}}{L} \left[ \frac{e^{-\frac{r^2}{c^2}}}{c^2} \left( \text{Ei}\left(\frac{r^2}{c}\right) - 2\text{Ei}\left(\frac{(\tau - c)r^2}{\tau c}\right) + \text{Ei}\left(\frac{(\tau - c)r^2}{c(\tau + c)}\right) \right) \right. \\ &\quad \left. + \frac{2\tau e^{-\frac{r^2}{\tau}}}{cr^2(\tau - c)} - \frac{(\tau + c)e^{-\frac{2r^2}{\tau + c}}}{cr^2(\tau - c)} - \frac{1}{cr^2} \right]. \end{aligned} \quad (3.74)$$

Here  $Ei(x) = -\int_{-x}^\infty e^{-t} \mathcal{P}\left(\frac{1}{t}\right) dt$ . The last integral, over  $s, \tilde{s}$  must be done numerically and we discuss that in section 3.3.3.

$\langle(\mathbf{f}_1 - \mathbf{1})^2\rangle_\beta$ : It is convenient to first differentiate with respect to  $\chi, \tilde{\chi}$  before performing the  $t, \tilde{t}$  integrals. These derivatives lead to a complicated expression. However, it is important to realize that this expression involves terms that appear at different orders in  $\frac{1}{\beta}$ .

The reader can persuade herself through inspection, or through an explicit calculation that the dominant terms at small  $\beta$  occur only when the  $\chi, \tilde{\chi}$  derivatives act on the  $\chi_k^2$  and  $(\tilde{\chi}^k)^2$  terms inside  $z$  in (3.70).

This leads to the simple result

$$\langle (f_1 - 1)^2 \rangle_\beta = \frac{64\pi^8 \mu^4}{9L^4 \beta^4} \langle (f_5 - 1)^2 \rangle_\beta (1 + \mathcal{O}(\beta)) = \frac{Q_1^2}{Q_5^2} \langle (f_5 - 1)^2 \rangle_\beta (1 + \mathcal{O}(\beta)), \quad (3.75)$$

where we have used the ratio between coefficients displayed in (3.51) and neglected the  $\mathcal{O}(\beta)$  terms in the last equality.

$\langle \mathbf{W}_i \mathbf{W}_j \rangle_\beta$ : The computation of  $\langle W_i W_j \rangle_\beta$  is rather involved. We do not give the details of all the intermediate steps, but simply note the final answer in the form of an integral over  $s, \tilde{s}$  that we will evaluate numerically below. We find that

$$\frac{1}{Q_5^2} \langle W_i W_j \rangle_\beta = \mathcal{A} \delta_{ij} + \mathcal{B} x_i x_j, \quad (3.76)$$

where

$$\begin{aligned} \mathcal{A} = & \frac{(c - \tau) e^{-\frac{r^2}{c}} (r^2(c - \tau) + 3c(\tau + c)) \left( -2\text{Ei} \left( \frac{(\tau - c)r^2}{\tau c} \right) + \text{Ei} \left( \frac{(\tau - c)r^2}{c(\tau + c)} \right) + \text{Ei} \left( \frac{r^2}{c} \right) \right)}{12c^4} \\ & + \frac{\tau e^{-\frac{r^2}{\tau}} (-\tau c^2(\tau + 3c) + r^4(\tau - c)^2 + cr^2(c - \tau)(2\tau + 3c))}{6c^3 r^4 (\tau - c)} \\ & + \frac{(\tau + c) e^{-\frac{2r^2}{\tau + c}} (c^2 r^2 (\tau + c)^2 + r^6 (-\tau - c)^2 + 2cr^4(\tau - c)(\tau + c))}{12c^3 r^6 (\tau - c)}, \end{aligned} \quad (3.77)$$

and

$$\begin{aligned} \mathcal{B} = & \frac{(\tau^2 + 4\tau c + c^2) e^{-\frac{r^2}{c}} \left( -2\text{Ei} \left( \frac{(\tau - c)r^2}{\tau c} \right) + \text{Ei} \left( \frac{(\tau - c)r^2}{c(\tau + c)} \right) + \text{Ei} \left( \frac{r^2}{c} \right) \right)}{6c^4} \\ & + \frac{\tau e^{-\frac{r^2}{\tau}} (\tau^2 (2c^2 + cr^2 + r^4) + \tau c (6c^2 + 5cr^2 + 4r^4) + c^2 r^2 (6c + r^2))}{3c^3 r^6 (\tau - c)} \\ & - \frac{(\tau + c) e^{-\frac{2r^2}{\tau + c}} (\tau^2 (2c^2 + cr^2 + r^4) + 2\tau c (2c^2 + 3cr^2 + 2r^4) + c^2 (2c^2 + 5cr^2 + r^4))}{6c^3 r^6 (\tau - c)}. \end{aligned} \quad (3.78)$$

### 3.3.3 Analysis of the results

We now proceed to analyze the results obtained. We will compute the “difference” and “quantumness” parameters defined in (3.13) and (3.14). For the harmonic functions, we compute the following expressions both of which depend on  $\vec{x}$ .

$$\begin{aligned} \mathbf{d}_5 &= \left| \frac{\langle (f_5 - 1) \rangle_\beta - f_5^{\text{bh}} + 1}{\langle (f_5 - 1) \rangle_\beta} \right|; \\ \mathbf{q}_5 &= \left| \frac{(\langle (f_5 - 1)^2 \rangle_\beta - \langle (f_5 - 1) \rangle_\beta^2)^{\frac{1}{2}}}{\langle (f_5 - 1) \rangle_\beta} \right|. \end{aligned} \quad (3.79)$$

We do not need to compute these parameters separately for  $f_1$  since as we have found above,  $\langle f_1 - 1 \rangle_\beta = \frac{Q_1}{Q_5} \langle f_5 - 1 \rangle_\beta$  and also  $\langle (f_1 - 1)^2 \rangle_\beta = \frac{Q_1^2}{Q_5^2} \langle (f_5 - 1)^2 \rangle_\beta$ . Therefore  $\mathbf{q}_1 = \mathbf{q}_5$ ;  $\mathbf{d}_1 = \mathbf{d}_5$ .

Since  $W_i = 0$  in the conventional black-hole geometry, we find  $\mathbf{d}_W = 1$ . Then, to measure the size of quantum fluctuations, we compute

$$\mathbf{q}_W = \left| \frac{(x^i x^j \langle W_i W_j \rangle_\beta - x^i x^j \langle W_i \rangle_\beta \langle W_j \rangle_\beta)^{\frac{1}{2}}}{x^i x^j \langle W_i \rangle_\beta \langle W_j \rangle_\beta} \right|. \quad (3.80)$$

### Difference and quantumness parameters for the harmonic functions, $f_1$ and $f_5$

We start by evaluating (3.79). Let us consider the remaining integrals over  $s, \tilde{s}$  in the results (3.74).

First note that  $s, \tilde{s}$  only appear in these expressions through  $w = e^{\frac{2\pi i(s-\tilde{s})}{L}}$ . Moreover, each integrand has a Laurent series expansion in  $w$ , and so the integral over  $s, \tilde{s}$  simply picks out the  $w^0$  term. Note also, that the integrand has potential singularities at  $\tau = c$ . These poles arise when  $w$  solves

$$\frac{\pi^2}{6} - \frac{1}{2} \left( \text{Pl}(2, w) + \text{Pl}(2, 1/w) + \frac{2\pi\beta}{L} \log(1-w) \right) = 0. \quad (3.81)$$

At small  $\beta$  the pole is *almost* at  $w = 1$  but the last term moves the pole slightly off the  $|w| = 1$  contour to  $|w| = 1 + \mathcal{O}(\beta)$ . Other than the effect above, the normal ordering term is negligible. For ease with the final numerical integrals, we deal with this as follows. We drop the term  $c_{\mathcal{N}}$  in (3.70) and instead add a small real regulator

to  $c$  so that  $c_\epsilon = c - \epsilon$ . We then compute (3.74) and (3.76) with  $c \rightarrow c_\epsilon$ . Numerically, it is easy to check that the value of this regulator does not alter any of the answers provided it is kept small enough.

It is of interest to consider the behaviour near  $r = 0$ , where the fuzzball solution differs from the conventional solution. We find that, in this limit (3.74)

$$\begin{aligned} \frac{1}{Q_5^2} \langle (f_5 - 1)^2 \rangle_\beta &= Q_5^2 \int_0^L \frac{ds d\tilde{s}}{L^2} \frac{\log\left(\frac{\tau^2}{\tau^2 - c^2}\right)}{c^2} + \frac{r^2 \left( \tau(\tau + c) \log\left(1 - \frac{c^2}{\tau^2}\right) + c^2 \right)}{\tau c^3 (\tau + c)} + O(r^4) \\ &= 1.182 \frac{1}{\tau^2} - 1.283 \frac{r^2}{\tau^3}, \end{aligned} \tag{3.82}$$

which leads to

$$q_5 = 0.426 - 0.119 \frac{r^2}{\tau}. \tag{3.83}$$

The key point is that, just as expected  $q_5$  becomes of order 1 just in the region where  $\frac{r^2}{\tau} \ll 1$  and the average fuzzball geometry starts to differ appreciably from the conventional solution. Therefore, in precisely the region where the average fuzzball geometry predicts interesting effects, it becomes unreliable.

It is possible to numerically compute both  $d_5$  and  $q_5$  for larger values of  $x$  and we display this in Figure 3.5. As we move to larger values of  $\frac{r^2}{\tau}$  the solution becomes more reliable, but then it also becomes indistinguishable from the conventional black hole.

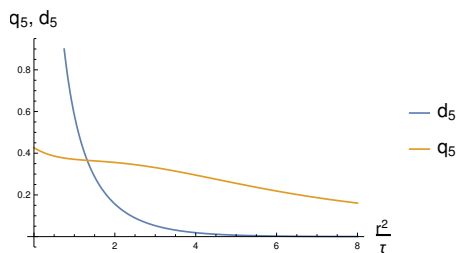


Figure 3.5: A plot of the “difference parameter”,  $d_5$  and the “quantumness parameter”,  $q_5$  for the harmonic functions  $f_5$  and  $f_1$ . The plot shows that in the average fuzzball geometry, precisely in the region where  $f_5, f_1$  differ significantly from their conventional value, quantum fluctuations becomes large and the fuzzball geometry becomes unreliable.

### Difference and quantumness parameters for $W_i$

We now turn to the difference and quantumness parameters for  $W_i$ . The difference parameter is uniformly equal to 1 since  $W_i = 0$  in the conventional black hole.

At small  $\frac{r^2}{\tau}$  we find that

$$\begin{aligned} & \hat{x}^i \hat{x}^j \langle W_i W_j \rangle_\beta \\ &= \int_0^L \frac{ds}{L} \frac{d\tilde{s}}{L} \left[ \frac{(\tau^2 - c^2) \log\left(\frac{\tau^2 - c^2}{\tau^2}\right) + c^2}{4c^3} - \frac{r^2(\tau + c) \left(\tau^2 \log\left(\frac{\tau^2 - c^2}{\tau^2}\right) + c^2\right)}{2\tau c^4} \right] + O\left(\frac{r^4}{\tau^3}\right) \\ &= \frac{0.00489}{\tau} + \frac{0.355r^2}{\tau^2} + O\left(\frac{r^4}{\tau^3}\right). \end{aligned} \tag{3.84}$$

At small values of  $r$ , when we combine this with the series expansion of (3.49), this leads to

$$\mathfrak{q}_W = 0.140 \frac{\sqrt{\tau}}{r} + 1.587 \frac{r}{\sqrt{\tau}}. \tag{3.85}$$

Therefore, quantum fluctuations diverge near  $r = 0$  and the expected value of  $W_i$  in the average geometry becomes completely unreliable.

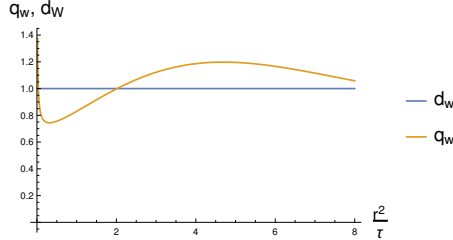


Figure 3.6: A plot of the “difference parameter”,  $\mathfrak{d}_W$  and the “quantumness parameter”,  $\mathfrak{q}_W$  for the one-form  $W_i$ . The difference parameter is uniformly 1, since this function vanishes in the conventional black hole. But, the value it ostensibly takes in the average fuzzball solution is always unreliable since quantum fluctuations are the same size as its expectation value

We can numerically plot the quantumness parameter for larger values of  $r$  and this leads to the curve shown in Figure 3.6. At both small  $\frac{r^2}{\tau}$  and larger values of  $\frac{r^2}{\tau}$  the value for  $W_i$  given by the average fuzzball geometry is unreliable.

**Fuzzballs and entropy counting:** In this section, we have argued that the average fuzzball geometry is unreliable in the interesting region near  $r = 0$ . By result 3.1, the geometry corresponding to a typical state in the Hilbert space produced by quantizing fuzzball solutions is also unreliable near  $r = 0$ . Away from  $r = 0$ , this average geometry is effectively indistinguishable from the conventional geometry since its deviation from the conventional geometry is of the same order as quantum fluctuations.

The reader might wonder how — in spite of this fact — counting the entropy of fuzzball solutions succeeds in getting the correct form for the number of Ramond ground states in the D1-D5 system.

The puzzle is made more acute by recognizing that most of the contribution to this entropy comes from Planck-size fuzzballs. For small  $\beta$ , the reader can check that  $\tau$  also measures the average size of the profile function

$$\sum_i \int_0^L \langle : F^i(s) F^i(s) : \rangle_\beta \frac{ds}{L} = 2\tau. \quad (3.86)$$

Fluctuations in the size of the fuzzball are also controlled by  $\tau$ . At high temperatures,

$$\sum_{i,j} \int_0^L \langle : F^i(s) F^i(s) :: F^j(\tilde{s}) F^j(\tilde{s}) : \rangle_\beta \frac{ds}{L} \frac{d\tilde{s}}{L} = \frac{22}{5} \tau^2. \quad (3.87)$$

This tells us that if we consider the entropy corresponding to fuzzballs that are *parametrically* larger than (3.86), then this entropy is highly suppressed.

We do not have a complete explanation for the fact that quantizing the space of fuzzballs gives approximately the correct counting — even though individual fuzzball solutions that contribute dominantly to the entropy are unreliable. Our best guess is as follows. We can consider the solutions (3.21) for profile functions,  $F^i(s)$  that are *parametrically larger* than (3.86). In this regime, the solutions are reliable. Since they also saturate the BPS condition, they must correspond to some ground-states of the D1-D5 system. This subclass of solutions can be quantized and counted reliably. Then — perhaps as a result of one of the fortuitous coincidences that occur while counting supersymmetric states — this counting formula can be extrapolated to obtain a count of all ground states. Perhaps this last step can be explained by going to some other point in parameter space, where these solutions

can be mapped to better controlled states; this deserves to be understood better.

However, we emphasize that the entropy-formula itself cannot be taken as evidence that fuzzballs are giving us an accurate picture of physics near  $r = 0$  at the supergravity point in moduli space, since the solutions that dominate the entropy are unreliable in that region. It would be nice to understand the physics near  $r = 0$  better but this clearly requires some other technique.

Another interesting open question is as follows. What is the basis whose elements minimize  $\mathbf{q}_5, \mathbf{q}_1, \mathbf{q}_W$  so that the fluctuations in a typical state — as calculated in (3.74), (3.75) and (3.76) — come from differences between elements of this basis rather than fluctuations of the operator within given basis states? We do not expect, that even in such a basis,  $\mathbf{q}_5, \mathbf{q}_1, \mathbf{q}_W$  will be parametrically suppressed near  $r = 0$ , but in such a basis the fuzzball microstates would be reliable as possible.

### 3.4 Probing multi-charge solutions

In the previous section, we provided a detailed discussion of the two-charge fuzzballs. However, the corresponding conventional solution has vanishing horizon area. So, it is of interest to investigate fuzzballs that have the same charges as black holes with a macroscopic horizon.

In this section, we will consider the class of asymptotically AdS fuzzball solutions discovered in [44] following previous work in [85]. The conventional black-hole geometry corresponding to these charges is given in [45]. We cannot repeat the analysis of section 3.3 and compute quantum expectations and fluctuations since (a) all fuzzball solutions with the charges of [44] have not been discovered and (b) these solutions have not been quantized. Moreover, even in the set of solutions of [44], we will consider only a subset for which the form of the metric was explicitly given in [44].

These solutions are macroscopically distinguishable from the conventional black hole. Therefore, if we believe expectation 2 then result 3.2 immediately tells us that they cannot be typical elements of a basis. The calculations in this section show that one can reach this conclusion even without assuming expectation 2 and simply by considering asymptotic observables.

The solutions of [44] are asymptotically AdS, and the asymptotic observable we

will focus on is a two-point function of a marginal scalar operator in the boundary CFT. We will use this two-point function to investigate the energy-gap between successive excitations of the fuzzball solutions. We find that this gap is too large and violates expectation 1. We will also investigate whether fuzzball solutions satisfy a specific bound for the falloff of the two-point function for large spacelike momenta. This bound holds in any conformal field theory, and is saturated by the black-hole geometry. However, fuzzballs fail to saturate this bound, indicating that they cannot be typical microstates.

### 3.4.1 Review of the solution

The metric given in [44] is

$$\begin{aligned}
 ds_6^2 &= -\frac{2}{\sqrt{\mathcal{P}}}(dv + \beta)(du + \omega + \frac{1}{2}\mathcal{F}(dv + \beta)) + \sqrt{\mathcal{P}}ds_4^2; \\
 u &= (t - y)/\sqrt{2}; v = (t + y)/\sqrt{2}; y \sim y + 2\pi R_y; \\
 ds_4^2 &= \frac{\Sigma dr^2}{r^2 + a^2} + \Sigma d\theta^2 + (r^2 + a^2) \sin^2 \theta d\phi^2 + r^2 \cos^2 \theta d\psi^2; \\
 \mathcal{P} &= Z_1 Z_2 - Z_4^2; \quad \beta = \frac{a^2 R_y}{\sqrt{2\Sigma}}(\sin^2 \theta d\phi - \cos^2 \theta d\psi); \quad \Sigma = (r^2 + a^2 \cos^2 \theta).
 \end{aligned} \tag{3.88}$$

The functions  $Z_1, Z_4, \mathcal{F}$  in the metric above depend on three integer parameters  $k, m, n$ . We will consider the simplest case,  $k = 1, m = 0, n$  arbitrary, for which it is easy to write down explicit expressions for these quantities. For this case, we find that

$$\begin{aligned}
 Z_1 &= \frac{(a^2 + r^2)^{-n-1} \left( a^2 b^2 R_y^2 \sin^2(\theta) r^{2n} \cos \left( 2 \left( \frac{n(t+y)}{R_y} + \phi \right) \right) + 2Q_1 Q_5 (a^2 + r^2)^{n+1} \right)}{2Q_5 (a^2 \cos^2(\theta) + r^2)}; \\
 Z_4 &= \frac{abR_y \sin(\theta) r^n (a^2 + r^2)^{-\frac{n}{2} - \frac{1}{2}} \cos \left( \frac{n(t+y)}{R_y} + \phi \right)}{a^2 \cos^2(\theta) + r^2}; \\
 \mathcal{F} &= -\frac{1 - r^{2n} (a^2 + r^2)^{-n}}{a^2}.
 \end{aligned} \tag{3.89}$$

The parameters in the solution are related through the constraint

$$\frac{Q_1 Q_5}{R_y^2} = a^2 + b^2/2. \quad (3.90)$$

The asymptotic geometry of these solutions is  $\text{AdS}_3 \times S^3$  with an AdS radius  $\lambda = (Q_1 Q_5)^{\frac{1}{4}}$ . By the standard formula for the AdS central charge, we also have

$$\frac{3\lambda}{2G_3} = 6N_1 N_5, \quad (3.91)$$

where  $N_1, N_5$  are the number of D1 and D5 branes and  $G_3$  is the 3-dimensional Newton's constant. In addition we set  $\mathcal{N} = N_1 N_5 / (a^2 + b^2/2)$ .

The charges of the solutions — the angular momenta along the  $S^3$  ( $J_L, J_R$ ), the mass ( $M$ ) and the momentum along the  $y$ -direction  $P_y$  are given by

$$J_L = J_R = \frac{\mathcal{N}}{2} a^2; \quad M = P_y = \frac{\mathcal{N} n}{2R_y} b^2. \quad (3.92)$$

### 3.4.2 Physical quantities of interest

Let us consider a marginal scalar operator in the boundary theory. We will consider the Fourier transform of its *Wightman function* in a state dual to the fuzzball solution

$$G(\omega, \gamma) = \int \langle f | O(t, y) O(0, 0) | f \rangle e^{\frac{i\omega t}{R_y}} e^{\frac{i\gamma y}{R_y}} dt dy. \quad (3.93)$$

It will also be useful to consider the Fourier transform of the *commutator* which is just the difference of two Wightman functions

$$J(\omega, \gamma) = \int \langle f | [O(t, y), O(0, 0)] | f \rangle e^{\frac{i\omega t}{R_y}} e^{\frac{i\gamma y}{R_y}} dt dy = G(\omega, \gamma) - G(-\omega, -\gamma). \quad (3.94)$$

This Wightman function can be computed using the standard AdS/CFT dictionary by considering the boundary limit of a bulk minimally coupled massless scalar,  $\phi$ , with no motion along the  $S^3$  coordinates.

$$G(\omega, \gamma) = \lim_{r \rightarrow \infty} r^4 \int \langle f | \phi(r, t, y) \phi(r, 0, 0) | f \rangle e^{\frac{i\omega t}{R_y}} e^{\frac{i\gamma y}{R_y}} dt dy. \quad (3.95)$$

This follows from the standard “extrapolate” dictionary in AdS/CFT.<sup>3</sup>

It was shown in [87, 50] that, in the fuzzball background under consideration, the massless scalar equation is separable. Furthermore,  $t$  and  $y$  are Killing vectors for the metric, and therefore it is convenient to expand the bulk scalar field as

$$\phi(r, t, y) = \sum_{\omega, \gamma} a_{\omega, \gamma} R_{\omega, \gamma}(r) e^{\frac{-i\omega t}{R_y}} e^{\frac{-i\gamma y}{R_y}} + \text{h.c.}, \quad (3.96)$$

where the bulk operators are normalized so that  $[a_{\omega, \gamma}, a_{\omega', \gamma'}^\dagger] = \delta_{\omega\omega'} \delta_{\gamma\gamma'}$ . We take the radial wave-functions corresponding to different  $\omega, \gamma$  to be orthonormal in the Klein Gordon norm. Therefore they satisfy

$$\int h(r) \omega R_{\omega, \gamma}(r) R_{\omega', \gamma'}^*(r) dr = 1. \quad (3.97)$$

where the measure factor,  $h(r) = 8\pi^3 \sqrt{-g}/(\sin \theta \cos \theta)$  depends only on  $r$ . Note that this requires us to consider only *normalizable* radial bulk solutions.

The boundary Wightman function is then just given by

$$G(\omega, \gamma) = N_{\omega, \gamma} |C_{\omega, \gamma}|^2, \quad (3.98)$$

where

$$C_{\omega, \gamma} = \lim_{r \rightarrow \infty} r^2 R_{\omega, \gamma}(r). \quad (3.99)$$

and

$$\langle f | a_{\omega, \gamma} a_{\omega', \gamma'}^\dagger | f \rangle = N_{\omega, \gamma} \delta_{\omega, \omega'} \delta_{\gamma, \gamma'}. \quad (3.100)$$

If the fuzzball state is approximately thermal, we expect that  $N_{\omega, \gamma} = \frac{1}{1 - e^{-\beta\omega}}$  and *independent* of  $\gamma$ . However, we can avoid any assumptions about the function  $N_{\omega, \gamma}$  by considering the *commutator*. Then by using the fact that

$$\langle f | [a_{\omega, \gamma}, a_{\omega', \gamma'}^\dagger] | f \rangle = \delta_{\omega, \omega'} \delta_{\gamma, \gamma'}. \quad (3.101)$$

---

<sup>3</sup>In some special cases in  $d = 4$  that correspond to Coulomb branch solutions of  $\mathcal{N} = 4$  SYM, there are subtleties with the standard extrapolate dictionary [86] but these subtleties are irrelevant here.

we see that the commutator is simply given by

$$J(\omega, \gamma) = |C_{\omega, \gamma}|^2. \quad (3.102)$$

Therefore, the computation of the Wightman function and the commutator reduces essentially to a computation of  $C_{\omega, \gamma}$  which can be obtained by solving the bulk radial equation and normalizing it under (3.97).

We will be particularly interested in the behaviour of these function in the limit where  $\gamma \gg 1$ . In this limit, we can perform analytic calculations using a WKB approximation. We will show that  $G(\omega, \gamma)$  and  $J(\omega, \gamma)$  have support on a *discrete* set of frequencies with a *gap* between successive excitations that scales with  $\frac{a^2}{b^2}$ . Therefore, even if we take  $\frac{a}{b} \ll 1$  (but not suppressed by an exponent of  $N_1 N_5$ ), we see by expectation 1 that these states are very atypical.

The large- $\gamma$  limit of the Wightman function and the commutator is also of interest because, by virtue of having a horizon, black holes saturate a *bound* on how slowly these functions can decay at large- $\gamma$ . We will show, again, that the fuzzball solutions do *not* saturate this bound in the limit where  $\frac{a^2}{b^2 n} = \mathcal{O}(1)$ . Therefore, these fuzzball solutions also do *not* obey the ETH.

### 3.4.3 Propagation of a massless scalar

When the angular momentum of the mode along  $S^3$  is zero, the wave-equation,  $\square\phi = 0$  yields the following equation for the radial mode

$$\begin{aligned} R''_{\omega, \gamma}(r) + Q(r)R'_{\omega, \gamma}(r) + P(r)R_{\omega, \gamma}(r) &= 0; \\ Q(r) &= \frac{a^2 + 3r^2}{a^2 r + r^3}; \\ P(r) &= \frac{1}{4a^2 r^2 (a^2 + r^2)^{n+2}} \left( -b^4 r^2 (\omega - \gamma)^2 (r^{2n} - (a^2 + r^2)^n) - 4a^6 \gamma^2 (a^2 + r^2)^n \right. \\ &\quad \left. - 2a^2 r^2 (b^2 (\omega - \gamma) (r^{2n} (\omega - \gamma) - 2\omega (a^2 + r^2)^n)) + 4a^4 r^2 (a^2 + r^2)^n (\omega^2 - \gamma^2) \right). \end{aligned} \quad (3.103)$$

With the appropriate translation of notation, this is the same as the wave-equation derived in [50]. To put the equation in WKB form, we redefine

$$R_{\omega,\gamma}(r) = \alpha \frac{\psi(r)}{\sqrt{r(r^2 + a^2)}}. \quad (3.104)$$

Here  $\alpha$  is a normalization constant that we will turn to in section 3.4.5 and we have suppressed the  $\omega, \gamma$  dependence on  $\psi$  and  $\alpha$ . Further, changing variables to  $\xi = \frac{r}{a}$  and setting  $b = a\kappa$ , we can put the equation for  $\psi$  in WKB form,

$$\frac{d^2\psi(\xi)}{d\xi^2} - V(\xi)\psi(\xi) = 0, \quad (3.105)$$

with

$$V(\xi) = \frac{1}{4(\xi^2 + 1)^2} \left[ \frac{4\gamma^2 - 1}{\xi^2} + 4\gamma^2 + 3\xi^2 + \kappa^2(\kappa^2 + 2)(\omega - \gamma)^2 \frac{\xi^{2n}}{(\xi^2 + 1)^n} - (\kappa^2(\omega - \gamma) + 2\omega)^2 + 6 \right]. \quad (3.106)$$

The potential has two turning points, and we can understand its qualitative behaviour as follows. We see that at small  $\xi$  ( $r \ll a$ ), the potential is positive since it is dominated by the  $\frac{4\gamma^2 - 1}{\xi^2}$  term in the numerator of (3.106). We remind the reader that  $\gamma \gg \omega$  and we will primarily be interested in a regime where  $\kappa \gg 1$ . Then it is clear that for a range of values of  $\xi$  near  $\xi = 1$ , the potential becomes negative before becoming positive again for large  $\xi$  due to the  $3\xi^2$  term in the numerator. A graph of the potential is shown in Figure 3.7 for some typical values of  $\kappa, n, \gamma$  with  $\omega = 0$  for simplicity.

For large values of  $\gamma$ , the WKB approximation is valid everywhere except very close to the two turning points or when  $\xi = O(\gamma)$ . In this large  $\xi$  region, we will match the WKB solution to a Bessel function, and we will deal with the turning points by interpolating between the two sides using the Airy-functions.

Let us denote the position of the first turning point by  $\xi_1$  and the second turning point by  $\xi_2$ . Then, for small  $\xi$  if we insist that the solution be normalizable, we can write

$$\psi(\xi) = \frac{1}{V(\xi)^{\frac{1}{4}}} e^{\int_{\xi_1}^{\xi} \sqrt{V(\zeta)} d\zeta}, \quad \xi < \xi_1, \quad (3.107)$$

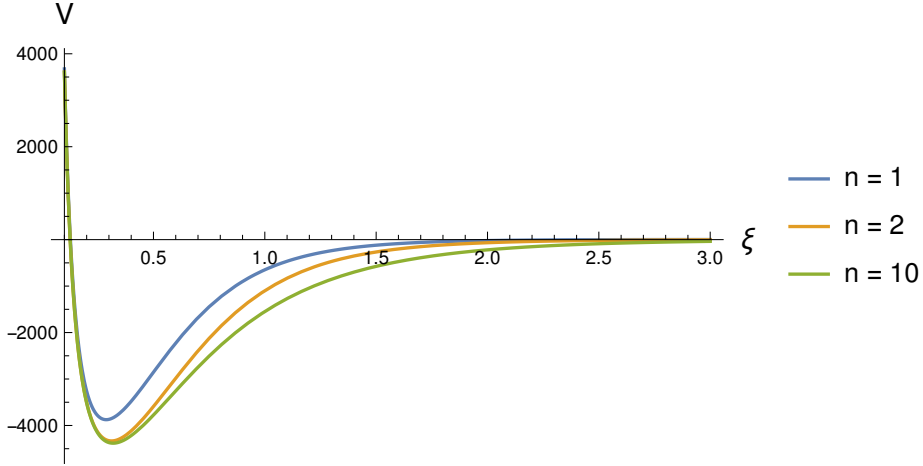


Figure 3.7: A graph of  $V(\xi)$  vs  $\xi$  with  $\gamma = 10, \omega = 0, \kappa = 4$  and different values of  $n$ .

Near  $\xi = \xi_1$ , we can approximate  $V(\xi) \approx |V'(\xi_1)|(\xi_1 - \xi)$  and therefore we have

$$\psi(\xi) = \frac{2\sqrt{\pi}}{|V'(\xi_1)|^{\frac{1}{6}}} \text{Ai}(|V'(\xi_1)|(\xi_1 - \xi)), \quad \xi \approx \xi_1, \quad (3.108)$$

where we have chosen the Airy Ai-function based on the expected asymptotics for  $\xi < \xi_1$ . Matching again with the WKB solution we find that

$$\begin{aligned} \psi(\xi) &= \frac{1}{|V(\xi)|^{\frac{1}{4}}} \left[ e^{i\frac{\pi}{4}} e^{-i\int_{\xi_1}^{\xi} \sqrt{|V(\zeta)|} d\zeta} + e^{-i\frac{\pi}{4}} e^{i\int_{\xi_1}^{\xi} \sqrt{|V(\zeta)|} d\zeta} \right] \\ &= \frac{1}{|V(\xi)|^{\frac{1}{4}}} \left[ A_- e^{i\frac{\pi}{4}} e^{i\int_{\xi_2}^{\xi} \sqrt{|V(\zeta)|} d\zeta} + e^{-i\frac{\pi}{4}} A_+ e^{-i\int_{\xi_2}^{\xi} \sqrt{|V(\zeta)|} d\zeta} \right], \quad \xi_1 < \xi < \xi_2, \end{aligned} \quad (3.109)$$

where

$$A_{\pm} = e^{\pm i\int_{\xi_1}^{\xi_2} \sqrt{|V(\zeta)|} d\zeta}. \quad (3.110)$$

Near  $\xi \approx \xi_2$  we need to use the Airy-function interpolation again and find that the solution matches to

$$\psi(\xi) = \frac{1}{|V(\xi)|^{\frac{1}{4}}} \left[ B_+ e^{\int_{\xi_2}^{\xi} \sqrt{|V(\zeta)|} d\zeta} + B_- e^{-\int_{\xi_2}^{\xi} \sqrt{|V(\zeta)|} d\zeta} \right], \quad \xi_2 < \xi \ll \gamma, \quad (3.111)$$

with  $B_+ = \frac{A_- + A_+}{2}$ ;  $B_- = \frac{i}{2}(A_- - A_+)$ . Now, for very large  $\xi$ , we can also solve for the wave-equation in terms of Bessel functions

$$\psi(\xi) = \frac{2C}{\delta} \sqrt{\xi} I_1 \left( \frac{\delta}{\xi} \right), \quad \xi \gg 1, \quad (3.112)$$

where  $\delta^2 = \frac{1}{2}(\gamma^2 - \omega^2)(2 + \kappa^2)$ , and we have picked the Bessel ‘‘I’’ function by demanding that the solution be normalizable at infinity. Matching the solutions (3.111) and (3.112) in the neighbourhood of some point  $\xi_3$  which satisfies  $1 \ll \xi_3 \ll \gamma$ , where both solutions are valid, we see that the solutions can only match if  $B_+ = 0$ . This simply tells us that in the region where the potential becomes positive again, the magnitude of the wave-function cannot grow exponentially.

This gives us a *quantization condition* on the potential:

$$2 \int_{\xi_1}^{\xi_2} |V(\zeta)|^{\frac{1}{2}} d\zeta = (2m + 1)\pi, \quad (3.113)$$

for some integer  $m$ . From the formula above, we have  $B_- = (-1)^m$  and this additionally tells us that

$$\frac{2C}{\sqrt{2\pi}} \frac{\xi_3}{\delta^{\frac{3}{2}}} e^{\frac{\delta}{\xi_3}} = \frac{(-1)^m}{V(\xi_3)^{\frac{1}{4}}} e^{-\int_{\xi_2}^{\xi_3} |V(\zeta)|^{\frac{1}{2}} d\zeta} \implies C = (-1)^m \frac{\delta}{2} \sqrt{2\pi} e^{-\int_{\xi_2}^{\xi_3} |V(\zeta)|^{\frac{1}{2}} d\zeta - \frac{\delta}{\xi_3}}. \quad (3.114)$$

It is clear that the value of  $C$  does not depend on the precise value of  $\xi_3$  chosen to perform the matching.

We will now use this WKB solution to compute some physical quantities of interest.

### 3.4.4 Energy gap

First, we consider the gap in energies of states in the neighbourhood of the fuzzball state. This is a question of the values of  $\omega$  for which  $G(\omega, \gamma)$  has support.

Clearly  $G(\omega, \gamma)$  vanishes for those frequencies where no normalizable solution exists. (This is independent of any assumption about  $N_{\omega, \gamma}$ .) So, the energy gap can be obtained by examining the values of  $\omega$  for which the quantization condition (3.113) is satisfied. The quantization condition can be parsed as follows. First, in

the limit  $\xi_1 < \xi < \xi_2$ , we expand the square-root of the potential as

$$\begin{aligned}\sqrt{|V|} &= V_{\frac{1}{2},1}\gamma - \omega\kappa^2 V_{\frac{1}{2},0} + \mathcal{O}\left(\frac{1}{\gamma}\right), \\ V_{\frac{1}{2},1} &= \frac{\sqrt{\left|\kappa^4\left(\left(\frac{1}{\xi^2} + 1\right)^n - 1\right) - 2\kappa^2 - 4\left(\frac{1}{\xi^2} + 1\right)^{n+1}\right|}}{2\xi^2\left(\frac{1}{\xi^2} + 1\right)^{\frac{n}{2}+1}}, \\ V_{\frac{1}{2},0} &= \frac{(\kappa^2 + 2)\left(\left(\frac{1}{\xi^2} + 1\right)^n - 1\right)\left(\frac{1}{\xi^2} + 1\right)^{-\frac{n}{2}-1}}{2\xi^2\sqrt{\left|\kappa^4\left(\left(\frac{1}{\xi^2} + 1\right)^n - 1\right) - 2\kappa^2 - 4\left(\frac{1}{\xi^2} + 1\right)^{n+1}\right|}}.\end{aligned}\tag{3.115}$$

The absolute value sign inside the square-root is for later use and does not have any effect in the range under consideration.

Now, at large  $\gamma$ , the values of  $\xi_1$  and  $\xi_2$  are controlled by  $V_{\frac{1}{2},1}$  and do not depend on  $\omega$ . Therefore, if we consider two *consecutive* solutions of (3.113) that differ by an amount  $\delta\omega$ , then this difference must satisfy

$$\boxed{\delta\omega = \frac{\pi}{\kappa^2 g_n}}.\tag{3.116}$$

where

$$g_n = \int_{\xi_1}^{\xi_2} V_{\frac{1}{2},0} d\xi.\tag{3.117}$$

For general values of  $\kappa$ , this condition can only be solved numerically but it is of interest to examine the limit where  $\kappa \gg 1$ . In this limit, we can approximate  $\xi_1 \approx \frac{2}{\kappa^2}$  and  $\xi_2 \approx \kappa\sqrt{\frac{n}{2}}$ . For the calculation of  $g_n$ , these limits are effectively 0 and  $\infty$ . Therefore, expanding  $V_{\frac{1}{2},0}$  at large  $\kappa$ , we find

$$g_n = \int_0^\infty d\xi \frac{\sqrt{\left(\frac{1}{\xi^2} + 1\right)^n - 1} \left(\frac{1}{\xi^2} + 1\right)^{-n/2}}{2(\xi^2 + 1)} + \mathcal{O}\left(\frac{1}{\kappa}\right).\tag{3.118}$$

The first few values of  $g_n$  (for  $n = 1$  to  $n = 5$ ) are  $\{0.5, 0.574, 0.610, 0.632, 0.648\}$ .

Therefore, at large  $\gamma$  and large  $\kappa$ , the energy gap between consecutive excitations scales as  $\frac{1}{\kappa^2}$  with a simple numerical prefactor.

### 3.4.5 Large $\gamma$ Wightman function and commutator

We now briefly explain the significance of the behaviour of the Wightman function and the commutator at large  $\gamma$  but small  $\omega$ . As explained in [62], in any conformal field theory, the large- $\gamma$ , small- $\omega$ , limit of the *thermal* Wightman function/commutator must fall off exponentially, with an exponent that is bounded below. We review this argument below. In [62], it was also shown that black holes saturate this bound because of the presence of the horizon. It is therefore, of interest, to understand whether fuzzballs also saturate this bound.

We will perform the analysis for the Wightman function below, although the analysis for the commutator is precisely the same. To obtain the bound on the behaviour of the Wightman function, we consider this correlator in a state with a finite temperature and chemical potential for the momentum in the  $y$ -direction in some arbitrary two-dimensional conformal field theory living on a circle with radius  $R_y$ .

$$\begin{aligned} G(t, y) &= \text{Tr} \left( e^{-\beta(H - \mu P_y)} O(t, y) O(0, 0) \right) \\ &= \sum_{m, n} e^{-\beta(E_m - \mu P_m)} e^{-it(E_n - E_m) - iy(P_n - P_m)} |\langle m | O(0, 0) | n \rangle|^2, \end{aligned} \quad (3.119)$$

where the sum over  $m, n$  runs over a complete set of energy/momentum eigenstates and to lighten the notation we have the same symbol for the position-space Wightman function as for its Fourier transform. Now, by Fourier transforming in time, we find that

$$\begin{aligned} G(\omega, y) &= \int G(t, y) e^{\frac{i\omega t}{R_y}} dt \\ &= 2\pi \sum_{m, n} \delta\left(E_n - \frac{\omega}{R_y} - E_m\right) e^{-\beta(E_m - \mu P_m) - i(P_m - P_n)y} |\langle m | O(0, 0) | n \rangle|^2. \end{aligned} \quad (3.120)$$

Now, writing  $y = y_r + iy_i$ , and using the spectrum condition  $E_m \geq |P_m|$ , we see that

the real part of the exponent in the sum over  $m, n$  can be written as

$$\begin{aligned}
 \operatorname{Re}(-\beta(E_m - \mu P_m) - i(P_m - P_n)y) &\leq -\beta E_m(1 - |\mu|) + (|P_m| + |P_n|)|y_i| \\
 &= \beta(1 - |\mu|)\frac{\omega}{2R_y} - (E_m + E_n)\frac{\beta(1 - |\mu|)}{2} + (|P_m| + |P_n|)|y_i| \\
 &\leq \beta(1 - |\mu|)\frac{\omega}{2R_y} - (E_m + E_n)\left(\frac{\beta(1 - |\mu|)}{2} - |y_i|\right).
 \end{aligned} \tag{3.121}$$

Therefore the exponent always supplies a convergence factor in the sum over  $m, n$  provided that  $|\operatorname{Im}(y)| < \frac{\beta(1 - |\mu|)}{2}$  and therefore the Green's function can be analytically continued in the  $y$  plane in both directions up to this limit. But then writing

$$G(\omega, y_r - iy_i) = \int_{\gamma=-\infty}^{\infty} G(\omega, \gamma) e^{\frac{-i\gamma(y_r + iy_i)}{R_y}}, \tag{3.122}$$

we see that, in the regime where  $\gamma \rightarrow \infty$ , this is only possible if

$$\lim_{\gamma \rightarrow \infty} \frac{-\log |G(\omega, \gamma)|}{(|\gamma|/R_y)} \geq \frac{\beta(1 - |\mu|)}{2}. \tag{3.123}$$

Note that the minus sign outside the log indicates that the Wightman function must *decay* at large  $\gamma$ . Second, we also note that this bound can be written in terms of the left and right temperatures that couple to the left and right Virasoro charges:  $\beta_L = \frac{1}{R_y}\beta(1 - \mu)$ ;  $\beta_R = \frac{1}{R_y}\beta(1 + \mu)$ , if we recognize that  $\beta(1 - |\mu|) = R_y \min(\beta_L, \beta_R)$ . In this notation the bound simply becomes

$$\lim_{\gamma \rightarrow \infty} \frac{-\log |G(\omega, \gamma)|}{\gamma} \geq \frac{1}{2} \min(\beta_L, \beta_R). \tag{3.124}$$

Repeating the analysis above, we see that the *same* bound also applies to the commutator (3.94)

$$\lim_{\gamma \rightarrow \infty} \frac{-\log |J(\omega, \gamma)|}{\gamma} \geq \frac{1}{2} \min(\beta_L, \beta_R). \tag{3.125}$$

It was explained in [62] that black holes saturate this bound. Intuitively, this happens for the following reason. In general, modes with large  $\gamma$  but small  $\omega$  are unusual because they have larger momentum than frequency and are “spacelike” near the boundary. However, the black-hole horizon allows such modes to propagate in

the bulk because of the red-shift near the horizon. The fuzzball also has a red-shift but we will see below that fuzzballs do *not* saturate (3.124).

To calculate the large- $\gamma$  behaviour of the Wightman function and the commutator we need to compute  $\alpha$  defined in (3.104) and the asymptotic behaviour of  $\psi$ . We can compute

$$\alpha^{-2} = \int_0^\infty \omega \frac{|\psi(r)|^2}{r(r^2 + a^2)} h(r) dr, \quad (3.126)$$

where the measure factor,  $h(r)$ , is given below (3.97)

However, we see that the WKB wave-function given in (3.107), (3.109) and (3.112) has no growing exponential of  $\gamma$  and therefore

$$\lim_{\gamma \rightarrow \infty} \frac{\log(\alpha)}{\gamma} = 0. \quad (3.127)$$

This leaves us with the asymptotic part of the wave-function, which is controlled by the coefficient  $C$  in (3.114). A simple calculation yields that at large  $\gamma$  we have

$$-\log(C) = \int_{\xi_2}^{\xi_3} \sqrt{V(\xi)} d\xi + \frac{\delta}{\xi_3} + \mathcal{O}(1) = \frac{\pi\gamma((8\kappa^2 + 11)n - 1)}{32\kappa^2 n^{3/2}} + \mathcal{O}(1). \quad (3.128)$$

Using the formula (3.98) the falloff of the Wightman function and the commutator for the fuzzball geometry is given by

$$\lambda_{\text{fuzz}} \equiv \lim_{\gamma \rightarrow \infty} \frac{\log |G(\omega, \gamma)|}{\gamma} = \lim_{\gamma \rightarrow \infty} \frac{\log |J(\omega, \gamma)|}{\gamma} = \frac{\pi}{2\sqrt{n}} + \frac{(11n - 1)\pi}{16n^{\frac{3}{2}}\kappa^2}. \quad (3.129)$$

One subtlety in comparing the fuzzball result with the bound is that the fuzzballs also have angular momentum along the  $S^3$ . It is understood holographically that — at least for the purpose of computing correlation functions such as (3.93), which do not themselves depend on any  $S^3$  variable — black holes with angular momentum along the  $S^3$  direction behave as if they have an “effective” Virasoro charges given by-

$$L_0^{\text{eff}} = L_0 - \frac{J_L^2}{N_1 N_5}, \quad (3.130)$$

where we have recalled that the central charge of the theory is  $6N_1 N_5$ . (See, for example, the discussion below (5.17) of [88] and the original discussion in [89].) We emphasize that using this “effective charge” rather than the original charge only *weakens*

the bound (3.124) and so makes the comparison more favourable for fuzzballs.

The right inverse-temperature of the fuzzball is infinity because the solution satisfies  $\bar{L}_0 = 0$ . The effective left inverse-temperature corresponding to the effective charge above is given by

$$\beta_L = \pi (\kappa^2 + 2) \sqrt{\frac{1}{\kappa^2 (\kappa^2 + 2) n - 1}}. \quad (3.131)$$

Comparing the decay of the fuzzball Wightman function and the commutator to the bound we find that

$$\boxed{\lambda_{\text{fuzz}} - \frac{1}{2}\beta_L = \frac{\pi(3n-1)}{16\kappa^2 n^{3/2}} + \mathcal{O}\left(\frac{1}{\kappa^4}\right)}. \quad (3.132)$$

Therefore, fuzzballs *fail* to saturate the large- $\gamma$  bound (3.124) by the amount shown above.

### 3.4.6 Numerical verification

We can verify the analytic results above by direct numerical analysis of the propagation of a scalar field in the fuzzball background.

We consider a fuzzball background with a given value of  $\kappa$  and  $n$  and a scalar field excitation with a given value of  $y$ -momentum,  $\gamma$ . The equation (3.105) is subject to normalizability under the Klein-Gordon norm, and this fixes boundary conditions both at  $\xi = 0$  and at  $\xi = \infty$ . In fact, both  $\xi = 0$  and  $\xi = \infty$  are singular points of the equation, and to solve the equation numerically, we must expand in a series solution about the point  $\xi = 0$  out to  $\xi = \epsilon$ .

Near  $\xi = 0$ , we set the function and its derivative through the expansion

$$\psi^0(\xi) = \left(\frac{\xi}{\epsilon}\right)^{\frac{2\gamma-1}{2}} (1 + a_0 \xi^2), \quad 0 < \xi \leq \epsilon, \quad (3.133)$$

with

$$a_0 = -\frac{\gamma^2 (\kappa^4 + 4) + (\kappa^2 + 2)^2 w^2 - 2\gamma\kappa^2 (\kappa^2 + 2) w - 8}{16(\gamma + 1)}. \quad (3.134)$$

Note that, for numerical convenience, the normalization used here is *different* from

the normalization used in (3.107).

Near  $\xi = \infty$ , we set the function and its derivative through the expansion

$$\psi^\infty = \frac{1}{\sqrt{\xi}} \left( 1 + \frac{a_\infty}{\xi^2} \right), \quad \frac{1}{\epsilon} \leq \xi < \infty, \quad (3.135)$$

with

$$a_\infty = \frac{1}{32} (-\gamma^2 \kappa^4 + 4\gamma^2 - \omega^2 \kappa^4 - 4\kappa^2 \omega^2 - 4\omega^2 + 2\gamma \kappa^4 \omega + 4\gamma \kappa^2 \omega). \quad (3.136)$$

Note that, for numerical convenience, this normalization is also chosen to be different from the normalization used in (3.112).

The allowed values of  $\omega$  can then be fixed by a *shooting* procedure. Given a guess for  $\omega$ , starting from  $\xi = \epsilon$ , we solve the equation to the mid-point of the trough of the potential:  $\xi_m = \frac{1}{2}(\xi_1 + \xi_2)$ . This solution yields some values for the function and its derivative:  $\psi^0(\xi_m)$  and  $\frac{d\psi^0(\xi_m)}{d\xi}$ . Similarly, for the same value of  $\omega$ , we can start from  $\xi = \frac{1}{\epsilon}$  and solve inwards to obtain a second set of values for the function and its derivative:  $\psi^\infty$  and  $\frac{d\psi^\infty}{d\xi}$ . These values define a difference function for any given value of  $\omega$

$$\mathcal{D}(\omega) = \frac{d\psi^\infty}{d\xi} \psi^0(\xi_m) - \frac{d\psi^0(\xi_m)}{d\xi} \psi^\infty. \quad (3.137)$$

We then use non-linear root-finding techniques to find the roots of  $\mathcal{D}(\omega)$ . In our analysis, we first bracketed the root, and then used the Brent method as implemented in the GNU Scientific Library [90]. Bracketing methods are robust and guaranteed to converge to a root in the bracketed interval.

Note that it is because the equation is linear that we can get away by just matching the *ratio* of the function and its derivative at the point  $\xi_m$ . If this had not been the case, we would have had to match both these quantities separately; this would have forced us to use two-dimensional root finding, which is far less robust.

The asymptotic value of the function,  $C$ , as defined above, can be fixed as follows. We denote the value that the solution starting at  $\xi = 0$  takes at  $\xi_1$  by  $\psi^0(\xi_1)$ . Then  $C$  is given by

$$C = \frac{\psi^0(\xi_m)}{\psi^{\text{inf}}(\xi_m)} \times \frac{2\sqrt{\pi} \text{Ai}(0)}{|V'(\xi_1)|^{\frac{1}{6}}} \times \frac{1}{\psi^0(\xi_1)}. \quad (3.138)$$

Note that  $\text{Ai}(0) \approx 0.355028$ . This formula implements the following procedure:

First we normalize the solution on the left so that it takes on the value given by (3.108) at  $\xi_1$ . Then, we normalize the solution on the right so that it matches the left solution at the mid-point.

Unlike the WKB analysis, the numerical analysis is not restricted to large  $\gamma$ . However, we can use it in the same regime to verify the results of the WKB approximation above.

In Figure 3.8, we show how the gap between the first two non-zero solutions of  $\omega$  matches with the analytic formula (3.116). We see that, at large  $\kappa$  (which is the

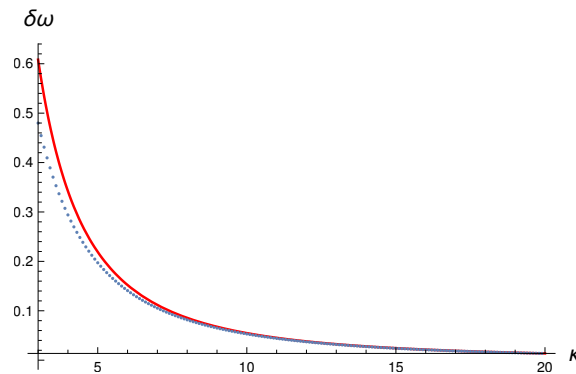


Figure 3.8: Comparison between a numerical calculation (dots) of the gap between the first two allowed frequencies and the formula (3.116) (solid curve). Other parameters are  $\gamma = 100, n = 2$ . In its regime of validity (large  $\kappa$ ) the formula (3.116) shows excellent agreement with the numerical results.

regime in which (3.116) is derived), the agreement is excellent. In Figure 3.9, we show a comparison of the numerically computed asymptotic value for  $C$  with the analytic formula (3.114) for a fixed value of  $\kappa = 5, n = 2$  and varying values of  $\gamma$ . We see, once again, that the agreement is excellent in the regime where the analytic formula is valid.

### 3.4.7 Analysis of the result

The key results derived above are the formula for the mass-gap (3.116) and the decay of the Wightman function (3.129) at large  $\gamma$ , which we also verified numerically. We discuss their significance in turn.

The formula for the gap (3.116) tells us that the gap between the frequency of

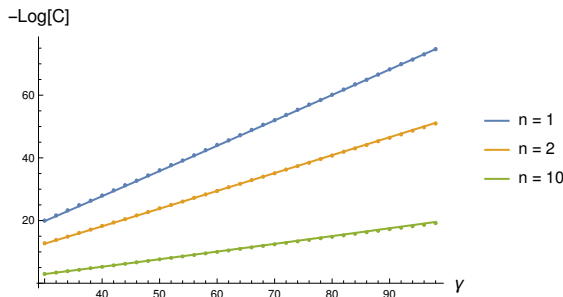


Figure 3.9: Comparison between a numerical calculation (dots) of the asymptotic value  $C$  with the formula (3.114) (solid curves) for different values of  $n$  and  $\gamma$ . Here,  $\kappa = 5$  is held fixed. In the appropriate regime of validity of the analytic formula (large  $\gamma$ ), it agrees very well with the numerical results.

successive excitations of these solutions is *far too large* for a typical microstate. As described in the discussion around (3.8), expectation (1) tells us that the Wightman function (after a small amount of local smearing) should have continuous support in frequency space. As explained there, this should be true even of the Wightman function in a BPS state. Even though the original state is BPS, the scalar excitation should connect these states to nearby non-BPS states that are expected to satisfy expectation 1.

However, for the fuzzball solutions we find that the support is concentrated on discretely spaced frequencies with a gap between consecutive frequencies that scales with  $\frac{1}{\kappa^2}$ . This means that the fuzzball solutions that we have analyzed, with any finite value of  $\kappa$  (provided  $\kappa$  does not scale with the central charge) *cannot* serve as microstates of a black hole.

Instead, the finite energy gap is reminiscent of a phase of zero-entropy — like thermal AdS as explained below (3.9). This suggests that the states corresponding to this set of fuzzball solutions belong to such a phase — which comprises exponentially atypical states.

The formula for the decay at large- $\gamma$  (3.129) tells us that if fuzzballs are microstates, then the set of fuzzball solutions correspond to states that violate the ETH. This is because, on the basis of the black-hole calculation, the thermal state is expected to saturate the bound (3.124). The ETH would then suggest that eigenstates of the Hamiltonian, or indeed, typical elements of any other basis that spans

that microcanonical ensemble should also saturate the bound.

We expect that the holographic theory dual to black holes should be chaotic in supergravity regime, and therefore it should satisfy the ETH: the hypothesis that fuzzballs are black-hole microstates contradicts this expectation.

Second, note that even if we disregard the ETH, the idea that fuzzballs are black-hole microstates leads to a strange conclusion: since the set of fuzzballs we have analyzed are below the bound, there must be some other fuzzballs that violate the bound (3.124). This is the only way that the microcanonical average can saturate the bound. Now, strictly speaking, this is not a contradiction since the bound (3.124) is a bound for the behavior of the thermal state in different *theories* and does not control the behaviour of specific pure states. But, on the other hand, we are not aware of *any* geometry that violates the bound (3.124). In the absence of such an example, it seems difficult to understand how the fuzzball geometries could represent black-hole microstates.

**Very large values of  $\kappa$ .** We now briefly consider the limit where we take  $a \sim \ell_{\text{pl}}$ . In this limit  $\kappa$  becomes large, and the decay of the large- $\gamma$  Wightman function approaches the bound (3.124). The energy-gap becomes small.<sup>4</sup> However, this energy-gap is still *too large* since it scales with an inverse power of the central charge rather than being exponentially suppressed. So, even in this limit, the fuzzball solutions do not yield the correct gap expected in the boundary theory. This, by itself, ensures that even Planck-sized fuzzballs do not have the right properties expected of a typical microstate.

We now discuss some independent problems with the idea of considering fuzzballs with Planckian features. We will argue that for  $a \sim \ell_{\text{pl}}$ , such solutions become indistinguishable from the black hole in most of space, and quantum fluctuations are likely to be large in the near-horizon region where the fuzzball deviates from the black hole.

First, note that in this limit, the angular momentum in the  $S^3$  directions, which is proportional to  $a^2$ , vanishes. So, in the subsector under consideration, solutions with very long throats (small values of  $a$ ) cannot correspond to states with arbitrary charges. However, for the remainder of this section, we will assume that when the

---

<sup>4</sup>This is the gap computed in [50] by taking  $\kappa = N_1 N_5$ .

full set of fuzzball-geometries is found, it will be possible to keep  $a$  arbitrarily small, while keeping the charges constant by changing some other parameters.

Second, we note that the  $a \rightarrow 0$  limit of (3.88) does not commute with the  $r \rightarrow 0$  limit. If we first take  $a \rightarrow 0$  so that we can neglect terms of order  $\frac{a}{r}$ , the metric has the following smooth limit:

$$\begin{aligned}
 ds_6^2 \xrightarrow{a \rightarrow 0} & \frac{(b^2 n - 2r^2)}{\sqrt{2bR_y}} dt^2 + \frac{(b^2 n + 2r^2)}{\sqrt{2bR_y}} dy^2 + \frac{bR_y}{\sqrt{2r^2}} dr^2 + \frac{\sqrt{2bn}}{R_y} dt dy \\
 & + \frac{bR_y \cos^2(\theta)}{\sqrt{2}} d\psi^2 + \frac{bR_y \sin^2(\theta)}{\sqrt{2}} d\phi^2 + \frac{bR_y}{\sqrt{2}} d\theta^2.
 \end{aligned} \tag{3.139}$$

A change of variables to  $\rho = \left(r^2 + \frac{b^2 n}{2}\right)^{\frac{1}{2}}$  shows that this is the metric of an extremal BTZ black hole  $\times S^3$ .

On the other hand, even when  $\frac{b}{a} \gg 1$ , if we explore the regions of the geometry where  $r = O(a)$ , we find a different answer. In coordinates where  $r = a\xi$ , the metric expanded to  $O(\xi^2)$  near  $\xi = 0$  is given by

$$\begin{aligned}
 ds_6^2 = & -\frac{(2a^2 - b^2)(\cos^2(\theta) + \xi^2)}{2\lambda^2} dt^2 + \frac{b^2(\cos^2(\theta) + \xi^2)}{\lambda^2} dt dy + \frac{(2a^2 + b^2)(\cos^2(\theta) + \xi^2)}{2\lambda^2} dy^2 \\
 & + \lambda^2 (1 - \xi^2) d\xi^2 - 2\frac{a^2 \sin^2(\theta)}{\sqrt{a^2 + \frac{b^2}{2}}} dt d\phi - \frac{b^2 \cos^2(\theta)}{\sqrt{a^2 + \frac{b^2}{2}}} dt d\psi - 2\sqrt{a^2 + \frac{b^2}{2}} \cos^2(\theta) dy d\psi \\
 & + \lambda^2 d\theta^2 + \lambda^2 \sin^2 \theta d\phi^2 + \lambda^2 \cos^2 \theta d\psi^2.
 \end{aligned} \tag{3.140}$$

If we take  $a \sim \ell_{\text{pl}}$ , then the fuzzball metric has Planckian structures near  $r = 0$  and these structures are given by the metric in (3.140). Remarkably, curvature invariants such as the Ricci scalar and even the square of the Riemann tensor,  $R_{\mu\nu\rho\sigma}R^{\mu\nu\rho\sigma}$ , which can be computed from (3.140) remain *finite* in limit as  $a \rightarrow 0$ . So, in this limit, the fuzzball metric cleverly introduces Planckian structures, without introducing Planckian curvatures! This is a surprising and nice feature of the solution.

However, it would be *incorrect* to imagine that this makes the classical metric immune to quantum fluctuations in this region. The study of section 3.3 tells us that we must also take into account quantum fluctuations in the *parameters* that specify a solution. In the two-charge case, the solution was specified by a profile

function  $F^i(s)$ . But, in the quantum theory, the profile function did not have a definite value because of the non-zero commutator,  $[F^i(s), F^i(\tilde{s})]$ . We saw that when the metric had Planck scale features, the uncertainties in the profile function were enough to make these features unreliable.

In the absence of a moduli-space quantization of the solutions examined in this section, we cannot make analogous precise statements for the multi-charge solutions. However, a rule of thumb is that we do not expect to pin down bulk length-scales in a theory of quantum gravity with perfect certainty. Therefore, it is fair to estimate that in the quantum states corresponding to the metrics examined in this section, the length-scale  $a$  will itself fluctuate and that  $\delta a = O(\ell_{\text{pl}})$ .

If this is correct, then in the regime where  $a = O(\ell_{\text{pl}})$  we also have  $\frac{\delta a}{a} = O(1)$ . But then, examining the metric (3.140), we see that such fluctuations will *induce* fluctuations in the metric so that  $\delta g_{\mu\nu} = O(g_{\mu\nu})$ . For example, we see that for the determinant of the metric (3.140)

$$g = \det(g_{\mu\nu}) = a^4 \lambda^4 \xi^2 (\xi^4 - 1) \sin^2(\theta) \cos^2(\theta), \quad (3.141)$$

and therefore

$$\delta g = \frac{\partial g}{\partial a} \delta a = 4g \frac{\delta a}{a}. \quad (3.142)$$

If  $\frac{\delta a}{a} = O(1)$  then  $\frac{\delta g}{g} = O(1)$ . So, while the Planckian structures are smooth, in the sense that local curvature invariants remain bounded, they are nevertheless not reliable features of the metric.

We caution the reader that our arguments in this last paragraph have been necessarily somewhat imprecise. This is because the fuzzball program has itself not been carried through to completion in this setting. But we believe that our reasoning is robust for a simple reason. The parameters that specify a fuzzball solution are coordinates on the phase space of gravity. Usually, we do not consider classical solutions whose distinctive features depend on specifying phase-space coordinates to an accuracy that depends on  $\hbar$ . Conversely, if we attempt to do so, we should expect that the minimal fluctuations on phase space induced by the uncertainty principle will wash out these features.

### 3.5 Discussion

In this chapter we explored the viability of the fuzzball proposal to the black hole information paradox. We argued that the fuzzball geometries that differ from the conventional black hole geometries cannot parameterize the phase space of all black hole microstates. Hence, these geometries are not relevant for the black hole information paradox. Classical geometries which differ from the conventional black hole geometry only within Planck scale from the horizon are not reliable due to large quantum fluctuations. Hence, one cannot argue that typical black hole microstates do not have a horizon. We realized these expectations explicitly for two-charge fuzzball geometries.

We studied asymptotically AdS fuzzball geometries corresponding to black holes with finite horizon radius. The solutions which we analyzed were too atypical. The deviations from the conventional geometry could be detected by simple asymptotic correlators. We also showed that fuzzballs that cap off a macroscopic distance away from the horizon have a gap between the frequency of allowed excitations that is too large for black-hole microstates. We expect our results to generalize to arbitrary solutions that have macroscopic features.

We note that structure at horizon is not required to resolve the information paradox. As we have already seen in chapter 2, holographic encoding of information is a feature of quantum gravity. This feature is sufficient to resolve the strong subadditivity and cloning paradox.

## Chapter 4

### Bound on thermal Wightman correlators

#### 4.1 Introduction

In this chapter, based on [14], we consider a novel limit of thermal correlation functions in a relativistic quantum field theory in  $d$  spacetime dimensions. Let  $\mathcal{O}(t, \vec{x})$  be any local operator, which may be the elementary field itself or a more complicated operator. Then consider the Fourier transformed correlation function at finite temperature  $\beta^{-1}$

$$G(\omega_i, \vec{k}_i) \delta_\omega \delta_{\vec{k}} \equiv \int \prod_i dt_i d\vec{x}_i \frac{1}{Z} \text{Tr} [e^{-\beta H} \mathcal{O}(t_1, \vec{x}_1) \dots \mathcal{O}(t_n, \vec{x}_n)] e^{i \sum (\omega_i t_i - \vec{k}_i \cdot \vec{x}_i)}, \quad (4.1)$$

where  $Z$  is the partition function and we use the shorthand notation  $\delta_\omega \equiv (2\pi) \delta(\sum \omega_i)$ , and  $\delta_{\vec{k}} \equiv (2\pi)^{d-1} \delta(\sum \vec{k}_i)$  to indicate the delta functions that appear because the position-space correlator on the right is invariant under overall spacetime translations.

The correlator above is a Wightman correlator which means that we just evaluate the quantum expectation value of the product of operators shown and do not impose time-ordering. We now consider the limit of this correlator where  $|\vec{k}_i| \rightarrow \infty$  but  $\omega_i = \text{fixed}$ .

About the vacuum, this limit would just yield zero since the spectrum condition,  $H \geq |\vec{P}|$ , in relativistic quantum field theories tells us that we cannot have excitations with energy smaller than momentum. However, in a thermal state such excitations can exist. For example, the operator  $\mathcal{O}$  could create a particle with large momentum  $\vec{k}$  and simultaneously destroy a particle from the thermal background with the opposite momentum. This would change the momentum of the state by a large amount but the energy by only a small amount.

In this chapter, we show that the correlators (4.1) are constrained by a beautiful geometric bound. We prove, using analytic properties of correlation functions that hold in any relativistic quantum field theory, that

$$\lim_{\substack{|\vec{k}_i| \rightarrow \infty \\ \omega_i = \text{const}}} \frac{1}{R(\vec{k}_i)} \log |G(\omega_i, \vec{k}_i)| \leq -\beta, \tag{4.2}$$

where  $R(\vec{k}_i)$  is the radius of the smallest sphere that encloses the unique (non-planar) polygon with  $i^{\text{th}}$  edge labeled by  $\vec{k}_i$ . Less formally, our bound states that in this limit,  $G(\omega_i, \vec{k}_i)$  must die off *at least as fast as*  $e^{-\beta R(\vec{k}_i)}$ . Two examples of this geometric radius are shown in Figure 4.1; these are relevant for a three-point and a four-point function respectively.

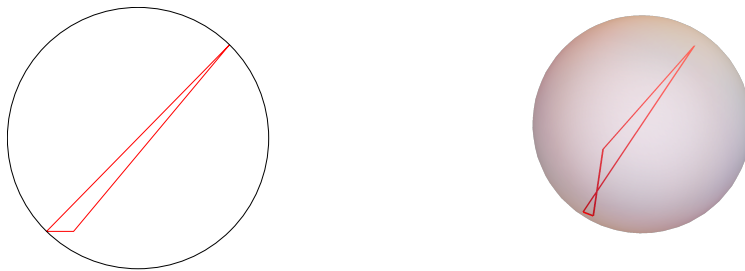


Figure 4.1: *The bounding sphere for a three-point function (left) and a four-point function (right). The red polygon in both cases shows the spatial momenta.*

Operators whose momentum is much larger than their frequency appear in the map between bulk and boundary operators in the AdS/CFT correspondence [2, 4, 3]. The reconstruction of the field operator at a local bulk point at finite temperature necessarily makes reference to such operators. Such operators also appear if one attempts to reconstruct a causal wedge in the bulk from a boundary causal diamond [57]. This led [57] to analytically continue their bulk-boundary smearing function and has led to some claims that the bulk-boundary map is ill-defined or discontinuous in black-hole backgrounds [91, 92].

This issue was examined in [62] and in [68], it was pointed out that the map was still well-defined since it should be properly thought of as a *distribution* that acts on

operators whose natural “size” at large spacelike momenta is small. (This idea was subsequently also elaborated in [93].) For the purpose of the bulk-boundary map at leading order, the only correlator that is relevant is the two-point function and so [62] proved the bound (4.2) for two-point functions. In this chapter, we present a generalization of this bound for arbitrary point functions, and also examine its behaviour in various theories.

In section 4.3 we study correlators of the form (4.1) in weakly coupled theory. We show that if we take the operators  $\mathcal{O}(t_i, \vec{x}_i)$  to be the elementary fields themselves, then this bound is *not saturated* by the leading tree-level interaction. However, once one goes to high-enough loop order, then the perturbative expansion always contains a term that saturates (4.2).

This may suggest that holographic theories would always saturate the bound as these theories are strongly coupled. However, as explored in section 4.4, this is not always true. We consider holographic correlators of operators dual to propagating fields in anti-de Sitter space. Although in  $d = 2$ , the leading order holographic two-point function in a black-hole background saturates the bound, for higher  $d$ , the two-point function remains *below* the bound. While the bound would suggest that the two-point function could be as large as  $e^{-\frac{\beta|\vec{k}|}{2}}$  it turns out that in  $d$ -dimensions it is only as large as  $e^{-\alpha\frac{\beta|\vec{k}|}{2}}$  where  $\alpha = \frac{d\Gamma[1+\frac{1}{d}]}{\sqrt{\pi}\Gamma[\frac{1}{2}+\frac{1}{d}]}$ . For example, for  $d = 4$ ,  $\alpha = 1.67$ . This factor was noticed earlier in [94, 91], although no connection to the bound (4.2) was made.

While black-holes are sometimes believed to be “hypercompetitive” [95], this provides an example where the characteristic feature of a strongly coupled holographic theory in a state with a bulk horizon is the *under saturation* of a bound that is saturated by other theories. We do not have an intuitive understanding of this behaviour, and we believe that this is an important and striking feature that deserves further attention.

We believe that this bound is interesting and may have other applications. For example, the consideration of correlators with large spacelike momenta can serve as a diagnostic of whether the state is thermal or not. This diagnostic was used in in [10], where it was shown that fuzzball solutions do not saturate the bound even for  $d = 2$ , suggesting that the known fuzzball solutions are not good representatives of microstates of black-holes and are not dual to the boundary thermal state. The

behaviour of correlators of operators with large spacelike momenta may also serve as a diagnostic of when a theory is holographic, and when the bulk has a horizon, just like the chaos bound [96]. This diagnostic was also examined in [97].

A brief overview of this chapter is as follows. In section 4.2, we prove the bound for general relativistic quantum field theories. In section 4.3, we consider thermal Wightman correlators in perturbative quantum field theories and show that at sufficiently high-loop order we expect such theories to saturate the bound. In 4.4 we turn to holographic theories. Here, we first analyze holographic two-point functions, and then initiate a study of higher-point functions. The appendices contain a review of the formalism used to compute thermal Wightman functions, and some further details of the holographic analysis.

## 4.2 Proof of the bound

In this section, we will prove the bound (4.2). We consider a Wightman correlator of the form (4.1) and make the following assumptions

- 1 The correlator (4.1) is well defined at all values of the temperature.
- 2 The underlying theory obeys the spectrum condition, so that states which are simultaneous eigenstates of the energy and momentum, with eigenvalues  $E$  and  $\vec{P}$ , satisfy  $E \geq |\vec{P}|$ .

Due to energy momentum conservation, note that the correlation function (4.1) only has support on the submanifold where  $\sum \omega_i = \sum \vec{k}_i = 0$ . In particular, this means that the momenta  $\vec{k}_i$  generically form a non-planar polygon in  $(d - 1)$ -dimensions. We now wish to prove the bound (4.2) where  $R$  is the radius of the smallest  $(d - 1)$ -sphere that encloses this polygon.

We will establish the proof in three steps. In the first step we will start with thermal correlators in coordinate space and we will argue that the correlators can be analytically continued to a particular domain of complexified coordinates. In the second step we will show how the analyticity domain of the correlators in coordinate space implies bounds for the momentum space correlators at large spacelike momenta. Finally in the third step, we will show that the optimal such bound is

related to a simple geometric extremization problem, whose solution we present. This leads to the bound (4.2) for correlators in momentum space.

#### 4.2.1 First part: on the analyticity domain of position-space thermal correlators

We start with finite temperature, real-time correlators in coordinate space

$$G(x_i) \equiv Z^{-1} \text{Tr}[e^{-\beta H} \mathcal{O}(x_1) \dots \mathcal{O}(x_n)]$$

These are Wightman correlators, so there is no time-ordering. For notational convenience we take all operators to be the same; the generalization to different operators is obvious. We use the notation  $x$  to denote  $d$ -vectors and  $x^0, \vec{x}$  to denote the timelike and spacelike components respectively. We wish to examine the domain of analyticity of these correlators. Our discussion closely follows [98], and a more detailed discussion is available in [39]. The domain of analyticity for thermal correlators was discussed in [99].

Using translational invariance we can parameterize this correlator as

$$\hat{G}(\xi_i) \equiv Z^{-1} \text{Tr}[e^{-\beta H} \mathcal{O}(0) \mathcal{O}(\xi_1) \mathcal{O}(\xi_1 + \xi_2) \dots \mathcal{O}(\xi_1 + \dots + \xi_{n-1})], \quad (4.3)$$

where  $\xi_1 \equiv x_2 - x_1, \xi_2 \equiv x_3 - x_2$  etc. We introduce the timelike vector  $e \equiv (1, 0, \dots, 0)$  and using the cyclicity of the trace we write this correlator as

$$\hat{G}(\xi_i) = Z^{-1} \text{Tr}[\mathcal{O}(0) e^{-iP \cdot \xi_1} \mathcal{O}(0) e^{-iP \cdot \xi_2} \mathcal{O}(0) \dots e^{-iP \cdot \xi_{n-1}} \mathcal{O}(0) e^{P \cdot [\beta e + i(\xi_1 + \dots + \xi_{n-1})]}], \quad (4.4)$$

where  $P \equiv (H, \vec{P})$  are the operators for space-time translations and the inner-product between  $d$ -vectors is taken using the  $(-, + \dots +)$  metric. We insert complete sets of states between these operators, which leads to an expansion of the form

$$\hat{G}(\xi_i) = Z^{-1} \sum_{i_1, \dots, i_n} \mathcal{O}_{i_n i_1} e^{-iP_{i_1} \cdot \xi_1} \mathcal{O}_{i_1 i_2} e^{-iP_{i_2} \cdot \xi_2} \dots \mathcal{O}_{i_{n-1} i_n} e^{P_{i_n} \cdot [\beta e + i(\xi_1 + \dots + \xi_{n-1})]}, \quad (4.5)$$

where we defined the matrix elements  $\mathcal{O}_{ij} \equiv \langle i | \mathcal{O}(0) | j \rangle$  on eigenstates of the energy-momentum  $P$ . Now we analytically continue the coordinates  $\xi_i$  as  $\xi_i \rightarrow \xi_i + i\eta_i$ .

Under this analytic continuation in (4.5) we get factors of the form  $e^{P_i \cdot \eta_i}$  in-between the various operators. Using the spectrum condition  $H \geq |\vec{P}|$ , the factors  $e^{P_i \cdot \eta_i}$  will improve the convergence of the sum over  $i_1, \dots, i_{n-1}$  provided that

$$\eta_i \in V^+, \quad (4.6)$$

where  $V^+$  denotes the future timelike cone.

On the other hand, the convergence of the sum over  $i_n$ , corresponding to the overall trace in (4.3), is improved provided that the last factor all the way to the right in (4.5) is suppressed. After analytic continuation that term gives a factor of  $e^{P_{i_n} \cdot (\beta e - (\eta_1 + \dots + \eta_{n-1}))}$ . From the spectrum condition this improves the convergence provided that

$$\beta e - (\eta_1 + \dots + \eta_{n-1}) \in V^+. \quad (4.7)$$

Let us call  $\mathcal{F}$  the domain of the coordinates  $\{\xi_i + i\eta_i\}$  defined by simultaneously imposing equations (4.6) and (4.7) for the imaginary parts  $\eta_i$ , i.e.

$$\mathcal{F} \equiv \{ \{ \xi_i + i\eta_i \} \in \mathbb{C}^{4n} : \eta_i \in V^+ \text{ and } \beta e - (\eta_1 + \dots + \eta_{n-1}) \in V^+ \}$$

Notice that  $\mathcal{F}$  must be least only *part* of the domain of analyticity of the correlator  $\hat{G}$ . This is because by assumption 1 above, the sum over  $i_1, \dots, i_n$  is convergent even for an infinitesimal value of  $\beta$ , and in the domain,  $\mathcal{F}$ , the analytic continuation only improves the convergence of the sum. Note that it may be possible to further analytically continue into a larger domain. But, for the purpose of our proof we only need that the correlators  $\hat{G}$  in (4.3) can be analytically continued at least in  $\mathcal{F}$  without encountering any singularities. The region  $\mathcal{F}$  is shown in Figure 4.2

Using the notation  $\eta_i = (\eta_i^0, \vec{\eta}_i)$ , equation (4.6) is equivalent to

$$\eta_i^0 \geq 0 \quad \text{and} \quad \eta_i^0 \geq |\vec{\eta}_i|$$

and (4.7) equivalent to

$$\beta - (\eta_1^0 + \dots + \eta_{n-1}^0) \geq 0$$

and

$$\beta - (\eta_1^0 + \dots + \eta_{n-1}^0) \geq |\vec{\eta}_1 + \dots + \vec{\eta}_{n-1}|$$

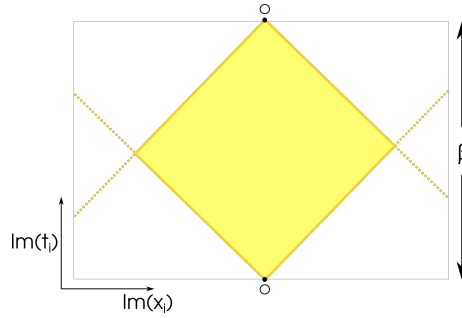


Figure 4.2: The domain of analyticity  $\mathcal{F}$ : if the first point is at  $O$ , then the correlator is analytic if the imaginary coordinates of successive points are chosen from any causal trajectory that lies within the shaded region.

Using these conditions, we find that any point in the domain  $\mathcal{F}$  defined by equations (4.6),(4.7) obeys

$$|\vec{\eta}_1| + \dots + |\vec{\eta}_{n-1}| + |\vec{\eta}_1 + \dots + \vec{\eta}_{n-1}| \leq \beta. \quad (4.8)$$

Moreover, it is easy to see that for any choice of the spatial vectors  $\vec{\eta}_i$  which satisfies (4.8), we can select their time-components  $\eta_i^0$  such that we are inside the domain of (4.6),(4.7). In addition, this choice can be made so that the point  $\{\eta^0, \vec{\eta}_i\}$  can be continuously connected to the real-plane  $\eta_i = 0$  by a path inside  $\mathcal{F}$ .

Hence we have established that the domain  $\mathcal{F}$  contains points which completely cover the domain in the *spatial coordinates*  $\vec{\eta}_i$  defined by equation (4.8).

Now, we remember that  $\vec{\eta}_i$  are defined as the spatial part of the imaginary part of the complexified *difference vectors*  $\xi_i + i\eta_i$ . Let us express the domain of analyticity in terms of the complexification of the original coordinates  $x_i \rightarrow x_i + iy_i$ . We have  $\vec{\eta}_1 = \vec{y}_2 - \vec{y}_1$   $\vec{\eta}_2 = \vec{y}_3 - \vec{y}_2$   $\dots$   $\vec{\eta}_{n-1} = \vec{y}_n - \vec{y}_{n-1}$  Then (4.8) can be written as  $|\vec{y}_1 - \vec{y}_2| + \dots + |\vec{y}_n - \vec{y}_1| \leq \beta$ .

So finally we reach the following conclusion: the thermal correlator

$$G(x_i) \equiv Z^{-1} \text{Tr}[e^{-\beta H} \mathcal{O}(x_1) \dots \mathcal{O}(x_n)]$$

can be analytically continued to complex space-time coordinates  $x_i + iy_i$  in (at least) a domain which contains points whose spatial imaginary parts can have any possible

value obeying

$$|\vec{y}_1 - \vec{y}_2| + \dots + |\vec{y}_n - \vec{y}_1| \leq \beta. \quad (4.9)$$

Moreover these points are continuously connected to the real-domain  $y_i = 0$  by a path in the domain of analyticity.

#### 4.2.2 Second part: decay of spacelike correlators

Now we will explain how the analyticity of position-space correlators discussed above is related to the decay of momentum space correlators at large spacelike momentum.

First we consider “mixed” correlators, where we Fourier transform in time but not in space

$$G(\omega_i, \vec{x}_i) \delta_\omega \equiv \int \prod_i dt_i G(t_i, \vec{x}_i) e^{i \sum \omega_i t_i}$$

Now we want to analytically continue in  $\vec{x}_i$ . Notice that we can not just analytically continue the integrand on the RHS in  $\vec{x}_i$  alone, as this would — in general — take us out of the domain of analyticity of the correlator. However, we can analytically continue the integrand in  $\vec{x}_i$ , provided that we shift, at the same time, the time arguments  $t_i$  in the complex plane (i.e. we shift the contours of integration by giving nonzero values to  $\text{Im}[t_i]$ ). While doing this we need to make sure that  $\text{Im}(t_i, \vec{x}_i)$  stays within the domain of analyticity determined at the end of the previous subsection. Notice that under this analytic continuation the factor  $e^{i\omega_1 t_1 + \dots + i\omega_n t_n}$  gives at most a growing exponential, but can not introduce any singularities.

From this follows that the correlator

$$G(\omega_i, \vec{x}_i)$$

can be analytically continued as  $\vec{x}_i \rightarrow \vec{x}_i + i\vec{y}_i$ , in (at least) the domain determined by

$$|\vec{y}_1 - \vec{y}_2| + \dots + |\vec{y}_n - \vec{y}_1| \leq \beta. \quad (4.10)$$

Finally we consider the fully Fourier transformed Wightman correlators in frequency momentum space

$$G(\omega_i, \vec{x}_i) = \int \prod_i \frac{d^{d-1} \vec{k}_i}{(2\pi)^{d-1}} G(\omega_i, \vec{k}_i) \delta_{\vec{k}} e^{i \sum \vec{k}_i \vec{x}_i}$$

We argued above that the LHS is analytic in the domain (4.10) upon  $\vec{x}_i \rightarrow \vec{x}_i + i\vec{y}_i$ . Under this analytic continuation, on the RHS we get the expression

$$\int \prod_i \frac{d\vec{k}_i}{(2\pi)^{d-1}} G(\omega_i, \vec{k}_i) \delta_{\vec{k}} e^{\sum \vec{k}_i \cdot \vec{y}_i}$$

In general the last factor grows exponentially. In order for the integral to be convergent it must be that  $G(\omega_i, \vec{k}_i)$  decays sufficiently fast at large  $\vec{k}_i$ , so as to suppress the growth of the last term. This is the origin of the bound (4.2).

The strictest possible bound on  $G$  from these considerations will come from maximizing the expression

$$I \equiv \left| \sum \vec{k}_i \cdot \vec{y}_i \right|, \quad (4.11)$$

where

$$|\vec{y}_1 - \vec{y}_2| + \dots + |\vec{y}_n - \vec{y}_1| \leq \beta, \quad (4.12)$$

and also

$$\sum \vec{k}_i = 0. \quad (4.13)$$

This last condition comes from the fact that the momentum space correlator has support only on momenta obeying this. Let us call  $I_{\max}$  the maximum of  $I$  defined by (4.11), where we vary the vectors  $\{\vec{y}_i\}$  over all possible values, subject to the constraints (4.12). The momentum vectors  $\vec{k}_i$  must obey (4.13). Then we find the optimal bound,  $G \sim e^{-I_{\max}}$ , or more precisely,

$$\lim_{\substack{|\vec{k}_i| \rightarrow \infty \\ \omega_i = \text{const}}} \frac{1}{I_{\max}} \log(|G|) \leq -1. \quad (4.14)$$

Determining  $I_{\max}$  corresponds to a simple geometric problem that we now consider.

### 4.2.3 Third part: an extremization problem

Above we found that the momentum-space correlator will have to decay like (4.14), where

$$I_{\max} = \left\{ \max \left| \sum \vec{k}_i \vec{y}_i \right| : \vec{y}_i \in \mathbb{R}^{d-1}, |\vec{y}_1 - \vec{y}_2| + \dots + |\vec{y}_n - \vec{y}_1| \leq \beta \right\}, \quad (4.15)$$

with  $\sum \vec{k}_i = 0$ .

It is easy to see that this extremization problem can equivalently be formulated slightly differently by redefining both the  $\vec{k}_i$  and the  $\vec{y}_i$  variables. First we introduce  $n$  new vectors  $\vec{P}_i$  such that  $\vec{k}_1 = \vec{P}_2 - \vec{P}_1$ ,  $\vec{k}_2 = \vec{P}_3 - \vec{P}_2$ ,  $\dots$ ,  $\vec{k}_{n-1} = \vec{P}_n - \vec{P}_{n-1}$ ,  $\vec{k}_n = \vec{P}_1 - \vec{P}_n$ . This does not uniquely fix the  $\vec{P}_i$ , as we can add to them an overall “center of mass” shift. However, this ambiguity will drop out in what follows. Also, notice that if we parameterize the  $\vec{k}_i$ ’s in terms of  $\vec{P}_i$ ’s as above, then the condition  $\sum \vec{k}_i = 0$  is automatic. We also redefine the  $\vec{y}$  variables by introducing  $\vec{a}_1 \equiv \vec{y}_n - \vec{y}_1$ ,  $\vec{a}_2 \equiv \vec{y}_1 - \vec{y}_2$ ,  $\dots$ ,  $\vec{a}_n \equiv \vec{y}_{n-1} - \vec{y}_n$ , where now we automatically have  $\sum \vec{a}_i = 0$ .

Now, it is a matter of simple algebra to check that the quantity  $I = |\sum \vec{k}_i \vec{y}_i|$  that we wanted to extremize takes the form

$$I = \sum |\vec{P}_i \vec{a}_i|, \quad (4.16)$$

where we extremize over  $\vec{a}_i$  subject to the condition that  $\sum \vec{a}_i = 0$  and the condition (4.12) which becomes

$$\sum |\vec{a}_i| \leq \beta$$

It is now obvious that since  $\sum \vec{a}_i = 0$  the overall center of mass shift ambiguity of the  $\vec{P}_i$ ’s that we mentioned earlier has no relevance for the extremization problem.

To summarize, we have shown that the original problem (4.15) is equivalent to the extremization problem

$$I_{\max} = \{\max |\sum \vec{P}_i \vec{a}_i| : \vec{a}_i \in \mathbb{R}^{d-1}, \sum \vec{a}_i = 0, \sum |\vec{a}_i| \leq \beta\}. \quad (4.17)$$

### The solution:

We now present the solution to the extremization problem (4.17). Consider  $n$  points  $\vec{P}_i$  in  $\mathbb{R}^{d-1}$ . We define the “minimal enclosing sphere” in the obvious way. We assume that this sphere has center  $\vec{C}$  and radius  $R$ . The radius  $R$  clearly does not depend on the overall center of mass position of the points  $\vec{P}_i$ .

Consider all possible  $n$ -tuples of vectors  $\vec{a}_i \in \mathbb{R}^{d-1}$ , with the properties required in (4.17), i.e. that

$$\sum \vec{a}_i = 0; \quad \sum |\vec{a}_i| \leq \beta. \quad (4.18)$$

We want to maximize

$$I \equiv \left| \sum_i \vec{P}_i \vec{a}_i \right|.$$

We will prove that

$$I_{\max} = \beta R. \tag{4.19}$$

. We first notice that for any  $\vec{a}_i$ 's obeying (4.18) we have the inequality  $I \leq \beta R$  since

$$I \equiv \left| \sum_i \vec{P}_i \vec{a}_i \right| = \left| \sum_i (\vec{P}_i - \vec{C}) \vec{a}_i \right| \leq R \left( \sum_i |\vec{a}_i| \right) \leq \beta R, \tag{4.20}$$

where in the second equality we used the fact that since  $\sum \vec{a}_i = 0$  we can shift the overall center of mass of the points by  $\vec{C}$  without changing the value of  $I$ . In the third equality we used  $|\vec{P}_i - \vec{C}| \leq R$ .

We have shown that for any  $\vec{a}_i$  obeying (4.18) we have  $I \leq \beta R$ . Will now identify a particular choice of  $\vec{a}_i$  which saturate the inequality (4.20). This will prove our claim that  $I_{\max} = \beta R$ .

First we will make use of a basic geometric result: the center  $\vec{C}$  of the minimal enclosing sphere of  $n$  points  $\vec{P}_i$  in  $\mathbb{R}^{d-1}$  is in the convex hull of the points  $\vec{P}_i$ . This means that we can find  $n$  real numbers  $\lambda_i$  obeying  $\lambda_i \geq 0$ ,  $\sum \lambda_i = 1$  such that  $\vec{C} = \sum \lambda_i \vec{P}_i$ . The proof of this result is simple: if  $\vec{C}$  is not in the convex hull of  $\vec{P}_i$  then the *hyperplane separation theorem* says that there is a hyperplane separating  $\vec{C}$  from all  $\vec{P}_i$ . If we move  $\vec{C}$  towards this hyperplane we reduce the distance from all points  $\vec{P}_i$ , contradicting the statement that  $\vec{C}$  was the center of the minimal enclosing sphere.

We will now consider a slight refinement of the aforementioned result. For a particular choice of the set of points  $\vec{P}_i$  we consider the minimal bounding sphere. Some of the points will be exactly on the sphere, while the remaining will be inside. We concentrate on the  $m$  points exactly on the sphere, let us call them *extremal points*. We select the index  $i$  labeling the points, so that the extremal points are the first  $m$  points  $\vec{P}_i, i = 1, \dots, m$ , The remaining points which are in the interior of the sphere are labeled as  $\vec{P}_i, i = m + 1, \dots, n$ . Notice that it may be that  $m = n$ . We consider the minimal bounding sphere of the extremal points alone (i.e. simply ignoring the interior points). It should be obvious that the sphere will be exactly the same as before. Applying the previous theorem to the set of extremal points,

we conclude that the center  $\vec{C}$  of the minimal enclosing sphere is also in the convex hull of the *extremal* points alone. This means that we can write

$$\vec{C} = \sum_{i=1}^m \lambda_i \vec{P}_i, \quad \lambda_i \geq 0 \quad \text{and} \quad \sum \lambda_i = 1. \quad (4.21)$$

Returning to the extremization problem (4.17), we then consider the following choice of the vectors  $\vec{a}_i$

$$\vec{a}_i = \frac{\beta}{R} \lambda_i (\vec{P}_i - \vec{C}) \quad i = 1, \dots, m \quad (4.22)$$

and

$$\vec{a}_i = 0, \quad i = m + 1, \dots, n. \quad (4.23)$$

It is easy to check, using (4.21), that the choice of  $\vec{a}_i$  given by (4.22) and (4.23) is consistent with conditions (4.18). For this choice we find

$$I = \beta R$$

which saturates the inequality (4.20). Hence we have shown that the solution to the geometric problem is given by (4.19).

From this, using (4.14) and the fact that the minimal size sphere  $R$  enclosing the vectors  $\vec{P}_i$  has the same radius as the minimal sphere enclosing the polygon of the difference vectors  $\vec{k}_i$  placed tip-to-tip, we find the claimed bound (4.2).

### 4.3 Weakly coupled theories

In this section, we consider the behaviour of thermal Wightman functions in weakly coupled perturbative quantum field theories in the limit where we take the momenta of the insertions to be large and spacelike. For simplicity, we will consider a scalar field,  $\phi$ , of mass  $m$ , in a thermal bath at inverse temperature  $\beta$  in flat space. However, our analysis can be easily generalized to weakly coupled gauge theories with a Gauss law constraint by using the techniques of [100].

We are interested in an interaction Hamiltonian that is polynomial in the fields

$$H_I = \sum_n a_n \int \phi_I^n(t, x_i) d^d x_i, \quad (4.24)$$

where  $\phi_I$  are the interaction picture operators and  $a_n$  the coupling constants. We will present two approaches to analyzing Wightman functions of the field  $\phi$  in perturbation theory for the couplings (4.24)— using a straightforward canonical formalism and thinking about (thermal) Wick contractions, or an equivalent set of diagrammatic rules derived using the Schwinger-Keldysh formalism. We explain these in turn.

**Canonical formalism** We consider the Fourier transformed Wightman functions of elementary fields, which are the same as (4.1) except that we focus on the case where the operators,  $\mathcal{O}$ , are the elementary fields themselves.

$$G(\omega_i, \vec{k}_i) \delta_\omega \delta_{\vec{k}} \equiv \int \prod_i dt_i d\vec{x}_i \frac{1}{Z} \text{Tr} [e^{-\beta H} \phi(t_1, \vec{x}_1) \dots \phi(t_n, \vec{x}_n)] e^{i \sum_i \omega_i t_i - \vec{k}_i \cdot \vec{x}_i}, \quad (4.25)$$

where  $\phi(t_i, x_i)$  are Heisenberg picture operators and  $Z = \text{Tr}(e^{-\beta H})$  is the partition function.

Perturbative Wightman functions can be computed in such theories using the formalism explained in Appendix B. The final result can be expressed in the following form

$$\begin{aligned} & G(\omega_i, \vec{k}_i) \delta_\omega \delta_{\vec{k}} \\ &= \sum_{\{s_j\}} \int \prod_{j,l} \frac{d\omega_l^j}{2\pi} \left( \prod_{j=1}^n 2\pi \delta \left( \sum_{l=1}^{s_j+1} \omega_l^j - \omega_j \right) g(\omega_l^j) \right) \times \frac{1}{Z} \text{Tr} \left[ (1 + Z_1) e^{-\beta H_0} \right. \\ & \times [H_I(\omega_1^1), \dots [H_I(\omega_{s_1}^1), \phi_I(\omega_{s_1+1}^1, \vec{k}_1)] \dots] \dots [H_I(\omega_1^n), \dots [H_I(\omega_{s_n}^n), \phi_I(\omega_{s_n+1}^n, \vec{k}_n)] \dots] + Z_2 \left. \right]. \end{aligned} \quad (4.26)$$

Notice that this expectation value is with respect to the thermal density matrix of the unperturbed Hamiltonian  $H_0$ . The term displayed appears at order  $\sum_i s_i$  in perturbation theory, and the leading sum runs over all such terms. In the expression above  $g$  is a rational function of the frequencies that is specified in the Appendix but is not important for our asymptotic analysis here.

The terms  $Z_1$  and  $Z_2$  are subtle terms that arise from infra-red effects in thermal field theory. In the Schwinger-Keldysh formalism, these terms arise from the “vertical part” of the contour as explained in Appendix B. In our calculations below, we will

naively assume that

$$(1 + Z_1) = \frac{\text{Tr}(e^{-\beta H})}{\text{Tr}(e^{-\beta H_0})}, \quad Z_2 = 0. \quad (4.27)$$

In Schwinger-Keldysh language, this corresponds to the assumption that the contribution from the vertical part of the contour decouples. In weakly-coupled field theories, the assumption (4.27) is believed to be justified provided we use a specific prescription for the two-point function in evaluating Wick contractions [101]. Moreover, we do not believe that the terms  $Z_1$  and  $Z_2$  will change our conclusions below, which are rather general and not specific to any particular field theory. Nevertheless, (4.27) requires further analysis that we postpone to a later study.

Now, we may expand out the interaction-picture field in terms of creation and annihilation operators

$$\phi_I(t, \vec{x}) = \int \frac{d^{d-1}\vec{k}}{(2\pi)^{d-1}} \frac{1}{\sqrt{2\omega_{\vec{k}}}} \left[ a_{\vec{k}} e^{-i\omega_{\vec{k}}t + i\vec{k}\cdot\vec{x}} + a_{\vec{k}}^\dagger e^{i\omega_{\vec{k}}t - i\vec{k}\cdot\vec{x}} \right], \quad (4.28)$$

where  $\omega_{\vec{k}} \equiv \sqrt{\vec{k}^2 + m^2}$  and the creation and annihilation operators satisfy

$$[a_{\vec{k}}, a_{\vec{k}'}^\dagger] = (2\pi)^{d-1} \delta(\vec{k} - \vec{k}'). \quad (4.29)$$

The thermal correlators of these operators follow from the commutators above using the KMS condition

$$\begin{aligned} \frac{1}{Z_0} \text{Tr}(e^{-\beta H_0} a_{\vec{k}} a_{\vec{k}'}^\dagger) &= \frac{1}{1 - e^{-\beta\omega_{\vec{k}}}} (2\pi)^{d-1} \delta(\vec{k} - \vec{k}'), \\ \frac{1}{Z_0} \text{Tr}(e^{-\beta H_0} a_{\vec{k}'}^\dagger a_{\vec{k}}) &= \frac{e^{-\beta\omega_{\vec{k}}}}{1 - e^{-\beta\omega_{\vec{k}}}} (2\pi)^{d-1} \delta(\vec{k} - \vec{k}'), \end{aligned} \quad (4.30)$$

where  $Z_0 = \text{Tr}(e^{-\beta H_0})$ . Note that the interaction Hamiltonian itself can be written as a polynomial in the creation and annihilation operators. Therefore, each commutator of the interaction Hamiltonian with the elementary fields that appears in the expression (4.26) leads to polynomials in the creation and annihilation operators. We denote a general such polynomial comprising *only* products of annihilation operators with  $c$ -number coefficients as  $X(\{\alpha\}, \omega, \vec{k})$ . For instance, at quadratic order,

an example of such a polynomial with frequency  $\omega$  and momentum  $\vec{k}$  would be

$$\int_0^\omega d\omega' \int d\vec{k}' a_{\omega', \vec{k}'} a_{\omega - \omega', \vec{k} - \vec{k}'}$$

Note that the energy,  $\omega$  and momentum  $\vec{k}$  of the polynomial is displayed explicitly in our notation. Specifying the frequency and momentum does not uniquely specify the polynomial and we have moved all the rest of the information about the polynomial into the parameter  $\{\alpha\}$ . This allows us to write

$$\begin{aligned} g(\omega_n^j) [H_I(\omega_1^j) \dots [H_I(\omega_{s_j}^j), \phi_I(\omega_{s_j+1}^j, \vec{k}_j)] \dots] &= \sum_{\alpha, \beta} \int d\omega_1 d\omega_2 d\vec{K}_1 d\vec{K}_2 \\ \times (2\pi)^d \delta(\omega_1 - \omega_2 - \sum_q \omega_q^j) \delta(\vec{K}_1 - \vec{K}_2 - \vec{k}_j) X(\{\alpha\}, \omega_1, \vec{K}_1) X^\dagger(\{\delta\}, \omega_2, \vec{K}_2) \end{aligned} \quad (4.31)$$

We include the rational function  $g$  that appears in (4.26) inside the polynomials to lighten the notation. At any order in perturbation theory, the polynomials that appear above can be systematically computed by using the form of the interaction Hamiltonian (4.24), the expansion (4.28) and the canonical commutators (4.29).

Note that the interaction Hamiltonian itself is integrated over all space, so it does not contribute any momentum, and the momentum on the right hand side comes purely from the insertion of  $\phi_I$ .

We now need three key facts about these polynomials that appear in the expansion of the Heisenberg picture operators. First, since all the annihilation operators that enter the polynomial are on-shell, this tells us that the integral only has support in the region  $\omega > |\vec{k}|$ . Second, while the precise correlation functions of these polynomials depend on the specific polynomial under consideration, we note that, generically, as  $\omega \rightarrow \infty$ ,

$$\begin{aligned} \frac{1}{Z_0} \text{Tr} \left( e^{-\beta H_0} X(\{\alpha\}, \omega, \vec{k}) X^\dagger(\{\delta\}, \omega', \vec{k}') \right) &\rightarrow \text{O}(1) \delta(\omega - \omega') \delta(\vec{k} - \vec{k}'), \\ \frac{1}{Z_0} \text{Tr} \left( e^{-\beta H_0} X^\dagger(\{\alpha\}, \omega, \vec{k}) X(\{\delta\}, \omega', \vec{k}') \right) &\rightarrow \text{O}(e^{-\beta\omega}) \delta(\omega - \omega') \delta(\vec{k} - \vec{k}'). \end{aligned} \quad (4.32)$$

These correlators follow from the elementary thermal correlators (4.30). We have suppressed the dependence on  $\{\alpha\}$  and  $\{\delta\}$  in the right hand side of the second line

although in any concrete calculation this dependence is important. It is possible to choose  $\{\alpha\}$  and  $\{\delta\}$  so that this coefficient is zero. The correlator is non-zero when the polynomials have the property that their constituent operators can be paired with each other as in (4.30) and, in the equation above, this is understood to be the case. Third, in a general correlation function one might have  $n$ -point correlators of such polynomials. These correlators can be combined by expanding each polynomial in its constituent creation and annihilation operators, and then using Wick's theorem.

We show below how this data is enough to argue that, at sufficiently high order in perturbation theory, the bound (4.2) is saturated. To lighten the notation we now denote  $\frac{1}{Z_0} \text{Tr}(e^{-\beta H_0} O) \equiv \langle O \rangle_\beta$ .

**Diagrammatic rules** As explained in Appendix B, the canonical formalism above can be recast in a set of diagrammatic rules using the Schwinger-Keldysh formalism [102]. The diagrammatic rules for computing thermal Wightman functions are more elaborate than the rules for computing the most-commonly considered time-ordered vacuum correlators.

In the Schwinger-Keldysh formalism, the subtlety corresponding to the factors of (4.27) corresponds to the fact that, as explained in Appendix B, one must carefully take into account the fact that the Schwinger-Keldysh propagators may receive contributions from very early and very late times. This leads to mixed Euclidean-real-time propagators that connect the vertical part of the Schwinger-Keldysh path-integral to the horizontal part. However, it is believed [101, 103] that this effect can be removed by using a specific prescription for the propagator that we adopt below.

This leads to the following simplified Feynman rules for our scalar theory are as follows and that do *not* account for the vertical part of the contour

1. To compute a  $n$ -point function we consider  $\tilde{n}$ -copies of the field, where  $\tilde{n} = n$  if  $n$  is even and  $\tilde{n} = n + 1$  if  $n$  is odd. We introduce  $n$ -different interaction vertices, each of which couples fields of type  $i$  only to other fields of type  $i$ . The  $i^{\text{th}}$  vertex comes with a sign of  $(-1)^{i+1}$ .
2. In position space, all interaction vertices are integrated from time  $-\infty$  to  $\infty$  and over all space. In frequency space, we just impose energy-momentum

conservation at each vertex.

3. There are  $\tilde{n}^2$ -types of propagators that connect fields of type  $i$  to fields of type  $j$ . For the scalar field, these propagators, in frequency space, are given by

$$D_{ij}(k) = \begin{cases} -\frac{i}{k^2+m^2-i\epsilon} + 2\pi\delta(k^2+m^2)n(|k^0|) & i = j \text{ and } n-i \text{ even,} \\ \frac{i}{k^2+m^2+i\epsilon} + 2\pi\delta(k^2+m^2)n(|k^0|) & i = j \text{ and } n-i \text{ odd,} \\ 2\pi\theta(k^0)\delta(k^2+m^2) + 2\pi\delta(k^2+m^2)n(|k^0|) & i < j, \\ 2\pi\theta(-k^0)\delta(k^2+m^2) + 2\pi\delta(k^2+m^2)n(|k^0|) & i > j. \end{cases} \quad (4.33)$$

4. The external legs are fields of type  $1 \dots n$ .

In the rules above,

$$n(|k^0|) \equiv \frac{1}{e^{\beta|k^0|} - 1}.$$

Since the reader may find these rules unfamiliar, we give a very explicit example in the case of the two-point function in Table 4.1 below.

We also note that for a  $n$ -point correlator, it is possible to extract information about all  $n!$  Wightman functions by considering a smaller basis of correlators and using the KMS relations to cleverly obtain information about other correlators [104]. Since our analysis is very simple, we will not utilize these techniques here although we expect that they may be required for concrete calculations of higher-point functions.

### 4.3.1 Two-point functions

Let us now consider the example of a two-point function. We will analyze this both using the canonical approach, and the diagrammatic approach.

**Canonical analysis** We consider

$$G(\omega_1, \vec{k}_1, \omega_2, \vec{k}_2) \delta_\omega \delta_{\vec{k}} = \sum_{\{\alpha\}, \{\delta\}, \{\alpha'\}, \{\delta'\}} \int \prod_{ij} [d\omega_{ij} d\vec{K}_{ij}] \mathcal{C},$$

$$\mathcal{C} = \langle X(\{\alpha\}, \omega_{11}, \vec{K}_{11}) X^\dagger(\{\delta\}, \omega_{12}, \vec{K}_{12}) X(\{\alpha'\}, \omega_{21}, \vec{K}_{21}) X^\dagger(\{\delta'\}, \omega_{22}, \vec{K}_{22}) \rangle_\beta. \quad (4.34)$$

In the expression above, we have absorbed the delta functions that appear in (4.26) and (4.31) into the measure, which we denote by the square brackets. The correlator itself gives an overall energy-momentum conserving delta function, which also appears on the left. These delta functions impose energy-momentum conservation that leads to the constraints

$$\begin{aligned}\vec{K}_{11} - \vec{K}_{12} &= \vec{k}_1; & \omega_{11} - \omega_{12} &= \omega_1 \\ \vec{K}_{21} - \vec{K}_{22} &= \vec{k}_2; & \omega_{21} - \omega_{22} &= \omega_2 \\ \vec{k}_1 + \vec{k}_2 &= 0; & \omega_1 + \omega_2 &= 0.\end{aligned}\tag{4.35}$$

The correlator can be calculated in terms of Wick contractions. In particular, one term that appears above is just the product of two-point correlators of polynomials

$$\begin{aligned}\langle X(\{\alpha\}, \omega_{11}, \vec{K}_{11}) X^\dagger(\{\delta\}', \omega_{22}, \vec{K}_{22}) \rangle_\beta \langle X^\dagger(\{\delta\}, \omega_{12}, \vec{K}_{12}) X(\{\alpha\}', \omega_{21}, \vec{K}_{21}) \rangle_\beta \\ \longrightarrow e^{-\beta\omega_{12}} \delta(\omega_{12} - \omega_{21}) \delta(\omega_{11} - \omega_{22}),\end{aligned}\tag{4.36}$$

for large values of  $\omega_{ij}$ . This is the limit that is relevant since we recall that the polynomials only have support for  $\omega_{ij} > |\vec{K}_{ij}|$ . In the limit where the mass becomes unimportant, the support of the polynomials actually starts from  $\omega_{ij} \approx |\vec{K}_{ij}|$ . This implies that the *largest* term in the two-point Wightman correlator above emerges from minimizing  $|\vec{K}_{12}|$  subject to all the delta function constraints above. It is clear that this is maximized when  $\vec{K}_{12} = \vec{K}_{21} = \frac{-\vec{k}_1}{2}$ ,  $\vec{K}_{11} = \vec{K}_{22} = \frac{\vec{k}_1}{2}$ .

But this means that in the limit under consideration

$$G(\omega_1, \vec{k}_1, \omega_2, \vec{k}_2) \longrightarrow e^{-\frac{\beta|\vec{k}_1|}{2}},\tag{4.37}$$

precisely consistent with our bound. Note that, such a term appears already at second order in perturbation theory for any  $\phi^n$  interaction.

What we have shown here is that there *exists* a term in the perturbative expansion that saturates the bound. The coefficient of this term depends on the precise polynomials that appear above, and the coefficient of this term could vanish. In fact, as we will see in the study of holographic theories for  $d > 2$ , these theories do *not* saturate the bound at leading order in bulk perturbation theory despite being strongly coupled in the boundary.

**Diagrammatic analysis** We now consider the example of a  $\phi^3$  interaction in some more detail. The Feynman rules for the two-point function are given in Table 4.1.

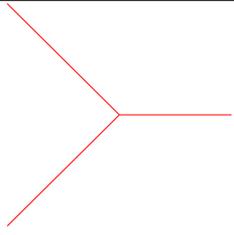
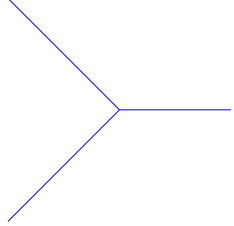
Diagram Element	Value
	$D_{11}(k)$
	$D_{12}(k)$
	$D_{21}(k)$
	$D_{22}(k)$
	$i\lambda$
	$-i\lambda$

Table 4.1: Feynman rules for a two-point Wightman function in a  $\phi^3$  theory. The explicit expressions for  $D_{ij}(k)$  are given in (4.33).

The reader will immediately see that these rules give rise to multiple diagrams. However, here we just want to show that the perturbative expansion *contains* a term that saturates the bound and not compute the full two-point function. To this end, we consider the diagram shown in figure 4.3. The corrections from this diagram can

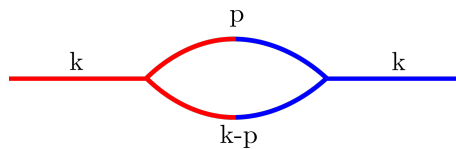


Figure 4.3: Correction to the 2-point correlator leading to saturation of the bound.

extend the support of the two-point Wightman function to off-shell momenta. In

fact, due to the absence of terms which mix different fields in the Lagrangian, figure 4.3 is the simplest diagram which achieves this feat. For simplicity we will study the behaviour of this diagram in the limit  $k^0 \rightarrow 0$ , similar statements can be made for finite  $k^0$ . We have

$$\lim_{|\vec{k}| \rightarrow \infty} \frac{\lambda^2}{(\vec{k}^2 + m^2)^2} \int \frac{d^d p}{(2\pi)^d} [2\pi\theta(p^0)\delta(p^2 + m^2) + 2\pi\delta(p^2 + m^2)n(|p^0|)] \\ [2\pi\theta((k-p)^0)\delta((k-p)^2 + m^2) + 2\pi\delta((k-p)^2 + m^2)n(|k-p^0|)]$$

Even without evaluating this expression exactly, we can estimate its behaviour in the limit of interest as follows. As the external frequency,  $k^0$ , is negligible,  $p$  and  $k-p$  must have approximately equal and opposite frequencies. This implies that  $\theta(p^0)\theta(k^0-p^0)$  does not contribute. Moreover, the on-shell condition for the internal propagator implies that  $|p^0| = |k^0-p^0| = |\vec{p}| = |\vec{k}-\vec{p}|$ . To estimate the slowest fall off, we want to minimize  $|p^0|$ . From momentum conservation, vectors  $\vec{k}$ ,  $\vec{p}$  and  $\vec{k}-\vec{p}$  form a triangle. Imposing  $|\vec{p}| = |\vec{k}-\vec{p}|$  would imply that the minimum value of  $|p^0|$  is  $|\vec{k}|/2$ . The Boltzmann factor would become  $e^{-\beta|\vec{k}|/2}$ . This implies that the diagram is proportional to  $e^{-\beta|\vec{k}|/2}$  and therefore, the two-point function saturates our bound at second order in perturbation theory.

This coefficient can be estimated by completing the evaluation of the diagram above and we find that, in the limit of large- $k$ , for  $d > 2$ , the diagram evaluates to

$$\frac{\lambda^2}{2} \frac{S_{d-3}}{(2\pi)^{d-2}} \frac{|\vec{k}|^{\frac{d}{2}-7}}{\beta^{\frac{d}{2}-1}} \Gamma\left(\frac{d}{2}-1\right) e^{-\beta\frac{|\vec{k}|}{2}}, \quad (4.38)$$

where  $S_{d-3}$  is the area of the unit sphere in  $d-3$  dimensions.

### 4.3.2 Three-point functions

We now move to a consideration of three-point functions and we again perform the analysis in two equivalent ways.

**Canonical analysis** Just as previously, we now find

$$G(\omega_1, \vec{k}_1, \omega_2, \vec{k}_2, \omega_3, \vec{k}_3) \delta_\omega \delta_{\vec{k}} = \sum_{\{\alpha\}_q, \{\delta\}_q} \int \prod_{ij} [d\omega_{ij} d\vec{K}_{ij}] \mathcal{C}, \quad (4.39)$$

$$\mathcal{C} = \left\langle \prod_{q=1}^3 X(\{\alpha\}_q, \omega_{q1}, \vec{K}_{q1}) X^\dagger(\{\delta\}_q, \omega_{q2}, \vec{K}_{q2}) \right\rangle_\beta,$$

and we have the constraints

$$\omega_{q1} - \omega_{q2} = \omega_q; \quad \vec{K}_{q1} - \vec{K}_{q2} = \vec{k}_q. \quad (4.40)$$

When the correlator above is expanded using Wick's theorem at finite temperature, we do *not* get only pairwise contractions of the  $X$ -polynomials, since some annihilation operators in the first polynomial may contract with creation operators from the second  $X^\dagger$  whereas some others may contract with creation operators from the third  $X^\dagger$ . However, of the multiple terms that appear, one particular term that appears in the Wick contraction is

$$\begin{aligned} \mathcal{C} = & \langle X(\{\alpha\}_1, \omega_{11}, \vec{K}_{11}) X^\dagger(\{\delta\}_2, \omega_{22}, \vec{K}_{22}) \rangle_\beta \langle X^\dagger(\{\delta\}_1, \omega_{12}, \vec{K}_{12}) X(\{\alpha\}_3, \omega_{31}, \vec{K}_{31}) \rangle_\beta \\ & \times \langle X(\{\alpha\}_2, \omega_{21}, \vec{K}_{21}) X^\dagger(\{\delta\}_3, \omega_{32}, \vec{K}_{32}) \rangle_\beta + \dots, \end{aligned} \quad (4.41)$$

where  $\dots$  denote the other possible Wick contractions.

In the displayed term, we find some additional constraints if the term is not to vanish

$$\begin{aligned} \omega_{11} = \omega_{22}; \quad \vec{K}_{11} = \vec{K}_{22}, \\ \omega_{12} = \omega_{31}; \quad \vec{K}_{12} = \vec{K}_{31}, \\ \omega_{21} = \omega_{32}; \quad \vec{K}_{21} = \vec{K}_{32}. \end{aligned} \quad (4.42)$$

In the limit where the  $\omega_1, \omega_2, \omega_3$  are negligible, this just sets all the  $\omega_{ij}$  equal to each other.

Now, we note that the displayed term is suppressed by a factor of  $e^{-\beta\omega_{11}}$ . In the regime where the mass is unimportant, each polynomial only has support in the

region where  $\omega_{ij} \geq |\vec{K}_{ij}|$  this means that we must have

$$\omega_{11} \geq |\vec{K}_{11}|; \quad \omega_{11} \geq |\vec{K}_{11} - \vec{k}_1|; \quad \omega_{11} \geq |\vec{k}_2 + \vec{K}_{11}|. \quad (4.43)$$

In the expansion of the Wightman function, we must integrate over all values of  $\omega_{ij}$  that are allowed. However, the constraints above tell us that the *largest* contribution to the integral comes precisely when  $\omega$  takes the smallest value that meets (4.43). This can be achieved by varying  $\vec{K}_{11}$  and it is clear that the resultant  $\omega_{11}$  is *precisely* the radius of the smallest circle that contains the triangle formed by  $\vec{k}_1, \vec{k}_2, \vec{k}_3$ .

For any given interaction we can estimate the lowest order in perturbation theory that the term above appears. For instance, consider a  $\phi^3$  theory. Then, in general, a non-trivial contraction above first appears at *third order* in perturbation theory, where each of the  $X$  polynomials are just single creation and annihilation operators. However, for such operators, the inequalities in (4.43) must actually be equalities since these operators have frequency equal to the norm of their momenta. Now, it is interesting that if the triangle formed by the three momenta  $\vec{k}_i$  is acute-angled, then all three-points of the triangle lie on the smallest circle that contains it (the so-called ‘‘circumcircle’’.) Thus, when the triangle formed by  $\vec{k}_i$  is acute angled, the minimum value of  $\omega$  dictated by (4.43) coincides with the value obtained by saturating all three inequalities. Therefore, for such configurations of momenta, the bound is saturated at third order in perturbation theory for a cubic interaction.

In general, it is *always* possible to keep two points of the triangle on the smallest circle that contains it. This corresponds to taking two out of three contractions in (4.41) to be contractions of single annihilation and creation operators, while taking the third contraction to comprise of polynomials that are at least quadratic in the elementary annihilation and creation operators. The lowest such term appears at *fifth* order in perturbation theory with a  $\phi^3$  interaction. On the other hand, if the interaction is  $\phi^5$  then such a term appears already at third-order in perturbation theory, and the bound can be saturated for all kinematic configurations at this order.

**Diagrammatic analysis:** The Feynman rules for the three-point function are a natural generalization of the rules above. We are interested in the one-loop diagram shown in Figure 4.4. This particular loop contribution is given by following integral.

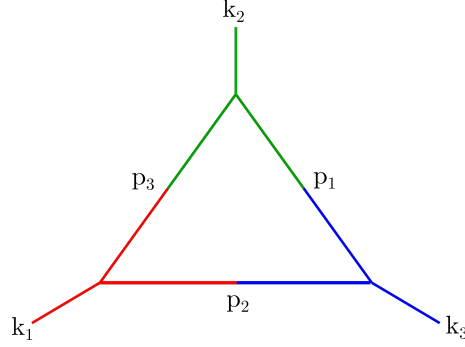


Figure 4.4: Contribution to the 3-point correlator that saturates the bound for special kinematics

$$\lim_{\vec{k}_i \rightarrow \infty} i\lambda^3 \prod \frac{1}{\vec{k}_i^2 + m^2} \int \prod_i \frac{d^d p_i}{(2\pi)^d} \delta(k_1 + p_3 - p_2) \delta(k_2 + p_1 - p_3) \delta(k_3 + p_2 - p_1) \\ (2\pi)^3 \delta(p_1^2 + m^2) \delta(p_2^2 + m^2) \delta(p_3^2 + m^2) [(\theta(-p_1^0) + n(|p_1^0|))] [\theta(p_2^0) + n(|p_2^0|)] [\theta(-p_3^0) + n(|p_3^0|)]$$

We are interested in the limit where the masses and external frequencies are negli-

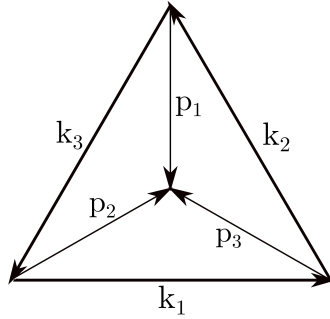


Figure 4.5: Momentum conservation for diagram 4.4.

gible. In this limit, the constraints imply that  $p_1^0 = p_2^0 = p_3^0$ . The on-shell condition, and momentum conservation (see Figure 4.5) then imposes  $|\vec{p}_1| = |\vec{p}_2| = |\vec{p}_3| = R_c$ , where  $R_c$  denotes circumradius of the triangle with sides  $\vec{k}_i$ . Due to the presence of both positive and negative signs in theta functions, we are forced to include at least one Boltzmann suppression factor,  $e^{-\beta R_c}$ . This diagram saturates the bound only for limited kinematic configurations, that is, when the triangle formed by external momenta is acute angled.

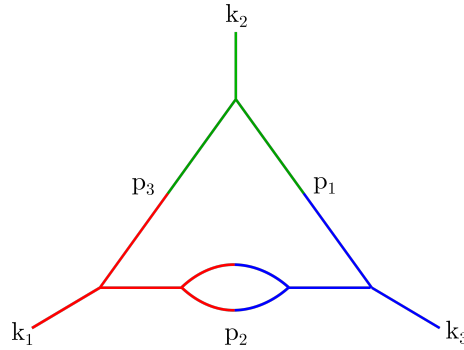


Figure 4.6: *Diagram for the three-point correlator that saturates the bound for all external kinematics*

In order to saturate the bound in all of kinematic space we require at least one off-shell (but time-like) internal propagator (as we can always keep 2 propagators on-shell and still saturate the bound). This can be achieved by correcting the internal propagator by introducing two additional vertices as shown in Figure 4.6. Note that no additional large- $k$  suppressions are introduced as we are interested in the regime where the internal propagators are time-like. Hence, for a  $\phi^3$  interactions we need 5<sup>th</sup> order corrections in the coupling to saturate the bound for all of kinematic space.

### 4.3.3 Higher-point functions

The generalization to higher-point functions is now quite simple.

**Canonical analysis** For a  $n$ -point function, we obtain the perturbative series

$$\begin{aligned}
 & G(\omega_i, \vec{k}_i) \delta_\omega \delta_{\vec{k}} \\
 &= \sum_{\{\alpha\}_q, \{\delta\}_q} \int \prod_{ij} [d\omega_{ij} d\vec{K}_{ij}] \langle \prod_{q=1}^n X(\{\alpha\}_q, \omega_{q1}, \vec{K}_{q1}) X^\dagger(\{\delta\}_q, \omega_{q2}, \vec{K}_{q2}) \rangle_\beta.
 \end{aligned} \tag{4.44}$$

The integral is subject to the constraints

$$\omega_{q1} - \omega_{q2} = \omega_q; \quad \vec{K}_{q1} - \vec{K}_{q2} = \vec{k}_q. \tag{4.45}$$

Expanding this using Wick's theorem, we now find the following term

$$\begin{aligned}
 & G(\omega_i, \vec{k}_i) \delta_\omega \delta_{\vec{k}} \\
 &= \sum_{\{\alpha\}_q, \{\delta\}_q} \int \prod_{ij} [d\omega_{ij} d\vec{K}_{ij}] \left[ \prod_{i=1}^{n-1} \langle X(\{\alpha\}_i, \omega_{i1}, \vec{K}_{i1}) X^\dagger(\{\delta\}_{i+1}, \omega_{i+1,2}, \vec{K}_{i+1,2}) \rangle_\beta \right] \\
 &\times \langle X^\dagger(\{\alpha\}_1, \omega_{12}, \vec{K}_{12}) X(\{\delta\}_n, \omega_{n1}, \vec{K}_{n1}) \rangle_\beta + \dots
 \end{aligned} \tag{4.46}$$

These correlators are additionally non-zero when the constraints

$$\omega_{i1} - \omega_{i+1,2} = 0; \quad \vec{K}_{i1} - \vec{K}_{i+1,2} = 0, \tag{4.47}$$

are satisfied. The only term that is exponentially suppressed in the expression above appears on the second line. In the limit where  $\omega_i \ll |\vec{k}_i|$ , it is clear that the *smallest* value of  $\omega_{12}$  that satisfies the constraints is the radius of the smallest sphere that contains the polygon formed by the  $\vec{k}_i$  precisely in line with our bound.

As in the discussion of the three-point function, since we can always place at least two points from this polygon on the sphere itself, this implies that two of the contractions in (4.46) (which involve four polynomials) can comprise polynomials of order 1. However the other  $(2n - 4)$  polynomials must be quadratic or higher. For a  $\phi^3$  interaction, this means that such a term first appears at order  $3n - 4$  in perturbation theory. For a  $\phi^5$  interaction on the other hand, such a term appears already at order  $n$  in perturbation theory.

**Diagrammatic analysis** It is also simple to see the diagram that contributes the relevant term in the  $n$ -point function. First, we need a minimum of  $n$ -th order correction to allow all the external momenta to be spacelike. Now we need  $n - 2$  internal momenta to be off-shell. This, in  $\phi^3$  theory, would require additional  $2(n - 2)$  vertices. So an  $n$ -point function will saturate the bound at order  $3n - 4$  in perturbation theory. For instance, Figure 4.7 shows the diagram that saturates the bound for 4-point function for the  $\phi^3$  theory.

If we work with  $\phi^5$  or higher interactions, then we can saturate the bound for  $n$ -point functions at  $n$ -th order in perturbation theory. This is because we can keep

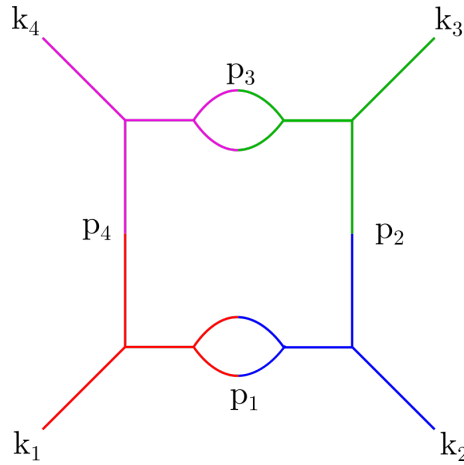


Figure 4.7: The bound for four-point function is expected to be saturated at eighth order in perturbation theory for arbitrary external kinematics by the diagram above.

all internal momenta off-shell without introducing additional vertices, as shown, for instance, in figure 4.8.

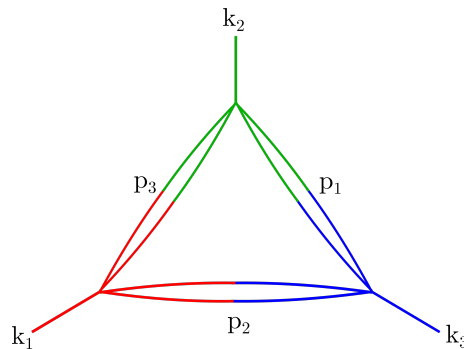


Figure 4.8: A  $\phi^5$  interaction can saturate the bound for  $n$ -point functions at  $n^{\text{th}}$  order in perturbation theory. The diagram above shows the relevant correction to the 3-point function.

In the case of a  $\phi^4$  interaction, odd-point functions vanish. Also, half of the internal momenta can be made off-shell by the same logic as above. An even  $n > 2$  point function could saturate the bound at order  $n + 2(n - 2 - n/2) = 2n - 4$  in perturbation theory.

In this section, we have considered correlators of elementary fields in weakly interacting theories. However, as the canonical analysis above makes clear, even in

a *free theory*, correlators of suitably complicated composite operators saturate the bound.

## 4.4 Holographic theories

We now consider a large- $N$  field theory with a gravitational holographic dual. In such a theory, the natural low-energy operators are generalized free-fields. So in this section, we analyze the behaviour of correlation functions of generalized free-fields at large spacelike momenta. While our proof of the large- $k$  bound is valid for such theories, there is a subtlety. The bound proved in 4.2 is strictly valid only for asymptotically large momenta. If we then consider a holographic correlator where the insertions have momenta such that  $|\vec{k}| \gg \omega, |\vec{k}| \gg T$  (where  $T$  is the temperature), but also  $|\vec{k}| \ll N$ , is the bound obeyed, or is the bound valid only for  $|\vec{k}| \gg N$ . In this section, we will make some progress towards understanding this question, but we will not reach a final answer.

We analyze both two-point functions and higher-point functions in a holographic theory at finite temperature. The two-point function can be analyzed by considering the propagation of bulk fields on top of a black-brane background. An interesting aspect of the holographic correlators, so obtained, is that their Fourier transforms have *non-zero* support in the regime of our interest (large spacelike momenta), even when the bulk theory is described by a free-field propagating in the curved background. We will show that, at this level, while the two-point function saturates the bound (4.2) for  $\text{AdS}_3$ , it remains *strictly below* the bound in higher dimensional AdS. We do not understand the reason for this curious behaviour particularly since the analysis of section 4.3 might have suggested that in a generic strongly coupled theory (where all orders in the perturbative expansion are important) the bound is always saturated.

In the second part of the section, we initiate the study of interactions for holographic correlators. Interactions introduce several dangerous terms in the bulk perturbative expansion that have the potential to violate the bound. This is because the bulk theory does *not* obey the spectrum condition and has excitations with frequency smaller than momentum. Nevertheless, by means of an analysis of the analytic structure of Witten diagrams, we argue that tree-level *contact* Witten dia-

grams do obey the bound. We make some brief comments about exchange diagrams in 4.4.2.

We should emphasize that at all points in this section, we are only interested in *boundary correlators*. Bulk correlators, where the operators are inserted at some finite value of the radial coordinate manifestly violate our bound. This is because these operators do *not* have well-defined correlators at all temperatures, which is one of the assumptions in our proof. In particular, if we keep the radial position of the operator fixed, and increase the temperature the operator will eventually fall behind the horizon, where it must be described by the state-dependent operators of [68, 67, 69, 70].

#### 4.4.1 Two-point functions

To analyze the behaviour of two-point functions of generalized free-fields, we consider free-fields in AdS, propagating on black brane backgrounds. For simplicity, we will only consider scalar fields. A similar analysis was also performed in [91].

We set the radius of AdS to 1 so that the metric of the black-brane in AdS is given by

$$ds^2 = \frac{1}{z^2} \left[ -h(z)dt^2 + \frac{1}{h(z)}dz^2 + d\vec{x}^2 \right], \quad (4.48)$$

where

$$h(z) = 1 - \frac{z^d}{z_0^d}.$$

The horizon is at  $z = z_0$ , the boundary at  $z = 0$  and  $\vec{x}$  is a  $(d - 1)$ -dimensional vector. The inverse-temperature of this brane is given by

$$\beta = \frac{4\pi z_0}{d}. \quad (4.49)$$

We will consider a massive scalar field in the bulk that satisfies the wave-equation

$$(\square - m^2)\phi = 0. \quad (4.50)$$

To analyze this wave-equation, it is useful to switch to coordinates defined by<sup>1</sup>

$$\frac{dz_*}{dz} = \frac{1}{zh(z)}. \quad (4.51)$$

The map and inverse-map between  $z_*$  and  $z$  is given by

$$z_* = -\frac{\log(z_0^d - z^d)}{d} + \frac{\log(z^d)}{d}; \quad z = \frac{z_0}{(1 + e^{-dz_*})^{\frac{1}{d}}}. \quad (4.52)$$

We make an ansatz of the form  $\phi = \chi_{\omega, \vec{k}}(z)e^{i\vec{k}\cdot x - i\omega t}$ . Further, it is convenient to substitute  $\chi_{\omega, \vec{k}}(z) = z^{\frac{d}{2}}\psi(z)$ , where we suppress the dependence of  $\psi$  on  $\omega, \vec{k}$  to lighten the notation. We now find that  $\psi(z)$  obeys the equation

$$\frac{d^2\psi}{dz_*^2} + V\psi = 0, \quad (4.53)$$

with

$$V = z^2\omega^2 + h(z) \left( -\frac{d^2}{4} - m^2 - z^2\vec{k}^2 - \frac{d^2 z^d}{4z_0^d} \right). \quad (4.54)$$

We now consider this equation in the limit that  $|\vec{k}| \rightarrow \infty$  with  $\omega$  fixed.

For this regime of parameters, it is most convenient to solve the equation in the following three regions

$$\begin{aligned} \text{Region I:} & \quad \frac{z_0 - z}{z_0} \ll 1, \\ \text{Region II:} & \quad h(z) \gg \frac{\omega^2}{|\vec{k}|^2} \quad \text{and} \quad |\vec{k}|^2 z^2 \gg 1, \\ \text{Region III:} & \quad z \ll 1, \end{aligned} \quad (4.55)$$

and then match the solutions in their overlapping regimes of validity. The potential has a turning point but this is included in region I above.

### Approximate solution in different regions

**Region I** — In this region we find that  $z_* \gg 1$  and we can approximate

$$z \approx z_0 \left( 1 - \frac{1}{d} e^{-dz_*} \right). \quad (4.56)$$

---

<sup>1</sup>Notice that the coordinate  $z_*$  is not the same as the tortoise coordinate.

We can also approximate the potential as

$$V \approx z^2 \left( \omega^2 - h\vec{k}^2 \right) \approx z_0^2 \left( \omega^2 - e^{-dz_*} \vec{k}^2 \right). \quad (4.57)$$

This leaves us with the differential equation

$$\ddot{\psi} + z_0^2 \left( \omega^2 - e^{-dz_*} \vec{k}^2 \right) \psi = 0, \quad \text{in Region I,} \quad (4.58)$$

This is just the modified Bessel equation (although the order is imaginary) and with  $\gamma = 2z_0 d^{-1}$ , the solution is

$$\psi = A_I K_{i\gamma\omega}(|\vec{k}|\gamma e^{-dz_*/2}) + B_I \mathcal{R} \left( I_{i\gamma\omega}(|\vec{k}|\gamma e^{-dz_*/2}) \right), \quad (4.59)$$

where  $\mathcal{R}$  yields the real part of its argument.

**Region II** — In region II, we will use a WKB approximation to solve the equation. We approximate the potential by

$$V \approx -z^2 h |\vec{k}|^2, \quad \text{Region II} \quad (4.60)$$

Then, with,

$$W(z) = \int \sqrt{-V} dz_* = \int \sqrt{-V} \frac{dz}{zh(z)} = |\vec{k}|z {}_2F_1 \left( \frac{1}{2}, \frac{1}{d}; 1 + \frac{1}{d}; \left( \frac{z}{z_0} \right)^d \right), \quad (4.61)$$

the solution is given by

$$\psi(z) = \frac{1}{(-V)^{\frac{1}{4}}} \left( A_{II} e^{W(z)} + B_{II} e^{-W(z)} \right). \quad (4.62)$$

**Region III**— In region III, we can neglect the non-linear terms inside  $h$  and approximate the potential by

$$V = -|\vec{k}|^2 z^2 - \left( \frac{d}{2} \right)^2 - m^2. \quad (4.63)$$

In this region, we also have

$$z = z_0 e^{z^*}, \quad \text{Region III}, \quad (4.64)$$

The solution to the differential equation is

$$\psi = A_{III} I_\nu(|\vec{k}|z) + B_{III} K_\nu(|\vec{k}|z), \quad (4.65)$$

with  $\nu = \sqrt{(\frac{d}{2})^2 + m^2}$ .

### Matching

We now match the three solutions, given in (4.59), (4.62), (4.65) to relate the constants above to each other.

Now, as we enter the range where  $|\vec{k}|z \gg 1$ , but  $z \ll 1$ , which is the overlap between region III and region II, we find that the solution can be written by considering the asymptotics of both (4.65) and of (4.62). In this region,

$$\psi = \frac{A_{III}}{\sqrt{2\pi|\vec{k}|z}} e^{|\vec{k}|z} + \frac{e^{-|\vec{k}|z}}{\sqrt{2\pi|\vec{k}|z}} (\pi B_{III} + i A_{III} e^{i\pi\nu}) = \frac{1}{\sqrt{|\vec{k}|z}} (A_{II} e^{|\vec{k}|z} + B_{II} e^{-|\vec{k}|z}). \quad (4.66)$$

There is a subtlety about whether we should match both the positive and the negative exponential terms in (4.66). However, note that first the leading constants  $A_{II}$  and  $B_{II}$  that multiply these terms could make them of the same magnitude. Second, we can also imagine continuing the exponential into the imaginary plane so that the exponents become phases, and then match them.

This leads to the relations

$$A_{II} = \frac{A_{III}}{\sqrt{2\pi}}; \quad B_{II} = \frac{\pi B_{III} + i A_{III}}{\sqrt{2\pi}}. \quad (4.67)$$

Now we turn to region I. First, by extending from region II towards region I, we find

$$W(z) \xrightarrow{z \rightarrow z_0} \frac{|\vec{k}| \sqrt{\pi} z_0 \Gamma[1 + \frac{1}{d}]}{\Gamma[\frac{1}{2} + \frac{1}{d}]} - 2|\vec{k}| d^{-\frac{1}{2}} z_0^{\frac{1}{2}} \sqrt{z_0 - z}. \quad (4.68)$$

For convenience below we define

$$\kappa = \frac{|\vec{k}|\sqrt{\pi}z_0\Gamma[1 + \frac{1}{d}]}{\Gamma[\frac{1}{2} + \frac{1}{d}]}.$$
 (4.69)

So, the WKB solution, as we approach region I becomes

$$\psi = \frac{1}{\sqrt{|\vec{k}|z_0e^{-dz_*/2}}} \left( A_{II}e^{\kappa-2|\vec{k}|d^{-\frac{1}{2}}z_0^{\frac{1}{2}}\sqrt{z_0-z}} + B_{II}e^{-\kappa+2|\vec{k}|d^{-\frac{1}{2}}z_0^{\frac{1}{2}}\sqrt{z_0-z}} \right).$$
 (4.70)

On the other hand, we have a regime where  $|\vec{k}|e^{-dz_*} \gg 1$ , but nevertheless,  $z_* \gg 1$  that overlaps with the regime above and is part of region I. This happens for  $1 \ll z_* \ll \ln(|\vec{k}|)$ . In this region, the expansion of the Bessel functions is

$$\begin{aligned} K_{i\gamma\omega}(\gamma|\vec{k}|e^{-dz_*/2}) &\approx \frac{1}{\sqrt{\frac{4}{d\pi}|\vec{k}|z_0e^{-dz_*/2}}} e^{-2z_0|\vec{k}|d^{-1}e^{-dz_*/2}} \\ \mathcal{R} \left( I_{i\gamma\omega}(\gamma|\vec{k}|e^{-dz_*/2}) \right) &\approx \frac{1}{\sqrt{\frac{4\pi}{d}|\vec{k}|z_0e^{-dz_*/2}}} e^{2z_0|\vec{k}|d^{-1}e^{-dz_*/2}}. \end{aligned}$$
 (4.71)

We can match these asymptotics with the asymptotics of region II, by using the fact that in the overlapping region

$$e^{-\frac{dz_*}{2}} = \sqrt{d\left(1 - \frac{z}{z_0}\right)} = d^{\frac{1}{2}}z_0^{-\frac{1}{2}}\sqrt{z_0-z}.$$
 (4.72)

Therefore the solution from region I as we approach region II becomes

$$\psi = A_I \frac{1}{\sqrt{\frac{4}{\pi d}|\vec{k}|z_0e^{-dz_*/2}}} e^{-2|\vec{k}|z_0^{\frac{1}{2}}d^{-\frac{1}{2}}\sqrt{z_0-z}} + B_I \frac{1}{\sqrt{\frac{4\pi}{d}|\vec{k}|z_0e^{-dz_*/2}}} e^{2|\vec{k}|z_0^{\frac{1}{2}}d^{-\frac{1}{2}}\sqrt{z_0-z}}.$$
 (4.73)

Now matching (4.73) and (4.70) we see that we need

$$\begin{aligned} A_I &= \sqrt{\frac{4}{\pi d}} e^{\kappa} A_{II}, \\ B_I &= \sqrt{\frac{4\pi}{d}} B_{II} e^{-\kappa}. \end{aligned}$$
 (4.74)

Combining (4.74) and (4.67) we find that

$$\begin{aligned} A_{III} &= \pi A_I e^{-\kappa} \sqrt{\frac{d}{2}}, \\ B_{III} &= \sqrt{\frac{2}{\pi}} (B_{II} - iA_{II}) = \sqrt{\frac{2}{\pi}} \left( e^\kappa B_I \sqrt{\frac{d}{4\pi}} - i e^{-\kappa} A_I \sqrt{\frac{\pi d}{4}} \right). \end{aligned} \quad (4.75)$$

### Normalization

Finally, we need to normalize the solutions above so that they can be used as a basis for expanding a quantum field. First, near the boundary we note that

$$\begin{aligned} \psi &= A_{III} I_\nu(|\vec{k}|z) + B_{III} K_\nu(|\vec{k}|z) \\ &\xrightarrow{z \rightarrow 0} (|\vec{k}|z)^\nu \left( B_{III} \Gamma(-\nu) 2^{-\nu-1} + A_{III} \frac{2^{-\nu}}{\Gamma(1+\nu)} \right) + (|\vec{k}|z)^{-\nu} 2^{\nu-1} \Gamma(\nu) B_{III}. \end{aligned} \quad (4.76)$$

Since we are looking for normalizable solutions, we set

$$B_{III} = 0. \quad (4.77)$$

This also tells us that  $|B_I| \ll |A_I|$  in the large  $|\vec{k}|$  limit, and so we can neglect  $B_I$  in what follows. Next, in the region near the horizon, where  $z_* \gg 1$ , we have the expansion

$$K_{i\gamma\omega}(\gamma|\vec{k}|e^{-dz_*/2}) \xrightarrow{z_* \rightarrow \infty} - \left( \frac{\pi}{\gamma\omega \sinh(\pi\gamma\omega)} \right)^{1/2} \sin(-d\gamma\omega z_*/2 + \log(\gamma|k|/2)\gamma\omega - \delta). \quad (4.78)$$

where the phase  $\delta = \arg(\Gamma(1+i\gamma\omega))$  and we have ignored the expansion of the Bessel “T” function since  $B_I$  is negligible.

We can use this to set the normalization of the field as follows. We expand the bulk quantum field as

$$\phi = \int \frac{d\omega d^{d-1}\vec{k}}{(2\pi)^d} \frac{1}{\sqrt{2\omega}} a_{\omega,\vec{k}} \psi(z) e^{-i\omega t} e^{i\vec{k}\cdot\vec{x}}, \quad (4.79)$$

with the creation and annihilation operators normalized so that

$$[a_{\omega, \vec{k}}, a_{\omega', \vec{k}'}^\dagger] = (2\pi)^d \delta(\omega - \omega') \delta(\vec{k} - \vec{k}'). \quad (4.80)$$

The correct normalization of  $\psi_{\omega, \vec{k}}(z)$  can then be determined through the canonical commutation relations

$$[\phi(t, z, \vec{x}), g^{tt} \dot{\phi}(t, z', \vec{x}')] = \frac{i}{\sqrt{-g(z_*)}} \delta(z_* - z'_*) \delta(\vec{x} - \vec{x}') \quad (4.81)$$

By examining these commutation relations in the near-horizon region where the wave-function varies exponentially, we find that

$$A_I^2 = \frac{8z_0^d \omega \sinh(\frac{2\pi z_0 \omega}{d})}{\pi}$$

## Two-point functions

The analysis above permits us to calculate the two-point correlation function of the generalized free-field on the boundary,  $\mathcal{O}$ , that is dual to the bulk field  $\phi$  through

$$\langle \mathcal{O}_{\omega, \vec{k}} \mathcal{O}_{\omega', \vec{k}'} \rangle_\beta = \lim_{z \rightarrow \infty} z^{-2\Delta} \langle \phi_{\omega, \vec{k}}(z) \phi_{\omega', \vec{k}'}(z) \rangle_\beta. \quad (4.82)$$

Note that this two-point function is sometimes defined with a “wave-function renormalization” factor that we have set to 1. The quantum expectation value on the right hand-side can be computed by using

$$\begin{aligned} \langle a_{\omega, \vec{k}} a_{\omega', \vec{k}'}^\dagger \rangle &= \frac{1}{1 - e^{-\beta\omega}} (2\pi)^d \delta(\omega - \omega') \delta(\vec{k} - \vec{k}'); \\ \langle a_{\omega, \vec{k}}^\dagger a_{\omega', \vec{k}'} \rangle &= \frac{e^{-\beta\omega}}{1 - e^{-\beta\omega}} (2\pi)^d \delta(\omega - \omega') \delta(\vec{k} - \vec{k}'). \end{aligned} \quad (4.83)$$

This leads to the result

$$\lim_{|\vec{k}| \rightarrow \infty} \langle \mathcal{O}_{\omega, \vec{k}} \mathcal{O}_{\omega', \vec{k}'} \rangle_\beta = 2\pi d z_0^d \cosh\left(\frac{2\pi z_0 \omega}{d}\right) |\vec{k}|^{2\nu} \frac{2^{-2\nu}}{\Gamma(1 + \nu)^2} e^{-2\kappa} \delta(\omega + \omega') \delta(\vec{k} + \vec{k}'). \quad (4.84)$$

Apart from some leading constants, the important part of this result for us is that in the large- $k$  limit, the two-point function scales like  $e^{\frac{-\alpha\beta|\vec{k}|}{2}}$  where<sup>2</sup>

$$\alpha = \frac{d\Gamma[1 + \frac{1}{d}]}{\sqrt{\pi}\Gamma[\frac{1}{2} + \frac{1}{d}]} \tag{4.85}$$

While, for  $d = 2$ , we have  $\alpha = 1$  for  $d > 2$ , we have  $\alpha > 1$ . In particular, for  $d = 3, 4, 5, 6$  we have  $\alpha = 1.34, 1.67, 2.00, 2.32$  respectively.

This means that while the bound is saturated in  $d = 2$ , it is under-saturated for  $d > 2$ . It would be nice to understand the reason for this phenomenon.

#### 4.4.2 Interactions and higher-point functions

We now examine how the correlators above behave when interactions are included. We will prove that, at tree-level, holographic correlators computed via *contact Witten diagrams obey the bound (4.2)*. Our arguments do not immediately show that the bound is saturated, and we postpone a more-complete discussion of exchange diagrams to future work. Interactions in holographic theories at finite temperature have been considered extensively in the literature starting with the work of [94, 105]. We refer the reader to [106] for more details.

Our analysis proceeds as follows. We consider Witten diagrams in the background of the *Euclidean black brane*. The Euclidean black brane metric is given by the continuation of (4.48)

$$ds_E^2 = \frac{1}{z^2} \left[ h(z)d\tau^2 + \frac{1}{h(z)}dz^2 + d\vec{x}^2 \right], \tag{4.86}$$

with a periodic identification of Euclidean time through  $\tau \sim \tau + \beta$ . This metric is completely regular and the  $\tau$ -circle shrinks smoothly to zero at  $z = z_0$ . For notational consistency we will continue to use the coordinate  $t = -i\tau$ .

In this section, we assume that the boundary correlator at real time and finite temperature can be computed as follows

1. We integrate all bulk points and bulk to bulk propagators over the Euclidean black-brane geometry.

---

<sup>2</sup>A similar factor appears in [91], although our expression is different. The discrepancy may be due to a typographical error.

2. We analytically continue the bulk to boundary propagators to account for complexified positions of the boundary insertions.

This seems to be a natural prescription for computing finite-temperature, real time correlators and avoids some of the difficulties that appear in the Schwinger-Keldysh formalism, which are explained in Appendix B.

For simplicity, we will consider scalar fields dual to operators of dimension  $\Delta$ . We consider contact interactions in some detail, and then briefly mention exchange interactions.

### Contact interactions

Witten diagrams with contact interactions can be computed using the bulk-boundary propagator in this background,  $K_{\Delta}(t_0, \vec{x}_0, t, \vec{x}, z)$  from a boundary point  $(t_0, \vec{x}_0)$  to a bulk point  $(t, \vec{x}, z)$  and a typical diagram is evaluated through an integral of the form

$$W(t_i, x_i) = \int \prod_i K_{\Delta_i}(t_i, \vec{x}_i, t, \vec{x}, z) dt d^{d-1} \vec{x} \frac{dz}{z^{d+1}}, \quad (4.87)$$

where the contour of integration is

$$0 \leq z \leq z_0; \quad \vec{x} \in R^{d-1} \quad 0 \leq it \leq \beta.$$

The purely Euclidean computation would involve purely imaginary values for the boundary points  $t_i$  and purely real values for  $x_i$ . For such values, the bulk to boundary propagator has *no* singularities. However, here, we will allow the boundary points to be at general complex values of  $t_i, \vec{x}_i$ , which can be done by analytically continuing the bulk to boundary propagator.

Now, the key point is as follows. As we start with Euclidean boundary points and continue them to complex values, the bulk to boundary propagator in (4.87) may develop singularities. Nevertheless, the *integral* itself can usually still be defined through analytic continuation. The *integral* develops singularities only when the contour of integration gets *pinched* between two or more singularities of the integrand [107].<sup>3</sup>

---

<sup>3</sup>This is similar to the method used in [108] to locate singularities in holographic correlators. However, since the bulk background is that of a black brane rather than empty AdS, the

Although, in general, we cannot find explicit analytic expressions for the bulk-boundary propagator for higher than two boundary dimensions, we can still isolate its singularities. The bulk-boundary propagator is singular whenever the boundary point  $(t_i, x_i)$  is connected to the bulk point  $(t, x, z)$  by a null geodesic. Since the boundary points are at complex positions, we consider *complexified* geodesics.

**Conditions for the Contour to be Pinched** We now review the conditions under which the contour of integration may be pinched. Let the equation of the light-cone emanating from a boundary point  $(t_i, x_i)$  to a boundary point  $(t, x, z)$  be given by  $S_i = 0$ . Then for the integral (4.87) to be singular, we require the following *necessary condition*. For some  $q$  *distinct* values  $i_1, i_2 \dots i_q$ , we should have

$$S_{i_1} = S_{i_2} = \dots S_{i_q} = 0; \quad \sum_{j=1}^q \gamma_j \frac{\partial S_{i_j}}{\partial w} = 0; \quad (4.88)$$

where  $\gamma_1, \gamma_2 \dots \gamma_q$  are arbitrary complex numbers and  $w_k$  runs over  $t, \vec{x}, z$ .

The first condition in (4.88) expresses the fact that the singularities are coincident. The second condition expresses the fact that the normals to the light-cone at the point of coincidence are linearly dependent on each other.

In addition, it is important that the singularities do not approach the contour of integration from the “same” side. Let  $\delta \vec{x}_i = x_i - x$  and  $\delta t = t_i - t$ . Then we require the following condition: *if the vectors  $\text{Im}(\delta \vec{x}_i)$  are on the same side of any  $(d - 2)$ -dimensional hyperplane that runs through the origin, then the singularity is not pinched*. Mathematically, this condition can be expressed by stating

$$\nexists \vec{b} \in R^{d-1}, \quad \text{such that} \quad \text{Im}(\delta \vec{x}_i) \cdot \vec{b} > 0, \quad \forall i. \quad (4.89)$$

The reason for this is that, in such a case, by deforming the contour of integration to give  $\vec{x}$  a small imaginary part in the direction perpendicular to this hyperplane, we simultaneously move away from all singularities.

We now prove that in a contact Witten diagram, the contour of integration *cannot* be pinched between the singularities of the bulk-boundary propagators.

---

analysis here is considerably more involved.

**Sketch of Proof** The proof below is somewhat involved, so we provide a brief sketch of the steps involved.

1. First we show that, if the contour of integration lies on a real value of  $z$  then singularities of the analytically continued bulk-boundary propagator only occur when the imaginary part of the displacement from the boundary to the bulk point is null or spacelike:

$$[\text{Im}(\delta t)]^2 \leq \text{Im}(\delta \vec{x}) \cdot \text{Im}(\delta \vec{x}). \quad (4.90)$$

2. Simple geometry then shows that if the boundary points are in the domain of analyticity, then (4.89) cannot be met.

**An analysis of complexified geodesics in higher-dimensional black branes**

The null geodesic equations, written in terms of an affine parameter,  $\lambda$  tell us that

$$\frac{dt}{d\lambda} = -\frac{k_{0i}z^2}{h(z)}; \quad \frac{d\vec{x}}{d\lambda} = \vec{k}_i z^2; \quad -\frac{h(z)}{z^2} \left(\frac{dt}{d\lambda}\right)^2 + \frac{1}{z^2 h(z)} \left(\frac{dz}{d\lambda}\right)^2 + \frac{1}{z^2} \left(\frac{d\vec{x}}{d\lambda}\right)^2 = 0, \quad (4.91)$$

where the subscript  $i$  indicates the different geodesics that end up at boundary points  $(t_i, x_i)$ . We remind the reader that these geodesics can move along the *complexified*  $(t, \vec{x}, z)$  manifold. Nevertheless, we will consider geodesics that originate at real  $z$  since the contour of integration originally runs along real  $z$ . For bulk to boundary propagators, the geodesic runs from a bulk point at an initial real value of  $z$ , which we denote by  $z_r$ , to the boundary, which is at  $z = 0$  and so we are interested in geodesics whose imaginary part again becomes zero when  $\text{Re}(z) = 0$ .

Using the last equation to solve for  $\frac{dz}{d\lambda}$  we find that

$$\frac{dz}{d\lambda} = -z^2 \left( k_{0i}^2 - \vec{k}_i^2 h(z) \right)^{\frac{1}{2}}. \quad (4.92)$$

The  $z$ -equation can be integrated to yield

$$\lambda = \frac{1}{z \sqrt{k_{0i}^2 - \vec{k}_i^2}} {}_2F_1 \left( \frac{1}{2}, -\frac{1}{d}; \frac{d-1}{d}; \frac{\vec{k}_i^2}{\vec{k}_i^2 - k_{0i}^2} \frac{z^d}{z_0^d} \right) - f_0, \quad (4.93)$$

where the constant  $f_0$  is set according to the convention that the affine parameter is 0 for  $z = z_r$ . Near the boundary, we have

$$\lambda \xrightarrow{z \rightarrow 0} \frac{1}{\sqrt{k_{0i}^2 - \vec{k}_i^2 z}}, \quad (4.94)$$

and so  $\lambda$  tends to  $\infty$  near the boundary.

Since the geodesic must reach the boundary at a real value of  $z = 0$ , the allowed geodesics must satisfy

$$k_{0i}^2 - \vec{k}_i^2 > 0. \quad (4.95)$$

We now proceed to prove that null geodesics obey (4.90). Our proof proceeds in two steps.

- 1 First we show that the equation (4.91) where the derivatives of  $t$  and  $\vec{x}$  need to be integrated along the curve (4.93) to obtain the full displacement  $\delta t$  and  $\delta \vec{x}$  can also be integrated along the real  $z$ -axis by considering the equations

$$\frac{dt}{dz} = \frac{1}{\frac{dz}{d\lambda}} \frac{dt}{d\lambda} = \frac{1}{h(z)\sqrt{1 - \vec{c}_i^2 h(z)}}; \quad \frac{d\vec{x}}{d\lambda} = \frac{1}{\frac{dz}{d\lambda}} \frac{d\vec{x}}{d\lambda} = \frac{\vec{c}_i}{\sqrt{1 - \vec{c}_i^2 h(z)}}, \quad (4.96)$$

where  $\vec{c}_i = \frac{\vec{k}_i}{k_{i0}}$ . What we need to prove here is that  $\frac{dz}{d\lambda} \neq 0$  at any point between the trajectory of the original geodesic and the real  $z$ -axis. If so, then we can deform the integration contour of the equations (4.96) from the original geodesic to the real  $z$ -axis.

- 2 Then we show that along the real  $z$  axis, the condition (4.90) is satisfied.

We will assume, throughout this analysis that  $\text{Im}(\vec{c}_i) \neq 0$ . This is the generic case, and our proof is easily generalized to the special case where  $\text{Im}(\vec{c}_i) = 0$ .

To prove property 1, we first note that along real  $z$ -axis,  $\text{Im}(\sqrt{1 - \vec{c}_i^2 h(z)})$  cannot change signs. This quantity can only change sign if, at some point on the real  $z$ -axis, we have  $1 - \vec{c}_i^2 h(z) > 0$  as a real number. But this is impossible since  $h(z) \in \mathbb{R}$  but  $\text{Im}(\vec{c}_i^2) \neq 0$ .

Now consider the *family* of geodesics with the same value of  $\vec{k}_i$  and  $k_{i0}$  but starting at different initial values of the  $z$ -coordinate:  $0 < z(0) < z_r$ . These geodesics *cannot* intersect the original geodesic that starts at  $z(0) = z_r$  because

the derivative along the curve is purely a function of  $z$  so a unique curve passes through each complex value of  $z$  where  $\frac{dz}{d\lambda} \neq 0$ . These geodesics also cannot intersect the  $z$ -axis. This is because if the geodesic intersects the  $z$ -axis, then  $\frac{d\text{Im}(z)}{d\lambda} = \text{Im} \left( -z^2 \sqrt{(k_{0i}^2 - \vec{k}_i^2) - \vec{k}_i^2 (h(z) - 1)} \right)$  must have different signs at  $z = z_r$  and the point where it returns to the  $z$ -axis. However, by (4.95) and a simple extension of the argument above,  $\frac{d\text{Im}(z)}{d\lambda}$ , keeps a fixed sign for real  $z$ . Therefore these geodesics must stay *between* the real  $z$ -axis and the trajectory of the original geodesic that starts at  $z_r$ . If we additionally assume that the geodesic curve varies continuously as the initial starting point varies then it follows that *all points* in the complex  $z$ -plane between the original geodesic and the real  $z$ -axis can be reached by varying  $z(0)$ . But since all geodesics terminate at the boundary, this means that  $\frac{dz}{d\lambda} \neq 0$  for any point between the original geodesic and the real  $z$ -axis.

This implies that to obtain the displacement  $\delta\vec{x}$  and  $\delta t$  we may integrate their derivatives, given by (4.96) along the real  $z$ -axis. Note that this immediately allows us to obtain explicit formulas for  $\delta t$  and  $\delta\vec{x}$  by explicit integration

$$\begin{aligned} \delta t_i &= \frac{z F_1 \left( \frac{1}{d}; \frac{1}{2}, 1; 1 + \frac{1}{d}; \frac{\vec{c}_i^2 z^d}{\vec{c}_i^2 - 1}, z^d \right)}{\sqrt{1 - \vec{c}_i^2}}, \\ \delta \vec{x}_i &= \vec{c}_i \frac{z {}_2F_1 \left( \frac{1}{2}, \frac{1}{d}; 1 + \frac{1}{d}; \frac{\vec{c}_i^2 z^d}{\vec{c}_i^2 - 1} \right)}{\sqrt{1 - \vec{c}_i^2}}, \end{aligned} \quad (4.97)$$

where  $F_1$  is the ‘‘Appell F-function’’.

Now we show property 2. First we perform a rotation in the transverse directions so that  $\vec{k}_i = (k_i, 0, \dots, 0)$  and therefore  $\vec{c}_i = (c, 0, \dots, 0)$  with  $c = \frac{k_i}{k_{i0}}$ . Second, for convenience, we consider the case where  $\text{Im}(c) > 0$  so that  $\text{Im}\left(\frac{1}{\sqrt{1 - c^2 h(z)}}\right) > 0$  and  $\text{Im}\left(\frac{c}{\sqrt{1 - c^2 h(z)}}\right) > 0$ . The other cases can be treated by trivially changing some signs below.

We define

$$D(d, z) = \text{Im} \left[ \frac{c}{\sqrt{1 - c^2 h(z)}} - \frac{1}{h(z) \sqrt{1 - c^2 h(z)}} \right]. \quad (4.98)$$

We noting that, through some simple algebra, if  $D(d, z)$  vanishes for  $0 < h < 1$ , this

can only happen at

$$h = \frac{-1 + \operatorname{Re}(c)}{|c|^2 - \operatorname{Re}(c)}. \quad (4.99)$$

Since  $D(d, z) > 0$  at  $z = 0$  ( $h = 1$ ) this means that  $D(d, z)$  is positive near  $z = 0$  and can cross the real axis *at most once* between the boundary and  $z_r$ .

To prove (4.90), we only need to integrate  $D(d, z)$  from the position of the contour to the boundary. However, the property of  $D(z)$  above tells us that (4.90) will be implied if we prove that

$$H(d) = \int_0^{z_0} D(d, z) > 0. \quad (4.100)$$

We will prove this as follows. First, we will show that once  $H(d)$  becomes positive, it remains positive as we increase  $d$ . Then we will check that for  $d = 2$ , the integral is positive which proves that it is positive for all  $d$ .

First, we note that

$$\frac{\partial D(d, z)}{\partial d} = \frac{\partial D(d, z)}{\partial z} \frac{z}{d} \log\left(\frac{z}{z_0}\right). \quad (4.101)$$

Therefore

$$d \frac{\partial}{\partial d} H(d) = d \frac{\partial}{\partial d} \int_0^{z_0} D(d, z) = \int_0^{z_0} \frac{\partial D(d, z)}{\partial z} z \log\left(\frac{z}{z_0}\right) = - \int_0^{z_0} D(d, z) \log\left(\frac{z}{z_0}\right) - H(d). \quad (4.102)$$

The boundary terms in the integration by parts vanish because the log vanishes at  $z = z_0$ , while at the boundary  $z = 0$ .

The differential equation above can be written as

$$\frac{\partial}{\partial d} dH(d) = - \int_0^{z_0} D(d, z) \log\left(\frac{z}{z_0}\right). \quad (4.103)$$

Now by the assumption about  $D$  above we also have that

$$\int_0^{z_0} D(d, z) \log\left(\frac{z}{z_0}\right) < 0. \quad (4.104)$$

since  $\log(\frac{z}{z_0}) < 0$  and moreover  $|\log(\frac{z}{z_0})|$  becomes larger as we go closer to  $z = 0$ . Therefore in the integral above  $\log(z)$  weights the positive section of  $D$  with a weight that is larger in magnitude than the weight for the section where  $D$  is negative.

Turning now to  $H(2)$  this can be analytically computed using the formulas above

to be  $H(2) = \text{Im}(\log(1+c))$ . Recall that we are considering the case where  $\text{Im}(c) > 0$  so that clearly  $H(2) > 0$ . Therefore  $H(d) > 0, \forall d \geq 2$ . The result (4.90) now follows immediately.

**Analyticity of correlators in the domain  $\eta_i \in \mathcal{F}$**  The analyticity of correlators in the required domain can now be proved. We let  $\eta_i$  be the *imaginary part* of the displacement of the boundary points from each other and let  $(\delta t_i, \delta \vec{x}_i)$  be the displacement in time and space from the point where the contour may be pinched in the bulk. Then, we see that the imaginary parts of these displacements are given by

$$(\text{Im}(\delta t_1), \text{Im}(\delta x_1)), (\text{Im}(\delta t_1), \text{Im}(\delta x_1)) + \eta_1, \dots, (\text{Im}(\delta t_1), \text{Im}(\delta x_1)) + \eta_1 + \dots + \eta_{n-1}. \quad (4.105)$$

However starting from a null or spacelike vector and adding future directed timelike vectors, it is *not* possible to obtain a configuration of spacelike vectors whose spatial parts are *not* on one-side of some codimension 1 hyperplane. So the singularity cannot be pinched by boundary points whose imaginary displacements are in the future timelike direction.

In fact, starting with the initial contour that runs from  $\text{Im}(t) = 0$  to  $\text{Im}(t) = -\beta$  and along  $\text{Im}(\vec{x}) = 0$ , we can deform the contour as shown in Figure 4.9. In the  $\text{Im}(t), \text{Im}(\vec{x})$  plane, the contour follows a *causal path* that tracks all the boundary points. Such a path must exist since the imaginary displacement between each point and the next point in the Wightman correlator is timelike and future directed.

On this contour of integration, it is clear that there are *no* singularities that remain even in the integrand. this is because a singularity can only arise when one of the boundary points is separated from a point on the contour by a spacelike imaginary displacement. However, in Figure 4.9 the imaginary displacement between every boundary point and every point on the contour is timelike.

It is also clear why the proof breaks down if the condition  $\beta e_i - \sum \eta_i \in \mathcal{V}^+$  is not met. Since the boundary is identified in Euclidean time, it is possible for geodesics to go both “forward” and “backward” in imaginary time. For points that are outside the diamond of analyticity, what may seem like a timelike displacement  $\eta_i \in \mathcal{V}^+$  may nevertheless be reached by a light ray going in the “wrong” direction in time.

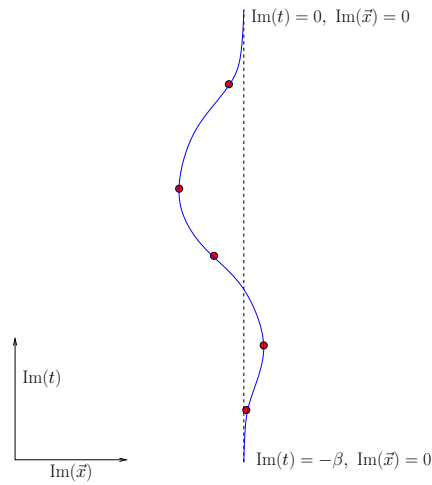


Figure 4.9: A deformation of the integration contour that explicitly avoids all singularities for a contact Witten diagram. The boundary points are displayed as red dots. The original contour is the dashed line along  $\text{Im}(\vec{x}) = 0$ . The final deformed contour is the blue line. The red dots are the imaginary coordinates of the boundary insertions.

See Figure 4.10. In this situation, it is clear that the proof of the previous section

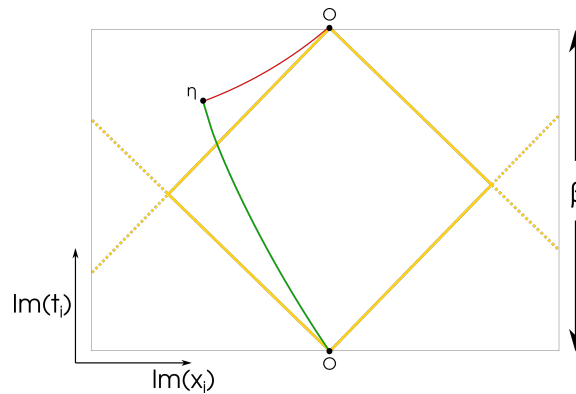


Figure 4.10: It seems like the vector  $\eta$ 's imaginary coordinates are “timelike” separated from  $\mathcal{O}$ . But if we take into account the periodic identification of Euclidean time, it is also possible to reach  $\eta$  from  $\mathcal{O}$  via a “spacelike” imaginary displacement.

does not hold.

### Exchange interactions

We now turn to exchange interactions. Let  $G(t, x, z, t', x', z')$  be the bulk-bulk propagator. Then exchange interactions are given by summing Witten diagrams which yield integrals of the form

$$\begin{aligned}
 W(t_i, x_i) = & \int \prod_{i_1=1}^{n_1} K_{\Delta_{i_1}}(t_i, \vec{x}_{i_1}, t, \vec{x}, z) G(t, \vec{x}, z, t', \vec{x}', z') \\
 & \times \prod_{i_2=1}^{n_2} K_{\Delta_{i_2}}(t_{i_2}, \vec{x}_{i_2}, t', \vec{x}', z') G(t', \vec{x}', z', t'', \vec{x}'', z'') \dots dt dt' d^{d-1} \vec{x} d^{d-1} \vec{x}' \frac{dz dz'}{z^{d+1} (z')^{d+1}} \dots
 \end{aligned}
 \tag{4.106}$$

Now the singularities of the bulk to bulk propagator are also along the light-cone, and so we need to repeat the analysis of the previous subsection for bulk-bulk propagators.

Some parts of the previous argument go through. For example, if the bulk-bulk propagator starts and ends at real values of  $z$ , then the displacement of  $\delta \vec{x}$  and  $\delta t$  between the two end-points of the bulk-bulk propagator can again be obtained by integrating the geodesic equations along the real  $z$  axis. For such geodesics, the condition (4.95) may not hold. Instead, such geodesics are separated by a point on the real  $z$ -axis, where the sign of  $\text{Im}(\frac{dz}{d\lambda})$  changes sign. This is because if this quantity has one sign at one endpoint (as the geodesic departs the real- $z$ -axis), it must have the opposite sign at the other endpoint (as the geodesic returns to the real- $z$ -axis). This point occurs at the unique value of  $h(z)$  for  $0 < z < 1$  where

$$h(z_t) = \frac{\text{Im}(k_0^2)}{\text{Im}(k_i^2)}
 \tag{4.107}$$

provided that we also have  $\text{Re}(k_0^2) - h(z_t)\text{Re}(k_i^2) > 0$ . Consider a geodesic that starts at  $z_r$  and terminates at  $z'_r$ . Once again we consider geodesics with the same value of  $k_0$  and  $\vec{k}_i$  that start between  $z_r$  and  $z_t$ . Since these geodesics cannot intersect the original geodesic they must intersect the  $z$  axis at some point between  $z_t$  and  $z'_r$ . Proceeding this way, by starting with different initial conditions, we can “fill up” the entire region between the real  $z$ -axis and original geodesic with other geodesics. This means that there are no points where  $\frac{dz}{d\lambda}$  vanishes in the region between the

trajectory of the geodesic and the real  $z$ -axis.

However, it is *not* true that for the bulk-bulk propagator, the vector  $(\text{Im}(\delta t), \text{Im}(\delta \vec{x}))$  must be spacelike. To consider a trivial counter-example, consider a geodesic that propagates from a value of  $z$  close to the horizon to another value of  $z$  close to the horizon. In the near-horizon region, we can make  $|\text{Im}\left(\frac{1}{h(z)\sqrt{1-c^2h(z)}}\right)| > |\text{Im}\frac{c}{\sqrt{1-c^2h(z)}}|$  and therefore we can easily achieve  $|\text{Im}(\delta t)|^2 > \text{Im}(\delta \vec{x}_i) \cdot \text{Im}(\delta \vec{x}_i)$ .

This means that the proof of the previous subsection, that applied to contact Witten diagrams is not immediately applicable.

This does not mean that exchange diagrams violate our bound. For example, in some cases, such as the BTZ black hole, exchange Witten diagrams can be reduced to sums of contact diagrams by extending the techniques of [109]. Then the proof of the previous subsection indirectly implies that exchange diagrams also have the correct analytic properties. However, for the more general case, we have not yet been able to find an appropriate proof that exchange Witten diagrams lead to boundary correlators obeying our bound. We leave the question of the analytic properties of exchange Witten diagrams as an open problem.

## 4.5 Discussion

We studied the limit of Wightman correlators in a relativistic quantum field theory at finite temperature, where the spatial momenta of the insertions became large while their frequencies remained finite. Based on general properties of quantum field theories, we showed that the correlator was bounded by the exponential of a specific geometric term: the radius of the smallest sphere that could contain the non-planar polygon of the momenta in units of the temperature.

We showed that this bound is saturated in weakly coupled theory at high enough loop order for arbitrary  $n$ -point functions. However, we found that this bound is not always saturated in holographic theories at leading order. This was surprising as holographic theories are strongly coupled.

In the context of holographic theories, it would be interesting to explore whether or not the bound holds for momenta which are much larger than the temperature, yet parametrically smaller than  $N$ . It would also be interesting to understand whether behaviour of correlators in this limit can help in identifying holographic theories.



## Chapter 5

### A quantum test for strong cosmic censorship

#### 5.1 Introduction

It is often believed, or at least hoped, that all *fundamental* theories of nature are *deterministic*. In a deterministic theory, if the initial condition is specified, i.e., all information about the *system* under consideration is supplied at some initial time, then we can determine everything about the system at any later time. As an example, if we know the initial position and velocity of a free particle in classical mechanics, we can determine the trajectory of the particle completely. Often, we may need to specify *boundary conditions* as well. For instance, we can confine the free particle in a box. Now, the initial condition is not sufficient to determine the trajectory of the particle. We also need to supply the boundary condition, which in this case would be the shape of the box and its interaction with the particle. Nonetheless, once the boundary condition is also specified, we can predict the position of particle at any later time. The theory remains deterministic.

Of course, not all physical processes fall under this category. The simplest example of a non-deterministic process is the motion of a *Brownian* particle in a fluid, described by a *stochastic* equation. However, such an equation does not describe a *fundamental* process. The Brownian motion is an *effective* description of a particle in a fluid. The *exact*, and deterministic, description would take into account the motion of all fluid particles and interactions. In principle, a deterministic description is achievable, even if not very illuminating.

One may argue that quantum mechanics is not deterministic. However calling quantum mechanics non-deterministic is misleading. Even in quantum mechanics, once the initial condition is supplied, we can evolve forward in time. In quantum mechanics, a modification of what is meant by knowing everything about a system is

required. Position and momentum no longer describes a particle. Rather, a quantum system is described by a *state* in an abstract *Hilbert space*. However, once the state of a closed quantum system is given at some time, we can determine the state at all times. In this sense, even quantum mechanics is deterministic.

However it is not clear whether general relativity is deterministic. In general relativity, the initial data can be specified over any *Cauchy slice*, a spacelike slice that foliates the spacetime. Cauchy slice is a generalization of the notion of a constant time surface. Once the *Cauchy data* is specified, it is expected that the full non-linear equations of motion can be solved, in principle, to determine the metric and other dynamical fields everywhere.

This expectation seems to fall apart even in some of the simplest solutions of Einstein's equation. Black holes in outer space are typically described by additional *asymptotic charges* apart from mass, such as angular momentum and electromagnetic charge. Such black holes have multiple horizons. Apart from the event horizon, these black holes have an *inner horizon* with following interesting properties.

1. Cauchy data on any spacelike slice cannot specify the evolution of fields beyond the inner horizon. Note that this is very different from what happens for Schwarzschild black holes. If the data is specified on a slice which has no support in the interior of a black hole, then we cannot evolve the fields beyond the outer horizon. However, we can extend the spacelike slice to include the interior region. Cauchy data on such achronal<sup>1</sup> *nice slice* is sufficient to determine the metric and other fields everywhere in the spacetime<sup>2</sup>. However, in the case of black holes with inner horizons, no such achronal slice exists. Data on a Cauchy slice only allows unique evolution of fields up to the inner horizon. The inner horizon is a *Cauchy horizon*, the boundary of domain of validity of the Cauchy problem.
2. Timelike geodesics can reach the inner horizon in finite proper time and curvature invariants do not diverge at the inner horizon. Hence, it should be possible to extend the spacetime beyond the inner horizon.

---

<sup>1</sup>No two points in an achronal set can be connected by a timelike trajectory.

<sup>2</sup>Except near the singularity. It is expected that a complete theory of quantum gravity would resolve the singularity.

Cauchy data giving rise to such black holes are examples of Cauchy data for which the *maximal Cauchy development*<sup>3</sup> is *incomplete*. This seems to be a scenario where determinism *fails*.

To sidestep this problem and restore determinism in gravity, Penrose proposed the strong cosmic censorship conjecture [15], which can be phrased as follows.

**Strong cosmic censorship conjecture** - *Maximal Cauchy development of a generic Cauchy data is complete.*

This suggests that initial data giving rise to spacetimes with *traversable* inner horizons must be of *measure zero* in the space of all initial conditions. Hence, generic perturbations to such solutions should render the inner horizon unstable. For instance, if we study propagation of a scalar field on such spacetimes, then the *stress tensor* of the scalar field at the inner horizon should be divergent. Hence, any observer that approaches the inner horizon would be destroyed by an infinite flux of radiation.

A physical intuition behind such an expectation is that the inner horizon is to the future of all events in the exterior. Hence, perturbations outside the black hole stretched over an infinite time, are experienced by an observer in finite proper time near the inner horizon. This infinite *blue-shift* effect, characterized by the *surface gravity* at inner horizon, could destabilize the inner horizon [110].

However, the decay of exterior perturbations at late times is controlled by the *quasinormal modes*. If the decay is sufficiently fast, then the perturbations in the exterior wouldn't be strong enough to render the inner horizon unstable. Hence, stability of the inner horizon is subject to two competing physical effects, namely quasinormal frequencies and surface gravity at the inner horizon [111].

The validity of strong cosmic censorship conjecture under classical perturbations has been a subject to extensive debate [112, 113]. Somewhat surprisingly, in several cases, it is possible to extend the metric continuously across the horizon [114] and only the derivatives of the metric diverge. The classical analysis has therefore focused on the severity of this divergence and the question of whether solutions to the equations of motion can be continued weakly past the horizon. The answer to this

---

<sup>3</sup>Maximal Cauchy development is the domain of validity of a Cauchy problem.

question depends on the precise smoothness conditions that are placed on the initial data [115].

In this chapter we explore quantum effects on the stability of inner horizon. Can quantum effects rule out, or constrain the violations of strong cosmic censorship conjecture? One way to understand the quantum effects is to study the *renormalized quantum stress tensor* near the inner horizon [116, 117, 118, 119]. However, computation of quantum stress tensor is very involved, and often impractical. Ambiguities due to the renormalization procedure add another layer of complexity to the problem.

In this chapter we develop of simple necessary criteria for a quantum state to be smooth across any null surface. We study a quantum scalar field propagating in the background of some  $d + 1$ -dimensional spacetime. We assume that the two point function of the scalar field with insertions near the null surface should reduce to the two point function in flat space, in the limit when the insertions approach each other. In fact, in the computation of renormalized stress tensor, contribution of this term is subtracted to get a finite answer. If this assumption fails, the stress tensor would diverge, making the spacetime singular near the null surface.

This seemingly trivial assumption is sufficient to greatly restrict the quantum state near the null surface. We define local modes near the null surface by integrating the fields in local Rindler coordinates on both sides of the surface. Since Rindler modes oscillate infinitely near the null surface, we can extract a mode even by restricting the integral to a neighbourhood of the null surface. We show that these local modes must be *correctly entangled* for the state to be smooth in the vicinity of the null surface. We explore how this entanglement constraints the two point function of global modes. For instance, if we apply this test to the horizon of a Schwarzschild black hole, then we can show that the two-point function of Schwarzschild modes must contain a piece proportional to a delta function in the frequency-difference with a coefficient that is precisely the Boltzmann factor corresponding to the temperature of the horizon.

We use this condition to develop a test for violations of strong cosmic censorship conjecture. Recall that the conjecture can be violated if the inner horizon of a black hole is smooth. However, the quantum state is already constrained due to smoothness of outer horizon. It is non-trivial for this state to also be smooth across

the inner horizon.

In section 5.2, we develop the precise quantum criteria for smoothness of a quantum state across a null surface. In section 5.3 we implement this criteria to study the violations of strong cosmic censorship in asymptotically AdS Reissner Nordström (RN-AdS) black holes. We show that the cosmic censorship conjecture is *not* violated in RN-AdS. In section 5.4, we study BTZ black holes and show that our tests do not rule out violations of the conjecture, as expected from the analysis of [119]. We point that this doesn't imply violations of the conjecture, since our criteria is only a *necessary* condition for smoothness. In particular, stress tensor at the inner horizon can still be divergent even if our smoothness condition is satisfied.

We also study the possibility of extension of spacetime beyond the inner horizon. We show that our smoothness criteria greatly constraints any violations of strong cosmic censorship conjecture. This extension turns out to be nontrivial since the standard construction of mirror operators [67, 68] that applies to the outer horizon cannot be directly applied to the inner horizon of the BTZ black hole. This can be understood in terms of the monogamy of entanglement. In the free-field limit, the modes near the inner horizon can be written as linear-combinations of modes near the outer horizon. Since the modes near the outer horizon are entangled with modes outside the outer horizon, they cannot also be entangled with new modes behind the inner horizon. It is possible to reuse the modes between the inner and outer horizon in such a manner that not only are the constraints of locality respected, the modes also have the correct two-point function dictated by the temperature of the inner horizon. This also provides the *unique* extension of quantum fields in the near-horizon region just beyond the inner horizon if the inner horizon is traversable.

Finally we close the chapter with some discussions in section 5.5. This chapter is based on [16].

## 5.2 Entangled modes across a null surface

In quantum field theory, to test whether the spacetime in the vicinity of a surface is smooth, we can test whether it is possible to transmit “messages” in that region by turning on a source for a field at one point and measuring the response of the field at another. While the long-distance propagation of the source will depend on

the nature of the spacetime, in the short-distance limit, we expect that fields in the neighbourhood of the source will respond in a universal manner. The response of the one-point function of the field to a source depends only on the commutator, but the response of higher-point functions also requires a specific short-distance behaviour for the two-point function. This, in turn, requires degrees of freedom that constitute the quantum field to be entangled with each other in a specific manner, as we now explain.

In the neighbourhood of any null surface, the quantum fields can be expanded in a set of modes corresponding to left and right movers. We will choose the convention that the “left movers” are those that smoothly cross the surface, so that the phase factor multiplying these modes varies smoothly as we move along the surface. On the other hand, the modes that move parallel to the null surface (i.e. whose surfaces of constant phase are parallel to the null surface) will be called “right movers”. See Figure 5.1.

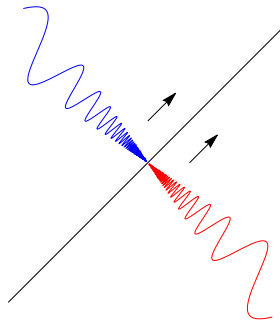


Figure 5.1: *Near horizon right-moving modes of a free scalar field near a null surface (black line). The red modes correspond to the operator  $\mathbf{a}$  while the blue ones to  $\tilde{\mathbf{a}}$  (see eq. (5.12)). The arrows indicate that the modes propagate parallel to the surface.*

The specific technical result that we intend to show is that it is possible to define appropriate “right moving” modes on the two sides of the null surface, so that their action on the state of the system is related in a specific manner.<sup>4</sup>

---

<sup>4</sup>We use the term “entanglement” to denote this relationship although our result is primarily about correlation functions, and not about any quantum-information measure of entanglement. The reason for our terminology is that — as shown in [120] — it is possible to use these correlators between near-horizon modes to extract Bell pairs from opposite sides of the horizon.

We consider a small portion of a null surface, such that the metric is continuous across the surface. In  $(d + 1)$ -dimensions, we introduce coordinates  $\mathcal{U}, \mathcal{V}$  and transverse coordinates,  $\xi^a$  with  $2 \leq a \leq d$ . We use a calligraphic font for these coordinates in this section to distinguish them from the coordinates that appear in the black-hole geometry. The Greek indices below can take values in a larger range,  $0 \leq \mu, \nu \leq d$ , and we set  $\xi^0 = \mathcal{U}$  and  $\xi^1 = \mathcal{V}$ . The null surface under consideration is that of  $\mathcal{U} = 0$ , and on this surface, we will consider the small patch near  $\xi^\mu = 0$ , where we write the metric as

$$ds^2 = -d\mathcal{U}d\mathcal{V} + \delta_{\alpha\beta}d\xi^\alpha d\xi^\beta + g_{\mu\nu}^{(1)}d\xi^\mu d\xi^\nu. \quad (5.1)$$

We will assume that  $g_{\mu\nu}^{(1)} \rightarrow 0$  as  $\xi^\mu \rightarrow 0$  i.e. as we approach the patch under consideration the metric is well approximated by the first two terms in (5.1).

**Near-horizon 2-point function:** Now consider a scalar field propagating in this background. The precise assumption that we will make is that if the spacetime is “reasonable” then, in the short-distance limit the two-point function of the scalar field will be given simply by an inverse power of the geodesic distance. This is true at least if the ultraviolet physics of the scalar operator is controlled by a free-fixed point (at scales much lower than the Planck scale). A similar assumption can be made for fermions, or fields with spin.

Consider two insertions of the field at two nearby, but distinct points, which may be on the same side or on opposite sides of the null surface. We denote the state of the full system by  $|\Psi\rangle$ . In AdS/CFT, this state may be considered to be a state in the Hilbert space, as defined by the boundary conformal field theory. The assumption above implies that if this state is “reasonable” then

$$\langle \Psi | \phi(\mathcal{U}_1, \mathcal{V}_1, \xi_1^\alpha) \phi(\mathcal{U}_2, \mathcal{V}_2, \xi_2^\alpha) | \Psi \rangle = \mathcal{N} \frac{1}{s^{\frac{d-1}{2}}} + \mathcal{R}. \quad (5.2)$$

In the equation above, the leading-order square of the geodesic distance  $s$  is given by

$$s = (-\delta\mathcal{U} \delta\mathcal{V} + \delta_{\alpha\beta} \delta\xi^\alpha \delta\xi^\beta), \quad (5.3)$$

where  $\delta\mathcal{U} = \mathcal{U}_1 - \mathcal{U}_2 - i\epsilon$ ;  $\delta\mathcal{V} = \mathcal{V}_1 - \mathcal{V}_2 - i\epsilon$  and we use the  $(d - 1)$ -vector,  $\delta\vec{\xi}$ , with

components  $\delta\vec{\xi}^a = \xi_1^a - \xi_2^a$  to denote the displacement in the transverse directions between the two points. Here,  $\mathcal{R}$  can be any function of the variables  $(\mathcal{U}_i, \mathcal{V}_i, \xi_i^a)$  that is less-singular than the displayed leading term as the points come close to each other. We have also introduced  $-i\epsilon$  regulators with  $\delta\mathcal{U}$  and  $\delta\mathcal{V}$ , which reflect that fact that we are interested in a Wightman function. This will be important when we consider commutators below. The normalization of the short-distance singularity

$$\mathcal{N} = \frac{\Gamma(d-1)}{2^d \pi^{\frac{d}{2}} \Gamma(\frac{d}{2})}, \quad (5.4)$$

can be fixed by considering a canonically normalized field in flat-space and explicitly checking its short-distance behaviour.

The important equation (5.2) makes the assumptions that the short-distance singularities of the two-point function arise only when the geodesic distance vanishes. Note that the remaining part of the metric  $g_{\mu\nu}^{(1)}$  does not appear in the leading singular part of this expression, although it is important for the subleading terms captured in the function  $\mathcal{R}$ .

We will show that (5.2) forces a specific form of entanglement between right movers across the surface  $\mathcal{U} = 0$ . To see this, we take a further limit of (5.2) and repeat the manipulations that led to equation (4.3) of [70]. If we first differentiate the two-point function, we will find that

$$\langle \Psi | \partial_{\mathcal{U}_1} \phi(\mathcal{U}_1, \mathcal{V}_1, \xi_1^a) \partial_{\mathcal{U}_2} \phi(\mathcal{U}_2, \mathcal{V}_2, \xi_2^a) | \Psi \rangle = -\frac{d^2-1}{4} \mathcal{N} \frac{(\delta\mathcal{V})^2}{s^{\frac{d+3}{2}}} + \partial_{\mathcal{U}_1} \partial_{\mathcal{U}_2} \mathcal{R}. \quad (5.5)$$

We now consider the limit  $\delta\mathcal{V} \rightarrow 0$ . In this limit the derivative of the two-point function above goes to zero unless  $\delta\vec{\xi}^a = 0$ . But this point, where the transverse displacement vanishes, gives a delta function contribution. We can check this, and also determine the normalization of the delta function by performing an integral over the transverse coordinates

$$\begin{aligned} \lim_{\delta\mathcal{V} \rightarrow 0} \int d^{d-1} \delta\vec{\xi}^a \frac{(\delta\mathcal{V})^2}{s^{\frac{d+3}{2}}} &= \lim_{\delta\mathcal{V} \rightarrow 0} \frac{1}{(\delta\mathcal{U})^2} \frac{1}{(-\delta\mathcal{U}\delta\mathcal{V})^{\frac{d-1}{2}}} \int d^{d-1} \delta\vec{\xi}^a \left( 1 + \frac{1}{(-\delta\mathcal{U}\delta\mathcal{V})} \delta\vec{\xi}^2 \right)^{-\frac{d+3}{2}} \\ &= \frac{1}{(\delta\mathcal{U})^2} \kappa_N, \end{aligned} \quad (5.6)$$

where

$$\kappa_N = \int d^{d-1} \delta \vec{\xi} \frac{1}{(1 + \delta \vec{\xi}^2)^{\frac{d+3}{2}}} = \frac{4}{d^2 - 1} \frac{\pi^{\frac{d-1}{2}}}{\Gamma(\frac{d-1}{2})}. \quad (5.7)$$

It is important that, in the integral above, we take the range of the integral over the transverse coordinates to be  $(-\infty, \infty)$  in order to be able to change variables from  $\delta \vec{\xi} \rightarrow \frac{\delta \vec{\xi}}{\sqrt{-\delta \mathcal{U} \delta \mathcal{V}}}$ . This is only a trick to determine the normalization. It does *not* require that the expression for the two-point function remain valid for an infinite separation in transverse coordinates or even that the transverse coordinates have an infinite extent.

The various normalization constants in the equations above simplify when taken together using

$$\frac{d^2 - 1}{4} \kappa_N \mathcal{N} = \frac{1}{4\pi}. \quad (5.8)$$

Note that if we were to perform the operations above on a term in the two-point function that diverges with a smaller power of geodesic distance or on a regular function, which may appear inside  $\mathcal{R}$ , we would obtain a result that is non-singular in the limit  $\mathcal{U}_1 \rightarrow \mathcal{U}_2$ .

So we finally find

$$\begin{aligned} \lim_{\mathcal{V}_1 - \mathcal{V}_2 \rightarrow 0} \langle \Psi | \partial_{\mathcal{U}_1} \phi(\mathcal{U}_1, \mathcal{V}_1, \xi_1^a) \partial_{\mathcal{U}_2} \phi(\mathcal{U}_2, \mathcal{V}_2, \xi_2^a) | \Psi \rangle &= -\frac{1}{4\pi} \frac{1}{(\mathcal{U}_1 - \mathcal{U}_2 - i\epsilon)^2} \delta^{d-1}(\delta \vec{\xi}) \\ &+ \lim_{\mathcal{V}_1 - \mathcal{V}_2 \rightarrow 0} \partial_{\mathcal{U}_1} \partial_{\mathcal{U}_2} \tilde{R}. \end{aligned} \quad (5.9)$$

If the reader is worried about the ultralocal delta function that appears above, she should note that in the applications below we will always use (5.9) after integrating both sides with test functions. Typically, we will consider fields that are separated by  $\epsilon_{\mathcal{V}}$  in the  $\mathcal{V}$  coordinate, and smeared over a range  $\epsilon_{\mathcal{U}}$  in the  $\mathcal{U}$  coordinate and  $\epsilon_{\xi}$  in the transverse coordinates. Then the formula above holds provided we take  $\epsilon_{\mathcal{V}} \ll \epsilon_{\mathcal{U}} \ll \epsilon_{\xi}$ .

**Near-horizon modes:** We now define some modes by integrating the field over a very short distance on both sides of the  $\mathcal{U} = 0$  surface and for a very short distance over the transverse coordinates. We will show that the short distance structure of the two-point function above forces these modes to have a specific two-point correlation

function. We follow the procedure given in [120] to define the modes.

The intuition is the following: as we approach the null surface from below  $\mathcal{U} \rightarrow 0^-$  we can find solutions of the wave equation that behave like  $(-\mathcal{U})^{i\omega_0}$ . These solutions undergo an infinite number of oscillations until  $\mathcal{U} = 0$ . If we think in terms of the tortoise-like coordinate  $u = \log(-\mathcal{U})$  these solutions behave like plane waves. This approximation becomes better as we approach the null surface at  $\mathcal{U} \rightarrow 0$  or  $u = -\infty$ . We define modes  $\mathbf{a}$  corresponding to wave packets with highly peaked frequency  $\omega_0$  and centered very far towards  $u = -\infty$ , or equivalently around a point  $\mathcal{U}_0$  very near the null surface  $\mathcal{U} = 0$ . We make sure that these modes are unit-normalized (as opposed to having delta-function normalization). We define these modes as Fourier modes with approximate frequency  $\omega_0$  characterized by a window of support in position space centered around  $\mathcal{U}_0$  and with a very large width in  $u$ -coordinates (though a small region in  $\mathcal{U}$  coordinates).

This is achieved by introducing a “tuning function”  $\mathcal{T}(\mathcal{U})$  which has the property that  $\mathcal{T}(\mathcal{U})$  is real and has support only for  $\mathcal{U} \in [\mathcal{U}_l, \mathcal{U}_h]$ , where  $0 < \mathcal{U}_l \ll \mathcal{U}_0 \ll \mathcal{U}_h$  and so that  $\mathcal{U}_h$  is much smaller than the characteristic curvature scale of the geometry. This tuning function is assumed to vanish smoothly at the end-points of its support and normalized carefully as follows. First, we define its Fourier transform via

$$\mathcal{T}(\mathcal{U}) = \int_{-\infty}^{\infty} \mathfrak{s}(\nu) \left(\frac{\mathcal{U}}{\mathcal{U}_0}\right)^{i\nu} d\nu; \quad \mathfrak{s}(\nu) = \frac{1}{2\pi} \int_0^{\infty} \frac{d\mathcal{U}}{\mathcal{U}} \mathcal{T}(\mathcal{U}) \left(\frac{\mathcal{U}}{\mathcal{U}_0}\right)^{-i\nu}. \quad (5.10)$$

Then we normalize the “tuning function” by demanding

$$\int |\mathfrak{s}(\nu)|^2 d\nu = 1. \quad (5.11)$$

We choose  $\mathfrak{s}(\nu)$  to be sharply peaked around  $\nu = 0$ , which corresponds to  $\mathcal{T}(\mathcal{U})$  being almost constant in the domain  $[\mathcal{U}_l, \mathcal{U}_h]$ .

We now also integrate over a small volume  $V_{\text{ol}}$  in the transverse coordinates and define the modes

$$\begin{aligned} \mathbf{a} &= \frac{1}{\sqrt{\pi\omega_0}} \int \frac{d^{d-1}\xi^a}{\sqrt{V_{\text{ol}}}} \int_0^{-\infty} d\mathcal{U} \partial_{\mathcal{U}} \phi(\mathcal{U}, \mathcal{V} = 0, \xi^a) \left(\frac{-\mathcal{U}}{\mathcal{U}_0}\right)^{-i\omega_0} \mathcal{T}(-\mathcal{U}), \\ \tilde{\mathbf{a}} &= \frac{1}{\sqrt{\pi\omega_0}} \int \frac{d^{d-1}\xi^a}{\sqrt{V_{\text{ol}}}} \int_0^{\infty} \partial_{\mathcal{U}} \phi(\mathcal{U}, \mathcal{V} = -\epsilon, \xi^a) \left(\frac{\mathcal{U}}{\mathcal{U}_0}\right)^{i\omega_0} \mathcal{T}(\mathcal{U}). \end{aligned} \quad (5.12)$$

The domain of integration, which is controlled by  $\mathcal{T}(\mathcal{U})$  is a very small region on both sides of the null surface and also a very small patch in the transverse coordinates. The modes have a nontrivial dependence on the choice of  $\omega_0$  and, moreover, such modes can be defined in the vicinity of any point of the null surface. But we have suppressed this dependence on the left hand sides of (5.12) to lighten the notation.

In the rest of this section we will show how the short-distance behaviour of the two-point function (5.9) determines the two-point correlators of these modes.

Before moving on, we emphasize that the modes  $\mathbf{a}, \tilde{\mathbf{a}}$  depend on the choice of  $\mathcal{U}_0, \mathcal{U}_l, \mathcal{U}_h$  and also the precise choice of the tuning function. We are interested in the behavior of these modes in the limit  $\mathcal{U}_0 \rightarrow 0$  and  $\frac{\mathcal{U}_h}{\mathcal{U}_0}, \frac{\mathcal{U}_0}{\mathcal{U}_l} \gg 1$  and where  $\mathfrak{s}(\nu)$  is sharply peaked. The statements we are going to make about the modes  $\mathbf{a}, \tilde{\mathbf{a}}$  correspond to the behavior of these modes in this particular limit. However, in the equations below, we will not display the dependence on these various cutoffs explicitly, since the equations can be made arbitrarily precise by taking these cutoffs to be as small as necessary.

**Commutators:** If we assume that the field operators satisfy canonical commutation relations then we find that at equal values of  $\mathcal{V}$  we have

$$[\phi(\mathcal{U}_1, \mathcal{V}, \xi_1^a), \partial_{\mathcal{U}_2} \phi(\mathcal{U}_2, \mathcal{V}, \xi_2^a)] = \frac{i}{2} \delta^{d-1}(\delta \vec{\xi}) \delta(\mathcal{U}_1 - \mathcal{U}_2). \quad (5.13)$$

This commutator has, inbuilt into it, the fact that the fields commute at spacelike separation. We note that the commutator is also consistent with the two-point correlator that we found above because

$$\begin{aligned} \text{Im} (\langle \partial_{\mathcal{U}_1} \phi(\mathcal{U}_1, \mathcal{V}, \xi_1^a), \partial_{\mathcal{U}_2} \phi(\mathcal{U}_2, \mathcal{V}, \xi_2^a) \rangle) &= \text{Im} \left[ -\frac{1}{4\pi} \frac{1}{(\mathcal{U}_1 - \mathcal{U}_2 - i\epsilon)^2} \right] \\ &= \frac{1}{4} \delta'(\mathcal{U}_1 - \mathcal{U}_2) \delta^{d-1}(\delta \vec{\xi}), \end{aligned} \quad (5.14)$$

which can be seen from the identity  $-\frac{1}{(x-i\epsilon)^2} = \frac{\partial}{\partial x} \frac{1}{x-i\epsilon} = \frac{\partial}{\partial x} \mathcal{P} \frac{1}{x} + i\pi \delta'(x)$ .

We can substitute these commutation relations into the definition of the modes

to compute their commutators.

$$\begin{aligned}
 [\mathbf{a}, \mathbf{a}^\dagger] &= \frac{1}{\pi\omega_0 V_{\text{ol}}} \int [\partial_{\mathcal{U}_1} \phi(\mathcal{U}_1, \mathcal{V} = 0, \xi_1^a), \partial_{\mathcal{U}_2} \phi(\mathcal{U}_2, \mathcal{V} = 0, \xi_2^a)] \\
 &\quad \times \left(-\frac{\mathcal{U}_1}{\mathcal{U}_0}\right)^{-i\omega_0} \left(-\frac{\mathcal{U}_2}{\mathcal{U}_0}\right)^{i\omega_0} \mathcal{T}(-\mathcal{U}_1) \mathcal{T}(-\mathcal{U}_2) d\mathcal{U}_1 d\mathcal{U}_2 d^{d-1}\xi_1^a d^{d-1}\xi_2^a.
 \end{aligned} \tag{5.15}$$

Using the canonical commutators (5.13), and doing the trivial integral in the transverse directions, we find that

$$\begin{aligned}
 [\mathbf{a}, \mathbf{a}^\dagger] &= \frac{i}{2\pi\omega_0} \int \partial_{\mathcal{U}_1} \delta(\mathcal{U}_1 - \mathcal{U}_2) \left(-\frac{\mathcal{U}_1}{\mathcal{U}_0}\right)^{-i\omega_0} \left(-\frac{\mathcal{U}_2}{\mathcal{U}_0}\right)^{i\omega_0} \mathcal{T}(-\mathcal{U}_1) \mathcal{T}(-\mathcal{U}_2) d\mathcal{U}_1 d\mathcal{U}_2 \\
 &= \frac{i}{2\pi\omega_0} \int_0^{-\infty} \partial_{\mathcal{U}_1} \mathcal{T}(-\mathcal{U}_1) \mathcal{T}(-\mathcal{U}_1) d\mathcal{U}_1 + \frac{1}{2\pi} \int_0^{-\infty} \mathcal{T}(-\mathcal{U}_1)^2 \frac{d\mathcal{U}_1}{\mathcal{U}_1}.
 \end{aligned} \tag{5.16}$$

In doing the integral over the delta function in the  $\mathcal{U}$  coordinates, we were careful that the  $\mathcal{U}_2$  integral proceeds with  $d\mathcal{U}_2 < 0$ , and so the delta function sets  $\mathcal{U}_1 = \mathcal{U}_2$  and gives an additional minus sign. The first term above vanishes if the tuning function vanishes at both its end points. For the second term, using the normalization of the tuning function above we find

$$[\mathbf{a}, \mathbf{a}^\dagger] = 1. \tag{5.17}$$

A similar calculation for  $\tilde{\mathbf{a}}$  leads to

$$[\tilde{\mathbf{a}}, \tilde{\mathbf{a}}^\dagger] = 1, \tag{5.18}$$

and also

$$[\mathbf{a}, \tilde{\mathbf{a}}] = [\mathbf{a}, \tilde{\mathbf{a}}^\dagger] = 0. \tag{5.19}$$

**Cross-correlators:** For the cross-correlators we have

$$\begin{aligned} \langle \Psi | \mathbf{a}\tilde{\mathbf{a}} | \Psi \rangle &= \frac{1}{\pi V_{\text{ol}} \omega_0} \int d\mathcal{U}_1 d\mathcal{U}_2 \partial_{\mathcal{U}_1} \partial_{\mathcal{U}_2} \langle \Psi | \phi(\mathcal{U}_1, \mathcal{V} = 0, \xi_1^a) \phi(\mathcal{U}_2, \mathcal{V} = 0, \xi_2^a) | \Psi \rangle \\ &\quad \times (-\mathcal{U}_1)^{-i\omega_0} (\mathcal{U}_2)^{i\omega_0} \mathcal{T}(-\mathcal{U}_1) \mathcal{T}(\mathcal{U}_2) d^{d-1} \xi_1^a d^{d-1} \xi_2^a. \end{aligned} \quad (5.20)$$

In the small domain where the integrand above has support, note that the regular parts of the two-point function just drop out and the only contribution comes from the singular terms identified above.

Now, note that we may write

$$\frac{1}{(\mathcal{U}_1 - \mathcal{U}_2)^2} = \frac{1}{(-\mathcal{U}_1)\mathcal{U}_2} \int_{-\infty}^{\infty} \omega \frac{e^{-\pi\omega}}{1 - e^{-2\pi\omega}} \left( -\frac{\mathcal{U}_2}{\mathcal{U}_1} \right)^{-i\omega} d\omega, \quad (5.21)$$

where  $\mathcal{U}_1 < 0$  and  $\mathcal{U}_2 > 0$ . If  $|\mathcal{U}_1| > |\mathcal{U}_2|$  this identity follows from completing the  $\omega$  integral in the upper half plane and picking up the poles at  $\omega = in$ ; else we close the contour in the lower half-plane and pick up the poles at  $\omega = -in$ .

Substituting the short distance limit (5.9) into the expression above and doing the transverse integral we find that

$$\begin{aligned} \langle \Psi | \mathbf{a}\tilde{\mathbf{a}} | \Psi \rangle &= \frac{1}{4\pi^2 \omega_0} \int \frac{d\mathcal{U}_1}{\mathcal{U}_1} \frac{d\mathcal{U}_2}{\mathcal{U}_2} \omega \frac{e^{-\pi\omega}}{1 - e^{-2\pi\omega}} \left( -\frac{\mathcal{U}_2}{\mathcal{U}_1} \right)^{-i\omega} d\omega \mathcal{T}(-\mathcal{U}_1) \mathcal{T}(\mathcal{U}_2) (-\mathcal{U}_1)^{-i\omega_0} (\mathcal{U}_2)^{i\omega_0} \\ &= \frac{1}{\omega_0} \int \omega \frac{e^{-\pi\omega}}{1 - e^{-2\pi\omega}} |\mathfrak{s}(\omega - \omega_0)|^2 d\omega. \end{aligned} \quad (5.22)$$

In the limit where  $\mathfrak{s}(\omega)$  is very sharply peaked around  $\omega = 0$ , and using the normalization condition (5.11), the two-point function just reduces to

$$\langle \Psi | \mathbf{a}\tilde{\mathbf{a}} | \Psi \rangle = \frac{e^{-\pi\omega_0}}{1 - e^{-2\pi\omega_0}}. \quad (5.23)$$

This gives us the universal form of entanglement for short distance modes on opposite sides of the horizon. As in [120], this two-point function can be used to extract Bell pairs from either side of the null surface.

Taking the Hermitian conjugate of this relation leads to

$$\langle \Psi | \mathbf{a}^\dagger \tilde{\mathbf{a}}^\dagger | \Psi \rangle = \frac{e^{-\pi\omega_0}}{1 - e^{-2\pi\omega_0}}. \quad (5.24)$$

Finally, by a similar calculation we find

$$\langle \Psi | \mathbf{a}^\dagger \tilde{\mathbf{a}} | \Psi \rangle = \langle \Psi | \mathbf{a} \tilde{\mathbf{a}}^\dagger | \Psi \rangle = 0. \quad (5.25)$$

**Self-correlators:** We can also determine correlators of the  $\mathbf{a}$  and  $\tilde{\mathbf{a}}$  modes with their own conjugates. In this case, we need the identity

$$\frac{-1}{(\mathcal{U}_1 - \mathcal{U}_2 - i\epsilon)^2} = \frac{1}{\mathcal{U}_1 \mathcal{U}_2} \int_{-\infty}^{\infty} \omega \frac{1}{1 - e^{-2\pi\omega}} \left( \frac{\mathcal{U}_2}{\mathcal{U}_1} e^{-i\epsilon} \right)^{-i\omega} d\omega, \quad (5.26)$$

when  $\mathcal{U}_1 < 0$  and  $\mathcal{U}_2 < 0$ . The integral on the right can again be done by closing the  $\omega$  contour in the upper or the lower half plane and picking up the poles at  $\omega = in$ . Note that the  $i\epsilon$  term ensures that the integral converges both at large positive and large negative  $\omega$ .

Using this identity, we see that

$$\begin{aligned} \langle \Psi | \mathbf{a} \mathbf{a}^\dagger | \Psi \rangle &= \int \frac{d\mathcal{U}_1 d\mathcal{U}_2}{\mathcal{U}_1 \mathcal{U}_2} \frac{1}{1 - e^{-2\pi\omega}} \left( \frac{\mathcal{U}_2}{\mathcal{U}_1} \right)^{-i\omega} d\omega \mathcal{T}(-\mathcal{U}_1) \mathcal{T}(-\mathcal{U}_2) \left( -\frac{\mathcal{U}_1}{\mathcal{U}_0} \right)^{-i\omega_0} \left( -\frac{\mathcal{U}_2}{\mathcal{U}_0} \right)^{i\omega_0} \\ &= \int \frac{1}{1 - e^{-2\pi\omega}} |\mathfrak{s}(\omega - \omega_0)|^2 d\omega. \end{aligned} \quad (5.27)$$

Again, in the limit where  $\mathfrak{s}(\omega)$  is sharply peaked we find that

$$\langle \Psi | \mathbf{a} \mathbf{a}^\dagger | \Psi \rangle = 1 + \langle \Psi | \mathbf{a}^\dagger \mathbf{a} | \Psi \rangle = \frac{1}{1 - e^{-2\pi\omega_0}}. \quad (5.28)$$

A small subtlety that we note is that it is the  $i\epsilon$  prescription that is important for ensuring that  $\langle \mathbf{a} \mathbf{a}^\dagger \rangle$  and  $\langle \mathbf{a}^\dagger \mathbf{a} \rangle$  have distinct values. Indeed, the reader might have wondered whether it is possible to replace  $\frac{1}{1 - e^{-2\pi\omega}} \rightarrow \frac{e^{-2\pi\omega}}{1 - e^{-2\pi\omega}}$  in the identity (5.26) since both these terms have the same residues at the pole  $\omega = \pm in$ . However, with an additional factor of  $e^{-2\pi\omega}$  in the numerator, the integral will not converge for large negative  $\omega$  since the numerator and the denominator now grow at the same

rate but the factor of  $e^{-\epsilon\omega}$  grows in that regime. It is the  $i\epsilon$  prescription that forces us to use the measure displayed in the equation (5.26) rather than the one with an additional exponential factor. This, in turn, ensures that there is no exponential factor in the numerator on the right hand side of (5.28).

**Relating the action of modes on the state:** Above, we derived the two-point functions between the various modes. However, by putting these results together, we can derive a stronger relationship that relates the action of the left-movers on the quantum state to the action of the right movers.

Let us write

$$\tilde{\mathbf{a}}|\Psi\rangle = c_1\mathbf{a}|\Psi\rangle + c_2\mathbf{a}^\dagger|\Psi\rangle + |\chi\rangle, \quad (5.29)$$

where  $c_1, c_2$  are constants to be determined and  $|\chi\rangle$  is orthogonal to the vectors produced by the action of  $\mathbf{a}$  and  $\mathbf{a}^\dagger$  on  $|\Psi\rangle$  so that

$$\langle\chi|\mathbf{a}|\Psi\rangle = \langle\chi|\mathbf{a}^\dagger|\Psi\rangle = 0. \quad (5.30)$$

Now, from (5.25) we have

$$\langle\Psi|\mathbf{a}^\dagger\tilde{\mathbf{a}}|\Psi\rangle = 0 \Rightarrow c_1 = 0. \quad (5.31)$$

We can now set  $c_2$  using

$$\langle\Psi|\mathbf{a}\tilde{\mathbf{a}}|\Psi\rangle = \frac{e^{-\pi\omega_0}}{1 - e^{-2\pi\omega_0}} \Rightarrow c_2 = e^{-\pi\omega_0}. \quad (5.32)$$

Finally, note that

$$\langle\Psi|\tilde{\mathbf{a}}^\dagger\tilde{\mathbf{a}}|\Psi\rangle = \frac{e^{-2\pi\omega_0}}{1 - e^{-2\pi\omega_0}} \Rightarrow \langle\chi|\chi\rangle = 0. \quad (5.33)$$

where we have also used the two-point correlator of  $\mathbf{a}$  with its conjugate. As similar procedure can be followed for the action of  $\tilde{\mathbf{a}}^\dagger$ . Therefore, we reach the simple relations

$$\tilde{\mathbf{a}}|\Psi\rangle = e^{-\pi\omega_0}\mathbf{a}^\dagger|\Psi\rangle; \quad \tilde{\mathbf{a}}^\dagger|\Psi\rangle = e^{\pi\omega_0}\mathbf{a}|\Psi\rangle. \quad (5.34)$$

**Null surfaces with spherical or translational symmetry:** The analysis above can be simplified slightly if the null surface under consideration has spherical or

translational symmetry. Since the case of spherical symmetry is the case that will be important for us later, we indicate the generalization explicitly.

Consider a spherically symmetric null surface so that the metric is given by

$$ds^2 = -d\mathcal{U}d\mathcal{V} + r_0^2 d\Omega_{d-1}^2 + g_{\mu\nu}^{(1)} d\xi^\mu d\xi^\nu. \quad (5.35)$$

We now impose that  $g_{\mu\nu}^{(1)} \rightarrow 0$  provided that  $\mathcal{U}, \mathcal{V} \rightarrow 0$ , and, as above, Greek indices,  $\mu, \nu$  run over all coordinates.

We can now define modes by integrating all over the  $(d-1)$ -sphere and extracting a particular spherical harmonic.

$$\begin{aligned} \mathbf{a} &= \frac{r_0^{\frac{d-1}{2}}}{\sqrt{\pi\omega_0}} \int \partial_{\mathcal{U}}\phi(\mathcal{U}, \mathcal{V} = 0, \Omega) \left(\frac{-\mathcal{U}}{\mathcal{U}_0}\right)^{-i\omega_0} \mathcal{T}(-\mathcal{U}) d\mathcal{U} Y_\ell^*(\Omega) d^{d-1}\Omega, \\ \tilde{\mathbf{a}} &= \frac{r_0^{\frac{d-1}{2}}}{\sqrt{\pi\omega_0}} \int \partial_{\mathcal{U}}\phi(\mathcal{U}, \mathcal{V} = -\epsilon, \Omega) \left(\frac{\mathcal{U}}{\mathcal{U}_0}\right)^{i\omega_0} \mathcal{T}(\mathcal{U}) d\mathcal{U} Y_\ell(\Omega) d^{d-1}\Omega, \end{aligned} \quad (5.36)$$

Now, rather than being defined in the neighbourhood of a point, the modes carry an angular momentum, denoted by  $\ell$ . These modes depend both on  $\ell$  and on  $\omega_0$  but we have suppressed that dependence to lighten the notation.

A precise repetition of the analysis above, leads to the same result for the action of these modes on the state

$$\tilde{\mathbf{a}}|\Psi\rangle = e^{-\pi\omega_0} \mathbf{a}^\dagger|\Psi\rangle; \quad \tilde{\mathbf{a}}^\dagger|\Psi\rangle = e^{\pi\omega_0} \mathbf{a}|\Psi\rangle. \quad (5.37)$$

Note that the orthogonality of the spherical harmonics implies that the modes are entangled only if the same value of  $\ell$  is used in both lines of (5.36).

**A note of caution:** The relation (5.37) holds for the special modes that we have defined, which use information from the field just next to the null surface. In particular, even in the simple background of a Schwarzschild black hole, these modes must be distinguished from the global Schwarzschild modes that are defined by integrating the field all over the exterior or all over the interior.

The difference between these modes is manifest in their response to perturbations. If we consider perturbations of the horizon generated by just throwing in some matter

on top of an equilibrium black hole then this will change the form of the two-point function between Schwarzschild modes in the interior and the exterior. However, this perturbation does not affect the nature of the entanglement very close to the horizon. In particular, the entanglement between the modes  $\mathbf{a}$  and  $\tilde{\mathbf{a}}$ , which are defined by integrals very close to the null surface  $\mathcal{U} = 0$ , is unaffected by a smooth deformation.

One way is that if we think of Schwarzschild modes with frequencies  $\omega$  and  $\omega'$ , then the near-horizon modes defined above pick up the coefficient of the  $\delta(\omega - \omega')$  term in their two-point function. The analysis above tells us that this coefficient must be universal and cannot be changed by a smooth deformation. We will elucidate this point further in our analysis of the Reissner-Nordström black hole below, where we discuss global modes and explicitly relate them to the near-horizon modes defined above.

### 5.3 The Reissner-Nordström black hole in AdS

We now apply the considerations above to the Reissner-Nordström (RN) geometry in anti-de Sitter space. The techniques that we have developed here can be just as easily applied to charged black holes in flat-space or in de Sitter space. The reason for considering AdS is not only that this allows us to make a link with the AdS/CFT conjecture but also because there is a canonical choice of a quantum state with asymptotically anti-de Sitter boundary conditions—the Hartle-Hawking state. In flat space, it was shown through an elaborate computation of the renormalized stress-tensor that the Hartle-Hawking state led to a singular stress-tensor on the horizon of this black hole [117, 118]. Here, we will show how a similar conclusion can be reached for charged black holes in flat space much more easily using our test.

This section is divided into four parts. First, we review the features of the classical RN geometry, which also serves to introduce necessary notation. Next, we describe the global expansion of fields propagating on this background. Then we relate these global modes to the near-horizon modes described in the previous section. The criterion that the near-horizon modes should be correctly entangled leads to specific constraints on the two-point functions of the global modes. Although we were not able to check these constraints analytically, it is easy to check them numerically

in any dimension. In the last subsection, we present evidence that the Hartle-Hawking/Kruskal state is singular at the inner horizon both for asymptotically AdS RN black holes and for asymptotically flat RN black holes in various dimensions.

### 5.3.1 The classical geometry

The classical geometry of the RN black hole in AdS, in general spacetime dimension  $d + 1$ , is described by the metric

$$ds^2 = -f(r)dt^2 + f(r)^{-1}dr^2 + r^2d\Omega_{d-1}^2, \quad (5.38)$$

where

$$f(r) = r^2 + 1 - \frac{A}{r^{d-2}} + \frac{B}{r^{2(d-2)}}. \quad (5.39)$$

Here we have set the radius of AdS to 1 and the constants  $A$  and  $B$  are related to the mass,  $M$  and charge  $Q$  by

$$A = \frac{16\pi M}{(d-1)V_{d-1}}; \quad B = \frac{(8\pi Q)^2}{2(d-1)(d-2)V_{d-1}}, \quad (5.40)$$

where  $V_{d-1}$  is the volume of the unit  $(d-1)$ -sphere [121]. We will consider non-extremal black holes where  $f(r)$  has first order zeros at  $r_-$  and  $r_+$ , which are the positions of the inner and outer horizons respectively.

As usual, it is convenient to introduce the tortoise coordinate

$$dr_* = \frac{dr}{f(r)}. \quad (5.41)$$

Near the outer horizon we have  $r_* \rightarrow -\infty$  and we choose the origin of  $r_*$  so that as one approaches the horizon, we have

$$(r - r_+) \rightarrow \frac{1}{2\kappa_+} e^{2\kappa_+ r_*}, \quad (5.42)$$

where the surface gravity at the horizons is, as usual, given by  $\kappa_+ = f'(r_+)/2$ . This fixes  $r_*$  to a constant asymptotic value near the boundary of AdS. Moreover, near the future outer horizon, we also have  $t \rightarrow \infty$  and, as usual, spacetime can be

continued past this horizon by introducing coordinates

$$U = -\frac{1}{\kappa_+} e^{\kappa_+(r_*-t)}; \quad V = \frac{1}{\kappa_+} e^{\kappa_+(r_*+t)}. \quad (5.43)$$

In these coordinates, the right future outer horizon is at  $U = 0, V > 0$ . After crossing this horizon, in the forward wedge, we define the  $t, r_*$  coordinates by

$$U = \frac{1}{\kappa_+} e^{\kappa_+(r_*-t)}; \quad V = \frac{1}{\kappa_+} e^{\kappa_+(r_*+t)}. \quad (5.44)$$

Within the forward wedge, we can move to the left outer horizon where, again,  $r_* \rightarrow -\infty$  but  $t \rightarrow -\infty$ . This horizon has  $V = 0$ . It is possible to cross this left horizon to reach a left asymptotic region.

However, in the forward wedge, it is also possible to reach the region  $r_* \rightarrow \infty$ , which marks the inner horizon. Within the forward wedge, the right inner horizon has  $t \rightarrow +\infty$ , and the left inner horizon has  $t \rightarrow -\infty$ . Near the inner horizon, the relationship between the tortoise and the ordinary radial coordinate becomes

$$r - r_- \rightarrow \frac{\zeta^2}{\kappa_-} e^{-2\kappa_- r_*}. \quad (5.45)$$

Here, the surface gravity of the inner horizon is  $\kappa_- = -f'(r_-)/2$ . Note that one unavoidably obtains an additional constant,  $\zeta$ , in the relationship between  $r - r_-$  and  $r_*$  having fixed a similar constant to 1 near the outer horizon. Naively, it appears that a simple change of coordinates will allow the continuation of the geometry beyond the inner horizon as well, and this naive extension leads to an extended spacetime diagram. In particular, define

$$U' = -\frac{\zeta}{\kappa_-} e^{-\kappa_-(r_*+t)} \quad V' = -\frac{\zeta}{\kappa_-} e^{\kappa_-(r_*+t)}. \quad (5.46)$$

This places the right inner horizon at  $U' = 0$  and the left inner horizon at  $V' = 0$ . When we cross the right inner horizon, we may use the coordinates

$$U' = \frac{\zeta}{\kappa_-} e^{-\kappa_-(r_*+t)} \quad V' = -\frac{\zeta}{\kappa_-} e^{\kappa_-(r_*+t)}. \quad (5.47)$$

A similar change of coordinates allows an extension across the left inner horizon.

The naive extended Penrose diagram is shown in Figure 5.2.

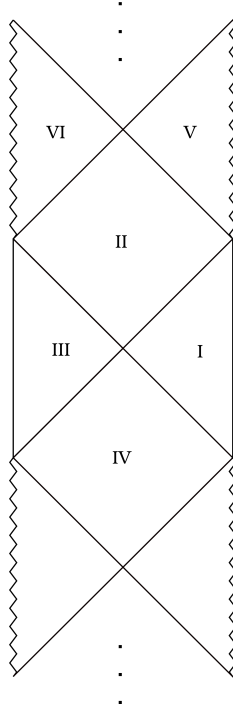


Figure 5.2: *Maximal extension of the Reissner Nordström spacetime. The dots indicate repetitions of the displayed pattern.*

### 5.3.2 Quantum fields on the RN background

We now consider a scalar quantum field propagating on the background above. We will assume that the scalar field is governed by an effective action

$$S_{\text{eff}} = \frac{1}{2} \int \sqrt{-g} [g^{\mu\nu} \partial_\mu \phi \partial_\nu \phi - m^2 \phi^2]. \quad (5.48)$$

Since the field equations are linear, we expect to be able to expand the field as

$$\phi = \sum_\ell \int \frac{d\omega}{\sqrt{2\pi}} F_{\omega,\ell}(r_*) e^{-i\omega t} Y_\ell(\Omega) + \text{h.c.}, \quad (5.49)$$

where  $F_{\omega,\ell}$  are operators. We now describe the operators  $F_{\omega,\ell}$  in more detail in various limits. This also serves to define our notation.

**Field expansion near the boundary of AdS:** Near the boundary of AdS, we demand that the field be normalizable. This corresponds to a situation where no sources have been turned on for the field. Near the boundary we have

$$\lim_{r \rightarrow \infty} [r^\Delta F_{\omega, \ell}(r)] = \mathcal{O}_{\omega, \ell}, \quad (5.50)$$

where  $\mathcal{O}_{\omega, \ell}$  are the modes of the boundary operator of dimension  $\Delta$  that is dual to the bulk field  $\phi$ .

**Field expansion just outside the outer horizon:** The normalizable boundary conditions link the left and right moving modes outside the horizon. As we approach the outer horizon, the tortoise coordinate  $r_* \rightarrow -\infty$ . A simple consideration of the wave-equation resulting from the action (5.48) shows that as we approach the horizon from outside, so that  $r \rightarrow r_+$  but  $r > r_+$ , the field has the expansion

$$F_{\omega, \ell} \xrightarrow{r \rightarrow r_+} \frac{1}{\sqrt{2\omega r_+^{\frac{d-1}{2}}}} a_{\omega, \ell} (e^{i\omega r_*} + e^{-i\delta_{\omega, \ell}} e^{-i\omega r_*}). \quad (5.51)$$

With the normalization above, the operators  $a_{\omega, \ell}$  are canonically normalized

$$[a_{\omega, \ell}, a_{\omega', \ell'}] = \delta(\omega - \omega') \delta_{\ell, \ell'}. \quad (5.52)$$

**Field expansion just inside the outer horizon:** Just inside the outer horizon, the left-moving modes must be the same as the left-movers outside the horizon by continuity of the field. However, it is possible to have new right-moving modes. Therefore, as  $r \rightarrow r_+$  but  $r < r_+$ , the field has the expansion

$$F_{\omega, \ell} \xrightarrow{r \rightarrow r_+} \frac{1}{\sqrt{2\omega r_+^{\frac{d-1}{2}}}} \left( \tilde{a}_{\omega, \ell}^\dagger e^{i\omega r_*} + a_{\omega, \ell} e^{-i\delta_{\omega, \ell}} e^{-i\omega r_*} \right). \quad (5.53)$$

**Field expansion just outside the inner horizon:** As we approach the inner horizon, we find that  $r_* \rightarrow \infty$ . As we approach it from outside, i.e.  $r \rightarrow r_-$  but  $r > r_-$ , we find that the radial mode functions simplify again and we may write

$$F_{\omega, \ell} \xrightarrow{r \rightarrow r_-} \frac{1}{\sqrt{2\omega r_-^{\frac{d-1}{2}}}} \left( \tilde{b}_{\omega, \ell}^\dagger e^{i\omega r_*} + b_{\omega, \ell} e^{-i\omega r_*} \right). \quad (5.54)$$

The modes  $b$  and  $\tilde{b}$  are not independent and must be related to the modes  $a, \tilde{a}$  just inside the outer horizon. The relationship can be obtained by evolving the expansion given in (5.53) forward in time until one reaches the inner horizon. We will consider this relationship in more detail in subsection 5.3.5.

**Field expansion just inside the inner horizon:** For the sake of completeness, we also describe the field expansion just inside the inner horizon. This is an academic exercise since we have not yet found any state where the conditions for smoothness are met even outside the inner horizon. However, if such a state were to be constructed, then the expansion behind the inner horizon would be relevant.

Just inside the inner horizon, with  $r \rightarrow r_-$  and also  $r < r_-$ , we may write

$$F_{\omega,\ell} \xrightarrow{r \rightarrow r_-} \frac{1}{\sqrt{2\omega r_-^{\frac{d-1}{2}}}} \left( \tilde{b}_{\omega,\ell}^\dagger e^{i\omega r_*} + c_{\omega,\ell}^\dagger e^{-i\omega r_*} \right). \quad (5.55)$$

Here we have imposed the fact that the “right movers”,  $\tilde{b}$  cross over smoothly whereas the  $c$  are some new modes which may or may not be related to the earlier modes. Notice that both  $\tilde{b}$  and  $c$  have the wrong energy with respect to the Schwarzschild Hamiltonian. This is because, in our coordinates as we move up on the diagram 5.2, the value of  $t$  decreases.

Note that this expansion relies only on the continuity of the metric, and does *not* make any assumptions about what happens deep inside the inner horizon.

### 5.3.3 Relationship between near-horizon modes and global modes

We can define near-horizon modes near all the horizons in this geometry. We will define modes on both sides of the right outer horizon, and on both sides of the right inner horizon. It is, of course, possible to define modes near the left-horizons but in our description (which treats the horizons symmetrically) this is redundant and so we will avoid it for now.

So we define

$$\begin{aligned}
 \mathbf{a} &= \frac{1}{\sqrt{\pi\omega_0}} \int \partial_U \phi(U, V=0, \Omega) \left(-\frac{U}{U_0}\right)^{-i\omega_0} \mathcal{T}(-U) Y_\ell^*(\Omega) dU d^{d-1}\Omega, \\
 \tilde{\mathbf{a}} &= \frac{1}{\sqrt{\pi\omega_0}} \int \partial_U \phi(U, V=-\epsilon, \Omega) \left(\frac{U}{U_0}\right)^{i\omega_0} \mathcal{T}(U) Y_\ell(\Omega) dU d^{d-1}\Omega, \\
 \mathbf{b} &= \frac{1}{\sqrt{\pi\omega_1}} \int \partial_{U'} \phi(U', V'=0, \Omega) \left(-\frac{U'}{U'_0}\right)^{-i\omega_1} \mathcal{T}(-U') Y_\ell^* dU' d^{d-1}\Omega, \\
 \mathbf{c} &= \frac{1}{\sqrt{\pi\omega_1}} \int \partial_{U'} \phi(U', V'=-\epsilon, \Omega) \left(\frac{U'}{U'_0}\right)^{i\omega_1} \mathcal{T}(U') Y_\ell(\Omega) dU' d^{d-1}\Omega.
 \end{aligned} \tag{5.56}$$

Here  $\omega_1 = \frac{\kappa_+ \omega_0}{\kappa_-}$ . All these modes depend on a choice of  $\omega_0$  and  $\ell_0$  and while we suppress these quantities in the notation we will make some choices for them later.

The integrals in (5.56) can be performed as follows. For the first line of (5.56) we find that

$$\mathbf{a} = \frac{1}{\pi\sqrt{2\omega_0}} \int \partial_U [F_{\omega,\ell}(r_*)e^{-i\omega t} + F_{\omega,\ell}^*(r_*)e^{i\omega t}] \left(-\frac{U}{U_0}\right)^{-i\omega_0} \mathcal{T}(-U) dU d\omega. \tag{5.57}$$

Now, since the tuning function has support for only very small values of  $U$ , we may expand the mode function using the approximation (5.51). We then find that up to the  $O(\epsilon)$  dependence on the cutoffs, described in section 5.2,

$$\begin{aligned}
 \mathbf{a} &= \frac{1}{2\pi\sqrt{\omega_0}} \int a_{\omega,\ell}(\kappa_+)^{\frac{i\omega}{\kappa_+}} \left(\partial_U(-U)^{\frac{i\omega}{\kappa_+}}\right) \left(\frac{-U}{U_0}\right)^{-i\omega_0} \mathcal{T}(-U) dU \frac{d\omega}{\sqrt{\omega}} \\
 &= \frac{1}{2\pi\sqrt{\omega_0}} \int \frac{i}{\kappa_+} \sqrt{\omega} (\kappa_+ U_0)^{\frac{i\omega}{\kappa_+}} a_{\omega,\ell} \left(\frac{-U}{U_0}\right)^{i\left(\frac{\omega}{\kappa_+} - \omega_0\right)} \mathcal{T}(-U) \frac{dU}{U} d\omega \\
 &= i \int \mathfrak{s}\left(\omega_0 - \frac{\omega}{\kappa_+}\right) (\kappa_+ U_0)^{\frac{i\omega}{\kappa_+}} \sqrt{\frac{\omega}{\omega_0}} a_{\omega,\ell} \frac{d\omega}{\kappa_+}.
 \end{aligned} \tag{5.58}$$

Note that the normalization of the modes is correct since, using the expression above, and also the identity  $[a_{\omega,\ell}, a_{\omega',\ell}] = \delta(\omega - \omega')$ , we can check that

$$\begin{aligned}
 [\mathbf{a}, \mathbf{a}^\dagger] &= \int \left|\mathfrak{s}\left(\omega_0 - \frac{\omega}{\kappa_+}\right)\right|^2 \frac{\omega}{\omega_0} \frac{d\omega}{\kappa_+^2} \\
 &= \int \left|\mathfrak{s}(\omega_0 - \omega')\right|^2 \frac{\omega'}{\omega_0} d\omega' = 1.
 \end{aligned} \tag{5.59}$$

where we used that  $\mathfrak{s}(\omega)$  is very sharply peaked around  $\omega = 0$ .

Similarly, we can express the near-horizon modes in terms of the global modes near the other horizons as well. We find that that in the limit under consideration precisely the same function  $\mathfrak{s}$  appears in these other expressions.

$$\begin{aligned}
 \tilde{\mathbf{a}} &= -i \int (\kappa_+ U_0)^{\frac{-i\omega}{\kappa_+}} \mathfrak{s}^* \left( \omega_0 - \frac{\omega}{\kappa_+} \right) \sqrt{\frac{\omega}{\omega_0}} \tilde{a}_{\omega,\ell} \frac{d\omega}{\kappa_+}, \\
 \mathbf{b} &= i \int \left( \frac{\kappa_-}{\zeta} U_0 \right)^{\frac{-i\omega}{\kappa_-}} \mathfrak{s} \left( \omega_1 - \frac{\omega}{\kappa_-} \right) \sqrt{\frac{\omega}{\omega_1}} b_{\omega,\ell} \frac{d\omega}{\kappa_-}, \\
 \mathbf{c} &= -i \int \left( \frac{\kappa_-}{\zeta} U_0 \right)^{\frac{i\omega}{\kappa_-}} \mathfrak{s}^* \left( \omega_1 - \frac{\omega}{\kappa_-} \right) \sqrt{\frac{\omega}{\omega_1}} c_{\omega,\ell} \frac{d\omega}{\kappa_-}.
 \end{aligned} \tag{5.60}$$

As advertised, in each case the near-horizon modes can be written as global modes smeared with a function that is sharply peaked in frequency space.

### 5.3.4 Constraints on two-point functions

From the results of section 5.2, we now find the following constraints on the near-horizon modes defined above. As explained there, smoothness of the outer horizon implies that

$$\begin{aligned}
 \langle \Psi | \tilde{\mathbf{a}} \tilde{\mathbf{a}}^\dagger | \Psi \rangle &= \langle \Psi | \mathbf{a} \mathbf{a}^\dagger | \Psi \rangle = \frac{1}{1 - e^{-2\pi\omega_0}}; \\
 \langle \Psi | \tilde{\mathbf{a}} \mathbf{a} | \Psi \rangle &= \langle \Psi | \tilde{\mathbf{a}}^\dagger \mathbf{a}^\dagger | \Psi \rangle = \frac{e^{-\pi\omega_0}}{1 - e^{-2\pi\omega_0}}.
 \end{aligned} \tag{5.61}$$

On the other hand, upon applying these constraints near the inner horizon we find that

$$\begin{aligned}
 \langle \Psi | \mathbf{b} \mathbf{b}^\dagger | \Psi \rangle &= \langle \Psi | \mathbf{c} \mathbf{c}^\dagger | \Psi \rangle = \frac{1}{1 - e^{-2\pi\omega_1}}; \\
 \langle \Psi | \mathbf{b} \mathbf{c} | \Psi \rangle &= \langle \Psi | \mathbf{b}^\dagger \mathbf{c}^\dagger | \Psi \rangle = \frac{e^{-\pi\omega_1}}{1 - e^{-2\pi\omega_1}},
 \end{aligned} \tag{5.62}$$

where  $\omega_1 = \frac{\kappa_+}{\kappa_-} \omega_0$  as above.

Now, as discussed earlier, the modes  $\mathbf{b}, \mathbf{b}^\dagger$  can in principle be expressed as linear combinations of  $\mathbf{a}, \tilde{\mathbf{a}}, \mathbf{a}^\dagger, \tilde{\mathbf{a}}^\dagger$  by solving the wave equation in the region between the two horizons. Hence it is not obvious whether equations (5.61) and (5.62) can hold

simultaneously. In fact as we will show numerically in the next subsections, these equations are incompatible in the case of the Hartle-Hawking state for the AdS-RN black hole. This statement implies that this state is singular on the inner horizon of the AdS-RN black hole.

Before we continue with this analysis, let us see what the constraints (5.61), (5.62) imply for the two-point function of the global modes  $a, b, \tilde{a}$ . Let us assume that the two-point function of the global modes is given by

$$\begin{aligned}
 \langle \Psi | a_{\omega, \ell} a_{\omega', \ell}^\dagger | \Psi \rangle &= \mathcal{A}_1(\omega) \delta(\omega - \omega') + \mathcal{A}_2(\omega, \omega'); \\
 \langle \Psi | \tilde{a}_{\omega, \ell} \tilde{a}_{\omega', \ell}^\dagger | \Psi \rangle &= \tilde{\mathcal{A}}_1(\omega) \delta(\omega - \omega') + \tilde{\mathcal{A}}_2(\omega, \omega'); \\
 \langle \Psi | a_{\omega, \ell} \tilde{a}_{\omega', \ell} | \Psi \rangle &= \mathcal{C}_1(\omega) \delta(\omega - \omega') + \mathcal{C}_2(\omega, \omega'); \\
 \langle \Psi | b_{\omega, \ell} b_{\omega', \ell}^\dagger | \Psi \rangle &= \mathcal{B}_1(\omega) \delta(\omega - \omega') + \mathcal{B}_2(\omega, \omega'),
 \end{aligned} \tag{5.63}$$

where, in each case, we have separated the correlator into one part that is proportional to a delta function and another part that is assumed to be smooth at  $\omega = \omega'$ . (We have also used the spherical symmetry to set the same value for  $\ell$  in all the operators above.) Then, substituting the formulas above, we find that the coefficients of the delta function are completely fixed by demanding smoothness at the outer and the inner horizon. In particular, we find that

$$\begin{aligned}
 \mathcal{A}_1(\omega) &= \tilde{\mathcal{A}}_1(\omega) = \frac{1}{1 - e^{-\frac{2\pi}{\kappa_+}\omega}}; \\
 \mathcal{C}_1(\omega) &= \frac{e^{-\frac{\pi}{\kappa_+}\omega}}{1 - e^{-\frac{2\pi}{\kappa_+}\omega}}; \\
 \mathcal{B}_1(\omega) &= \frac{1}{1 - e^{-\frac{2\pi}{\kappa_-}\omega}},
 \end{aligned} \tag{5.64}$$

where we have used the relationship between  $\omega_1 = \kappa_+ \omega_0 / \kappa_-$ . Note that the factors that appear in the exponentials above are just the standard inverse-temperatures of the inner and outer horizons given by  $\beta_\pm = \frac{2\pi}{\kappa_\pm}$ .

Therefore we see that the two-point function of the near-horizon modes picks only the delta-function piece in the two-point function of the global modes and completely fixes that piece. This explains why a smooth deformation of the geometry cannot change the two-point function of the near-horizon modes: a smooth deformation of

the geometry may change the smooth part of the two-point function of the global modes, but it cannot alter the coefficient of the delta function in this two-point function. This is the only term that the near-horizon modes are sensitive to and it must take a given value near a smooth horizon.

Now, as we explained above, in any given state of the system, the  $b$  modes are obtained by evolving the  $a$  and  $\tilde{a}$  modes in the region between the inner and outer horizon of the black hole. Therefore, given the correlators of those modes, it is possible to check whether the constraints (5.64) are satisfied. We will show that for the RN geometry, in various dimensions, these constraints cannot all be satisfied simultaneously.

### 5.3.5 Numerical results for the Reissner-Nordström black hole

We now check whether our constraints are satisfied in the AdS Reissner-Nordström geometry.

In this situation, where the propagation is linear, and using the time-translation isometry of the geometry we can write

$$\mathbf{b} = \kappa_1 \mathbf{a} + \tilde{\kappa}_2 \tilde{\mathbf{a}}^\dagger. \quad (5.65)$$

It is the time-translation invariance that allows us to relate modes with the same value of  $\omega$ , and we note that this equation may be modified if interactions are strong, or if the geometry is strongly time-dependent. Therefore,

$$\begin{aligned} \langle \mathbf{b} \mathbf{b}^\dagger \rangle &= \langle \mathbf{a} \mathbf{a}^\dagger \rangle |\kappa_1|^2 + |\tilde{\kappa}_2|^2 \langle \tilde{\mathbf{a}}^\dagger \tilde{\mathbf{a}} \rangle + 2 \operatorname{Re} (\kappa_1 \tilde{\kappa}_2^* \langle \mathbf{a} \tilde{\mathbf{a}} \rangle) \\ &= \frac{1}{1 - e^{-2\pi\omega_0}} (|\kappa_1|^2 + e^{-2\pi\omega_0} |\tilde{\kappa}_2|^2 + 2e^{-\pi\omega_0} \operatorname{Re} (\kappa_1 \tilde{\kappa}_2^*)). \end{aligned} \quad (5.66)$$

So the question of checking whether the near-horizon constraints (5.61),(5.62) are satisfied as we approach the near-horizon reduces to evaluating the Bogoliubov coefficients,  $\kappa_1, \tilde{\kappa}_2$  and determining if the combination above is in agreement with (5.62). By computing the two-point function of the modes near the inner horizon we define

$$\delta = \langle \mathbf{b}^\dagger \mathbf{b} \rangle (1 - e^{-2\pi\omega_1}) - 1. \quad (5.67)$$

which is the fractional difference from the expected Boltzmann factor. If the con-

straints are satisfied we will have  $\delta = 0$ .

**Description of the numerical algorithm:** These Bogoliubov coefficients can be computed by solving the radial (ordinary) differential equation that fixes the evolution of the field. We briefly describe our algorithm. A solution of the wave-equation with frequency  $\omega$  and angular momentum,  $\ell$  can be written in the form  $\phi_{\omega,\ell}(r_*)e^{-i\omega t}Y_\ell(\Omega)$ . The radial part of the solution  $\phi_{\omega,\ell}$  obeys the equation

$$\frac{d}{dr_*} \left( r^{d-1} \frac{d\phi_{\omega,\ell}}{dr_*} \right) + \omega^2 \phi_{\omega,\ell} - \ell(\ell + d - 2) f(r) \frac{\phi_{\omega,\ell}}{r^2} - m^2 \phi_{\omega,\ell} f(r) = 0, \quad (5.68)$$

where  $r$  is determined by solving the auxiliary equation  $r'(r_*) = f(r)$ . This auxiliary equation must be solved first; demanding the behaviour (5.42) near the outer horizon allows us to fix the value of  $r_*$  near the boundary of AdS as  $r \rightarrow \infty$ . Solving the auxiliary equation between the inner and outer horizon allows us to determine  $\zeta$ , which appears in (5.45).

The equation (5.68) is now solved, as a set of two first-order differential equations, starting from the boundary with initial conditions set by  $\phi_{\omega,\ell}(r) \rightarrow \frac{1}{r^\Delta}$  at large  $r$ . As  $r \rightarrow r_+$ , we can then read off the phase  $\delta_{\omega,\ell}$  by matching the behaviour of  $\phi_{\omega,\ell}$  and  $\phi'_{\omega,\ell} = \frac{d\phi_{\omega,\ell}}{dr_*}$  to (5.51).

Now, starting at a point in the middle of the inner and outer horizons, we solve the equation towards  $r_* \rightarrow -\infty$  (the outer horizon) and also  $r_* \rightarrow \infty$  (the inner horizon) with two separate initial conditions: once with  $\phi_{\omega,\ell} = 0, \phi'_{\omega,\ell} = 1$  and a second time with  $\phi_{\omega,\ell} = 1, \phi'_{\omega,\ell} = 0$ . Near both the inner and the outer horizons, the asymptotic behaviour of the mode is given by (5.53) and (5.54). By determining the coefficients of the terms that oscillate as  $e^{\pm i\omega r_*}$  for both sets of initial conditions, we can solve for the Bogoliubov coefficients  $\kappa_1$  and  $\tilde{\kappa}_2$ . This immediately leads to a result for  $\delta$ .

The procedure above is quite simple, and can be implemented using any standard numerical library. In our own case, to solve the differential equations, we used an eighth-order explicit Runge-Kutta solver with the Dormand and Prince coefficients [122] as implemented in C using code from CALCODE [123]. We also used the root-finding routines in the GNU scientific library [90] to locate the horizons and GNU parallel [124] to parallelize the calculations.

**Results:** In Figure 5.3 we present a plot for  $\delta$  vs the frequency for the angular momentum  $\ell = 0$  for various values of the radii of the inner and outer horizon and in dimensions  $d = 3, 4, 5, 6$ . The black holes range from those that are near-extremal to those where there is a significant separation of scales between the two horizons. The AdS radius is fixed to unity.

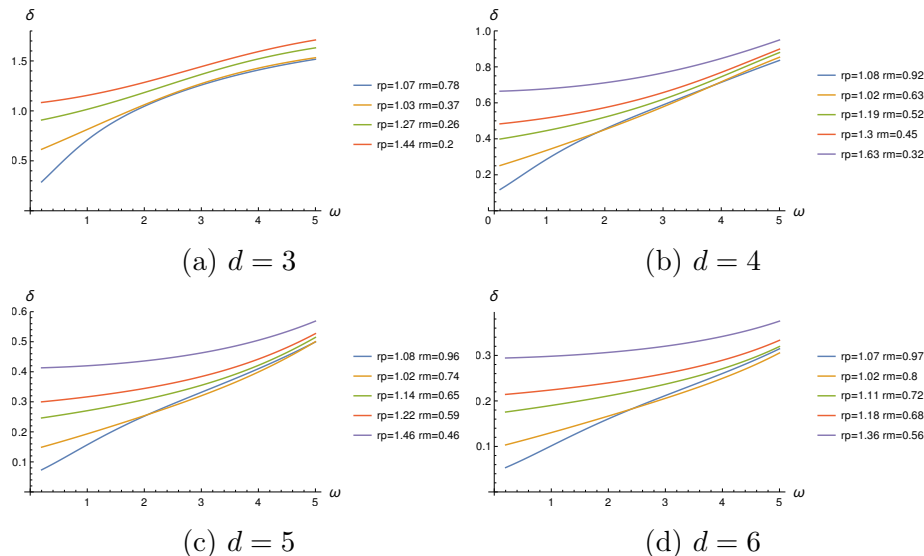


Figure 5.3: A plot of the fractional difference,  $\delta$ , vs the frequency for  $\ell = 0$  for various values of the inner and outer temperature. Non-zero values of  $\delta$  indicate that the constraints of section 5.2 are not satisfied.

These graphs are already sufficient to show that the Hartle-Hawking state is singular at the inner horizon of these geometries. This is because the criterion of section 5.2 must be satisfied for each value of frequency and angular momentum, as a necessary condition, for the state to be smooth. Instead the graphs above all display non-zero values of  $\delta$  for generic choices of frequency and angular momentum.

Our numerical results are quite robust. In fact, the largest source of numerical error arises from the relative phase between  $\kappa_1$  and  $\tilde{\kappa}_2$  in (5.66). This phase requires a careful determination of  $\zeta$  and a treatment of the wave-equation near the horizon. However, even this is not a significant source of error since, unlike the case of [125], we are considering a specific mode and so the wave-equation simplifies greatly near the horizon. Moreover, it is not difficult to check that if one keeps the angular momentum fixed and increases  $\omega$  then beyond a point, *no choice of relative phase*

between  $\kappa_1$  and  $\tilde{\kappa}_2$  will yield  $\delta = 0$ . This allows us to reach the physical conclusions above — that the inner horizon is not smooth in the Hartle-Hawking state — with confidence.

However, it is also interesting to understand how the fractional difference varies with angular momentum. In Figure 5.4, we present a plot for  $\delta$  vs the angular momentum for frequency fixed at the AdS scale for  $d = 4$ . The reader will note the remarkable fact that at large  $\ell$ , the fractional difference tends to zero. This can be explained via a semiclassical WKB analysis in this limit, as we demonstrate in Appendix C. This WKB analysis serves as an additional check on our numerical algorithm.

We note that in [118], it was pointed out that the renormalized expectation value of  $\phi^2$  is less singular than expected as one approaches the inner horizon. This is directly a consequence of the large  $\ell$  behaviour of Figure 5.4, since the fastest divergence of  $\phi^2$  as one approaches the inner horizon is controlled entirely by the large- $\ell$  modes.

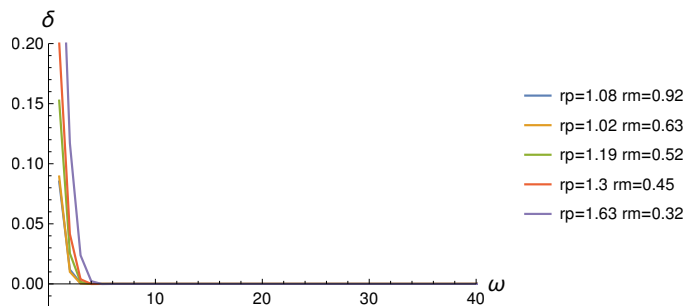


Figure 5.4: A plot of the fractional difference,  $\delta$ , vs the angular momentum with frequency fixed to the AdS scale for various sizes of the inner and outer horizons.

## 5.4 The BTZ black hole

We now turn to a discussion of the rotating BTZ black hole. It was argued in [119] that a rotating BTZ black hole that is close enough to extremality violates strong cosmic censorship, and so this presents an excellent test-case for our criterion.

We start by reviewing the geometry of the BTZ black hole, and the propagation of quantum fields in this geometry. We then show that it is indeed the case that

the near-horizon modes, as one approaches the inner horizon from the outside, have the correct occupation number. This corresponds to the fact that if we set the local temperature of the field correctly near the outer horizon, it is automatically red-shifted by the geometry so that the local temperature of the modes near the inner horizon coincides exactly with the temperature of the inner horizon! This is in contrast to what we found numerically in the previous section for the AdS-RN black hole in higher dimensions.

However, as explained in section 5.2, if we want to extend the spacetime behind the inner horizon, we also require the existence of modes behind the inner horizon. The reader may worry that the extension of quantum fields behind the inner horizon is not unique. Nevertheless, as we have emphasized *the near-horizon modes just behind the inner horizon are fixed by requirements of smoothness* and do not require knowledge of the dynamics deep behind the inner horizon.

When one crosses the outer horizon, interior modes can be understood using the standard construction of the mirror operators [68]. However, we show that this construction fails at the inner horizon due to the monogamy of entanglement. In particular, since the modes between the inner and the outer horizon are already entangled with the modes outside the outer horizon, they cannot also be entangled with new modes behind the inner horizon.

Nevertheless we show, remarkably, that it is possible to reuse the modes between the inner horizon and the outer horizon behind the inner horizon as modes for the field behind the inner horizon. This is dependent on the fact that the modes outside the inner horizon are correctly populated. The modes that we write down uniquely fix the behaviour of the field just behind the inner horizon although the usual ambiguities associated with a Cauchy horizon arise if we attempt to probe deeper into the geometry.

We will follow the notation of [119] in large part.

### 5.4.1 Classical geometry and propagation of fields

The BTZ solution can be written in the form

$$ds^2 = -f(r)dt^2 + \frac{dr^2}{f(r)} + r^2(d\phi - \Omega(r)dt)^2, \quad (5.69)$$

where

$$f(r) = \frac{(r^2 - r_+^2)(r^2 - r_-^2)}{r^2}; \quad \Omega(r) = \frac{r_+ r_-}{r^2}. \quad (5.70)$$

Here we have set the AdS radius to 1.

The positions of the inner and outer horizon are at  $r_+$  and  $r_-$ . The angular velocities  $\Omega_{\pm}$  and surface gravities  $\kappa_{\pm}$  of the two horizons are given by

$$\Omega_{\pm} = \frac{r_{\mp}}{r_{\pm}}; \quad \kappa_{\pm} = \frac{r_{\pm}^2 - r_{\mp}^2}{r_{\pm}}. \quad (5.71)$$

The tortoise coordinate is defined as in (5.41) and we once again adopt the convention that as one approaches the outer horizon,  $(r - r_+) = \frac{1}{\kappa_+} e^{2\kappa_+ r_*}$ . We can check that near the inner horizon this leads to a relationship of the form (5.45) with

$$\zeta = 2^{\frac{r_- + r_+}{2r_-}} (r_+ - r_-)^{\frac{r_+}{r_-} + 1}. \quad (5.72)$$

We note that our conventions for  $r_*$  differ from those of [119] by an overall additive constant.

We now consider a minimally coupled scalar field  $\phi$  propagating in this geometry. Just as above, we may expand the field in various regions. However, the expansion in terms of creation and annihilation operators is slightly more subtle than in the non-rotating case, as we explain below.

Near the boundary of AdS we may, as usual, expand the field as

$$\phi \xrightarrow{r \rightarrow \infty} \frac{1}{2\pi} \sum_m \int d\omega \frac{\mathcal{O}_{\omega, m}}{r^{\Delta}} e^{-i\omega t} e^{im\phi} + \text{h.c.}, \quad (5.73)$$

where  $\Delta(\Delta - 2) = m^2$  and  $\mathcal{O}_{\omega, m}$  are the Fourier modes of the primary operator of dimension  $\Delta$  that is dual to the field  $\phi$ .

Near the outer horizon, as we approach it from outside on the right, the expansion

of the field  $\phi$  is<sup>5</sup>

$$\phi \xrightarrow{r \rightarrow r_+} \sum_m \int \frac{d\omega_+}{2\pi\sqrt{r_+}\sqrt{2\omega_+}} a_{\omega_+,m} \left( e^{i\omega_+\kappa+r_*} + e^{-i\delta_{\omega_+,m}} e^{-i\omega_+\kappa+r_*} \right) e^{-i\kappa_+\omega_+t} e^{im(\phi-\Omega_+t)} + \text{h.c.}, \quad (5.74)$$

where

$$\omega_+ = \frac{\omega - m\Omega_+}{\kappa_+}; \quad \omega_- = \frac{\omega - m\Omega_-}{\kappa_-}. \quad (5.75)$$

A subtlety here is that in the expression above, the question of whether the coefficient of the mode function is a creation or annihilation operator is determined by the positivity of  $\omega_+$  and *not* of  $\omega$ . With this convention the operators above are canonically normalized

$$[a_{\omega_+,m}, a_{\omega'_+,m'}^\dagger] = \delta(\omega_+ - \omega'_+) \delta_{mm'}. \quad (5.76)$$

The expansions (5.73) and (5.74) fix the relationship between the operators  $a_{\omega_+,m}$  and  $\mathcal{O}_{\omega,m}$  and also the phase  $\delta$ . These can be determined by solving the wave-equation between the boundary and the outer horizon, which can be done analytically [126]. We will use the solutions as written in the conventions of [119].

$$\begin{aligned} a_{\omega_+,m} &= \frac{1}{C} \mathcal{O}_{\omega,m} \\ C &= \left( \frac{\kappa_+}{\sqrt{2}} \right)^{i\omega_+} (r_+^2 - r_-^2)^{\frac{\Delta}{2}} \frac{1}{\sqrt{r_+}\sqrt{2\omega_+}} \frac{\Gamma\left(\frac{1}{2}(\Delta - i\omega_+ - i\omega_-)\right) \Gamma\left(\frac{1}{2}(\Delta - i\omega_+ + i\omega_-)\right)}{\Gamma(\Delta)\Gamma(-i\omega_+)} \\ e^{-i\delta} &= \left( \frac{\kappa_+}{\sqrt{2}} \right)^{2i\omega_+} \frac{\Gamma(i\omega_+)\Gamma\left(\frac{1}{2}(\Delta - i\omega_+ - i\omega_-)\right) \Gamma\left(\frac{1}{2}(\Delta - i\omega_+ + i\omega_-)\right)}{\Gamma(-i\omega_+)\Gamma\left(\frac{1}{2}(\Delta + i\omega_+ - i\omega_-)\right) \Gamma\left(\frac{1}{2}(\Delta + i\omega_+ + i\omega_-)\right)}. \end{aligned} \quad (5.77)$$

We now proceed with the expansion of the field just inside the outer horizon

$$\begin{aligned} \phi \xrightarrow{r \rightarrow r_+} \sum_m \int \frac{d\omega_+}{2\pi\sqrt{r_+}\sqrt{2\omega_+}} & \left( a_{\omega_+,m} e^{-i\kappa_+\omega_+t} e^{im(\phi-\Omega_+t)} + \right. \\ & \left. \tilde{a}_{\omega_+,m} e^{i\kappa_+\omega_+t} e^{-im(\phi-\Omega_+t)} \right) e^{-i\omega_+\kappa_+r_*} + \text{h.c.} \end{aligned} \quad (5.78)$$

---

<sup>5</sup>We find it more convenient notationally to define the modes  $a_{\omega_+,m}$  in a somewhat asymmetric conventions, so that there is no phase factor  $e^{i\delta_{\omega_+,m}}$  in front of  $e^{i\omega_+\kappa_+r_*}$ .

Once we are near the inner horizon, we may write

$$\phi \xrightarrow{r \rightarrow r_-} \sum_m \int \frac{d\omega_-}{2\pi\sqrt{r_-}\sqrt{2\omega_-}} \left( b_{\omega_-,m} e^{-i\kappa_- \omega_- t} e^{im(\phi - \Omega_- t)} + \tilde{b}_{\omega_-,m} e^{i\kappa_- \omega_- t} e^{-im(\phi - \Omega_- t)} \right) e^{-i\omega_- \kappa_- r_*} + \text{h.c.}, \quad (5.79)$$

where

$$\omega_- = \frac{\omega - m\Omega_-}{\kappa_-}. \quad (5.80)$$

Note that in the expansion near the inner horizon, the classification of operators into creation and annihilation operators is determined by the sign of  $\omega_-$ . Finally, if the field extends across the inner horizon, we may write

$$\phi \xrightarrow{r \rightarrow r_-} \sum_m \int \frac{d\omega_-}{2\pi\sqrt{r_-}\sqrt{2\omega_-}} \left( c_{\omega_-,m} e^{i\omega_- \kappa_- r_*} + \tilde{b}_{\omega_-,m} e^{-i\omega_- \kappa_- r_*} \right) e^{i\kappa_- \omega_- t} e^{-im(\phi - \Omega_- t)} + \text{h.c.} \quad (5.81)$$

### 5.4.2 Near-horizon modes and constraints from entanglement

We now describe the relationship between the near-horizon modes and the global modes described above, and explain the constraints that the analysis of section 5.2 places on the two-point functions of the global modes.

Here, it is more convenient to use Eddington-Finkelstein coordinates, rather than Kruskal coordinates. These coordinates can be defined in the vicinity of both the inner and the outer horizon. Near the outer horizon, we set  $v_+ = r_* + t$  so that the metric is given by

$$ds^2 = -f(r)dv_+^2 + 2dv_+dr + r^2(d\phi - \Omega(r)dt)^2. \quad (5.82)$$

Now define  $x_+ = r_+ - r$  and  $\theta_+ = \phi - \Omega_+ t$ . Then, as we approach the horizon which is at  $x_+ = 0$ , the metric becomes

$$ds^2 = -2dv_+dx_+ + r_+^2 d\theta_+^2 + \text{O}(x_+), \quad (5.83)$$

which is the form that was required in section 5.2.

We now define near-horizon modes using the general prescription outlined in 5.2.

In particular, define

$$\begin{aligned}\mathbf{a} &= \frac{1}{\sqrt{\pi\omega_0}} \int \partial_{x_+} \phi(x_+, v_+ = 0, \theta_+) \left(-\frac{x_+}{U_0}\right)^{-i\omega_0} \mathcal{T}(-x_+) dx_+ e^{-im\theta_+} d\theta_+ \sqrt{\frac{r_+}{2\pi}}, \\ \tilde{\mathbf{a}} &= \frac{1}{\sqrt{\pi\omega_0}} \int \partial_{x_+} \phi(x_+, v_+ = -\epsilon, \theta_+) \left(-\frac{x_+}{U_0}\right)^{i\omega_0} \mathcal{T}(x_+) dx_+ e^{im\theta_+} d\theta_+ \sqrt{\frac{r_+}{2\pi}}.\end{aligned}\tag{5.84}$$

Such modes can be defined for any value of  $v_+$  but, as the reader can see from the relationship with the global modes below, shifting the value of  $v_+$  only rescales the mode by a phase.

Similarly, we can define near-horizon modes near the inner horizon. There, with  $v_- = r_* - t$ , and  $x_- = r_- - r$ , and  $\theta_- = \phi - \Omega_- t$ , as we approach the inner horizon at  $r_- = 0$ , the metric becomes

$$ds^2 = -2dv_- dx_- + r_+^2 d\theta_-^2 + \mathcal{O}(x_-).\tag{5.85}$$

Therefore, the prescription of section 5.2 tells us that near-horizon modes can be defined near the inner horizon using

$$\begin{aligned}\mathbf{b} &= \frac{1}{\sqrt{\pi\omega_1}} \int \partial_{x_-} \phi(x_-, v_- = 0, \theta_-) \left(-\frac{x_-}{U_0}\right)^{-i\omega_1} \mathcal{T}(-x_-) dx_- e^{im\theta_-} d\theta_- \sqrt{\frac{r_-}{2\pi}}, \\ \mathbf{c} &= \frac{1}{\sqrt{\pi\omega_1}} \int \partial_{x_-} \phi(x_-, v_- = -\epsilon, \theta_-) \left(-\frac{x_-}{U_0}\right)^{i\omega_1} \mathcal{T}(x_-) dx_- e^{-im\theta_-} d\theta_- \sqrt{\frac{r_-}{2\pi}}.\end{aligned}\tag{5.86}$$

As in the section above,  $\omega_1 = \frac{\kappa_+ \omega_0}{\kappa_-}$ .

Using the expansion of the field near the various horizons, we can relate these modes to the global modes. In doing the relevant integrals, the reader should keep in mind that the expressions above, which are given in terms of  $r_*$  and  $t$  need to be transformed to  $x_{\pm}, v_{\pm}$ . So, for instance,

$$e^{i\kappa_+ \omega_+ (r_* - t)} = e^{2i\kappa_+ \omega_+ r_*} e^{-i\kappa_+ \omega_+ v_+} = (\kappa_+ x_+)^{i\omega_+} e^{-i\kappa_+ \omega_+ v_+}.\tag{5.87}$$

Making similar substitutions in the other near-horizon expansions and using the

definition (5.10), we find

$$\begin{aligned}
 \mathbf{a} &= i \int \mathfrak{s}(\omega_0 - \omega_+) a_{\omega_+,m} (\kappa_+ U_0)^{i\omega_+} \sqrt{\frac{\omega_+}{\omega_0}} d\omega_+; \\
 \tilde{\mathbf{a}} &= -i \int \mathfrak{s}^*(\omega_0 - \omega_+) \tilde{a}_{\omega_+,m} (\kappa_+ U_0)^{-i\omega_+} \sqrt{\frac{\omega_+}{\omega_0}} d\omega_+; \\
 \mathbf{b} &= i \int \mathfrak{s}(\omega_1 - \omega_-) b_{\omega_-,m} \left(\frac{\kappa_- U_0}{\zeta}\right)^{i\omega_-} \sqrt{\frac{\omega_-}{\omega_0}} d\omega_-; \\
 \mathbf{c} &= -i \int \mathfrak{s}^*(\omega_1 - \omega_-) c_{\omega_-,m} \left(\frac{\kappa_- U_0}{\zeta}\right)^{-i\omega_-} \sqrt{\frac{\omega_-}{\omega_0}} d\omega_-.
 \end{aligned} \tag{5.88}$$

The constraints of section 5.2 now lead to the following constraints on these modes. At the outer horizon we have

$$\begin{aligned}
 (\mathbf{a} - e^{-\pi\omega_0} \tilde{\mathbf{a}}^\dagger) |\Psi\rangle &= 0; & (\mathbf{a}^\dagger - e^{\pi\omega_0} \tilde{\mathbf{a}}) |\Psi\rangle &= 0; & [\mathbf{a}, \tilde{\mathbf{a}}] &= 0; \\
 \langle \Psi | \mathbf{a} \mathbf{a}^\dagger | \Psi \rangle &= \langle \Psi | \tilde{\mathbf{a}} \tilde{\mathbf{a}}^\dagger | \Psi \rangle = \frac{1}{1 - e^{-2\pi\omega_0}}.
 \end{aligned} \tag{5.89}$$

These constraints are automatically met in the Hartle-Hawking state. For the occupation of  $\mathbf{a}$  this follows since, in that state, the global modes are populated as<sup>6</sup>

$$\langle \Psi | a_{\omega_+,m} a_{\omega'_+,m'}^\dagger | \Psi \rangle = \frac{1}{1 - e^{-2\pi\omega_+}} \delta(\omega_+ - \omega'_+) \delta_{mm'}. \tag{5.90}$$

Moreover, the global  $\tilde{a}$  modes can be constructed using the mirror-operator construction [68], which yields modes whose two-point function is again

$$\langle \Psi | \tilde{a}_{\omega_+,m} \tilde{a}_{\omega'_+,m'}^\dagger | \Psi \rangle = \frac{1}{1 - e^{-2\pi\omega_+}} \delta(\omega_+ - \omega'_+) \delta_{mm'}, \tag{5.91}$$

and which are moreover entangled with the modes outside the horizon through

$$\begin{aligned}
 a_{\omega_+,m} |\Psi\rangle &= e^{-\pi\omega_+} \tilde{a}_{\omega_+,m}^\dagger |\Psi\rangle; & a_{\omega_+,m}^\dagger |\Psi\rangle &= e^{\pi\omega_+} \tilde{a}_{\omega_+,m} |\Psi\rangle; \\
 \tilde{a}_{\omega_+,m} |\Psi\rangle &= e^{-\pi\omega_+} a_{\omega_+,m}^\dagger |\Psi\rangle; & \tilde{a}_{\omega_+,m}^\dagger |\Psi\rangle &= e^{\pi\omega_+} a_{\omega_+,m} |\Psi\rangle.
 \end{aligned} \tag{5.92}$$

Using (5.88), we can then check that all the relations in (5.89) are satisfied.

Of more interest to us are the constraints that the analysis of section 5.2 places

---

<sup>6</sup>Notice that the occupation levels in (5.90) know about the temperature of the black hole via the factor  $\kappa_+$  which enters in the relation (5.75) between  $\omega_+$  and  $\omega$ .

on the modes near the inner horizon. Here the constraints of section 5.2 can be divided into two parts. The first part is that as we approach the inner horizon from the exterior, the modes should be correctly populated

$$\langle \Psi | \mathbf{b} \mathbf{b}^\dagger | \Psi \rangle = \frac{1}{1 - e^{-2\pi\omega_1}}. \quad (5.93)$$

The second condition is that the modes behind the inner horizon should be correctly entangled with the modes in front

$$(\mathbf{b} - e^{-\pi\omega_1} \mathbf{c}^\dagger) | \Psi \rangle = 0; \quad (\mathbf{b}^\dagger - e^{\pi\omega_1} \mathbf{c}) | \Psi \rangle = 0; \quad [\mathbf{b}, \mathbf{c}] = 0. \quad (5.94)$$

We check (5.93) in section 5.4.3 and analyze (5.94) in section 5.4.4.

### 5.4.3 Checking the constraints on approaching the inner horizon

The constraint (5.93) can be checked by using the propagation of fields between the inner and outer horizon and the propagation of fields from the boundary to the outer horizon. First we note that by virtue of the Killing isometry of the geometry we have

$$\mathbf{b} = \kappa_1 \mathbf{a} + \tilde{\kappa}_2 \tilde{\mathbf{a}}^\dagger, \quad (5.95)$$

Here the Bogoliubov coefficients,  $\kappa_1$  and  $\tilde{\kappa}_2$  can be obtained from the reflection and transmission coefficients given in [119], after accounting for our different normalizations and also accounting for the relationship between local and global modes described. They are given by

$$\begin{aligned} \kappa_1 &= e^{i\delta_1} \left( \frac{\kappa_+}{\sqrt{2}} \right)^{i\omega_+} \frac{\sqrt{\frac{\omega_-}{\omega_+}} \Gamma(i\omega_-) \Gamma(1 + i\omega_+)}{\Gamma\left(\frac{1}{2}(-\Delta + i\omega_- + i\omega_+) + 1\right) \Gamma\left(\frac{1}{2}(\Delta + i\omega_- + i\omega_+)\right)} e^{i\delta} \\ \tilde{\kappa}_2 &= e^{i\delta_1} \left( \frac{\kappa_+}{\sqrt{2}} \right)^{-i\omega_+} \frac{\sqrt{\frac{\omega_-}{\omega_+}} \Gamma(i\omega_-) \Gamma(1 - i\omega_+)}{\Gamma\left(\frac{1}{2}(-\Delta + i\omega_- - i\omega_+) + 1\right) \Gamma\left(\frac{1}{2}(\Delta + i\omega_- - i\omega_+)\right)}, \end{aligned} \quad (5.96)$$

where the important phase  $e^{i\delta}$  is specified in (5.77) and the irrelevant common phase-factor is given by

$$e^{i\delta_1} = \left( \frac{\sqrt{2}\zeta}{\kappa_-} \right)^{i\omega_-} \frac{(U_0\kappa_+)^{\frac{i\omega_+}{\kappa_+}}}{(U_0\kappa_-)^{\frac{i\omega_-}{\kappa_-}}}. \quad (5.97)$$

Note that, as we will check below, these Bogoliubov coefficients correctly satisfy

$$|\kappa_1|^2 - |\tilde{\kappa}_2|^2 = 1. \quad (5.98)$$

Therefore we find that the condition that must be met for (5.93) to be satisfied is that

$$|\kappa_1|^2 \frac{1}{1 - e^{-2\pi\omega_+}} + |\tilde{\kappa}_2|^2 \frac{e^{-2\pi\omega_+}}{1 - e^{-2\pi\omega_+}} + (\kappa_1\tilde{\kappa}_2^* + \tilde{\kappa}_2\kappa_1^*) \frac{e^{-\pi\omega_+}}{1 - e^{-2\pi\omega_+}} = \frac{1}{1 - e^{-2\pi\omega_-}}. \quad (5.99)$$

At first sight this might seem a little surprising. But, in fact, the identity above is true as can be checked by just repeatedly using the Gamma-function identity  $\Gamma(iz)\Gamma(-iz) = \frac{\pi}{z \sinh(\pi z)}$ . In particular, we find that

$$\begin{aligned} \kappa_1\tilde{\kappa}_2^* &= -\frac{1}{2} \frac{1}{\sinh(\pi\omega_-)\sinh(\pi\omega_+)} (\cosh(\pi\omega_-) - \cosh(\pi(\omega_+ + i\Delta))); \\ \kappa_1^*\tilde{\kappa}_2 &= -\frac{1}{2} \frac{1}{\sinh(\pi\omega_-)\sinh(\pi\omega_+)} (\cosh(\pi\omega_-) - \cosh(\pi(\omega_+ - i\Delta))); \\ |\kappa_1|^2 &= \frac{1}{2} \frac{1}{\sinh(\pi\omega_-)\sinh(\pi\omega_+)} (\cosh(\pi(\omega_- + \omega_+)) - \cos(\pi\Delta)); \\ |\tilde{\kappa}_2|^2 &= \frac{1}{2} \frac{1}{\sinh(\pi\omega_-)\sinh(\pi\omega_+)} (\cosh(\pi(\omega_- - \omega_+)) - \cos(\pi\Delta)). \end{aligned} \quad (5.100)$$

Putting these results together, with a little algebra, we find that (5.99) follows!

We should emphasize that this result arises as a result of a nontrivial conspiracy between the reflection and transmission coefficients that control the propagation between the outer and the inner horizon, and the phase factor  $e^{-i\delta}$  that arises from propagation outside the outer horizon. This is reminiscent of the conspiracy between properties of the mode functions in these regions that the authors of [119] noticed when they were considering the *classical* problem in the same background.

Our test does not appear to be sensitive to the constraint,  $\frac{\Delta r_-}{r_+ - r_-} > 1$ , that was

found to be necessary in [119] for the stress-tensor to be regular at the inner horizon. Indeed, from our point of view, this constraint is somewhat surprising since (5.99) tells us that the state is *as smooth as possible* at the inner horizon: all the modes are occupied at just the right temperature. It would be interesting to understand this additional constraint through a mode-sum calculation of the stress-tensor near the inner horizon [59].

#### 5.4.4 Extending the field behind the inner horizon

The second part of our test in section 5.2 was that operators in front of the horizon must also be correctly entangled with operators behind it. In this case, the key-point is to focus on the operators  $\mathbf{c}$ . One might have thought that since the  $\mathbf{c}$  operators could, in principle, be “new” operators, one could just write them down using the standard mirror operator construction [68]. However, this is not possible due to the monogamy of entanglement. Since the modes just outside the inner horizon are linear combinations of modes near the outer horizon (5.95), and since those modes are already entangled with modes outside the outer horizon as in (5.88), (5.89), the modes near the inner horizon cannot also be entangled with fresh modes inside the inner horizon. Note that this application of the monogamy of entanglement is very different from the one used in the fuzzball or firewall arguments, since it can be phrased entirely at the level of effective field theory and involves only simple operators. Nevertheless, it turns out to be possible to cleverly reuse the modes behind the inner and outer horizon to generate modes behind the inner horizon.

**No new modes:** The fact that any new modes behind the inner horizon decouple can be seen from the following argument. Let us write

$$\mathbf{c} = \tilde{\kappa}_3 \tilde{\mathbf{a}} + \kappa_4 \mathbf{a}^\dagger + \kappa_5 \mathfrak{d} + \kappa_6 \mathfrak{e}^\dagger. \quad (5.101)$$

where  $\mathfrak{d}$  and  $\mathfrak{e}$  denote candidate new modes which commute with  $\tilde{\mathbf{a}}$  and  $\mathbf{a}^\dagger$ . We will first show that the new modes  $\mathfrak{d}$  and  $\mathfrak{e}^\dagger$  can consistently be set to zero above.

This is done as follows. First, we use the maximal entanglement of  $\mathbf{a}$  and  $\tilde{\mathbf{a}}$  to

show that the new modes cannot have any correlators with them. We start with

$$(\mathbf{a} - e^{-\pi\omega_0}\tilde{\mathbf{a}}^\dagger)|\Psi\rangle = 0, \quad (5.102)$$

and therefore,

$$\langle\Psi|\mathfrak{d}(\mathbf{a} - e^{-\pi\omega_0}\tilde{\mathbf{a}}^\dagger)|\Psi\rangle = 0. \quad (5.103)$$

But since  $\mathfrak{d}$  computes both with  $\mathbf{a}$  and with  $\tilde{\mathbf{a}}^\dagger$ ,

$$\langle\Psi|(\mathbf{a} - e^{-\pi\omega_0}\tilde{\mathbf{a}}^\dagger)\mathfrak{d}|\Psi\rangle = 0. \quad (5.104)$$

But note that we also have

$$\langle\Psi|\mathbf{a} = e^{\pi\omega_0}\langle\Psi|\tilde{\mathbf{a}}^\dagger. \quad (5.105)$$

Substituting this into the previous equation, we find that

$$2\sinh(\pi\omega_0)\langle\Psi|\tilde{\mathbf{a}}^\dagger\mathfrak{d}|\Psi\rangle = 0. \quad (5.106)$$

After employing similar reasoning for the two-point function with  $\mathbf{a}$ , we conclude that

$$\langle\Psi|\mathbf{a}\mathfrak{d}|\Psi\rangle = \langle\Psi|\tilde{\mathbf{a}}^\dagger\mathfrak{d}|\Psi\rangle = 0. \quad (5.107)$$

Similarly, we have

$$\langle\Psi|\mathbf{a}\mathbf{e}^\dagger|\Psi\rangle = \langle\Psi|\tilde{\mathbf{a}}^\dagger\mathbf{e}^\dagger|\Psi\rangle = 0. \quad (5.108)$$

The constraints (5.94) require

$$\mathbf{c}|\Psi\rangle = e^{-\pi\omega_1}\mathbf{b}^\dagger|\Psi\rangle. \quad (5.109)$$

Expanding both the left and the right hand sides using (5.101) and (5.95), we see that

$$(\tilde{\kappa}_3\tilde{\mathbf{a}} + \kappa_4\mathbf{a}^\dagger + \kappa_5\mathfrak{d} + \kappa_6\mathbf{e}^\dagger)|\Psi\rangle = e^{-\pi\omega_1}(\kappa_1^*\mathbf{a}^\dagger + \tilde{\kappa}_2^*\tilde{\mathbf{a}})|\Psi\rangle. \quad (5.110)$$

But since  $\mathfrak{d}|\Psi\rangle$  and  $\mathbf{e}^\dagger|\Psi\rangle$  are orthogonal to all the other vectors that appear above, we see immediately that

$$(\kappa_5\mathfrak{d} + \kappa_6\mathbf{e}^\dagger)|\Psi\rangle = 0. \quad (5.111)$$

But now using that

$$\mathbf{c}^\dagger|\Psi\rangle = e^{\pi\omega_1}\mathbf{b}|\Psi\rangle, \quad (5.112)$$

we can also conclude that

$$(\kappa_5^*\mathfrak{d}^\dagger + \kappa_6^*\mathfrak{e})|\Psi\rangle = 0. \quad (5.113)$$

But from (5.113) and (5.111), we find that

$$|\kappa_5|^2 - |\kappa_6|^2 = 0. \quad (5.114)$$

So not only are the new modes not entangled with the old modes, they cannot even contribute to the “norm” of the oscillators behind the horizon!

The results (5.107), (5.108) and (5.114) together constitute an important result. They show us that *we cannot define new modes behind the inner horizon that automatically have the right entanglement with modes in front of the inner horizon.* The reader might worry why the mirror operator construction [68] fails at the inner horizon. The reason is given by the equation (5.102). This means that if we look at the set of *simple operators* outside the inner horizon, the state is *not* separating with respect to these operators.

Therefore, for the remainder of this analysis, we will set

$$\kappa_5 = \kappa_6 = 0. \quad (5.115)$$

A pictorial representation of our result that one cannot arbitrarily define new modes behind the inner horizon is shown in Figure 5.5

**Reusing old modes:** At first the reader might conclude that the analysis above implies that it is impossible to extend the field behind the inner horizon. However, it turns out that is possible to cleverly *reuse* the old modes by choosing appropriate values for  $\tilde{\kappa}_3$  and  $\kappa_4$  in (5.101) so as to satisfy the entanglement constraints.

The concern is that the constraints might overdetermine  $\tilde{\kappa}_3$  and  $\kappa_4$ . However, the idea is to use the entanglement constraints between  $\mathbf{c}$  and  $\mathbf{b}$  to solve for  $\tilde{\kappa}_3$  and  $\kappa_4$  and then simply check whether  $[\mathbf{c}, \mathbf{b}] = 0$  and  $[\mathbf{c}, \mathbf{c}^\dagger] = 1$ . This is done as follows. We

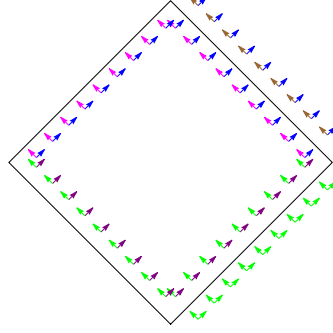


Figure 5.5: A figure of the outer and inner horizons and the modes near them. The purple modes near the right inner horizon are linear combinations of the green and violet modes near the outer horizons. But the green and violet modes are already entangled together. So, it is nontrivial to find the brown modes behind the inner horizon with the correct entanglement.

first note using (5.101) (and setting  $\kappa_5 = \kappa_6 = 0$ )

$$\mathbf{c}|\Psi\rangle = (\tilde{\kappa}_3\tilde{\mathbf{a}} + \kappa_4\mathbf{a}^\dagger)|\Psi\rangle = (\tilde{\kappa}_3 + \kappa_4e^{\pi\omega_0})\tilde{\mathbf{a}}|\Psi\rangle, \quad (5.116)$$

where we have used the entanglement between  $\mathbf{a}$  and  $\tilde{\mathbf{a}}$ . On the other hand, using the entanglement that is required between  $\mathbf{c}$  and  $\mathbf{b}$  and using (5.95) we find that

$$\begin{aligned} \mathbf{c}|\Psi\rangle &= e^{-\pi\omega_1}\mathbf{b}^\dagger|\Psi\rangle = e^{-\pi\omega_1}(\kappa_1^*\mathbf{a}^\dagger + \tilde{\kappa}_2^*\tilde{\mathbf{a}})|\Psi\rangle \\ &= e^{-\pi\omega_1}(\kappa_1^*e^{\pi\omega_0} + \tilde{\kappa}_2^*)\tilde{\mathbf{a}}|\Psi\rangle, \end{aligned} \quad (5.117)$$

where, in the last line, we again used the entanglement between the  $\mathbf{a}$  and the  $\tilde{\mathbf{a}}$  modes. Equating the final expressions on the two sides of the equations above, and using the fact that  $\tilde{\mathbf{a}}|\Psi\rangle \neq 0$  leads to the condition that

$$\tilde{\kappa}_3 + \kappa_4e^{\pi\omega_0} = e^{-\pi\omega_1}(\kappa_1^*e^{\pi\omega_0} + \tilde{\kappa}_2^*). \quad (5.118)$$

We can perform a similar analysis using the action of  $\mathbf{c}^\dagger$ . Here we find that

$$\mathbf{c}^\dagger|\Psi\rangle = (\tilde{\kappa}_3^*\tilde{\mathbf{a}}^\dagger + \kappa_4^*\mathbf{a})|\Psi\rangle = (\tilde{\kappa}_3^* + \kappa_4^*e^{-\pi\omega_0})\tilde{\mathbf{a}}^\dagger|\Psi\rangle. \quad (5.119)$$

On the other hand, the smoothness of the inner horizon requires

$$\begin{aligned} \mathbf{c}^\dagger|\Psi\rangle &= e^{\pi\omega_1}\mathbf{b}|\Psi\rangle = e^{\pi\omega_1}(\tilde{\kappa}_2\tilde{\mathbf{a}}^\dagger + \kappa_1\mathbf{a})|\Psi\rangle \\ &= e^{\pi\omega_1}(\kappa_1e^{-\pi\omega_0} + \tilde{\kappa}_2)\tilde{\mathbf{a}}^\dagger|\Psi\rangle. \end{aligned} \quad (5.120)$$

Taking the coefficients of the right hand sides of the two results above, and then taking the complex conjugate leads to the relation

$$\tilde{\kappa}_3 + \kappa_4e^{-\pi\omega_0} = e^{\pi\omega_1}(\kappa_1^*e^{-\pi\omega_0} + \tilde{\kappa}_2^*). \quad (5.121)$$

The relations (5.118) and (5.121) give linear equations for  $\tilde{\kappa}_3$  and  $\kappa_4$  that can be solved in terms of  $\kappa_1, \tilde{\kappa}_2$ . In particular the solution is

$$\begin{aligned} \tilde{\kappa}_3 &= \frac{1}{\sinh(\pi\omega_0)}[\kappa_1^* \sinh(\pi\omega_1) + \tilde{\kappa}_2^* \sinh[\pi(\omega_0 + \omega_1)]]; \\ \kappa_4 &= \frac{1}{\sinh(\pi\omega_0)}[\kappa_1^* \sinh[\pi(\omega_0 - \omega_1)] - \tilde{\kappa}_2^* \sinh(\pi\omega_1)]. \end{aligned} \quad (5.122)$$

These solutions are subject to further consistency checks. The first consistency check is that we need  $[\mathbf{c}, \mathbf{b}] = 0$ . This leads to the requirement

$$\kappa_1\kappa_4 - \tilde{\kappa}_2\tilde{\kappa}_3 = 0. \quad (5.123)$$

Using (5.118) and (5.121) we find, after some algebra, that

$$\kappa_1\kappa_4 - \tilde{\kappa}_2\tilde{\kappa}_3 = \frac{1}{2} \frac{e^{-\pi\omega_1}}{\coth(\pi\omega_0) - 1} (|\kappa_1e^{\pi\omega_0} + \tilde{\kappa}_2|^2 - |\kappa_1 + \tilde{\kappa}_2e^{\pi\omega_0}|^2 e^{2\pi\omega_1}). \quad (5.124)$$

On the other hand, from the relations

$$\langle\Psi|\mathbf{b}\mathbf{b}^\dagger|\Psi\rangle = 1 + \langle\Psi|\mathbf{b}^\dagger\mathbf{b}|\Psi\rangle = \frac{1}{1 - e^{-2\pi\omega_1}}, \quad (5.125)$$

we find that

$$|\kappa_1 + \tilde{\kappa}_2e^{\pi\omega_0}|^2 = e^{2\pi(\omega_0 - \omega_1)} \frac{1 - e^{-2\pi\omega_0}}{1 - e^{-2\pi\omega_1}}, \quad (5.126)$$

and also that

$$|\kappa_1 + \tilde{\kappa}_2e^{-\pi\omega_0}|^2 = \frac{1 - e^{-2\pi\omega_0}}{1 - e^{-2\pi\omega_1}}. \quad (5.127)$$

Substituting these relations in (5.124) we find that indeed (5.123) is satisfied.

The second consistency check is that the solution must satisfy  $[\mathfrak{c}, \mathfrak{c}^\dagger] = 1$ . This is just the requirement that

$$|\tilde{\kappa}_3|^2 - |\kappa_4|^2 = 1. \quad (5.128)$$

But this is also satisfied since

$$|\tilde{\kappa}_3|^2 - |\kappa_4|^2 = \frac{e^{-2\pi\omega_1}}{(e^{2\pi\omega_0} - 1)} \left[ -|\kappa_1 e^{\pi\omega_0} + \tilde{\kappa}_2|^2 + |\kappa_1 + \tilde{\kappa}_2 e^{\pi\omega_0}|^2 e^{4\pi\omega_0} \right] = 1. \quad (5.129)$$

One might have hoped that by placing reflecting boundary conditions at the singularity, one would correctly reproduce the coefficients  $\tilde{\kappa}_3$  and  $\kappa_4$  i.e. we quantize the field behind the inner horizon assuming that the geometry is given the naive analytic continuation and then also impose  $\phi = 0$  at the timelike singularity at  $r = 0$ . However, a simple calculation shows that this does *not* give the right values of  $\tilde{\kappa}_3$  and  $\kappa_4$ . It is possible that more sophisticated reflecting boundary conditions could be used to reproduce the values of  $\tilde{\kappa}_3$  and  $\kappa_4$  but we have not yet discovered them.

## 5.5 Discussion

### Summary

In this chapter we developed a necessary condition for a quantum state to be smooth in the vicinity of a null surface. The condition is that the near-horizon modes defined by (5.12), which have canonical commutators, must have the self-correlators given by (5.27) and must be entangled with each other through the correlators (5.23). This is a universal result, which relies just on the short-distance properties of the correlator of the scalar field.

For static black holes, implementation of this test at the horizon imposes a universal behaviour on the two-point correlator of global modes. The two-point function must have a delta-function piece in the frequency-difference, and the coefficient of this delta function is the same in any smooth state.

Since it is nontrivial for a state to satisfy the above condition for smoothness both at inner and outer horizon, this gives us a test for violations of strong cosmic censorship conjecture. We applied this test to charged black holes in anti-de Sitter space for boundary dimension, 3, 4, 5 and 6, where we were able to easily verify,

for a range of parameters, that the naturally defined Hartle-Hawking state was not smooth at the inner horizon. So, even in the absence of external perturbations, quantum fluctuations destabilize the inner horizon for such black holes.

In [119], it was argued that BTZ black holes violate strong cosmic censorship for a range of parameters. In this chapter, we found that our test was automatically satisfied in the Hartle-Hawking state as a result of some non-trivial identities involving the various reflection and transmission coefficients in the black-hole geometry.

We also explored the possibility of extension of spacetime behind the inner horizon. Entanglement across the inner horizon constrains the modes behind the horizon. We argued that expansion of fields in terms of new degrees of freedom is prohibited by monogamy of entanglement. Instead, we are forced to reuse old modes to construct near-horizon modes behind the inner horizon. We identified the correct combination that could be used to expand the field just behind the inner horizon. This does *not* completely fix the dynamics behind the inner horizon. If one considers points that are finitely separated from the inner horizon, then the correlators of field insertions at such points require information that is *not* contained in the near-horizon modes. The arbitrariness in these correlators corresponds to the freedom that one has in extending the metric and the fields behind the Cauchy horizon.

If BTZ black holes do violate strong cosmic censorship, the arbitrariness described above would present interesting challenges for the AdS/CFT interpretation of such black holes. The AdS/CFT conjecture suggests that a boundary CFT describes all phenomenon in the bulk geometry but a traversable inner horizon would imply that there are events (behind the inner horizon) that cannot be described by the boundary CFT in an obvious way.

However, before concluding that the conjecture is violated, we need to understand other effects that may influence traversability of the inner horizon. Since the inner horizon is to the future of all events in the exterior, we would need to understand non-perturbative effects as well. For instance, perturbations outside the horizon never go to zero, rather develop a fat tail of the order of  $e^{-S}$  after long time,  $O(S)$ . After this, the perturbations do not decay any further [127]. At even later times,  $O(e^{e^S})$ , effects such as Poincare recurrence may have some implications for the inner horizon.

## Outlook

Our work points to several directions for future work. One technical issue, which we believe would be interesting to understand better, is as follows. In the Hartle-Hawking state, the occupancy of the modes near the inner horizon of the BTZ black hole, which we presented in section 5.4, provides enough information to compute the stress-tensor at the inner horizon using mode sums. It would be nice to understand the constraint found in [119]— which suggests that the stress-tensor is finite only  $\beta = \frac{\Delta}{r_+ - 1} > 1$  — from the perspective of direct mode sums.

It is also natural to use our test to understand both flat-space and de Sitter black holes. The de Sitter case is particularly interesting because, classically, not only do charged de-Sitter black holes violate even the weak formulations of strong cosmic censorship [113], even non rotating and neutral black holes in de Sitter space have two horizons: the black-hole and the cosmological horizon. So an interesting exercise is to consider various possible quantum states and examine their smoothness on all these horizon by the methods discussed here.



## Chapter 6

### Conclusions

In chapter 2, we argued that the degrees of freedom are encoded holographically in a theory of quantum gravity in 4-dimensional asymptotically flat spacetimes. Hence, any information about a quantum state can be recovered from almost instantaneous measurements of boundary observables. Our analysis was based on assumptions motivated from semiclassical gravity.

We studied implications of holography for the black hole information paradox. Since all information is always present near the boundary, the notion of information escaping from the black hole through Hawking radiation is ill-founded. This implies that the often discussed Page curve is a wrong expectation based on incorrect assumptions about quantum gravity, namely locality. The true Page curve should be a constant. Strictly, this is not at odds with recent results on derivation of the Page curve of black hole radiation, [41], as these results work in a setup where gravity switches off and the Hilbert space factorizes. We also noted that mathematically, it may be possible to define a subalgebra for which the entanglement entropy follows the traditional Page curve. However, physical relevance of such subalgebra is unclear.

The loss of locality also resolves the strong subadditivity and cloning paradoxes, which incorrectly assume that the full Hilbert space can be thought of as a tensor product of subspace in the interior of a black hole and a subspace in the exterior. However, this doesn't resolve the paradoxes associated with the experience of an infalling observer. In [65], it was argued that operators behind the horizon are ill-defined. Non-locality discussed in chapter 2 does not shed light on this issue. To resolve this issue we need to invoke state-dependence [62, 67, 68, 70].

Apart from extension of our results to arbitrary spacetime dimensions and including massive excitations, an interesting direction for future work is to understand sub-region duality in semiclassical gravity. Can similar semiclassical analysis elucidate

the entanglement wedge reconstruction in AdS/CFT? It would also be interesting to explore sub-region duality in asymptotically flat spacetimes.

In chapter 3, we analyzed the fuzzball resolution to the information paradox. We argued that typical black hole microstates cannot be described by distinct classical geometries. We also showed that fuzzballs differ too much from black holes, and hence, cannot parameterize the phase space of black hole microstates.

In chapter 4, we derived a universal bound on the large spacelike limit of thermal Wightman correlators. This bound is saturated in perturbative theories via sufficiently high order loop diagrams. However, surprisingly, holographic theories do not always saturate this bound, at least at the leading order. This is unexpected as holographic theories are strongly coupled. It would be interesting to explore this bound in holographic theories in greater detail. An open problem is to understand whether our bound holds in holographic theories even for momenta that do not scale with the central charge. Another direction to explore is whether these correlators can be indicative of holography.

Finally, in chapter 5, we developed a quantum test for smoothness of a state across a null surface. This requires the local modes, obtained by integrating the quantum field in local Rindler coordinates near the null surface, to be entangled in a particular way. This imposes nontrivial conditions on two-point functions of global modes. We used this to develop a test for strong cosmic censorship. A violation of strong cosmic censorship conjecture requires the inner horizon of a black hole to be smooth. However, it is nontrivial for a state to be smooth at inner as well as outer horizon. We used this test to rule out violations in RN-AdS. Our test did not rule out violations in BTZ. We explored the possibility of extending the spacetime behind the inner horizon. Such an extension is only possible if modes behind the inner horizon are some combination of modes outside. No new mode can be defined behind the inner horizon.

Implementation of our test for the strong cosmic censorship conjecture for other black holes, such as black holes in de-Sitter space, is an immediate future direction to be pursued. Since de-Sitter black holes also have a cosmological horizon, it would be interesting to implement our analysis even for Schwarzschild black holes. It is also important to understand other quantum effects, including non-perturbative effects, that may have a bearing on stability of the inner horizon.

## Appendix A

### Asymptotic charges as observables

In this section, we will address the argument of [38] that the ADM mass, the Bondi mass and other asymptotic charges should not be observables at null infinity.

The argument of [38] is quite simple, and can be understood by considering even a free scalar theory. Usually, we define the vacuum as an eigenstate of the Hamiltonian which (after a possible shift in the zero-point energy) annihilates it.

$$H|0\rangle = 0. \tag{A.1}$$

In a local theory, the operator  $H$  above is an integral of a Hamiltonian density,  $\mathcal{H}(\vec{x}, t)$  over an entire Cauchy slice. However, now consider integrating the Hamiltonian density only inside some ball of large radius,  $B(R)$ ,

$$H(R, t) = \int_{B(R)} \mathcal{H}(\vec{x}, t) d^3\vec{x}. \tag{A.2}$$

The point made in [38] is that this truncated operator has large fluctuations: in fact,  $\langle 0|H(R)^2|0\rangle$  grows with  $R$  and so it appears that a naive  $R \rightarrow \infty$  limit will of  $H(R)$  will not yield the correct Hamiltonian,  $H$ .

Now, if one couples the scalar to gravity, the gravitational constraints relate some components of the metric on a sphere of radius  $R$  to the energy contained inside the sphere. Therefore [38] argued that these metric components would also have large fluctuations that could only be tamed by smearing  $H(R)$  over a large time. Their smearing prescription is shown in Figure A.1a. If such a smearing were indeed necessary, it would be impossible to assign a meaning to the ADM mass or assign a Bondi mass to a cut of future (or past) null infinity, since as we take  $R \rightarrow \infty$  in figure A.1a, the smeared operator of [38] appears to have support over a semi-infinite region of future null infinity.

In this Appendix, we show that this conclusion is unwarranted. The large quantum fluctuations can also be avoided by smearing  $H(R, t)$  *radially* before taking the  $R \rightarrow \infty$  limit. Said another way, to obtain asymptotic charges at null infinity, we first smear the bulk metric radially and then take its large-radius limit.

The ADM mass defined in this manner is related by the constraints to the following operator  $H$ .

$$H = \lim_{R \rightarrow \infty} H_{\text{sm}}(R) = \lim_{R \rightarrow \infty} \int dt' dR' \mathfrak{g}(t') \mathfrak{F}_R(R') \int_{B(R')} \mathcal{H}(\vec{x}, t) d^3\vec{x}. \quad (\text{A.3})$$

The smearing in time is controlled by  $\mathfrak{g}(t)$  and has support over a small user-defined length scale,  $\eta$  around  $t = 0$ . The smearing function in the radial direction,  $\mathfrak{F}_R$ , varies the radius of the ball in the range  $R \pm R^{1-\delta}\eta^\delta$ , where  $\delta$  can be chosen to be any number satisfying  $0 < \delta < \frac{1}{3}$ . We show that the fluctuations of  $H_{\text{sm}}(R)$  in a massless scalar field theory are then suppressed as

$$\langle 0 | H_{\text{sm}}(R)^2 | 0 \rangle = \frac{1}{120\pi} \frac{1}{R\eta} \left( \frac{R}{\eta} \right)^{3\delta}, \quad (\text{A.4})$$

up to terms that fall off even faster with  $R$ . So this has a good limit as  $R \rightarrow \infty$ . We derive this result below.

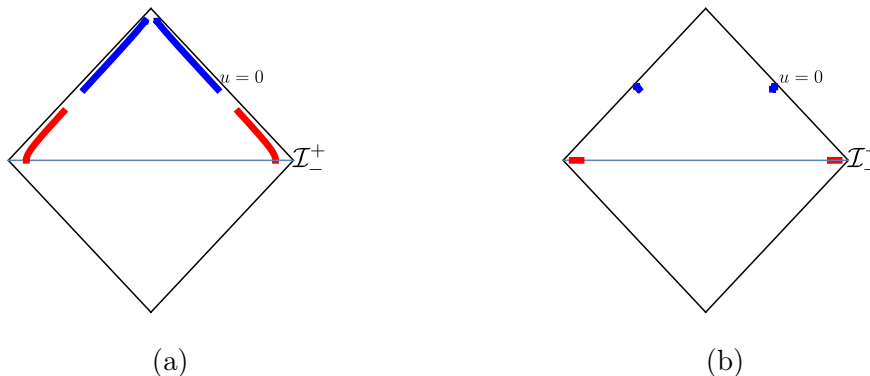


Figure A.1: The protocol of [38] (left) associates large regions of  $\mathcal{I}^+$  with each measurement of Bondi mass making it impossible to associate a value with a cut. In contrast, our protocol (right) reduces quantum fluctuations by averaging over the radial direction, associating an infinitesimal interval of  $\mathcal{I}^+$  to each measurement of the Bondi mass.

---

## Fluctuations of the smeared Hamiltonian

Consider the free massless scalar field in 3 + 1-dimensional spacetime.

$$\phi(x) = \int \frac{d^3k}{(2\pi)^{3/2}} \frac{1}{\sqrt{2\omega_{\vec{k}}}} \left[ a_{\vec{k}} e^{ik \cdot x} + a_{\vec{k}}^\dagger e^{-ik \cdot x} \right]. \quad (\text{A.5})$$

The field satisfies canonical commutation relations provided

$$[a_{\vec{k}}, a_{\vec{k}'}^\dagger] = \delta^3(\vec{k} - \vec{k}'). \quad (\text{A.6})$$

The Hamiltonian density is

$$\mathcal{H}(x, t) = \frac{1}{2} : \left[ (\partial_t \phi(x))^2 + (\vec{\nabla} \phi(x))^2 \right] :. \quad (\text{A.7})$$

As usual, we normal order the Hamiltonian so that the divergent contribution of the zero-point energies is removed. Using the mode expansion we find

$$H(R, t) = -\frac{1}{2} \int_{|\vec{x}| \leq R} d^3x \frac{d^3k d^3p}{(2\pi)^3} \frac{(\omega_{\vec{k}} \omega_{\vec{p}} + \vec{k} \cdot \vec{p})}{2\sqrt{\omega_{\vec{k}} \omega_{\vec{p}}}} \left[ a_{\vec{k}} a_{\vec{p}} e^{i(k+p) \cdot x} + a_{\vec{k}}^\dagger a_{\vec{p}}^\dagger e^{-i(k+p) \cdot x} - a_{\vec{k}}^\dagger a_{\vec{p}} e^{-i(k-p) \cdot x} - a_{\vec{p}}^\dagger a_{\vec{k}} e^{i(k-p) \cdot x} \right]. \quad (\text{A.8})$$

Usually, we integrate over all  $\vec{x}$  to define the Hamiltonian and then we just drop the terms with two creation and two annihilation operators. However, if we integrate over a finite region, these terms remain and the discussion here has to do with their effect.

$$H(R, t) = \int \frac{d^3k d^3p}{(2\pi)^2} \frac{(\omega_{\vec{k}} \omega_{\vec{p}} + \vec{k} \cdot \vec{p})}{2\sqrt{\omega_{\vec{k}} \omega_{\vec{p}}}} \left( \mathcal{D}(k-p, R, t) a_{\vec{p}}^\dagger a_{\vec{k}} - \mathcal{D}(k+p, R, t) a_{\vec{k}} a_{\vec{p}} + \text{h.c.} \right), \quad (\text{A.9})$$

with

$$\mathcal{D}(q, R, t) = \frac{\sin(|\vec{q}|R) - |\vec{q}|R \cos(|\vec{q}|R)}{|\vec{q}|^3} e^{-iq^0 t}. \quad (\text{A.10})$$

In the large  $R$  limit, the function  $\mathcal{D}(q, R, t)$  is sharply peaked around  $|\vec{q}| \rightarrow 0$ .

As discussed earlier, we are interested in the smeared operator (A.3). We make the following choices for the smearing functions.

$$\mathfrak{F}_R(R') = \frac{1}{\lambda\sqrt{\pi}} e^{-\frac{(R'-R)^2}{\lambda^2}}; \quad \mathfrak{g}(t') = \frac{1}{\eta\sqrt{\pi}} e^{-\frac{t'^2}{\eta^2}}, \quad (\text{A.11})$$

where

$$\lambda = R^{1-\delta} \eta^\delta, \quad (\text{A.12})$$

and  $\eta$  is chosen to be a small length scale that does not scale with  $R$ .

Now we proceed to the computation of fluctuations of smeared Hamiltonian.

$$\langle 0 | H_{\text{sm}}^2(R) | 0 \rangle = \int dt_1 dt_2 dR_1 dR_2 \mathfrak{F}_R(R_1) \mathfrak{F}_R(R_2) \mathfrak{g}(t_1) \mathfrak{g}(t_2) \langle \Omega | H(t_1, R_1) H(t_2, R_2) | \Omega \rangle. \quad (\text{A.13})$$

Expanding out both factors of  $H$  in creation and annihilation operators, we see that the only term that contributes towards vacuum fluctuations is the one which picks up creation operators from the second factor and annihilation operators from the first. This leads to correlators of the form  $\langle 0 | a_{\vec{k}} a_{\vec{p}} a_{\vec{k}'}^\dagger a_{\vec{p}'}^\dagger | 0 \rangle = \delta(\vec{k} - \vec{k}') \delta(\vec{p} - \vec{p}') + \delta(\vec{k} - \vec{p}') \delta(\vec{p} - \vec{k}')$ . We then find

$$\begin{aligned} \langle \Omega | H_{\text{sm}}^2(R) | \Omega \rangle &= \int \frac{d^3 k d^3 p}{(2\pi)^4} \frac{(\omega_{\vec{k}} \omega_{\vec{p}} + \vec{k} \cdot \vec{p})^2}{2\omega_{\vec{k}} \omega_{\vec{p}}} \mathcal{D}(k+p, R_1, t_1) \mathcal{D}^*(k+p, R_2, t_2) \\ &\quad \times \mathfrak{F}_R(R_1) \mathfrak{F}_R(R_2) \mathfrak{g}(t_1) \mathfrak{g}(t_2) dR_1 dR_2 dt_1 dt_2 \end{aligned} \quad (\text{A.14})$$

Now we will perform all the smearing integrals to get the following.

$$\begin{aligned} \langle \Omega | H_{\text{sm}}^2(R) | \Omega \rangle &= \int \frac{d^3 k d^3 p}{(2\pi)^4} \frac{(\omega_{\vec{k}} \omega_{\vec{p}} + \vec{k} \cdot \vec{p})^2}{2\omega_{\vec{k}} \omega_{\vec{p}}} e^{-\frac{1}{2}\eta^2(\omega_{\vec{k}} + \omega_{\vec{p}})^2} \frac{1}{4} e^{-\frac{1}{2}\lambda^2(|\vec{k} + \vec{p}|)^2} \frac{1}{|\vec{k} + \vec{p}|^6} \\ &\quad \times \left[ (2 + \lambda^2(|\vec{k} + \vec{p}|)^2) \sin(|\vec{k} + \vec{p}|R) - 2|\vec{k} + \vec{p}|R \cos(|\vec{k} + \vec{p}|R) \right]^2. \end{aligned} \quad (\text{A.15})$$

To simplify the above integral, we change variables to  $\vec{q} = \vec{k} + \vec{p}$  and  $\vec{r} = \vec{k} - \vec{p}$ .

---

Then we see that the integral above only receives contributions from the range where  $|\vec{q}|\eta \ll 1$ . This allows us to series expand all terms in a series in  $|\vec{q}|$  (except for those that involve  $|\vec{q}|R$ ) and do the integrals explicitly leading to

$$\langle 0|H_{\text{sm}}^2(R)|0\rangle = \frac{R^2}{120\pi\eta\lambda^3} \left(1 + \mathcal{O}\left(\frac{\lambda}{R}\right)\right) = \frac{1}{120\pi} \frac{1}{R\eta} \left(\frac{R}{\eta}\right)^{3\delta} \left(1 + \mathcal{O}\left(\frac{\lambda}{R}\right)\right), \quad (\text{A.16})$$

as advertised.

While we also required a small smearing over time, this only provided us with a UV-momentum cutoff. However, our radial smearing was over a *parametrically* larger region. This provided us with another momentum cut-off that was parametrically smaller than the cutoff provided by the time-smearing. This is the crucial difference with [38]. In fact, we can recover the results of [38] just by taking  $\lambda = \mathcal{O}(\eta)$  in our calculation. Then the fluctuations of our smeared Hamiltonian again start to diverge with  $R$  as is evident above.

The fluctuations of the Bondi mass can be similarly suppressed by taking  $t = u + R$  in the expression above, and smearing by a small amount in  $u$  and a large amount in  $R$ .

The discussion here has had to do with the *definition* of asymptotic observables as limits of bulk observables and not with the “difficulty” of measuring them practically. To summarize, we do not see any, in-principle, obstacle to taking this limit and obtaining asymptotic charges as observables in a quantum theory, provided the limit is taken carefully.



## Appendix B

### Thermal perturbation theory

In this appendix, we review the elements of thermal perturbation theory. Our analysis applies to any perturbative quantum field theory and is applied in the main text, both to holographic correlators, and to weakly-coupled theories. We first describe a canonical formulation of thermal perturbation theory, and then describe a diagrammatic formulation that naturally arises from the Schwinger-Keldysh representation. The material covered here is standard, but we include it here for the sake of completeness and also because it is somewhat difficult, in the extant literature, to find a clear and concise description of the rules to carry out perturbation theory for relativistic field theories.

#### Canonical formulation

We are interested in evaluating

$$\mathrm{Tr}(e^{-\beta H} \phi(t_1, x_1) \dots \phi(t_n, x_n)). \quad (\text{B.1})$$

At some point of time,  $\tau$  we split the Hamiltonian into a free and an interacting part

$$H = H_0[\tau] + H_I[\tau]. \quad (\text{B.2})$$

Here  $H_I$  is the interaction Hamiltonian evaluated at real time  $\tau$  and  $H_0$  is the “free Hamiltonian”, also evaluated at time  $\tau$ . Note that both  $H_0$  and  $H_I$  depend on the time we choose to make this split,  $\tau$ , although this dependence on  $\tau$  must eventually drop out. Below, whenever  $H_I$  is evaluated at time  $\tau$ , we will suppress this dependence to lighten the notation.

Now consider

$$T(z) = e^{zH_0} e^{-zH}. \quad (\text{B.3})$$

This satisfies

$$\begin{aligned} T'(z) &= e^{zH_0} H_0 e^{-zH_0} e^{zH_0} e^{-zH} - e^{zH_0} H e^{-zH_0} e^{zH_0} e^{-zH} \\ &= -e^{zH_0} H_I e^{-zH_0} T(z). \end{aligned} \quad (\text{B.4})$$

The solution to this is just

$$T(\beta) = \mathcal{T}_c e^{-\int_0^\beta H_I(\tau - iz) dz}. \quad (\text{B.5})$$

where

$$H_I(\tau - iz) = e^{zH_0} H_I e^{-zH_0}, \quad (\text{B.6})$$

and  $\mathcal{T}_c$  denotes a contour-ordering sign, where the contour moves down in imaginary time from  $\text{Im}(t) = 0$  to  $\text{Im}(t) = -\beta$ . In the expression above larger values of  $z$  are placed to the left. More explicitly, we have

$$T(\beta) = \sum_n \frac{(-1)^n}{n!} \int \mathcal{T}_c \{H_I(\tau - iz_1) \dots H_I(\tau - iz_n)\} dz_1 \dots dz_n. \quad (\text{B.7})$$

Therefore we have

$$e^{-\beta H} = e^{-\beta H_0} T(\beta). \quad (\text{B.8})$$

We can expand the interaction Hamiltonian as a sum of terms with various frequencies (as measured by the free Hamiltonian). If we then write

$$H_I(t) = \int_{-\infty}^{\infty} H_I(\omega) e^{-i\omega t} \frac{d\omega}{2\pi}, \quad (\text{B.9})$$

then we have

$$H_I(t - iz) = \int_{-\infty}^{\infty} e^{-i\omega t - z\omega} H_I(\omega) \frac{d\omega}{2\pi}, \quad (\text{B.10})$$

and

$$T(\beta) = \sum_n (-1)^n \int \prod \frac{d\omega_i}{2\pi} \int_0^\beta dz_1 \int_0^{z_1} dz_2 \dots \int_0^{z_{n-1}} dz_n e^{-i\sum \omega_i(\tau - iz_i)} H(\omega_1) \dots H(\omega_n). \quad (\text{B.11})$$

---

We now turn to the real-time part of the correlator. Using standard arguments we have

$$\phi(t_i, x_i) = \overline{\mathcal{T}} \left[ e^{i \int_{\tau}^t H_I(x) dx} \right] \phi_I(t, x_i) \mathcal{T} \left[ e^{-i \int_{\tau}^t H_I(x) dx} \right], \quad (\text{B.12})$$

where  $\phi_I(t, x_i)$  is the interaction-picture operator at time  $t$ .

With a little algebra this can be written as

$$\phi(t_i, x_i) = \sum_{N=0}^{\infty} i^N \int_{\tau}^t dt_N \dots \int_{\tau}^{t_2} dt_1 [H_I(t_1), [H_I(t_2) \dots [H_I(t_N), \phi_I(t, x_i)] \dots]]. \quad (\text{B.13})$$

Combining (B.13) and (B.7) we immediately obtain a perturbative expansion for (B.1).

For consistency, we would like to see the following two effects emerge from the expressions above

1. Although we have suppressed this dependence, in fact both the free Hamiltonian and the interaction Hamiltonian depend on the time at which we make the split,  $\tau$ , and correspondingly  $\tau$  also appears in the lower limit of the integral.
2. Second, the correlator above should be time-translationally invariant. So if we shift  $t_i \rightarrow t_i + x$ , the correlator should not change.

This is obvious in the original expression (B.1). However, in perturbation theory this appears to be a little puzzling. To see the puzzle, let us suppress the separate time-dependence and instead consider a single operator  $C(t)$ . The generalization to operators at different times will be given later, and will be obvious.

Therefore, we consider the expression  $\text{Tr}(e^{-\beta H} C(t))$ . We will expand this out to second order in perturbation theory to check the two consistency properties above. To second order we have

$$\begin{aligned} T(\beta) = & 1 - \int H_I(\omega) e^{-i\omega\tau} \frac{1 - e^{-\beta\omega}}{\omega} \frac{d\omega}{2\pi} \\ & + \int H_I(\omega) H_I(\omega') e^{-i(\omega+\omega')\tau} \left[ \frac{1 - e^{-\beta\omega}}{\omega\omega'} + \frac{e^{-\beta(\omega+\omega')} - 1}{(\omega + \omega')\omega'} \right] \frac{d\omega}{2\pi} \frac{d\omega'}{2\pi}. \end{aligned} \quad (\text{B.14})$$

Further, we write the interaction picture operator as

$$C_I(t) = \int C_I(\omega) e^{-i\omega t} \frac{d\omega}{2\pi}. \quad (\text{B.15})$$

Inserting this into the nested commutators above yields an expression for the Heisenberg-picture operator, which we will use below.

Before we turn to the general structure of the perturbative expansion we work out the first order terms and the quadratic terms explicitly. The reader may skip these explicit calculations if she is interested only in the results.

**First order terms:** The first order terms are

$$\int F \frac{d\omega}{2\pi} \frac{d\omega'}{2\pi},$$

where

$$F = -\text{Tr} e^{-\beta H_0} \left[ H_I(\omega) \frac{1 - e^{-\beta\omega}}{\omega} C_I(\omega') e^{-i\omega' t} e^{-i\omega\tau} - \frac{1}{\omega} [H_I(\omega), C_I(\omega')] e^{-i\omega' t} (e^{-i\omega t} - e^{-i\omega\tau}) \right]. \quad (\text{B.16})$$

In general, we expect this correlator to have support for all values with  $\omega + \omega' = 0$ . However, this is puzzling, since in some of the terms above, we appear to get a non-zero dependence on both  $t$  and  $\tau$ .

This can be resolved by imposing the *KMS condition*.

$$\begin{aligned} \text{Tr} (e^{-\beta H_0} H_I(\omega) C_I(\omega')) &= e^{\beta\omega} \text{Tr} (H_I(\omega) e^{-\beta H_0} C_I(\omega')) = e^{\beta\omega} \text{Tr} (e^{-\beta H_0} C_I(\omega') H_I(\omega)) \\ &= e^{\beta\omega} \text{Tr} (e^{-\beta H_0} (H_I(\omega) C_I(\omega') - [H_I(\omega), C_I(\omega')])). \end{aligned} \quad (\text{B.17})$$

In particular this means that

$$(1 - e^{-\beta\omega}) \text{Tr} (e^{-\beta H_0} H_I(\omega) C_I(\omega')) = \text{Tr} (e^{-\beta H_0} [H_I(\omega), C_I(\omega')]). \quad (\text{B.18})$$

Therefore, we have

$$F = \frac{-1}{\omega} \text{Tr} (e^{-\beta H_0} [H_I'(\omega), C_I(\omega')]) e^{-i\omega' t} e^{-i\omega t}, \quad \omega, \omega' \neq 0. \quad (\text{B.19})$$

---

Since the trace is proportional to  $\delta(\omega+\omega')$ , in this form, it is clear that the correlator is independent of both  $\tau$  and  $t$ .

However, the contribution above is *not* the full contribution to the correlator since in writing the final expression for  $F(\omega, \omega')$  we divided by  $\omega$ . This is not allowed at  $\omega = 0$ . In particular, if the thermal expectation of  $H_I(\omega)C_I(\omega')$  has a term proportional to  $\delta(\omega)\delta(\omega')$ . This term is not cancelled off by the KMS condition. However, this term is also manifestly independent of  $\tau$  and  $t$  so the puzzle above does not arise here. We will return to these correction terms below.

**Second order terms:** Now let us consider the second order terms. We need to include the second order term from  $T(\beta)$  the second order term from the real-time evolution, and the product of the first order terms. Therefore the full expression we need to consider is as follows

$$\begin{aligned}
S &= \int \frac{d\omega_1 d\omega_2 d\omega_3}{(2\pi)^3} \text{Tr} e^{-\beta H_0} [T_1 + T_2 + R] \\
T_1 &= e^{-i(\omega_1+\omega_2)\tau - i\omega_3 t} \int_0^\beta dz_1 \int_0^{z_1} dz_2 e^{-z_1\omega_1 - z_2\omega_2} H_I(\omega_1) H_I(\omega_2) C_I(\omega_3) \\
T_2 &= -ie^{-i\omega_1\tau - i\omega_3 t} \int_0^\beta dz_1 e^{-z_1\omega_1} \int_\tau^t dt_2 e^{-i\omega_2 t_2} H_I(\omega_1) [H_I(\omega_2), C_I(\omega_3)] \\
R &= - \int_\tau^t dt_2 \int_\tau^{t_2} dt_1 e^{-i\omega_1 t_2 - i\omega_2 t_2 - i\omega_3 t} [H_I(\omega_1), [H_I(\omega_2), C_I(\omega_3)]] .
\end{aligned} \tag{B.20}$$

We again consider the case where  $\omega_1 \neq 0, \omega_2 \neq 0, \omega_3 \neq 0$ . For the term denoted by  $T_1$  above we need to use the KMS relations twice. This yields

$$\begin{aligned}
\text{Tr}(e^{-\beta H_0} H_I(\omega_1) H_I(\omega_2) C_I(\omega_3)) &= \frac{\text{Tr}(e^{-\beta H_0} [H_I(\omega_2), [H_I(\omega_1), C_I(\omega_3)]])}{(1 - e^{-\beta\omega_1})(1 - e^{-\beta\omega_2})} \\
&- \frac{e^{-\beta\omega_3}}{(1 - e^{-\beta\omega_1})(1 - e^{-\beta\omega_3})} \text{Tr}(e^{-\beta H_0} [C_I(\omega_3), [H_I(\omega_1), H_I(\omega_2)]]).
\end{aligned} \tag{B.21}$$

We can put both these terms in the form of the commutator that appears in the real-time expression by using the Jacobi identity for the second expression

$$[C_I(\omega_3), [H_I(\omega_1), H_I(\omega_2)]] = -[H_I(\omega_1), [H_I(\omega_2), C_I(\omega_3)]] + [H_I(\omega_2), [H_I(\omega_1), C_I(\omega_3)]] . \tag{B.22}$$

After these steps, we find that

$$\begin{aligned}
 T_1 &= \frac{(\omega_1 (e^{-\beta\omega_2} - 1) + \omega_2 (e^{\beta\omega_1} - 1)) e^{-i\tau(\omega_1+\omega_2)}}{\omega_1\omega_2 (e^{\beta\omega_1} - 1) (e^{\beta\omega_2} - 1) (e^{\beta\omega_3} - 1) (\omega_1 + \omega_2)} e^{-i\omega_3 t} \\
 &\times \left[ (e^{\beta(\omega_2+\omega_3)} - 1) \text{Tr}(e^{-\beta H_0} [H_I(\omega_2), [H_I(\omega_1), C_I(\omega_3)]]) \right. \\
 &\left. - (e^{\beta\omega_2} - 1) \text{Tr}(e^{-\beta H_0} [H_I(\omega_1), [H_I(\omega_2), C_I(\omega_3)]]) \right]. \tag{B.23}
 \end{aligned}$$

We also find that

$$T_2 = \frac{e^{-i\omega_3 t - i\tau\omega_1}}{\omega_1\omega_2} (e^{-it\omega_2} - e^{-i\tau\omega_2}) \text{Tr}(e^{-\beta H_0} [H_I(\omega_1), [H_I(\omega_2), C_I(\omega_3)]]), \tag{B.24}$$

whereas the real-time term is given by

$$\begin{aligned}
 R &= -e^{-i\omega_3 t} \frac{((\omega_1 + \omega_2)e^{-i(t\omega_2 + \tau\omega_1)} - \omega_2 e^{-it(\omega_1 + \omega_2)} + \omega_1 (-e^{-i\tau(\omega_1 + \omega_2)}))}{\omega_1\omega_2(\omega_1 + \omega_2)} \\
 &\times \text{Tr}(e^{-\beta H_0} [H_I(\omega_1), [H_I(\omega_2), C_I(\omega_3)]]). \tag{B.25}
 \end{aligned}$$

Upon adding these terms, and noting that within the integral we can switch the dummy variables  $\omega_2 \leftrightarrow \omega_1$  we find that the full quadratic term in the integrand for  $\omega_i \neq 0$  is

$$\begin{aligned}
 T_1 + T_2 + R &= \frac{e^{-i\omega_3 t}}{\omega_1\omega_2} \text{Tr}(e^{-\beta H_0} [H_I(\omega_1), [H_I(\omega_2), C_I(\omega_3)]]) \left[ \right. \\
 &\frac{e^{-(\beta+i\tau)(\omega_1+\omega_2)}}{(e^{\beta\omega_1} - 1) (e^{\beta\omega_2} - 1) (e^{\beta\omega_3} - 1) (\omega_1 + \omega_2)} \times \left( \omega_1 \left( e^{\beta(2(\omega_1+\omega_2)+\omega_3)} - e^{\beta(\omega_1+\omega_2)} + e^{\beta\omega_1} \right) \right. \\
 &\left. - (\omega_1 + \omega_2) e^{\beta(2\omega_1+\omega_2+\omega_3)} + \omega_2 \left( e^{\beta(\omega_1+2\omega_2)} - e^{\beta\omega_2} + e^{\beta(\omega_1+\omega_2+\omega_3)} - e^{2\beta(\omega_1+\omega_2)} + e^{\beta(2\omega_1+\omega_2)} \right) \right) \\
 &\left. + \frac{\omega_2 e^{-it(\omega_1+\omega_2)} + \omega_1 e^{-i\tau(\omega_1+\omega_2)}}{\omega_1 + \omega_2} + e^{-i\tau(\omega_1+\omega_2)} + \dots, \right. \\
 &\left. \right) \tag{B.26}
 \end{aligned}$$

where  $\dots$  indicates terms that either integrate to 0 or contribute only when one of the  $\omega_i$ 's is 0.

---

However, recall that the thermal trace has support only on  $\omega_3 = \omega_1 + \omega_2$ . This is because the trace can be evaluated in any basis, including the basis of eigenstates of  $H_0$  in which the total  $H_0$ -eigenvalue of the insertion inside the trace must vanish. Imposing this condition, we find a tremendous simplification in the expression above and the full quadratic term becomes

$$T_1 + T_2 + R = \frac{1}{\omega_1^2 + \omega_1\omega_2} \text{Tr}(e^{-\beta H_0} [H_I(\omega_1), [H_I(\omega_2), C_I(\omega_3)]]) + \dots \quad (\text{B.27})$$

Even though the integral above is over three variables it is understood that when we evaluate the trace, this will force the constraint  $\omega_3 = \omega_1 + \omega_2$ .

**Result: General structure of the perturbative expansion:** From the examples above, we arrive at the following general structure of the perturbative expansion. In the perturbative expansion, there are two terms that are multiplied by phases dependent linearly on  $\tau$ . One term comes from the expansion of  $T(\beta)$ . the other term comes from the *lower* limit of the time-integrals. The two example calculations above show that these two terms cancel with each other.

Since the full amplitude cannot depend on  $\tau$  in any manner, this cancellation *must* continue to all orders. Therefore, *for generic frequencies of the operators* that appear in the perturbative expansion, the only term that can survive from the multiple time-integrals comes from the *upper limit* of integration. The contribution from the lower-limit of integration cancels with the contribution from (B.11) for generic values of  $\omega_i$ .

However, this is *not* the full contribution to the correlation function. As pointed out below (B.19) and in the discussion leading to (B.27), there may be terms in the correlation function that, in the space of frequencies of the insertions, appear on surfaces of codimension 1 or higher. These terms are, by themselves, independent of  $\tau$  and, in general, our argument that they cancel does not apply.

For instance, in (B.11) we may expect to get a finite contribution to the correlator from frequencies that satisfy  $\sum \omega_i = 0$ . We can quantify this contribution by extracting the part in the product of the interaction Hamiltonians that is proportional

a delta function in the  $\omega_n$  (B.11)

$$(-1)^n \int_0^\beta dz_1 \int_0^{z_1} dz_2 \dots \int_0^{z_{n-1}} dz_n e^{-i \sum \omega_i (\tau - iz_i)} H(\omega_1) \dots H(\omega_n) = Z_1(\omega_i) 2\pi \delta(\sum \omega_i) + \dots, \quad (\text{B.28})$$

where  $\dots$  indicates terms that contribute for generic values of  $\omega_i$ . Then we set

$$(1 + Z_1) = \sum_n \int \prod \frac{d\omega_i}{2\pi} Z_1(\omega_i) 2\pi \delta(\sum \omega_i). \quad (\text{B.29})$$

However, one may also have contributions that appear from terms where the sum of frequencies in (B.7) cancels with a frequency from the lower-limit of real-time integration from the commutators. We write this contribution as  $Z_2$  and we will quantify it when we turn to the Schwinger-Keldysh formalism.

This leads to the following general result At  $n^{\text{th}}$  order in perturbation theory we find that

$$\begin{aligned} & \text{Tr}(e^{-\beta H} C(t)) \\ &= \sum_n \int \prod_{i=1}^{n+1} \frac{d\omega_i}{2\pi} \text{Tr}(e^{-\beta H_0} (1 + Z_1) g(\omega_i) [H_I(\omega_1), \dots, [H_I(\omega_n), C_I(\omega_{n+1})]]) e^{i \sum \omega_i t} + Z_2), \end{aligned} \quad (\text{B.30})$$

where the factors  $Z_1$  and  $Z_2$  are discussed above. Even though the integral runs over  $n + 1$  variables, the thermal trace yields  $\delta(\omega_1 + \dots \omega_{n+1})$  and therefore all functions depend only on  $n$  variables. The function  $g(\omega_i)$  comes from the upper limit of time-integration and is therefore given by

$$g(\omega_i) = \frac{(-1)^n}{\prod_{k=1}^n \sum_{j=1}^k \omega_j} = \frac{(-1)^n}{\omega_1(\omega_1 + \omega_2) \dots (\omega_1 + \dots \omega_n)}. \quad (\text{B.31})$$

The alert reader might worry that (B.30) that  $H_0$ ,  $H_I$  and also  $C_I$  are all implicitly dependent on  $\tau$ . However, consider making the split between the free and the interacting part at a different time  $\tau' = \tau + x$ . Then we note immediately that

$$H'_0 = e^{iHx} H_0 e^{-iHx}; \quad H'_I = e^{iHx} H_I e^{-iHx}. \quad (\text{B.32})$$

---

However, denoting the *Heisenberg picture* operator by  $C_H$ , we have

$$\begin{aligned}
C'_I(\omega) &= \int_{-\infty}^{\infty} e^{iH_0 t} C_H(\tau') e^{-iH_0 t} e^{i\omega t} dt \\
&= \int_{-\infty}^{\infty} (e^{iHx} e^{iH_0 t} e^{-iHx}) (e^{iHx} C_H(\tau) e^{-iHx}) (e^{iHx} e^{-iH_0 t} e^{-iHx}) \\
&= e^{iHx} C_I(\omega) e^{-iHx}.
\end{aligned} \tag{B.33}$$

We now see, using the cyclicity of the trace that the factors of  $e^{-iHx}$  all cancel on the right hand side of (B.30) so this correlator does not depend on  $\tau$  as expected.

The result (B.30) can be easily generalized to evaluate a Wightman function that involves insertions at different times. We find that

$$\begin{aligned}
\text{Tr}(e^{-\beta H} C(t_1) \dots C(t_n)) &= \sum \int \left( \prod_{j,l} \frac{d\omega_l^j}{2\pi} \right) \prod_j g(\omega_l^j) e^{i \sum_{j,l} \omega_l^j t_j} \text{Tr} \left( e^{-\beta H_0} (1 + Z_1) \right. \\
&\times [H_I(\omega_1^1) \dots [H_I(\omega_{s_1}^1), C_I(\omega_{s_1+1}^1) \dots] \dots [H_I(\omega_1^n), \dots [H_I(\omega_{s_n}^n), C_I(\omega_{s_n+1}^n)] \dots] + Z_2 \Big).
\end{aligned} \tag{B.34}$$

Physically, this formula can be understood as follows. Consider taking  $\tau \rightarrow -\infty$ . This means that the split between the free and the interaction Hamiltonian is performed at  $t = -\infty$ . Then, if we proceed *naively* we might imagine that

1. By means of a suitable turning on/off function for the interaction we can make the full Hamiltonian coincide with the free Hamiltonian at  $\tau = -\infty$ .
2. In the time-integrals that arise from the Dyson expansion, we can ignore all the terms that arise from the lower limit of integration.

These steps are too naive because in the thermal case, as we adiabatically turn on the interaction we may heat or cool the state or change it in some other manner. This is the explanation for the term  $Z_1$  above. In fact, if the system does not *thermalize* effectively, then some contributions from early times may remain important even at late times and this is the physical explanation for the term  $Z_2$  above.

If we choose the interaction-term carefully so that it does not change the temperature of the system then  $Z_1$  may just be a numerical factor that will cancel when we compute thermal expectation values since it will also appear in the partition

function. If the system thermalizes effectively then  $Z_2 = 0$  but this is a very subtle issue as we discuss below.

## Schwinger-Keldysh formalism

In this section we will briefly describe the Schwinger-Keldysh formalism, which yields a diagrammatic approach to computing thermal Wightman functions in relativistic field theories. In the process we will also clarify the functions  $Z_1$  and  $Z_2$  above. Consider again the thermal expectation value (B.1). We now give small negative imaginary parts to the time coordinates  $t_i \rightarrow t_i - i\epsilon_i$  so that  $\epsilon_1 > \epsilon_2 > \dots \epsilon_n$ . At the end of the calculation we will take  $\epsilon_i \rightarrow 0$ . Then we can represent all the points on a time-contour that runs from  $-\infty - i\epsilon_n \rightarrow \infty - i\epsilon_n$ , snakes back to  $-\infty - i\epsilon_n$ , then moves down in imaginary time to  $-\infty - i\epsilon_{n-1}$  goes to  $+\infty - i\epsilon_{n-1}$  and so on. At the end the contour moves in imaginary time and ends up at  $t = -\infty - i\beta$  as shown in Figure B.1a.

To write an expression for the correlator using this contour, we adopt the notation

$$U_{I_i}(t_1, t_2) \equiv e^{-i \int_{t_1}^{t_2} H_{I_i}(\bar{t} - i\epsilon_i) d\bar{t}}. \quad (\text{B.35})$$

Then we can write, using the analysis of the previous section,

$$\begin{aligned} & \text{Tr}(e^{-\beta H} \phi(t_1, \vec{x}_1) \phi(t_2, \vec{x}_2) \dots \phi(t_n, \vec{x}_n)) \\ &= \text{Tr}(e^{-\beta H_0} \mathcal{T}_c \left\{ T(\beta) U_{I_1}(-\infty, \infty) \phi_I(t_1, \vec{x}_1) U_{I_1}(\infty, -\infty) \right. \\ & \left. U_{I_2}(-\infty, \infty) \phi_I(t_2, \vec{x}_2) U_{I_2}(\infty, -\infty) \dots U_{I_n}(-\infty, \infty) \phi_I(t_n, \vec{x}_n) U_{I_n}(\infty, -\infty) \right\}), \end{aligned} \quad (\text{B.36})$$

where  $\mathcal{T}_c$  denotes ordering *along* the contour.

Now, in the limit where the  $\epsilon_i \rightarrow 0$ , note that the expression (B.36) has multiple redundancies since parts of the various  $U_I$  operators cancel with each other. In Figure B.1a, for instance, the red parts of the contour cancel and so do the blue parts, leaving only the thick black part. This allows us to collapse the contour of B.1a to B.1b. Even the contour of B.1b has redundancies. However, it is convenient to retain these redundancies in order to obtain easy Feynman rules.

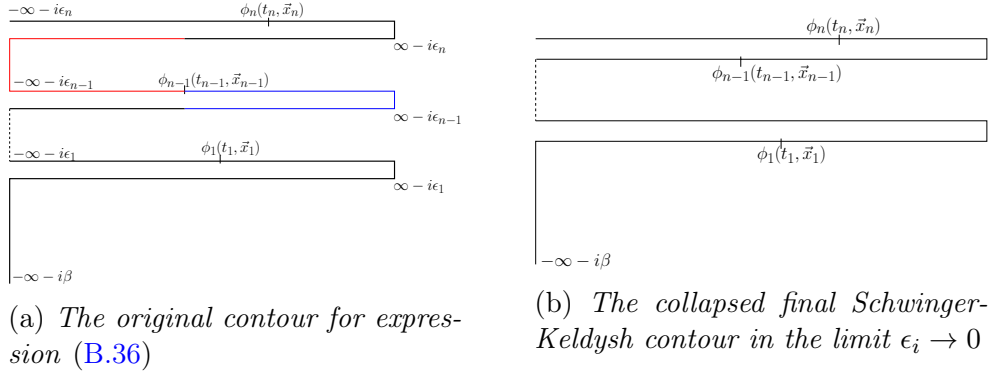


Figure B.1: The Schwinger-Keldysh contour

Note that the final number of horizontal legs in the collapsed contour of Figure B.1b is  $\tilde{n}$  where  $\tilde{n} = n$  if  $n$  is even and  $\tilde{n} = n + 1$  if  $n$  is odd. This is because the contour must return to  $-\infty$  before descending to  $-\infty - i\beta$ .

To obtain the Feynman rules, we now introduce  $\tilde{n} + 1$  types of fields, corresponding to the factors  $\tilde{n}$  horizontal legs of the contour and the single vertical leg. We can define a contraction<sup>1</sup> of these  $\tilde{n} + 1$  fields that can be evaluated in terms of ordinary interaction-picture fields as follows

$$D_{ij}(t_1, \vec{x}_1, t_2, \vec{x}_2) = \frac{1}{Z_0} \times \begin{cases} \text{Tr}(e^{-\beta H_0} \mathcal{T} \phi_I(t_1, \vec{x}_1) \phi_I(t_2, \vec{x}_2)) & i = j \text{ and } n - i \text{ even,} \\ \text{Tr}(e^{-\beta H_0} \overline{\mathcal{T}} \phi_I(t_1, \vec{x}_1) \phi_I(t_2, \vec{x}_2)) & i = j \text{ and } n - i \text{ odd,} \\ \text{Tr}(e^{-\beta H_0} \phi_I(t_1, \vec{x}_1) \phi_I(t_2, \vec{x}_2)) & i > j, \\ \text{Tr}(e^{-\beta H_0} \phi_I(t_2, \vec{x}_2) \phi_I(t_1, \vec{x}_1)) & i < j. \end{cases} \quad (\text{B.37})$$

The first two lines above correspond to time-ordered and anti-time-ordered thermal expectation values whereas the last two lines correspond to Wightman functions where the field that appears later on the contour is placed first. These two-point functions can be calculated using (4.28) and (4.30). For instance, the time-ordered

<sup>1</sup>The contraction can be defined, as usual, as the difference of the contour-ordered product and the “normal ordered product”. However, the “normal ordered product” must be defined, by making a Bogoliubov transform of the creation and annihilation operators so that its *thermal* expectation value vanishes. This is explained in [128]

propagators are,

$$\frac{1}{Z_0} \text{Tr}(e^{-\beta H_0} \mathcal{T} \phi_I(t_1, \vec{x}_1) \phi_I(t_2, \vec{x}_2)) = \int \frac{d^{d-1} \vec{k}}{2(2\pi)^d \omega_k} e^{i\vec{k} \cdot (\vec{x}_1 - \vec{x}_2)} \frac{e^{-i\omega_k |t_1 - t_2|} + e^{-\beta \omega_k} e^{i\omega_k |t_1 - t_2|}}{1 - e^{-\beta \omega_k}}. \quad (\text{B.38})$$

We can Fourier transform the propagator to obtain a momentum-space expression.

$$D_{ij}(k_1)(2\pi)^d \delta(k_1 + k_2) = \int d^d x_1 d^d x_2 D_{ij}(x_1, x_2) e^{-ik_1 \cdot x_1 - ik_2 \cdot x_2}, \quad (\text{B.39})$$

and these are the expressions listed in (4.33).

The second feature that will appear when we expand out (B.36) using Wick's theorem is that the interaction Hamiltonian appears with a positive sign for odd legs of the contour and a negative sign for even legs of the contour. These rules also apply to the vertical segment where we take the value of  $t$  to be complex. If both legs are on the vertical segment, then the propagator is the Euclidean two-point function and if one leg is on the vertical segment and another is on a horizontal segment then the propagator is the analytically continued Wightman function.

Therefore, in the end, when we expand out (B.36) and take  $\epsilon_i \rightarrow 0$ , we get the following Feynman rules

1. There are  $\tilde{n} + 1$ -types of interaction vertices. Of these  $\tilde{n}$  correspond to the different  $H_I(t)$  on the horizontal parts of the contour. The 0<sup>th</sup> vertex corresponds to the interaction vertex on the vertical part of the contour. The  $j^{\text{th}}$  vertex connects only fields of type  $i$  to each other and has a coefficient  $(-1)^{n-j}(-i)$ . The 0<sup>th</sup> vertex comes has a coefficient  $(-1)$ .
2. All interaction vertices on the horizontal parts of the contour are integrated from time  $-\infty$  to  $\infty$  and over all space.
3. The interaction vertex on the vertical part of the contour is integrated in Euclidean time from  $[0, \beta]$  and over all space.
4. There are  $(\tilde{n} + 1)^2$ -types of propagators that connect fields of type  $i$  to fields of type  $j$  as given in (B.37)
5. The external legs correspond to fields of type  $1 \dots n$ .

---

**More on the vertical part** The vertical part of the contour corresponds to a very subtle term. First note that the Feynman-diagram expansion yields terms where interaction Hamiltonians from the vertical part only contract with each other through a Euclidean propagator. These terms contribute a disconnected set of graphs that are not connected to the external points. This is an overall numerical prefactor that is clearly just  $\frac{\text{Tr}(e^{-\beta H})}{\text{Tr}(e^{-\beta H_0})}$ .

Now, as we take the vertical part of the contour in real time to  $-\infty$ , we may expect that the mixed propagators that connect the vertical and horizontal part die off due to the Riemann-Lebesgue lemma. However, this does not always happen because some terms in the Feynman diagram may continue to contribute at  $t = -\infty$ . This is in contrast to the situation in perturbation theory about the vacuum, where by evolving infinitely along a slightly imaginary direction we can project out all contributions except those corresponding to the vacuum. It is this contribution from the vertical part of the contour that leads to the factors  $Z_1$  and  $Z_2$  in (B.30). This subtlety has been discussed in the thermal field theory literature and we refer the reader to [101, 103, 129] for more details. In our calculations in the main text, we will *not* include the contribution of the vertical part of the contour. We do not believe that this will materially affect our results, but we leave a more detailed discussion of these effects to a later study.

## Interactions in the BTZ black hole

In this appendix, we provide some more details of holographic contact Witten diagrams for the BTZ black hole. We consider a four-point interaction between scalar field with dimensions  $\Delta_i$ . In the BTZ black-hole we can explicitly compute the bulk-boundary propagators, but our analysis here is entirely *complementary* to the analysis in the main text. The alert reader may have noticed that in using (4.88) in the main text, we did not need to use the condition of linear dependence of the normals. This condition is only meaningful if less than  $d + 1$ -singularities collide since otherwise it is met trivially. In this Appendix, we will see the relevance of this condition for a four-point function and we will not need to use (4.89) at all in this Appendix.

We will consider the *Euclidean, planar* BTZ black hole with metric

$$ds^2 = (r^2 - r_+^2)d\tau^2 + \frac{1}{r^2 - r_+^2}dr^2 + r^2d\phi^2. \quad (\text{B.40})$$

Here the temperature is given by  $\beta = T^{-1} = \frac{2\pi}{r_+}$ . The coordinate  $r$  here is related to the coordinate  $z$  used in the main text through  $r = \frac{1}{z}$ .

The bulk to boundary propagator in this geometry between a boundary point  $(\tau_i, \phi_i)$  and a bulk point  $(\tau, r, \phi)$  can then be found to be [130]

$$K_{\Delta_i} = \frac{N_{\Delta_i}}{\left( \cosh(r_+(\phi_i - \phi))\frac{r}{r_+} - \cos(r_+(\tau_i - \tau))\sqrt{\frac{r^2}{r_+^2} - 1} \right)^{\Delta_i}}. \quad (\text{B.41})$$

A contact Witten diagram in Euclidean space can then be calculated to be

$$G(t_i, \phi_i) = \int r dr d\tau d\phi \prod_{i=1}^4 \frac{N_{\Delta_i}}{\left( \cosh(r_+(\phi_i - \phi))\frac{r}{r_+} - \cos(r_+(\tau_i - \tau))\sqrt{\frac{r^2}{r_+^2} - 1} \right)^{\Delta_i}}, \quad (\text{B.42})$$

where  $\Delta_i$  are the dimensions of the fields that participate in the interaction and  $N_{\Delta_i}$  is a normalization that will be irrelevant for us.

To get the Lorentzian Wightman function with arguments extended in imaginary time, we can write  $\tau_i = it_i + \delta_i$  and the ordering in the Wightman correlator is set by the ordering of the  $\delta_i$ . Similarly, we can extend the transverse coordinates in the imaginary direction through  $\phi_i = x_i + i\epsilon_i$  in the imaginary direction inside the integral expression (B.42). Let us order the  $\delta_i$  so that  $\delta_1 < \delta_2 < \delta_3 < \delta_4$ . Without loss of generality, we set  $\delta_1 = \epsilon_1 = 0$ ; this just corresponds to setting the first point in the four-point function to the origin, which can be done by a translation. Then, to check the analyticity properties in position space, we need to check the following property: *Provided (i)  $\delta_i - \delta_{i-1} > 0$  and (ii)  $|\delta_i - \delta_{i-1}| > |\epsilon_i - \epsilon_{i-1}|$  and (iii)  $|\beta - \delta_4| > |\epsilon_4|$ , the integral should not have any singularities.*

Notice that the *integrand* in (B.42) then has singularities whenever

$$S_i = \cosh(r_+(x_i + i\epsilon_i - \phi))\frac{r}{r_+} - \cos(r_+(it_i + \delta_i - \tau))\sqrt{\frac{r^2}{r_+^2} - 1} = 0. \quad (\text{B.43})$$

---

We see that the first bulk-boundary propagator cannot encounter a singularity. But the other three bulk-boundary propagators can encounter singularities and in principle, either two or three singularities can collide at a point on the integration contour. We now show that this cannot happen in such a way as to satisfy (4.88).

**Two singularities colliding** We will now prove that that contour cannot be pinched by the meeting of any *two* singularities. Notice that when  $S_i = 0$ , we have

$$\begin{aligned} \frac{\partial S_i}{\partial r} &= \frac{1}{r_+} \left( \cosh(r_+(x_1 + i\epsilon_1 - \phi)) - \frac{\frac{r}{r_+}}{\sqrt{(\frac{r}{r_+})^2 - 1}} \cos(r_+(it_i + \delta_i - \tau)) \right) \\ &= \frac{-1}{r_+} \cosh(r_+(x_1 + i\epsilon_1 - \phi)) \frac{1}{(\frac{r}{r_+})^2 - 1}. \end{aligned} \quad (\text{B.44})$$

If the contour is pinched between two singularities, and if  $r < \infty$ , we would find, by demanding linear dependence of the derivatives, that

$$\begin{aligned} \frac{\sinh(r_+(x_1 + i\epsilon_1 - \phi))}{\sinh(r_+(x_2 + i\epsilon_2 - \phi))} &= \frac{\sin(r_+(it_1 + \delta_1 - \tau))}{\sin(r_+(it_2 + \delta_2 - \tau))} = \frac{\cosh(r_+(x_1 + i\epsilon_1 - \phi))}{\cosh(r_+(x_2 + i\epsilon_2 - \phi))} \\ &= \frac{\cos(r_+(it_1 + \delta_1 - \tau))}{\cos(r_+(it_2 + \delta_2 - \tau))}. \end{aligned} \quad (\text{B.45})$$

These conditions require the points to be either coincident or else separated by  $\Delta\epsilon = \Delta\delta = \frac{2\pi}{r_+}$ . The second case, requires the imaginary shift to be larger than  $\beta$ , whereas the first case involves a coincident singularity.

**Three singularities colliding** We may also consider the case, where three  $S_i$  vanish simultaneously for some  $r < \infty$ . In this case, imposing the linear dependence of derivatives implies that, for some constants  $\gamma_1, \gamma_2$  we have

$$\begin{aligned} \cosh(r_+(x_3 + i\epsilon_3 - \phi)) &= \gamma_1 \cosh(r_+(x_1 + i\epsilon_1 - \phi)) + \gamma_2 \cosh(r_+(x_2 + i\epsilon_2 - \phi)); \\ \sinh(r_+(x_3 + i\epsilon_3 - \phi)) &= \gamma_1 \sinh(r_+(x_1 + i\epsilon_1 - \phi)) + \gamma_2 \sinh(r_+(x_2 + i\epsilon_2 - \phi)); \\ \cos(r_+(it_3 + \delta_3 - \tau)) &= \gamma_1 \cos(r_+(it_1 + \delta_1 - \tau)) + \gamma_2 \cos(r_+(it_2 + \delta_2 - \tau)); \\ \sin(r_+(it_3 + \delta_3 - \tau)) &= \gamma_1 \sin(r_+(it_1 + \delta_1 - \tau)) + \gamma_2 \sin(r_+(it_2 + \delta_2 - \tau)). \end{aligned} \quad (\text{B.46})$$

Using the fact that  $\cosh^2 x - \sinh^2 x = \cos^2 x + \sin^2 x = 1$  we see that the equations above imply that we must have

$$\cosh(r_+(x_1 - x_2 + i\epsilon_1 - i\epsilon_2)) = \cos(r_+(i(t_1 - t_2) + (\delta_1 - \delta_2))), \quad (\text{B.47})$$

which immediately tells us that (by writing the  $\cos$  as a  $\cosh$  and equating the imaginary part of the argument and excluding the case where the shift in imaginary coordinates is larger than  $\beta$ ) that  $|\epsilon_1 - \epsilon_2| = |\delta_1 - \delta_2|$  at the singularity. Namely that the singularity cannot occur if we keep the difference of  $\delta$ 's larger than the difference of  $\epsilon$ .

For the four-point function, we cannot have the situation where four or more singularities coincide in the interior. This situation is relevant for higher-point functions and in such a case, the linear dependence of the normals can be met trivially. We now need to impose the additional condition, (4.89) imposed in the text: the contour cannot be pinched if the imaginary part of the boundary points are on one side of a hyperplane since by deforming the contour, we can remove the singularities. However, it is interesting that this condition does not seem to be required for Witten diagrams with a small number of external legs.

## Appendix C

### Scattering in the Reissner-Nordström geometry at large angular momenta

In Section 5.3.5, we noticed that the fractional difference between the expected Boltzmann factor and the numerical Boltzmann factor at the inner horizon for large  $\ell$  modes in Reissner-Nordström black holes tends to zero. Here, we will explain this feature by using WKB approximation to solve wave the equation at large  $\ell$ . The exact form of the metric is given in Section 5.3.

$$ds^2 = -f(r)dt^2 + f(r)^{-1}dr^2 + r^2d\Omega_{d-1}^2. \quad (\text{C.1})$$

We reproduce the near horizon form of  $f(r)$ .

$$f(r) = 2\kappa_{\pm}(r - r_{\pm}); \quad r \rightarrow r_{\pm}. \quad (\text{C.2})$$

We consider a massless scalar Klein-Gordon field  $\phi$ . The wave equation can be solved with an ansatz of the form

$$\phi_{\omega,\ell}(r, t, \Omega) = \frac{1}{r^{(d-1)/2}}\psi_{\ell,\omega}(r_*)e^{-i\omega t}Y_{\ell}^m(\Omega), \quad (\text{C.3})$$

which leads to

$$\begin{aligned} \psi_{\ell,\omega}''(r_*) - V(r_*)\psi_{\ell,\omega}(r_*) &= 0, \\ V(r_*) &= -\omega^2 + \frac{f(r)}{r^2} \left( \ell(\ell + d - 2) + \frac{(d-3)(d-1)}{4}f(r) + \frac{(d-1)}{2}rf'(r) \right), \end{aligned} \quad (\text{C.4})$$

where  $r_*$  is the *tortoise* coordinate, defined by  $dr_* = \frac{dr}{f(r)}$ .

## Large- $\ell$ behaviour

At large  $\ell$ , the potential near outer horizon takes the following form.

$$V(r_*) \approx -\omega^2 + \frac{2\kappa_+(r-r_+)}{r_+^2} \ell^2. \quad (\text{C.5})$$

Solving the  $\psi$ -equation, Eq. (C.4), with the above potential yields,

$$\psi_{\ell,\omega}(r_*) \approx A_B K_{i\omega/\kappa_+} \left( \frac{\ell}{r_+\kappa_+} \sqrt{f(r)} \right) + B_B I_{i\omega/\kappa_+} \left( \frac{\ell}{r_+\kappa_+} \sqrt{f(r)} \right). \quad (\text{C.6})$$

In the regime,  $\ell(r-r_+) \gg 1$  and  $r-r_+ \ll r_+$ , this solution can be approximated as

$$A_B \sqrt{\frac{\pi}{2}} \left( \frac{r_+\kappa_+}{\ell\sqrt{f(r)}} \right)^{\frac{1}{2}} e^{-\frac{\ell\sqrt{f(r)}}{r_+\kappa_+}} + B_B \sqrt{\frac{1}{2\pi}} \left( \frac{r_+\kappa_+}{\ell\sqrt{f(r)}} \right)^{\frac{1}{2}} \left[ i e^{-\pi\omega} e^{-\frac{\ell\sqrt{f(r)}}{r_+\kappa_+}} + e^{\frac{\ell\sqrt{f(r)}}{r_+\kappa_+}} \right]. \quad (\text{C.7})$$

The near horizon Bessel solution can be matched with a WKB solution in the large- $\ell$  limit. For large- $\ell$ , the WKB approximation is valid at all radial points where  $f(r)$  is finite (and nonzero).

$$\psi_{\text{wkb}}(r_*) \approx A_{\text{wkb}} e^{-\int^{r_*} \sqrt{V} dr_*} + B_{\text{wkb}} e^{\int^{r_*} \sqrt{V} dr_*}. \quad (\text{C.8})$$

Near the boundary,

$$\psi_{\text{wkb}}(r_*) \approx A_{\text{wkb}} e^{-\ell r_*} + B_{\text{wkb}} e^{\ell r_*}, \quad 1 \ll r \ll \ell. \quad (\text{C.9})$$

Near the outer horizon,

$$\psi(r_*) \approx A_{\text{wkb}} e^X e^{-\frac{\ell}{r_+\kappa_+} \sqrt{f(r)}} + B_{\text{wkb}} e^{-X} e^{\frac{\ell}{r_+\kappa_+} \sqrt{f(r)}}, \quad \frac{1}{\ell} \ll r-r_+ \ll r_+, \quad (\text{C.10})$$

where,

$$X = \int_{\zeta_*^+}^{\zeta_*^\infty} \sqrt{V(r)} dr_* \quad (\text{C.11})$$

with  $\frac{1}{\ell} \ll \zeta_+ - r_+ \ll r_+$  and  $1 \ll \zeta_\infty \ll \ell$  close to boundary.

---

To a very good approximation, we can write

$$X \approx l \int_{-\infty}^0 \frac{\sqrt{f(r)}}{r} dr_* \equiv l\Lambda, \quad \Lambda > 0. \quad (\text{C.12})$$

Near the boundary, the normalizable mode behaves as

$$\psi(r_*) \approx N \sqrt{r_*} J_{\frac{d}{2}} \left( -ir_* \sqrt{\ell^2 - \omega^2} \right), \quad r \gg \ell, \quad (\text{C.13})$$

where  $N$  is a normalization constant. For large- $\ell$ , the normalizable mode behaves as

$$\psi(r_*) \approx N \frac{i}{\sqrt{\ell}} \frac{1}{\sqrt{2\pi}} \left( e^{-\ell r_*} e^{\frac{i\pi}{8}d} + i e^{\ell r_*} e^{\frac{3i\pi}{8}d} \right), \quad 1 \ll r \ll \ell. \quad (\text{C.14})$$

Matching this with the WKB solution Eq. (C.9), we get

$$\frac{A_{\text{wkb}}}{B_{\text{wkb}}} = -i e^{-\frac{i\pi}{4}d}. \quad (\text{C.15})$$

Near horizon behaviour would now become

$$\psi(r_*) \approx N \frac{i}{\sqrt{\ell}} \frac{1}{\sqrt{2\pi}} \left( -i e^{-\frac{i\pi}{4}d} e^{l\Lambda} e^{-\frac{\ell}{r_+\kappa_+} \sqrt{f(r)}} + e^{-l\Lambda} e^{\frac{\ell}{r_+\kappa_+} \sqrt{f(r)}} \right). \quad (\text{C.16})$$

We see that the coefficient of  $e^{\frac{\ell}{r_+\kappa_+} \sqrt{f(r)}}$  is exponentially suppressed. Hence, in the large  $\ell$  limit,

$$B_B = 0 \quad (\text{C.17})$$

Close to horizon,

$$\psi_{\ell,\omega}(r_*) = A_B K_{i\omega/\kappa_+} \left( \frac{\ell}{r_+\kappa_+} \sqrt{f(r)} \right) \quad (\text{C.18})$$

Now we consider the near horizon ( $\ell(r - r_+) \ll 1$ ) limit.

$$\begin{aligned} \psi_{\ell,\omega}(r_*) &= \frac{A_B}{2} \left[ \left( \frac{\ell}{2r_+\kappa_+} \right)^{\frac{i\omega}{\kappa_+}} \Gamma\left(-\frac{i\omega}{\kappa_+}\right) e^{i\omega r_*} + (\omega \rightarrow -\omega) \right] \\ &= \frac{A_B}{2} \left( \frac{\pi\kappa_+}{\omega \sinh\left(\frac{\pi\omega}{\kappa_+}\right)} \right)^{1/2} \left[ e^{\frac{i\delta_{\omega,\ell}}{2}} e^{i\omega r_*} + e^{\frac{-i\delta_{\omega,\ell}}{2}} e^{-i\omega r_*} \right], \end{aligned} \quad (\text{C.19})$$

where

$$\frac{\delta_{\omega,\ell}}{2} = \arg \left( \left( \frac{\ell}{2r_+\kappa_+} \right)^{\frac{i\omega}{\kappa_+}} \Gamma\left(-\frac{i\omega}{\kappa_+}\right) \right); \quad \text{large-}\ell. \quad (\text{C.20})$$

The mode expansion of the scalar field just outside the horizon as  $r \rightarrow r_+$  is

$$\phi(r, t, \Omega) = \int \frac{d\omega}{2\pi} \frac{1}{\sqrt{2\omega}} \frac{1}{r_+^{\frac{d-1}{2}}} \sum_{\ell,m} e^{-i\omega t} Y_{\ell,m}(\Omega) a_{\omega,\ell} \left[ e^{-i\delta_{\omega,\ell}} e^{-i\omega r_*} + e^{i\delta_{\omega,\ell}} e^{i\omega r_*} \right] + \text{h.c.} \quad (\text{C.21})$$

### Scattering between horizons for large $\ell$

The mode expansion just inside the outer horizon, as  $r \rightarrow r_+ + 0^-$  is as follows.

$$\phi(r, t, \Omega) = \int \frac{d\omega}{2\pi} \frac{1}{\sqrt{2\omega}} \frac{1}{r_+^{\frac{d-1}{2}}} \sum_{\ell,m} e^{-i\omega r_*} \left[ e^{-i\delta_{\omega,\ell}} a_{\omega,\ell} e^{-i\omega t} Y_{\ell,m}(\Omega) + \tilde{a}_{\omega,\ell} e^{i\omega t} \bar{Y}_{\ell,m}(\Omega) \right] + \text{h.c.} \quad (\text{C.22})$$

While, just outside the inner horizon, as  $r \rightarrow r_- + 0^+$ ,

$$\phi(r, t, \Omega) = \int \frac{d\omega}{2\pi} \frac{1}{\sqrt{2\omega}} \frac{1}{r_-^{\frac{d-1}{2}}} \sum_{\ell,m} e^{-i\omega r_*} \left[ b_{\omega,\ell} e^{-i\omega t} Y_{\ell,m}(\Omega) + \tilde{b}_{\omega,\ell} e^{i\omega t} \bar{Y}_{\ell,m}(\Omega) \right] + \text{h.c.} \quad (\text{C.23})$$

To compute the occupation numbers of the modes at the inner horizon, we need to relate the operators  $a$  and  $b$ . Consider a solution,  $Z(r)$ , to the wave equation such that

$$Z(r) \approx \Gamma\left(1 + i\frac{\omega}{\kappa_-}\right) \left( \frac{\ell\zeta}{2r_-\kappa_-} \right)^{-i\frac{\omega}{\kappa_-}} J_{i\frac{\omega}{\kappa_-}} \left( \frac{\ell}{r_-\kappa_-} \sqrt{|f(r)|} \right); \quad r - r_- \ll r_-, \quad (\text{C.24})$$

where  $\zeta$  is the factor introduced in the definition of the tortoise coordinate (5.45). Close to the inner horizon,

$$Z(r) = e^{-i\omega r_*}; \quad r \rightarrow r_- + 0^+ \quad (\text{C.25})$$

When we move slightly away from the inner horizon such that  $\ell(r - r_-) \gg 1$  but  $r - r_- \ll r_-$ ,

$$Z(r) \approx \Gamma\left(1 + i\frac{\omega}{\kappa_-}\right) \left(\frac{\ell\zeta}{2r - \kappa_-}\right)^{-i\frac{\omega}{\kappa_-}} \left(\frac{r - \kappa_-}{2\pi\ell\sqrt{|f(r)|}}\right)^{\frac{1}{2}} \times \left[ e^{-\frac{i\pi}{4}} e^{\frac{\pi\omega}{2\kappa_-}} e^{i\left(\frac{\ell}{r - \kappa_-}\sqrt{|f(r)|}\right)} + e^{\frac{i\pi}{4}} e^{-\frac{\pi\omega}{2\kappa_-}} e^{-i\left(\frac{\ell}{r - \kappa_-}\sqrt{|f(r)|}\right)} \right]. \quad (\text{C.26})$$

Away from the horizon, we can also use the large- $\ell$  WKB approximation.

$$Z(r) \approx \frac{1}{V^{1/4}} \left[ A_+ e^{i\int_{-\infty}^{r^*} \sqrt{V} dr^*} + B_+ e^{-i\int_{-\infty}^{r^*} \sqrt{V} dr^*} \right] \\ Z(r) \approx \frac{1}{V^{1/4}} \left[ A_- e^{i\int_{\infty}^{r^*} \sqrt{V} dr^*} + B_- e^{-i\int_{\infty}^{r^*} \sqrt{V} dr^*} \right], \quad (\text{C.27})$$

with,

$$A_- = A_+ e^{i\int_{-\infty}^{\infty} \sqrt{V} dr^*} = A_+ e^{i\theta} \quad B_- = B_+ e^{-i\int_{-\infty}^{\infty} \sqrt{V} dr^*} = B_+ e^{-i\theta}. \quad (\text{C.28})$$

Matching the WKB solution with the Bessel expansion near the inner horizon, we get

$$A_- = \Gamma\left(1 + i\frac{\omega}{\kappa_-}\right) \left(\frac{\ell\zeta}{2r - \kappa_-}\right)^{-i\frac{\omega}{\kappa_-}} \sqrt{\frac{\kappa_-}{2\pi}} e^{\frac{i\pi}{2}} e^{-\frac{\pi\omega}{2\kappa_-}}; \\ B_- = \Gamma\left(1 + i\frac{\omega}{\kappa_-}\right) \left(\frac{\ell\zeta}{2r - \kappa_-}\right)^{-i\frac{\omega}{\kappa_-}} \sqrt{\frac{\kappa_-}{2\pi}} e^{\frac{\pi\omega}{2\kappa_-}}. \quad (\text{C.29})$$

Close to the outer horizon,  $\ell(r_+ - r) \gg 1$  but  $r_+ - r \ll r_+$ , this solution can also be written as

$$Z(r) \approx \sqrt{\frac{2\pi}{\kappa_+} \frac{e^{\frac{\pi\omega}{2\kappa_+}}}{e^{\frac{2\pi\omega}{\kappa_+}} - 1}} \left[ (A_+ e^{i\frac{\pi}{4}} - B_+ e^{-i\frac{\pi}{4}} e^{\frac{\pi\omega}{\kappa_+}}) J_{-i\frac{\omega}{\kappa_+}} \left(\frac{\ell}{r_+ \kappa_+} \sqrt{|f(r)|}\right) \right. \\ \left. + (B_+ e^{-i\frac{\pi}{4}} - A_+ e^{i\frac{\pi}{4}} e^{\frac{\pi\omega}{\kappa_+}}) J_{i\frac{\omega}{\kappa_+}} \left(\frac{\ell}{r_+ \kappa_+} \sqrt{|f(r)|}\right) \right]. \quad (\text{C.30})$$

At the outer horizon, we can expand the Bessel function and substitute for  $A_+$

and  $B_+$  to get,

$$Z(r) = A_{\omega,\ell} e^{-i\omega r_*} + B_{\omega,\ell} e^{i\omega r_*}; \quad r \rightarrow r_+ - 0^+, \quad (\text{C.31})$$

where, for large- $\ell$ ,

$$\begin{aligned} A_{\omega,\ell} &= N_{\omega,\ell} \left[ e^{-\frac{\pi\omega}{2\kappa_-}} e^{i(\frac{\pi}{2}-\theta)} - e^{\frac{\pi\omega}{2\kappa_-}} e^{-i(\frac{\pi}{2}-\theta)} e^{\frac{\pi\omega}{\kappa_+}} \right] e^{-i\frac{\delta_{\omega,\ell}}{2}}; \\ B_{\omega,\ell} &= N_{\omega,\ell} \left[ e^{-\frac{\pi\omega}{2\kappa_-}} e^{i(\frac{\pi}{2}-\theta)} e^{\frac{\pi\omega}{\kappa_+}} - e^{\frac{\pi\omega}{2\kappa_-}} e^{-i(\frac{\pi}{2}-\theta)} \right] e^{i\frac{\delta_{\omega,\ell}}{2}}; \\ N_{\omega,\ell} &= e^{i\delta'_{\omega,\ell}} \sqrt{\frac{\sinh(\pi\frac{\omega}{\kappa_+}) e^{\frac{\pi\omega}{2\kappa_+}}}{\sinh(\pi\frac{\omega}{\kappa_-}) e^{\frac{2\pi\omega}{\kappa_+}} - 1}}; \\ e^{i\delta'_{\omega,\ell}} &= e^{\frac{i3\pi}{4}} \left( \frac{\ell\zeta}{2r_- \kappa_-} \right)^{-i\frac{\omega}{\kappa_-}} \sqrt{\frac{\Gamma(1+i\frac{\omega}{\kappa_-})}{\Gamma(1-i\frac{\omega}{\kappa_-})}}. \end{aligned} \quad (\text{C.32})$$

We can check that the Bogoliubov coefficients satisfy,

$$|A_{\omega,\ell}|^2 - |B_{\omega,\ell}|^2 = 1. \quad (\text{C.33})$$

Using the mode expansion near the horizons,

$$b_{\omega,\ell} = e^{-i\delta_{\omega,\ell}} A_{\omega,\ell}^* a_{\omega,\ell} - B_{\omega,\ell}^* \tilde{a}_{\omega,\ell}^\dagger. \quad (\text{C.34})$$

Using the constraints on operators  $a$  and  $\tilde{a}$ , Eq. (5.64), and large- $\ell$  Bogoliubov coefficients, Eq. (C.32), we get the Boltzmann factor at inner horizon.

$$\langle b_{\omega,\ell} b_{\omega',\ell'}^\dagger \rangle = \frac{1}{1 - e^{-\frac{2\pi\omega}{\kappa_-}}} \delta(\omega - \omega') \delta_{\ell,\ell'}, \quad \ell \gg 1. \quad (\text{C.35})$$

## References

- [1] J. D. Bekenstein, *Black holes and entropy*, *Phys. Rev. D* **7** (1973) 2333–2346.  
J. D. Bekenstein, *Generalized second law of thermodynamics in black hole physics*, *Phys. Rev. D* **9** (1974) 3292–3300. G. 't Hooft, *Dimensional reduction in quantum gravity*, *Conf. Proc. C* **930308** (1993) 284–296, [[gr-qc/9310026](#)].
- [2] J. M. Maldacena, *The Large  $N$  limit of superconformal field theories and supergravity*, *Int. J. Theor. Phys.* **38** (1999) 1113–1133, [[hep-th/9711200](#)].
- [3] E. Witten, *Anti-de Sitter space and holography*, *Adv. Theor. Math. Phys.* **2** (1998) 253–291, [[hep-th/9802150](#)].
- [4] S. S. Gubser, I. R. Klebanov and A. M. Polyakov, *Gauge theory correlators from noncritical string theory*, *Phys. Lett.* **B428** (1998) 105–114, [[hep-th/9802109](#)].
- [5] A. Laddha, S. G. Prabhu, S. Raju and P. Shrivastava, *The Holographic Nature of Null Infinity*, [2002.02448](#).
- [6] S. Raju, *Is Holography Implicit in Canonical Gravity?*, *Int. J. Mod. Phys.* **D28** (2019) 1944011, [[1903.11073](#)].
- [7] S. Banerjee, J.-W. Bryan, K. Papadodimas and S. Raju, *A toy model of black hole complementarity*, *JHEP* **05** (2016) 004, [[1603.02812](#)].
- [8] A. Strominger, *On BMS Invariance of Gravitational Scattering*, *JHEP* **07** (2014) 152, [[1312.2229](#)].
- [9] S. D. Mathur, *Fuzzballs and the information paradox: A Summary and conjectures*, [0810.4525](#).

- [10] S. Raju and P. Shrivastava, *Critique of the fuzzball program*, *Phys. Rev. D* **99** (2019) 066009, [[1804.10616](#)].
- [11] O. Lunin and S. D. Mathur, *Metric of the multiply wound rotating string*, *Nucl. Phys.* **B610** (2001) 49–76, [[hep-th/0105136](#)].
- [12] O. Lunin, S. D. Mathur and A. Saxena, *What is the gravity dual of a chiral primary?*, *Nucl. Phys.* **B655** (2003) 185–217, [[hep-th/0211292](#)].
- [13] V. S. Rychkov, *D1-D5 black hole microstate counting from supergravity*, *JHEP* **01** (2006) 063, [[hep-th/0512053](#)].
- [14] S. Banerjee, K. Papadodimas, S. Raju, P. Samantray and P. Shrivastava, *A Bound on Thermal Relativistic Correlators at Large Spacelike Momenta*, *SciPost Phys.* **8** (2020) 064, [[1902.07203](#)].
- [15] R. Penrose, *Structure of space-time*, in *Battelle Rencontres: 1967 lectures in mathematics and physics* (C. de Witt and J. Wheeler, eds.). New York: Benjamin, 1968.
- [16] K. Papadodimas, S. Raju and P. Shrivastava, *A simple quantum test for smooth horizons*, [1910.02992](#).
- [17] S. Hawking, *Particle Creation by Black Holes*, *Commun.Math.Phys.* **43** (1975) 199–220.
- [18] D. N. Page, *Average entropy of a subsystem*, *Phys. Rev. Lett.* **71** (1993) 1291–1294, [[gr-qc/9305007](#)].
- [19] D. N. Page, *Information in black hole radiation*, *Phys. Rev. Lett.* **71** (1993) 3743–3746, [[hep-th/9306083](#)].
- [20] S. D. Mathur, *The Information paradox: A Pedagogical introduction*, *Class. Quant. Grav.* **26** (2009) 224001, [[0909.1038](#)].
- [21] S. D. Mathur, *The Fuzzball proposal for black holes: An Elementary review*, *Fortsch. Phys.* **53** (2005) 793–827, [[hep-th/0502050](#)].

- 
- [22] A. Almheiri, D. Marolf, J. Polchinski and J. Sully, *Black Holes: Complementarity or Firewalls?*, *JHEP* **02** (2013) 062, [[1207.3123](#)].
- [23] T. Banks, M. R. Douglas, G. T. Horowitz and E. J. Martinec, *AdS dynamics from conformal field theory*, [hep-th/9808016](#).
- [24] J. de Boer and S. N. Solodukhin, *A Holographic reduction of Minkowski space-time*, *Nucl. Phys.* **B665** (2003) 545–593, [[hep-th/0303006](#)]. G. Arcioni and C. Dappiaggi, *Exploring the holographic principle in asymptotically flat space-times via the BMS group*, *Nucl. Phys.* **B674** (2003) 553–592, [[hep-th/0306142](#)]. G. Arcioni and C. Dappiaggi, *Holography in asymptotically flat space-times and the BMS group*, *Class. Quant. Grav.* **21** (2004) 5655, [[hep-th/0312186](#)]. M.-I. Park, *Testing holographic principle from logarithmic and higher order corrections to black hole entropy*, *JHEP* **12** (2004) 041, [[hep-th/0402173](#)]. S. N. Solodukhin, *Reconstructing Minkowski space-time*, *IRMA Lect. Math. Theor. Phys.* **8** (2005) 123–163, [[hep-th/0405252](#)]. F. Loran, *Phi<sup>4</sup>-model and holography in four dimensions*, *Phys. Lett.* **B605** (2005) 169–180, [[hep-th/0409267](#)]. C. Dappiaggi, *BMS field theory and holography in asymptotically flat space-times*, *JHEP* **11** (2004) 011, [[hep-th/0410026](#)]. G. Siopsis, *Correspondence principle for a brane in Minkowski space and vector mesons*, *JHEP* **10** (2005) 059, [[hep-th/0503245](#)]. C. Dappiaggi, V. Moretti and N. Pinamonti, *Rigorous steps towards holography in asymptotically flat spacetimes*, *Rev. Math. Phys.* **18** (2006) 349–416, [[gr-qc/0506069](#)]. R. B. Mann and D. Marolf, *Holographic renormalization of asymptotically flat spacetimes*, *Class. Quant. Grav.* **23** (2006) 2927–2950, [[hep-th/0511096](#)]. C. Dappiaggi, *BMS field theory and the open roads*, *J. Phys. Conf. Ser.* **33** (2006) 254–259. C. Dappiaggi, *Free field theory at null infinity and white noise calculus: A BMS invariant dynamical system*, [math-ph/0607055](#). D. Astefanesei, R. B. Mann and C. Stelea, *Note on counterterms in asymptotically flat spacetimes*, *Phys. Rev.* **D75** (2007) 024007, [[hep-th/0608037](#)]. G. Barnich and G. Compere, *Classical central extension for asymptotic symmetries at null infinity in three spacetime dimensions*, *Class. Quant. Grav.* **24** (2007) F15–F23, [[gr-qc/0610130](#)]. J. L. F. Barbon

- and C. A. Fuertes, *Holographic entanglement entropy probes (non)locality*, *JHEP* **04** (2008) 096, [[0803.1928](#)]. G. Barnich and C. Troessaert, *Symmetries of asymptotically flat 4 dimensional spacetimes at null infinity revisited*, *Phys. Rev. Lett.* **105** (2010) 111103, [[0909.2617](#)]. G. Barnich and C. Troessaert, *Aspects of the BMS/CFT correspondence*, *JHEP* **05** (2010) 062, [[1001.1541](#)]. A. Bagchi, *Correspondence between Asymptotically Flat Spacetimes and Nonrelativistic Conformal Field Theories*, *Phys. Rev. Lett.* **105** (2010) 171601, [[1006.3354](#)]. I. Papadimitriou, *Holographic renormalization as a canonical transformation*, *JHEP* **11** (2010) 014, [[1007.4592](#)]. W. Li and T. Takayanagi, *Holography and Entanglement in Flat Spacetime*, *Phys. Rev. Lett.* **106** (2011) 141301, [[1010.3700](#)]. G. Compere, F. Dehouck and A. Virmani, *On Asymptotic Flatness and Lorentz Charges*, *Class. Quant. Grav.* **28** (2011) 145007, [[1103.4078](#)]. A. Virmani, *Supertranslations and Holographic Stress Tensor*, *JHEP* **02** (2012) 024, [[1112.2146](#)]. G. Barnich, A. Gomberoff and H. A. Gonzalez, *The Flat limit of three dimensional asymptotically anti-de Sitter spacetimes*, *Phys. Rev.* **D86** (2012) 024020, [[1204.3288](#)]. R. N. C. Costa, *Holographic Reconstruction and Renormalization in Asymptotically Ricci-flat Spacetimes*, *JHEP* **11** (2012) 046, [[1206.3142](#)]. T. He, P. Mitra and A. Strominger, *2D Kac-Moody Symmetry of 4D Yang-Mills Theory*, *JHEP* **10** (2016) 137, [[1503.02663](#)]. I. Fujisawa and R. Nakayama, *Bondi-Metzner-Sachs surface-charge algebra via a Hamiltonian framework*, *Phys. Rev.* **D91** (2015) 126005, [[1503.03225](#)]. J. Gomis and G. Longhi, *Canonical realization of Bondi-Metzner-Sachs symmetry: Quadratic Casimir*, *Phys. Rev.* **D93** (2016) 025030, [[1508.00544](#)]. R. F. Penna, *BMS invariance and the membrane paradigm*, *JHEP* **03** (2016) 023, [[1508.06577](#)]. A. Vasy and M. Wrochna, *Quantum Fields from Global Propagators on Asymptotically Minkowski and Extended de Sitter Spacetimes*, *Annales Henri Poincaré* **19** (2018) 1529–1586, [[1512.08052](#)]. O. Baghchesaraei, R. Fareghbal and Y. Izadi, *Flat-Space Holography and Stress Tensor of Kerr Black Hole*, *Phys. Lett.* **B760** (2016) 713–719, [[1603.04137](#)]. M. R. Setare and H. Adami, *BMS type symmetries at null-infinity and near horizon of non-extremal black holes*, *Eur. Phys. J.* **C76** (2016) 687, [[1609.05736](#)]. D. Kapec, P. Mitra, A.-M.

- Raclariu and A. Strominger, *2D Stress Tensor for 4D Gravity*, *Phys. Rev. Lett.* **119** (2017) 121601, [[1609.00282](#)]. C. Cheung, A. de la Fuente and R. Sundrum, *4D scattering amplitudes and asymptotic symmetries from 2D CFT*, *JHEP* **01** (2017) 112, [[1609.00732](#)]. A. Strominger and A. Zhiboedov, *Superrotations and Black Hole Pair Creation*, *Class. Quant. Grav.* **34** (2017) 064002, [[1610.00639](#)]. T. McLoughlin and D. Nandan, *Multi-Soft gluon limits and extended current algebras at null-infinity*, *JHEP* **08** (2017) 124, [[1610.03841](#)]. S. Pasterski, S.-H. Shao and A. Strominger, *Flat Space Amplitudes and Conformal Symmetry of the Celestial Sphere*, *Phys. Rev. D* **96** (2017) 065026, [[1701.00049](#)]. S. Pasterski and S.-H. Shao, *Conformal basis for flat space amplitudes*, *Phys. Rev. D* **96** (2017) 065022, [[1705.01027](#)]. T. He, D. Kapec, A.-M. Raclariu and A. Strominger, *Loop-Corrected Virasoro Symmetry of 4D Quantum Gravity*, *JHEP* **08** (2017) 050, [[1701.00496](#)]. S. Pasterski, *Implications of Superrotations*, *Phys. Rept.* **829** (2019) 1–35, [[1905.10052](#)]. M. R. Setare and H. Adami, *Enhanced asymptotic  $BMS_3$  algebra of the flat spacetime solutions of generalized minimal massive gravity*, *Nucl. Phys.* **B926** (2018) 70–82, [[1703.00936](#)]. C. Batlle, V. Campello and J. Gomis, *Canonical realization of  $(2+1)$ -dimensional Bondi-Metzner-Sachs symmetry*, *Phys. Rev. D* **96** (2017) 025004, [[1703.01833](#)]. E. Melas, *On the representation theory of the Bondi–Metzner–Sachs group and its variants in three space–time dimensions*, *J. Math. Phys.* **58** (2017) 071705, [[1703.05980](#)]. M. Campiglia and R. Eyheralde, *Asymptotic  $U(1)$  charges at spatial infinity*, *JHEP* **11** (2017) 168, [[1703.07884](#)]. M. Campiglia, L. Coito and S. Mizera, *Can scalars have asymptotic symmetries?*, *Phys. Rev. D* **97** (2018) 046002, [[1703.07885](#)]. C. Batlle, D. Delmastro and J. Gomis, *Non-Relativistic  $BMS$  algebra*, [[1705.03739](#)]. G. Compère and A. Fiorucci, *Asymptotically flat spacetimes with  $BMS_3$  symmetry*, *Class. Quant. Grav.* **34** (2017) 204002, [[1705.06217](#)]. S. Pasterski, S.-H. Shao and A. Strominger, *Gluon Amplitudes as 2d Conformal Correlators*, *Phys. Rev. D* **96** (2017) 085006, [[1706.03917](#)]. H. Jiang, W. Song and Q. Wen, *Entanglement Entropy in Flat Holography*, *JHEP* **07** (2017) 142, [[1706.07552](#)]. R. K. Mishra and R. Sundrum, *Asymptotic Symmetries, Holography and Topological Hair*, *JHEP* **01** (2018)

- 014, [1706.09080]. I. Y. Park, *Foliation-based quantization and black hole information*, *Class. Quant. Grav.* **34** (2017) 245005, [1707.04803]. C. Batlle, D. Delmastro and J. Gomis, *Non-relativistic Bondi–Metzner–Sachs algebra*, *Class. Quant. Grav.* **34** (2017) 184002. C. S. Lam, *Holographic Scattering Amplitudes*, 1710.04302. D. Kapec and P. Mitra, *A  $d$ -Dimensional Stress Tensor for  $Mink_{d+2}$  Gravity*, *JHEP* **05** (2018) 186, [1711.04371].
- M. Campiglia and L. Coito, *Asymptotic charges from soft scalars in even dimensions*, *Phys. Rev.* **D97** (2018) 066009, [1711.05773]. H. T. Lam and S.-H. Shao, *Conformal Basis, Optical Theorem, and the Bulk Point Singularity*, *Phys. Rev.* **D98** (2018) 025020, [1711.06138]. N. Banerjee, S. Banerjee, S. Atul Bhatkar and S. Jain, *Conformal Structure of Massless Scalar Amplitudes Beyond Tree level*, *JHEP* **04** (2018) 039, [1711.06690].
- A. Schreiber, A. Volovich and M. Zlotnikov, *Tree-level gluon amplitudes on the celestial sphere*, *Phys. Lett.* **B781** (2018) 349–357, [1711.08435].
- S. Banerjee, *Null Infinity and Unitary Representation of The Poincare Group*, *JHEP* **01** (2019) 205, [1801.10171]. M. M. Caldarelli and K. Skenderis, *Kaluza–Klein reductions and AdS/Ricci-flat correspondence*, *Eur. Phys. J.* **C78** (2018) 590, [1802.06085]. L. Ciambelli, C. Marteau, A. C. Petkou, P. M. Petropoulos and K. Siampos, *Flat holography and Carrollian fluids*, *JHEP* **07** (2018) 165, [1802.06809]. S. Banerjee, *Symmetries of free massless particles and soft theorems*, *Gen. Rel. Grav.* **51** (2019) 128, [1804.06646]. A. Barducci, R. Casalbuoni and J. Gomis, *Confined dynamical systems with Carroll and Galilei symmetries*, *Phys. Rev.* **D98** (2018) 085018, [1804.10495]. S. Stieberger and T. R. Taylor, *Strings on Celestial Sphere*, *Nucl. Phys.* **B935** (2018) 388–411, [1806.05688]. R. K. Mishra, A. Mohd and R. Sundrum, *AdS Asymptotic Symmetries from CFT Mirrors*, *JHEP* **03** (2019) 017, [1809.07331]. G. Compère, A. Fiorucci and R. Ruzziconi, *Superboost transitions, refraction memory and super-Lorentz charge algebra*, *JHEP* **11** (2018) 200, [1810.00377]. L. Donnay, A. Puhm and A. Strominger, *Conformally Soft Photons and Gravitons*, *JHEP* **01** (2019) 184, [1810.05219]. S. Banerjee, P. Pandey and P. Paul, *Conformal properties of soft-operators - 1 : Use of null-states*, 1902.02309. M. Pate, A.-M. Raclariu and A. Strominger, *Conformally Soft Theorem in Gauge*

- Theory*, *Phys. Rev.* **D100** (2019) 085017, [[1904.10831](#)]. D. Nandan, A. Schreiber, A. Volovich and M. Zlotnikov, *Celestial Amplitudes: Conformal Partial Waves and Soft Limits*, *JHEP* **10** (2019) 018, [[1904.10940](#)].
- T. Adamo, L. Mason and A. Sharma, *Celestial amplitudes and conformal soft theorems*, *Class. Quant. Grav.* **36** (2019) 205018, [[1905.09224](#)]. A. Ball, E. Himwich, S. A. Narayanan, S. Pasterski and A. Strominger, *Uplifting  $AdS_3/CFT_2$  to flat space holography*, *JHEP* **08** (2019) 168, [[1905.09809](#)].
- S. Banerjee and P. Pandey, *Conformal properties of soft operators – 2 : Use of null-states*, [1906.01650](#). B. Chen, P.-X. Hao and Z.-F. Yu, *2d Galilean Field Theories with Anisotropic Scaling*, [1906.03102](#). A. Guevara, *Notes on Conformal Soft Theorems and Recursion Relations in Gravity*, [1906.07810](#).
- A. Fotopoulos and T. R. Taylor, *Primary Fields in Celestial CFT*, *JHEP* **10** (2019) 167, [[1906.10149](#)]. V. Godet and C. Marteau, *Gravitation in flat spacetime from entanglement*, *JHEP* **12** (2019) 057, [[1908.02044](#)]. H. Lü, P. Mao and J.-B. Wu, *Asymptotic Structure of Einstein-Maxwell-Dilaton Theory and Its Five Dimensional Origin*, *JHEP* **11** (2019) 005, [[1909.00970](#)]. E. Adjei, W. Donnelly, V. Py and A. J. Speranza, *Cosmic footballs from superrotations*, [1910.05435](#). R. Ruzziconi, *Asymptotic Symmetries in the Gauge Fixing Approach and the BMS Group*, [1910.08367](#).
- G. Compère, R. Oliveri and A. Seraj, *The Poincaré and BMS flux-balance laws with application to binary systems*, [1912.03164](#). K. Prabhu and I. Shehzad, *Asymptotic symmetries and charges at spatial infinity in general relativity*, [1912.04305](#). W. Merbis and M. Riegler, *Geometric actions and flat space holography*, [1912.08207](#). B. Bhattacharjee and C. Krishnan, *A General Prescription for Semi-Classical Holography*, [1908.04786](#).
- C. Krishnan, *Bulk Locality and Asymptotic Causal Diamonds*, *SciPost Phys.* **7** (2019) 057, [[1902.06709](#)].
- [25] A. Ashtekar, M. Campiglia and A. Laddha, *Null infinity, the BMS group and infrared issues*, *Gen. Rel. Grav.* **50** (2018) 140–163, [[1808.07093](#)].
- [26] A. Strominger, *Lectures on the Infrared Structure of Gravity and Gauge Theory*, [1703.05448](#). G. Compère and A. Fiorucci, *Advanced Lectures on General Relativity*, [1801.07064](#).

- [27] A. Ashtekar, *Asymptotic Quantization of the Gravitational Field*, *Phys. Rev. Lett.* **46** (1981) 573–576.
- [28] T. He, V. Lysov, P. Mitra and A. Strominger, *BMS supertranslations and Weinberg’s soft graviton theorem*, *JHEP* **05** (2015) 151, [[1401.7026](#)].
- [29] D. Kapec, M. Perry, A.-M. Raclariu and A. Strominger, *Infrared Divergences in QED, Revisited*, *Phys. Rev.* **D96** (2017) 085002, [[1705.04311](#)]. S. Choi, U. Kol and R. Akhoury, *Asymptotic Dynamics in Perturbative Quantum Gravity and BMS Supertranslations*, *JHEP* **01** (2018) 142, [[1708.05717](#)].
- [30] H. Bondi, M. G. J. van der Burg and A. W. K. Metzner, *Gravitational waves in general relativity. 7. Waves from axisymmetric isolated systems*, *Proc. Roy. Soc. Lond.* **A269** (1962) 21–52.
- [31] R. Sachs, *Gravitational waves in general relativity. 8. Waves in asymptotically flat space-times*, *Proc. Roy. Soc. Lond. A* **A270** (1962) 103–126.
- [32] A. Ashtekar and A. Magnon-Ashtekar, *Energy-Momentum in General Relativity*, *Phys. Rev. Lett.* **43** (1979) 181.
- [33] R. L. Arnowitt, S. Deser and C. W. Misner, *The Dynamics of general relativity*, *Gen. Rel. Grav.* **40** (2008) 1997–2027, [[gr-qc/0405109](#)]. T. Regge and C. Teitelboim, *Role of Surface Integrals in the Hamiltonian Formulation of General Relativity*, *Annals Phys.* **88** (1974) 286.
- [34] A. Ashtekar and M. Streubel, *Symplectic Geometry of Radiative Modes and Conserved Quantities at Null Infinity*, *Proc. Roy. Soc. Lond.* **A376** (1981) 585–607.
- [35] A. Ashtekar, *Radiative Degrees of Freedom of the Gravitational Field in Exact General Relativity*, *J. Math. Phys.* **22** (1981) 2885–2895.
- [36] A. Ashtekar, *ASYMPTOTIC QUANTIZATION: BASED ON 1984 NAPLES LECTURES*. 1987.

- 
- [37] J. Distler, R. Flauger and B. Horn, *Double-soft graviton amplitudes and the extended BMS charge algebra*, *JHEP* **08** (2019) 021, [[1808.09965](#)].  
M. Campiglia and J. Peraza, *Generalized BMS charge algebra*, *Phys. Rev. D* **101** (2020) 104039, [[2002.06691](#)].
- [38] R. Bousso, V. Chandrasekaran, I. F. Halpern and A. Wall, *Asymptotic Charges Cannot Be Measured in Finite Time*, *Phys. Rev.* **D97** (2018) 046014, [[1709.08632](#)].
- [39] R. F. Streater and A. S. Wightman, *PCT, spin and statistics, and all that*. Princeton University Press, 2016.
- [40] Chandramouli Chowdhury, Kyriakos Papadodimas, Olga Papadoulaki and Suvrat Raju, “in progress.”
- [41] G. Penington, *Entanglement Wedge Reconstruction and the Information Paradox*, [1905.08255](#). G. Penington, S. H. Shenker, D. Stanford and Z. Yang, *Replica wormholes and the black hole interior*, [1911.11977](#).  
A. Almheiri, T. Hartman, J. Maldacena, E. Shaghoulian and A. Tajdini, *Replica Wormholes and the Entropy of Hawking Radiation*, [1911.12333](#).  
A. Almheiri, R. Mahajan, J. Maldacena and Y. Zhao, *The Page curve of Hawking radiation from semiclassical geometry*, [1908.10996](#).
- [42] I. Bena and N. P. Warner, *Black holes, black rings and their microstates*, *Lect. Notes Phys.* **755** (2008) 1–92, [[hep-th/0701216](#)]. I. Bena and N. P. Warner, *Resolving the Structure of Black Holes: Philosophizing with a Hammer*, [1311.4538](#).
- [43] O. Lunin and S. D. Mathur, *AdS / CFT duality and the black hole information paradox*, *Nucl. Phys.* **B623** (2002) 342–394, [[hep-th/0109154](#)].
- [44] I. Bena, S. Giusto, E. J. Martinec, R. Russo, M. Shigemori, D. Turton et al., *Smooth horizonless geometries deep inside the black-hole regime*, *Phys. Rev. Lett.* **117** (2016) 201601, [[1607.03908](#)].
- [45] M. Cvetič and F. Larsen, *Near horizon geometry of rotating black holes in five-dimensions*, *Nucl. Phys.* **B531** (1998) 239–255, [[hep-th/9805097](#)].

- [46] S. Lloyd, *Black Holes, Demons and the Loss of Coherence: How complex systems get information, and what they do with it*. PhD thesis, Rockefeller University, 1988.
- [47] J. Kinney, J. M. Maldacena, S. Minwalla and S. Raju, *An Index for 4 dimensional super conformal theories*, *Commun. Math. Phys.* **275** (2007) 209–254, [[hep-th/0510251](#)].
- [48] G. Casati, B. Chirikov and I. Guarneri, *Energy-level statistics of integrable quantum systems*, *Phys. Rev. Lett.* **54** (1985) 1350. M. V. Berry and M. Tabor, *Level clustering in the regular spectrum*, *Proc. R. Soc. Lond. A* **356** (1977) 375–394.
- [49] I. Bena, C.-W. Wang and N. P. Warner, *Mergers and typical black hole microstates*, *JHEP* **11** (2006) 042, [[hep-th/0608217](#)].
- [50] A. Tyukov, R. Walker and N. P. Warner, *Tidal Stresses and Energy Gaps in Microstate Geometries*, *JHEP* **02** (2018) 122, [[1710.09006](#)].
- [51] I. Bena, P. Heidmann and D. Turton, *AdS<sub>2</sub> Holography: Mind the Cap*, [1806.02834](#).
- [52] M. Srednicki, *Chaos and quantum thermalization*, *Phys. Rev. E* **50** (1994) 888. M. Srednicki, *The approach to thermal equilibrium in quantized chaotic systems*, *Journal of Physics A: Mathematical and General* **32** (1999) 1163.
- [53] N. Lashkari, A. Dymarsky and H. Liu, *Eigenstate Thermalization Hypothesis in Conformal Field Theory*, *J. Stat. Mech.* **1803** (2018) 033101, [[1610.00302](#)].
- [54] S. D. Mathur and D. Turton, *Comments on black holes I: The possibility of complementarity*, *JHEP* **01** (2014) 034, [[1208.2005](#)].
- [55] S. El-Showk and K. Papadodimas, *Emergent Spacetime and Holographic CFTs*, *JHEP* **10** (2012) 106, [[1101.4163](#)].
- [56] A. Hamilton, D. N. Kabat, G. Lifschytz and D. A. Lowe, *Local bulk operators in AdS/CFT: A Boundary view of horizons and locality*, *Phys. Rev.* **D73** (2006) 086003, [[hep-th/0506118](#)].

- 
- [57] A. Hamilton, D. N. Kabat, G. Lifschytz and D. A. Lowe, *Holographic representation of local bulk operators*, *Phys. Rev.* **D74** (2006) 066009, [[hep-th/0606141](#)].
- [58] A. Hamilton, D. N. Kabat, G. Lifschytz and D. A. Lowe, *Local bulk operators in AdS/CFT: A Holographic description of the black hole interior*, *Phys. Rev.* **D75** (2007) 106001, [[hep-th/0612053](#)]. A. Hamilton, D. N. Kabat, G. Lifschytz and D. A. Lowe, *Local bulk operators in AdS/CFT and the fate of the BTZ singularity*, *AMS/IP Stud. Adv. Math.* **44** (2008) 85–100, [[0710.4334](#)].
- [59] P. Candelas, *Vacuum Polarization in Schwarzschild Space-Time*, *Phys. Rev.* **D21** (1980) 2185–2202.
- [60] S. Ghosh and S. Raju, *Breakdown of String Perturbation Theory for Many External Particles*, *Phys. Rev. Lett.* **118** (2017) 131602, [[1611.08003](#)].
- [61] S. Ghosh and S. Raju, *Loss of locality in gravitational correlators with a large number of insertions*, *Phys. Rev.* **D96** (2017) 066033, [[1706.07424](#)].
- [62] K. Papadodimas and S. Raju, *An Infalling Observer in AdS/CFT*, *JHEP* **10** (2013) 212, [[1211.6767](#)].
- [63] K. Skenderis and M. Taylor, *The fuzzball proposal for black holes*, *Phys.Rept.* **467** (2008) 117–171, [[0804.0552](#)].
- [64] E. T. Jaynes, *Information theory and statistical mechanics*, *Physical review* **106** (1957) 620. E. T. Jaynes, *Information theory and statistical mechanics. ii*, *Phys. Rev.* **108** (1957) 171.
- [65] A. Almheiri, D. Marolf, J. Polchinski, D. Stanford and J. Sully, *An Apologia for Firewalls*, *JHEP* **09** (2013) 018, [[1304.6483](#)].
- [66] D. Marolf and J. Polchinski, *Gauge/Gravity Duality and the Black Hole Interior*, *Phys. Rev. Lett.* **111** (2013) 171301, [[1307.4706](#)].
- [67] K. Papadodimas and S. Raju, *Black Hole Interior in the Holographic Correspondence and the Information Paradox*, *Phys. Rev. Lett.* **112** (2014) 051301, [[1310.6334](#)].

- [68] K. Papadodimas and S. Raju, *State-Dependent Bulk-Boundary Maps and Black Hole Complementarity*, *Phys. Rev.* **D89** (2014) 086010, [[1310.6335](#)].
- [69] K. Papadodimas and S. Raju, *Local Operators in the Eternal Black Hole*, *Phys. Rev. Lett.* **115** (2015) 211601, [[1502.06692](#)].
- [70] K. Papadodimas and S. Raju, *Remarks on the necessity and implications of state-dependence in the black hole interior*, *Phys. Rev.* **D93** (2016) 084049, [[1503.08825](#)].
- [71] E. Verlinde and H. Verlinde, *Passing through the Firewall*, [1306.0515](#).  
E. Verlinde and H. Verlinde, *Behind the Horizon in AdS/CFT*, [1311.1137](#).  
E. Verlinde and H. Verlinde, *Black Hole Entanglement and Quantum Error Correction*, *JHEP* **10** (2013) 107, [[1211.6913](#)]. M. Guica and S. F. Ross, *Behind the geon horizon*, *Class. Quant. Grav.* **32** (2015) 055014, [[1412.1084](#)].
- [72] D. Harlow, *Aspects of the Papadodimas-Raju Proposal for the Black Hole Interior*, *JHEP* **11** (2014) 055, [[1405.1995](#)]. D. Marolf and J. Polchinski, *Violations of the Born rule in cool state-dependent horizons*, *JHEP* **01** (2016) 008, [[1506.01337](#)].
- [73] S. Raju, *Smooth Causal Patches for AdS Black Holes*, *Phys. Rev.* **D95** (2017) 126002, [[1604.03095](#)].
- [74] D. L. Jafferis, *Bulk reconstruction and the Hartle-Hawking wavefunction*, [1703.01519](#).
- [75] A. Bzowski, A. Gnechchi and T. Hertog, *Interactions resolve state-dependence in a toy-model of AdS black holes*, [1802.02580](#).
- [76] A. Sen, *Two Charge System Revisited: Small Black Holes or Horizonless Solutions?*, *JHEP* **05** (2010) 097, [[0908.3402](#)].
- [77] F. Chen, B. Michel, J. Polchinski and A. Puhm, *Journey to the Center of the Fuzzball*, *JHEP* **02** (2015) 081, [[1408.4798](#)].
- [78] E. J. Martinec, S. Massai and D. Turton, *String dynamics in NS5-F1-P geometries*, *JHEP* **09** (2018) 031, [[1803.08505](#)].

- 
- [79] K. Skenderis and M. Taylor, *Fuzzball solutions and D1-D5 microstates*, *Phys. Rev. Lett.* **98** (2007) 071601, [[hep-th/0609154](#)]. I. Kanitscheider, K. Skenderis and M. Taylor, *Holographic anatomy of fuzzballs*, *JHEP* **04** (2007) 023, [[hep-th/0611171](#)]. I. Kanitscheider, K. Skenderis and M. Taylor, *Fuzzballs with internal excitations*, *JHEP* **06** (2007) 056, [[0704.0690](#)].
- [80] J. de Boer, K. Papadodimas and E. Verlinde, *Black Hole Berry Phase*, *Phys. Rev. Lett.* **103** (2009) 131301, [[0809.5062](#)].
- [81] A. Bombini, A. Galliani, S. Giusto, E. Moscato and R. Russo, *Unitary 4-point correlators from classical geometries*, *Eur. Phys. J.* **C78** (2018) 8, [[1710.06820](#)]. A. Galliani, S. Giusto and R. Russo, *Holographic 4-point correlators with heavy states*, *JHEP* **10** (2017) 040, [[1705.09250](#)]. A. Galliani, S. Giusto, E. Moscato and R. Russo, *Correlators at large  $c$  without information loss*, *JHEP* **09** (2016) 065, [[1606.01119](#)].
- [82] O. Lunin, J. M. Maldacena and L. Maoz, *Gravity solutions for the D1-D5 system with angular momentum*, [hep-th/0212210](#).
- [83] P. Dedecker, *Calcul des variations, formes différentielles et champs géodésiques*, *Geometrie différentielle, Colloq. Intern. du CNRS LII, Strasbourg* (1953) 17–34. C. Crnkovic and E. Witten, *Covariant description of canonical formalism in geometrical theories*, *Three Hundred Years of Gravitation* (1987) 676–684. G. Zuckerman, *Action principles and global geometry*, *Mathematical Aspects of String Theory* **1** (1987) 259–284.
- [84] V. Balasubramanian, J. de Boer, S. El-Showk and I. Messamah, *Black Holes as Effective Geometries*, *Class. Quant. Grav.* **25** (2008) 214004, [[0811.0263](#)].
- [85] I. Bena, S. Giusto, R. Russo, M. Shigemori and N. P. Warner, *Habemus Superstratum! A constructive proof of the existence of superstrata*, *JHEP* **05** (2015) 110, [[1503.01463](#)].
- [86] K. Skenderis and M. Taylor, *Kaluza-Klein holography*, *JHEP* **05** (2006) 057, [[hep-th/0603016](#)].

- [87] I. Bena, D. Turton, R. Walker and N. P. Warner, *Integrability and Black-Hole Microstate Geometries*, *JHEP* **11** (2017) 021, [[1709.01107](#)].
- [88] O. Aharony, S. S. Gubser, J. M. Maldacena, H. Ooguri and Y. Oz, *Large  $N$  field theories, string theory and gravity*, *Phys. Rept.* **323** (2000) 183–386, [[hep-th/9905111](#)].
- [89] J. C. Breckenridge, D. A. Lowe, R. C. Myers, A. W. Peet, A. Strominger and C. Vafa, *Macroscopic and microscopic entropy of near extremal spinning black holes*, *Phys. Lett.* **B381** (1996) 423–426, [[hep-th/9603078](#)]. J. C. Breckenridge, R. C. Myers, A. W. Peet and C. Vafa, *D-branes and spinning black holes*, *Phys. Lett.* **B391** (1997) 93–98, [[hep-th/9602065](#)].
- [90] M. Galassi, J. Davies, J. Theiler, B. Gough, G. Jungman, M. Booth et al., *GNU Scientific Library Reference Manual (Network Theory Ltd.)*, 2009.
- [91] S.-J. Rey and V. Rosenhaus, *Scanning Tunneling Macroscopy, Black Holes, and AdS/CFT Bulk Locality*, *JHEP* **1407** (2014) 050, [[1403.3943](#)].
- [92] R. Bousso, B. Freivogel, S. Leichenauer, V. Rosenhaus and C. Zukowski, *Null Geodesics, Local CFT Operators and AdS/CFT for Subregions*, *Phys. Rev.* **D88** (2013) 064057, [[1209.4641](#)].
- [93] I. A. Morrison, *Boundary-to-bulk maps for AdS causal wedges and the Reeh-Schlieder property in holography*, *JHEP* **1405** (2014) 053, [[1403.3426](#)].
- [94] D. T. Son and A. O. Starinets, *Minkowski space correlators in AdS / CFT correspondence: Recipe and applications*, *JHEP* **0209** (2002) 042, [[hep-th/0205051](#)].
- [95] D. Stanford, *Black Holes and the Butterfly Effect*, *Institute for Advanced Study Newsletter* (2017) .
- [96] J. Maldacena, S. H. Shenker and D. Stanford, *A bound on chaos*, [1503.01409](#).
- [97] I. Amado, B. Sundborg, L. Thorlacius and N. Wintergerst, *Black holes from large  $N$  singlet models*, *JHEP* **03** (2018) 075, [[1712.06963](#)].

- 
- [98] R. Haag, *Local quantum physics: Fields, particles, algebras, 2nd ed.* Springer, 1992.
- [99] J. Bros and D. Buchholz, *Towards a relativistic kms-condition*, *Nuclear Physics B* **429** (1994) 291–318.
- [100] M. Brigante, G. Festuccia and H. Liu, *Inheritance principle and non-renormalization theorems at finite temperature*, *Phys. Lett.* **B638** (2006) 538–545, [[hep-th/0509117](#)].
- [101] A. Niegawa, *Path-integral formulation of real-time quantum field theories at finite temperature*, *Physical Review D* **40** (1989) 1199.
- [102] T. Evans, *N-point finite temperature expectation values at real times*, *Nuclear Physics B* **374** (1992) 340–370. H. Mabilat, *Derivation of the real-time formalism from first principles in thermal field theory*, *Zeitschrift für Physik C Particles and Fields* **75** (1997) 155–166. U. Kraemmer and A. Rebhan, *Advances in perturbative thermal field theory*, *Reports on Progress in Physics* **67** (2004) 351.
- [103] F. Gelis, *A New approach for the vertical part of the contour in thermal field theories*, *Phys. Lett.* **B455** (1999) 205–212, [[hep-ph/9901263](#)].
- [104] F. M. Haehl, R. Loganayagam, P. Narayan, A. A. Nizami and M. Rangamani, *Thermal out-of-time-order correlators, KMS relations, and spectral functions*, *JHEP* **12** (2017) 154, [[1706.08956](#)]. S. Chaudhuri, C. Chowdhury and R. Loganayagam, *Spectral Representation of Thermal OTO Correlators*, *JHEP* **02** (2019) 018, [[1810.03118](#)]. S. Chaudhuri and R. Loganayagam, *Probing Out-of-Time-Order Correlators*, [1807.09731](#).
- [105] C. Herzog and D. Son, *Schwinger-Keldysh propagators from AdS/CFT correspondence*, *JHEP* **0303** (2003) 046, [[hep-th/0212072](#)].
- [106] E. Barnes, D. Vaman, C. Wu and P. Arnold, *Real-time finite-temperature correlators from AdS/CFT*, *Phys. Rev.* **D82** (2010) 025019, [[1004.1179](#)]. K. Skenderis and B. C. van Rees, *Real-time gauge/gravity duality: Prescription, Renormalization and Examples*, *JHEP* **05** (2009) 085,

- [0812.2909]. K. Skenderis and B. C. van Rees, *Real-time gauge/gravity duality*, *Phys. Rev. Lett.* **101** (2008) 081601, [0805.0150].
- V. Balasubramanian, A. Bernamonti, J. de Boer, N. Copland, B. Craps, E. Keski-Vakkuri et al., *Holographic Thermalization*, *Phys. Rev.* **D84** (2011) 026010, [1103.2683]. V. Balasubramanian, A. Bernamonti, J. de Boer, N. Copland, B. Craps, E. Keski-Vakkuri et al., *Thermalization of Strongly Coupled Field Theories*, *Phys. Rev. Lett.* **106** (2011) 191601, [1012.4753].
- [107] R. Eden, P. Landshoff and D. Olive, *The Analytic S-Matrix*. Cambridge University Press, London, 1966.
- [108] J. Maldacena, D. Simmons-Duffin and A. Zhiboedov, *Looking for a bulk point*, *JHEP* **01** (2017) 013, [1509.03612].
- [109] E. D'Hoker, D. Z. Freedman and L. Rastelli, *AdS / CFT four point functions: How to succeed at  $z$  integrals without really trying*, *Nucl.Phys.* **B562** (1999) 395–411, [hep-th/9905049].
- [110] M. Simpson and R. Penrose, *Internal instability in a Reissner-Nordstrom black hole*, *Int. J. Theor. Phys.* **7** (1973) 183–197. J. M. McNamara, *Instability of black hole inner horizons*, *Proceedings of the Royal Society of London. A. Mathematical and Physical Sciences* **358** (1978) 499–517. S. Chandrasekhar and J. B. Hartle, *On crossing the cauchy horizon of a reissner–nordström black-hole*, *Proceedings of the Royal Society of London. A. Mathematical and Physical Sciences* **384** (1982) 301–315. E. Poisson and W. Israel, *Inner-horizon instability and mass inflation in black holes*, *Phys. Rev. Lett.* **63** (1989) 1663–1666. E. Poisson and W. Israel, *Internal structure of black holes*, *Phys. Rev.* **D41** (1990) 1796–1809.
- [111] V. Cardoso, J. L. Costa, K. Destounis, P. Hintz and A. Jansen, *Quasinormal modes and Strong Cosmic Censorship*, *Phys. Rev. Lett.* **120** (2018) 031103, [1711.10502].
- [112] A. Ori, *Inner structure of a charged black hole: An exact mass-inflation solution*, *Phys. Rev. Lett.* **67** (1991) 789–792. A. Ori, *Structure of the singularity inside a realistic rotating black hole*, *Phys. Rev. Lett.* **68** (1992)

- 2117–2120. F. Mellor and I. Moss, *Stability of Black Holes in De Sitter Space*, *Phys. Rev.* **D41** (1990) 403. C. M. Chambers and I. G. Moss, *Stability of the Cauchy horizon in Kerr-de Sitter space-times*, *Class. Quant. Grav.* **11** (1994) 1035–1054, [[gr-qc/9404015](#)]. P. R. Brady, C. M. Chambers, W. Krivan and P. Laguna, *Telling tails in the presence of a cosmological constant*, *Phys. Rev.* **D55** (1997) 7538–7545, [[gr-qc/9611056](#)]. M. Dafermos, *The Interior of charged black holes and the problem of uniqueness in general relativity*, *Commun. Pure Appl. Math.* **58** (2005) 0445–0504, [[gr-qc/0307013](#)]. M. Dafermos, *Stability and instability of the Reissner-Nordstrom Cauchy horizon and the problem of uniqueness in general relativity*, *Contemp. Math.* **350** (2004) 99–113, [[gr-qc/0209052](#)]. K. Murata, H. S. Reall and N. Tanahashi, *What happens at the horizon(s) of an extreme black hole?*, *Class. Quant. Grav.* **30** (2013) 235007, [[1307.6800](#)]. D. Christodoulou, *The formation of black holes in general relativity*, in *The Twelfth Marcel Grossmann Meeting: On Recent Developments in Theoretical and Experimental General Relativity, Astrophysics and Relativistic Field Theories (In 3 Volumes)*, pp. 24–34, World Scientific, 2012. S. Bhattacharjee, S. Sarkar and A. Virmani, *Internal Structure of Charged AdS Black Holes*, *Phys. Rev.* **D93** (2016) 124029, [[1604.03730](#)]. S. Hod, *Strong cosmic censorship in charged black-hole spacetimes: As strong as ever*, *Nucl. Phys.* **B941** (2019) 636–645, [[1801.07261](#)]. O. J. C. Dias, H. S. Reall and J. E. Santos, *Strong cosmic censorship for charged de Sitter black holes with a charged scalar field*, *Class. Quant. Grav.* **36** (2019) 045005, [[1808.04832](#)]. Y. Mo, Y. Tian, B. Wang, H. Zhang and Z. Zhong, *Strong cosmic censorship for the massless charged scalar field in the Reissner-Nordstrom–de Sitter spacetime*, *Phys. Rev.* **D98** (2018) 124025, [[1808.03635](#)]. S. Hod, *Quasinormal modes and strong cosmic censorship in near-extremal Kerr–Newman–de Sitter black-hole spacetimes*, *Phys. Lett.* **B780** (2018) 221–226, [[1803.05443](#)]. J. Luk and S.-J. Oh, *Strong cosmic censorship in spherical symmetry for two-ended asymptotically flat initial data I. The interior of the black hole region*, [1702.05715](#). R. Luna, M. Zilhão, V. Cardoso, J. L. Costa and J. Natário, *Strong Cosmic Censorship: the nonlinear story*, *Phys. Rev.* **D99** (2019) 064014, [[1810.00886](#)].

- [113] O. J. C. Dias, F. C. Eperon, H. S. Reall and J. E. Santos, *Strong cosmic censorship in de Sitter space*, *Phys. Rev.* **D97** (2018) 104060, [[1801.09694](#)].
- [114] M. Dafermos, *Black holes without spacelike singularities*, *Commun. Math. Phys.* **332** (2014) 729–757, [[1201.1797](#)]. M. Dafermos and J. Luk, *The interior of dynamical vacuum black holes I: The  $C^0$ -stability of the Kerr Cauchy horizon*, [1710.01722](#).
- [115] M. Dafermos and Y. Shlapentokh-Rothman, *Rough initial data and the strength of the blue-shift instability on cosmological black holes with  $\lambda > 0$* , *Classical and Quantum Gravity* **35** (2018) 195010.
- [116] W. A. Hiscock, *Stress-energy tensor near a charged, rotating, evaporating black hole*, *Physical Review D* **15** (1977) 3054. A. R. Steif, *The Quantum stress tensor in the three-dimensional black hole*, *Phys. Rev.* **D49** (1994) 585–589, [[gr-qc/9308032](#)].
- [117] N. Birrell and P. Davies, *On falling through a black hole into another universe*, *Nature* **272** (1978) 35.
- [118] O. Sela, *Quantum effects near the Cauchy horizon of a Reissner-Nordström black hole*, *Phys. Rev.* **D98** (2018) 024025, [[1803.06747](#)].
- [119] O. J. C. Dias, H. S. Reall and J. E. Santos, *The BTZ black hole violates strong cosmic censorship*, [1906.08265](#).
- [120] S. Raju, *A Toy Model of the Information Paradox in Empty Space*, [1809.10154](#).
- [121] A. Chamblin, R. Emparan, C. V. Johnson and R. C. Myers, *Charged AdS black holes and catastrophic holography*, *Phys. Rev.* **D60** (1999) 064018, [[hep-th/9902170](#)].
- [122] E. Hairer, S. Nørsett and G. Wanner, *Solving ordinary differential equations I: nonstiff problems*. Springer-Verlag, New York, 1993.
- [123] C. K. Raju, *CALCODE: An ODE Solver*, 1999.

- 
- [124] O. Tange, *Gnu parallel - the command-line power tool*, *login: The USENIX Magazine* **36** (Feb, 2011) 42–47.
- [125] A. Lanir, A. Ori, N. Zilberman, O. Sela, A. Maline and A. Levi, *Analysis of quantum effects inside spherical charged black holes*, *Phys. Rev.* **D99** (2019) 061502, [[1811.03672](#)].
- [126] V. Balasubramanian and T. S. Levi, *Beyond the veil: Inner horizon instability and holography*, *Phys.Rev.* **D70** (2004) 106005, [[hep-th/0405048](#)].  
E. Keski-Vakkuri, *Bulk and boundary dynamics in BTZ black holes*, *Phys. Rev.* **D59** (1999) 104001, [[hep-th/9808037](#)].
- [127] J. M. Maldacena, *Eternal black holes in anti-de Sitter*, *JHEP* **0304** (2003) 021, [[hep-th/0106112](#)].
- [128] T. Evans and D. Steer, *Wick's theorem at finite temperature*, *Nuclear Physics B* **474** (1996) 481 – 496.
- [129] F. Gelis, *The Effect of the vertical part of the path on the real time Feynman rules in finite temperature field theory*, *Z. Phys.* **C70** (1996) 321–331, [[hep-ph/9412347](#)].
- [130] P. Kraus, H. Ooguri and S. Shenker, *Inside the horizon with AdS / CFT*, *Phys.Rev.* **D67** (2003) 124022, [[hep-th/0212277](#)].